EXPERIMENTAL INVESTIGATION ON THE EFFECTS OF BURNISHING PROCESS FOR TURNED TITANIUM ALLOY (Ti-6Al-4V)

Thesis

Submitted in partial fulfillment of the requirements for the degree of

DOCTOR OF PHILOSOPHY

by

GOUTAM D REVANKAR

DEPARTMENT OF MECHANICAL ENGINEERING

NATIONAL INSTITUTE OF TECHNOLOGY KARNATAKA

SURATHKAL, MANGALORE-575025

January, 2016

DECLARATION

By the Ph. D. Research Scholar

I hereby declare that the Research Thesis entitled ***"EXPERIMENTAL INVESTGATION ON THE EFFECTS OF BURNISHING PROCESS FOR TURNED TITANIUM ALLOY(Ti-6Al-4V)"*** which is being submitted to **National Institute of Technology Karnataka, Surathkal**in partial fulfillment of the requirements of award of the degree **Doctor of Philosophy** in **Department of Mechanical Engineering** *is a bonafide report of the research work carried out by me.* The material contained in this Research Thesis has not been submitted to any University or Institution for the award of any degree.

Register Number : ME09P11

Name of the Research Scholar : Goutam D Revankar

Signature of the Research Scholar :

Department of Mechanical Engineering

Place: NITK- Surathkal

Date:

CERTIFICATE

This is to certify that the Research Thesis entitled ***"EXPERIMENTAL INVESITGATION ON THE EFFECTS OF BURNISHING PROCESS FOR TURNED TITANIUM ALLOY (Ti-6AL-4V)"*** submitted by **Mr.Goutam D Revankar (Reg.No. ME09P11)** as the record of the research work carried out by him, is accepted as the Research Thesis submission in partial fulfillment of the requirements for the award of the degree of **Doctor of Philosophy.**

Dr. Shrikantha S. Rao
Date:
Research Guide

Chairman DRPC
Date:

Acknowledgement

It has been indeed a great honor and privilege for me to work under the guidance of my advisor **Dr. Shrikantha S. Rao,** Department of Mechanical Engineering, NITK Surathkal. With deep sense of gratitude and humility, I express my sincere thanks to him for his valuable guidance, untiring perseverance and unending patience which made the research not merely educational but also enjoyable.I also take this opportunity to thank the Director, NITK Surathkal and Head of Mechanical Engineering Department, NITK Surathkal for allowing me to carry out my doctoral studies.

I sincerely thank the Research Progress Assessment Committee consisting of Dr. Vijay. Desai (Mechanical Engineering Department), Dr. Sitaram. Nayak (Civil Engineering Department) for their valuable comments and constructive criticism which have helped the enrichment of this doctoral work. My heartfelt thanks to Dr.Raviraj Shetty, MIT Manipal, Dr.Mervin.A.Herbert, NITK Surathkal and Dr.V.N.Gaitonde, BVBCET Hubli for their valuable suggestions and constant support during my research work. I am indeed extremely indebted to all of them.

Seeking the blessings of His Holiness Tontadarya Swamiji, my sincere thanks to Management and Principal, Tontadarya College of Engineering Gadag, Mr.D.M.Goudar Head of Mechanical Dept. and my colleagues of mechanical department TCE Gadag for rendering their support and advice. I am immensely indebted to the unending help and support I received from my co-research colleagues Mr. Arun Kumar, Mr.Manjiah, Mr. I.S.Patil, Mrs. Rashmi, Mr Kathik Rao during the course of my research work. I also thank Mr.M.B.Uttarkar Chief Librarian TCE Gadag, Mr. Pawar, Mech-India Burnishing Ltd. Mumbai, Mr. Sivkumar Teli, Engineer HAL Bangalore, Mr.B.M.Vitlapur, NITK Surathkal who provided me continuous support during my research work. My sincere thanks to Mr.Puneet, Mr Challmarad, Mr. Raju.Deshanur, Mr Prakash.Badiger Department of Mechanical Engineering, TCE Gadag, Mr.Rehman and Mr. Shankar, GTTC Hubli, for extending their help while conducting the experiments. I also thank the faculties at CMTI Bangalore and IIT Mumbai ,for providing the testing facility at their organizations.

I am indebted to my grandfather Shri R.G.Raykar, my parents Mr. Devaraya.B.Revankar and Mrs. Prabhavathi. D.Revankar for inculcating in me the right values and virtues. I am indebted to my wife Mrs.Abhinetri.G.Revankar for her constant inspiration, encouragement and motivation during my research work. I am extremely grateful to my brother Mr. Raghavendra.D.Revankar for providing continuous encouragement and support. I wish to express my special thanks to all my family members and friends who were a constant source of motivation and encouragement during the entire course of my doctoral work.

_____

Goutam D Revankar

Abstract

Surface modifications and surface treatments play a very important role in increasing the service life of several critical parts of equipments that are employed in manufacturing and structural applications. Latest technologies utilize sophisticated surface modification methods like laser treatment and coatings to increase service life. But the biggest drawback of these technologies is the prohibitively high cost involved and hence is economically not viable for simple to moderate but vital applications like aerospace, automobiles, biomedical, gas turbines and machine parts. In this context an effective, efficient and economical option are the mechanical surface enhancement techniques that have been employed successfully over the years to increase the wear resistance, fatigue life and corrosion resistance of metallic components. These techniques improve surface finish, increase hardness and impart compressive residual stresses on component surfaces to counter the damage caused by the machining process. This is particularly the case in difficult-to-cut materials, namely titanium and nickel based alloys. Burnishing is a mechanical surface smoothing and surface enhancement technique, which can eliminate the damaging effects of machining processes like surface roughness, crack and tensile residual stress and improve the surface integrity of components. Development of a simplified burnishing process with parameters optimized to achieve fair levels of multiple responses is a need of the hour for industry and is attempted in the present work. The present research aims to study the effects of burnishing process on turned titanium alloy (Ti-6Al-4V) using Taguchi technique, response surface methodology and finite element method.

In the first phase of study, the analysis of surface roughness and hardness of titanium alloy, which is turned with polycrystalline diamond tool under different turning parameters, different lubricating modes was carried out. The optimum conditions of machining for the best finish i.e., minimum quantity lubrication mode, high cutting speed, low feed rate, high nose radius with low depth of cut were established using Taguchi method. The second order surface roughness model based on response surface methodology (RSM) was developed using the experimental data obtained

from Taguchi's orthogonal array. The predicted values from the RSM model agreed with the experimentally obtained results.

In the second phase, the surface integrity of the above turned titanium specimens subjected to burnishing was investigated. The effect of burnishing parameters like burnishing force, feed, speed and number of passes was studied. The surface integrity factors investigated were surface roughness, hardness, residual stresses and micrography.The optimum conditions of burnishing i.e., a combination of burnishing speed in the medium range, small feed, low burnishing force with three passes was helpful for reduced surface roughness. However, burnishing with medium speed and feed, higher force and more number of tool passes improved the surface hardness. Greater improvements in surface finish (77%) and visible improvement in hardness (17%) were observed when compared with turned surfaces. A finite element method (FEM), model was developed to determine the residual stresses due to burnishing using the software LS-Pre Post. A comparison of residual stresses obtained by the FEM model and the experimental observations was made and validated.

A novel and improved burnishing tool was proposed and burnishing trials were conducted with this tool and the improvement was measured. A comparison of the performance of ball burnishing and roller burnishing was also carried out. Finally the improvement in wear resistance of ball burnished titanium was investigated using pin-on-disk wear testing equipment. Taguchi optimization in our investigation, showed greater improvements in specific wear rate (52% reduction) and coefficient of friction (64% reduction), when compared to turned surfaces. Thus, the study contributes a simple burnishing process which can be implemented by a small/medium enterprise to achieve better industrial components with improved surface hardness, surface finish and wear resistance.

Keywords: Burnishing, Titanium alloy (Ti-6Al-4V), Taguchi technique, Surface roughness, Surface hardness, Wear resistance

Contents

List of Figures

List of Tables

Nomenclature

Symbol	Description	Unit
η	Signal–Noise ratio	dB
Ra	Surface roughness	µm
H	Hardness	Hv
F_b	Force	N
Q	Quantity of lubricant	ml/hr
v	Cutting speed	m/min
f	Feed rate	mm/rev
A	Burnishing feed,	mm/rev
B	Burnishing speed	m/min
C	Burnishing Force	N
D	No of passes	
W_r	Specific wear rate	mm^3/Nm
Vs	Sliding velocity	m/s
Δm	Mass loss	gm
ρ	Density	g/cm^3
µ	Coefficient of friction	
F_N	Normal load	N
t	Test duration	s

Abbreviation	Description
2D	Two dimension
3D	Three dimension
ANOM	Analysis of means
ANOVA	Analysis of variance
BB	Ball burnishing
BUE	Built up edge
CI	Confidence interval
CNC	Computer Numerical Control
DOE	Design of experiments
DOF	Degrees of freedom
HRC	Hardness Rockwell C Scale
MOS	Mean square
MQL	Minimum quantity lubrication
OA	Orthogonal array
PCD	Polycrystalline Diamond
RB	Roller burnishing
RS	Residual stress
RSM	Response surface methodology
SEM	Scanning electron microscope
S/N	Signal to noise ratio
SS	Sum of squares
Ti-6Al-4V	Titanium alloy Grade 5
WEDM	Wire electro discharge machining

Chapter 1

INTRODUCTION

Most of the automobile and aerospace industries work under intense, dangerous and vibrant conditions. The industry demands materials having mechanical properties which provide efficient and extended performance under different working conditions (Tolga Bozdana 2005). The surface integrity of an engineered surface is generally characterized in terms of surface finish, state of residual stress, microstructure and micro hardness. Generally, good surface finish, high compressive strength and higher hardness of the surface layer increase the fatigue life, corrosion and wear resistance of the components. It is evident from the work of Kukielka, L. (1989) that, failure of about 85% of the modern machine components was due to improper physical and stereometrical properties of surface. Most of the machining processes cause damage to the surface integrity of the components resulting in rough surface, crack and tensile residual stress on the surface, particularly in difficult-to-cut materials, namely titanium alloys, nickel based alloys, magnesium alloys, refractory metals, superalloys and ferrous alloys frequently used in critical components. Surface modifications and surface treatments play a very important role in increasing the service life of several critical parts of materials and equipments that are employed for manufacturing and structural applications. Recent technologies utilize sophisticated surface modification methods, like laser treatment and coatings to increase service life. But the biggest drawbacks of these latest technologies is the prohibitively high cost involved and hence are economically not viable for simple to moderate vital applications like aerospace, automobiles, biomedical, gas turbines and machine parts. Most of these applications demand surface roughness values of the order of 0.1 to 0.2 μm, achievable through conventional surface modifications. A large number of studies have pointed that post-machining and metal-finishing operations are attractive (Papshev 1966, Torbilo&Markus 1969, Shapiro & Frolov 1970, Timoshchenko & Dubenko 1976, Ruseva & Fuks 1978, Kotiveerachari & Murthy 1989, Rajesham & Jem Cheong Tak 1989). One popular practice is ‘Burnishing’ which improves surface properties by plastically deforming the surface layers. Burnishing is categorized as

cold-working finishing process that results in good surface finish and generation of residual compressive stresses at metallic surface layers. Burnishing is a distinct process, when compared with the conventional chip-forming finishing processes such as grinding, honing, lapping and super finishing because it is a chip less process. Moreover, the traditional finishing process induces tensile stresses at the surface, whereas burnishing results in residual compressive stresses. The most important features that make it lucrative are that, burnishing is cheaper, consumes less time and skill to achieve a high quality surface finish. Burnishing is a mechanical surface smoothing and surface enhancement technique, which can eliminate these damaging effects of machining processes and improve the surface integrity of components. By displacing the asperities into the valleys of the machined surface, burnishing produces a smooth and compact surface and at the same time induces beneficial compressive residual stress and cold-work hardening, which retards crack nucleation and propagation to enhance component's functional properties. One of the best options to overcome and eliminate the damaging effects caused due to machining processes and enhance the surface integrity of components is burnishing. It is a mechanical surface smoothing and surface enhancement technique. An even and compact surface is produced during burnishing due to displacement of asperities into the valleys of the machined surface and additionally induces beneficial compressive residual stress and cold-work hardening. The result is the improvement of components functional properties, due to retardation of crack nucleation and propagation in the component. The objective of burnishing processes can be divided into three main sections, surface smoothing (geometrical), surface enhancement (mechanical) and the microstructural transformation (metallurgical).

Ti-6Al-4V is the most popular and widely used titanium alloy. Titanium alloy has been widely used in aviation, aerospace, ship building, biomedical, chemical and other industrial departments. It has excellent properties such as low density, high specific strength, corrosion resistance and fracture toughness. But one of the drawbacks of this alloy is its poor wear properties. To overcome this, large numbers of surface treatments are employed. However these surface treatment procedures are costly and require skilled labour. One promising alternative is the burnishing process

which is economical, easy to execute and highly effective. To conduct the burnishing process effectively on Ti-6Al-4V, it is essential to understand the machining characteristics of Ti-6Al-4V. Development of an economical ball burnishing process and its optimization to obtain enhanced wear resistance with good surface finish and hardness are the specific objectives of the present research work.

1.1 TITANIUM ALLOY (Ti-6Al-4V)

Titanium alloys contain a mixture of titanium and other chemical elements. The major strength of titanium-based alloys is their low density i.e about half the density of nickel-based alloys and almost similar to aluminum alloy. Futher, titanium alloys are attractive due to high strength to weight ratio, high yield stress, high tensile strength, toughness at elevated temperatures, corrosion resistivity, creep resistant, toughness, and durability (Q. Wu 2007, M'Saoubi et al. 2008,Y.B. Guo et al 2009). Another attractive property, the reason why it is used in medical industry is its biological compatibility. Titanium alloys are generally categorized into four main categories (Joshi 2006).

- Alpha alloys that consist of neutral alloying elements namely tin and/ or alpha stabilizers namely aluminium or oxygen. Such alloys cannot be subjected to heat treatment.
- Near-alpha alloys consist of minute amount of ductile beta-phase. Apart from alpha-phase stabilizers, near-alpha alloys are alloyed by 1-2% of beta phase stabilizers namely molybdenum, silicon or vanadium.
- Alpha and beta alloys can be characterized as meta stable and usually comprise of some combination of both alpha and beta stabilizers. Such alloys can be subjected to heat treatment
- Beta alloys, can be characterized as meta stable and consist of sufficient beta stabilizers namely molybdenum, silicon and vanadium to let them maintain the beta phase while being quenched. Such alloys can also be solution treated and aged to enhance strength.

Ti-6Al-4V is an alpha-beta alloy, where the alpha phase proportion usually varies from 60 to 90%. The alpha phase in pure titanium is characterized by a hcp crystalline structure that remains stable from room temperature to approximately 882°C. The beta phase in pure titanium has a bcc structure, and is stable from approximately 882°C to the melting point of about 1671°C (Schutz.R. et al. 1988). The addition of aluminium, results in stabilization of alpha phase, i.e, they tend to raise the temperature at which the alloy will be transformed completely to beta phase. This temperature is called beta-transus temperature. Whereas, the additions of chromium, copper, iron, manganese, molybdenum, and vanadium tend to stabilize the beta phase by reducing the temperature of transformation from alpha to beta phase (Schutz.R. et al. 1988). The typical microstructure is equiaxed (the same dimension in all directions), or contains elongated alpha grains in a transformed beta matrix (Rodney.B. et al. 1994). Figure 1.1 shows the alpha and the transformed beta phases. Some of its composition, physical and mechanical properties are given in Tables 1.1, 1.2 and 1.3 (Rodney.B. et al. 1994) respectively.

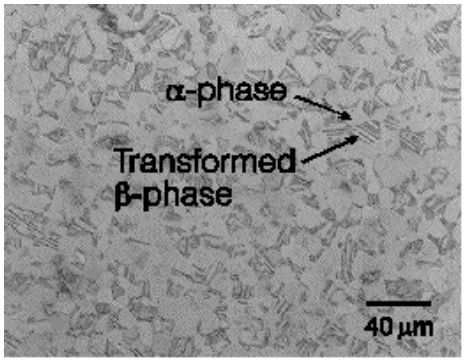

Figure 1.1 Microstructure of the primary (alpha) and transformed (beta) phases in Ti-6Al-4V (Rodney.B. et al. 1994)

There is a significant enhancement in corrosion resistivity due to the addition of 0.1% ruthenium (grade 29), 0.5% nickel (grade 25) and 0.05% palladium (grade 24), thereby reducing acid, chloride and sour environments, increasing the threshold temperature for attack to well above 200°C (Rodney.B. et al. 1994). Titanium alloy (Ti-6Al-4V) also known as aerospace Grade 5, is regarded as the workhorse alloy of the titanium industry. The most prominent, popular and extensively used titanium

alloy is Ti–6Al–4V and its share is more than 50% of the total world production of titanium alloys (Cui Chunxiang et al. 2011).

Table 1.1 Composition of Ti-6Al-4V (Rodney.B. et al. 1994)

Element	Composition
C	<0.08%
Fe	<0.25%
N_2	<0.05%
O_2	<0.2%
Al	5.5-6.76 %
V	3.5-4.5%
Ti	Balance

Table 1.2 Typical physical properties for Ti-6Al-4V (Rodney.B. et al. 1994)

Property	Typical Value
Density g/cm^3	4.42
Melting Range ^oC+/- 15 ^oC	1649
Specific Heat J/kg.°C	560
Volume Electrical Resistivity ohm.cm	170
Thermal Conductivity W/m.K	7.2

Table 1.3 Typical mechanical properties of Ti-6Al-4V (Rodney.B. et al. 1994)

Property	Typical Value
Hardness, Rockwell	36
Ultimate Tensile Strength MPa	950
Yield Tensile Strength	880
Modulus of Elasticity GPa	113.8
Poisson's ratio	0.342
Fatigue Strength MPa(at 1E+7 cycles .K_t stress concentration factor-3.3)	240

About 70% of all titanium alloys used is a sub-grade of Ti-6Al-4V. Some of its applications are in military , marine, power generation industries, chemical industries, aerospace, nuclear, spacecraft and biomedical devices. Other applications include connecting rods on expensive sports cars and some premium sports equipment and consumer electronics. Because of their durable properties in high stress engine environments, titanium alloys are used in engine components. This alloy is extensively used in the manufacture of the aerospace components because of the combination of high strength-to-weight ratio, excellent fatigue properties, fracture toughness and corrosion resistance. Compared to steel, titanium alloy has a high strength to weight ratio, only 60% of the density of steel and 55% of the modulus of stainless steel.

Titanium and its alloys are categorized as difficult-to-machine materials. High cutting temperatures and rapid tool wear are the major problems encountered during machining of titanium and its alloys (Machado et al. 1990). Inspite of having excellent biocompatibility, particularly in direct contact with bone or tissue is necessary, Ti-6Al-4V has a limitation due to reduced shear strength and poor surface wear properties during certain loading conditions (Velasco-Ortega E 2010).Because of the above stated limitation, Ti-6Al-4V alloy is not suitable for bone screws or plates. It also exhibits poor surface wear properties and also has a tendency to seize during sliding contact with itself and other metals. Thus, the challenge is to improve the wear properties of Ti-6Al-4V by surface treatment. Surface treatments such as nitriding, oxidizing carburizing and boriding are successfully employed to improve the surface wear properties. In this direction, an attempt is made in this research to modify the surface of Ti-6Al-4V alloy by ball burnishing.

1.2 POLYCRYSTALLINE DIAMOND

Polycrystalline Diamond (PCD) is a material that is almost as strong and as hard as a single crystal diamond and has two considerable advantages. Although single crystal diamonds are extremely strong, it fractures relatively easily along certain cleavage planes. In the case of PCD however, the crystals are oriented in different directions.

When a crack occurs along the cleavage plane of one of the crystals, the propagation tends to be held up when passing from one crystal to the other. PCD is therefore a much tougher material than single crystal diamonds. Due to the sintering process, the difficulties associated with the growing of large single crystals are solved. Substitutes for natural diamonds can be obtained through the sintering of fine diamond particles to form a polycrystalline mass. The sintering process for PCD relies on the same principles as other sintering processes, where intense heat and pressure are applied until particles fuse together. In the case of sintering for most of the metals, it is found that sintering proceeds quite rapidly at temperatures that are about 70% of the material's melting temperature. The melting point of diamond is about 3027 ^{o}C. This implies that the crystallites should be raised to a temperature of 2027 ^{o}C and a pressure of 70 kbar to maintain stability of the diamond (Wilks et al. 1991).When the diamond powder is compressed, the maximum pressure is experienced at the points of contact between the grains and not in the voids between the grains. The pressure in this region will be much lower. Due to high temperature, the diamond adjacent to the voids will transform to graphite. This is why the standard method of sintering with heat and pressure cannot be used successfully with diamond. To avoid the formation of graphite, the arrangement of reaction chamber prior to the sintering is used. Under these conditions, the cobalt will melt because of the high temperature and pressure. The melted cobalt will infiltrate into the voids and thus maintain the pressure on the diamond surfaces, preventing the formation of graphite. The strength of the PCD does not depend primarily on the cobalt acting as a binder, as would be the case in many other composite materials. The strength of PCD rather relies on the strength and extent to which the diamond-diamond bonds, produced by the crystallites, are grown together at their points of contact (Wilks et al. 1991).

PCD is normally used in high temperature environments. For this reason, the application fields of PCD can differ according to the thermal expansion coefficients of the binders used in the production of PCD. When ferrous metals are used as binders, it contributes to the formation of carbides and graphitization when the PCD blank is heated. This also implies that there exists a large difference in relative thermal expansion coefficients between the binder and the diamond. This will increase the risk

of blank fracture at temperatures above 727^{o}C. The thermal resistance of synthetic PCD can be improved by eliminating the cobalt binder. This can be done through chemical leaching and will cause the blank to have a porous structure (Narutaki et al. 1985). When sintering at very high pressure, diamond may react with the binder and form intermediate layers at the diamond-binder interfaces. The phase boundaries between the diamond and the binder material are made less abrupt due to the mechanical and thermal properties of these intermediate layers. The advantage of these intermediate layers is that abrupt phase boundaries normally lead to the generation of different kinds of thermo-mechanical stresses brought on by the difference in thermal expansion and mechanical properties of the different constituents in materials. These intermediate layers therefore make the material more thermo-mechanically stable (Bakon et al. 1993).

The typical uses of PCD include face milling of Al-alloys and other non-ferrous materials. Another application is for machining of medium high Si-AI alloys where the tools need to display high abrasion resistance. PCD inserts are also widely used in the automotive industry where parts like cylinder heads, transfer cases, intake manifolds and oil pump bodies are machined to specification (Webzell 2007).It is not advisable to use PCD for the machining of ferrous alloys, because these alloys chemically attack the diamond, resulting in an increased tool wear (Wilks et al. 1991).PCD is available in different grades that are differently suited for the machining of non- metals and nonferrous metals. The addition of other substances that act as a type of binder that facilitates the intergrowth of diamond crystals, will have an effect on the properties of the final product. This binder phase can be either a metal or carbide, although boride and nitride are also occasionally used. The binder can be added as a powder or as a coating on the diamonds (Webzell 2007).The goal of these elements is to support the production process or to improve certain properties. For example, the addition of boron oxide to the cutting material matrix increases the diamond grains' ability to resist oxidation. The property profile of PCD is thus determined by the cutting material components and their specific properties. These components are diamond grains of different sizes and an intermediate phase made of metal or ceramic. Other elements are also present in small amounts in the cutting

material matrix (Fowler 1988).Considering the above advantages of PCD i.e., high thermal conductivity, low wear rate and long tool life, it can be successfully used to machine titanium alloy.

1.3 MINIMUM QUANTITY LUBRICATION

In the present scenario, the use of flood cutting fluids in machining processes has been criticized largely due to the several negative effects on environment and health. Extensive attention has been given to reduce or completely omit the cutting fluids, and meet the demands for environment friendly cutting processes. One such alternative in this regards is the application of minimum quantity lubrication (MQL). In MQL, minute quantity of cutting fluid at the tool-work piece interface, usually at a flow rate of about 10 to 100 ml/hour is employed. The amount of cutting fluid in MQL is greatly reduced i.e., almost ten-thousandth of the quantity of cutting fluid utilized in flood lubrication (Autret et al. 2003). Minimum quantity lubrication (MQL) is also recognized as near dry machining. The working principle on which MQL, sometimes referred as near dry machining is based is on atomization principle i.e, a drop of liquid is split by an air flow dispersed in streaks and transported in the direction of flow of air. A large no of investigators have widely studied and successfully applied MQL in many machining processes such as turning, milling and drilling (Wakabayashi et al. 1998, Dhar et al. 2006, Davim et al. 2007, Kamata and Obikawa, 2007).

During metal cutting processes, the use of cutting fluids is inevitable because it helps to increase the tool life, prevent damage to the machined surface, enhance product surface finish and dimensional accuracy. Furthermore, the use of cutting fluid also aids in breaking of chips, chip-transport and trouble-free chip disposal. But the use of cutting fluids is associated with a large number of problems, mainly environmental pollution due to production of airborne mist, smoke and other particulates in the shop floor air quality. Thus , the health of the industrial workers is affected by exposure to cutting fluids through the inhalation of aerosols (mists) resulting in respiratory problems, for instance asthma, bronchitis, tuberculosis etc. and via skin contact with the fluid, causing allergic reactions and skin eruptions.

Because of the above mentioned setbacks, the mechanical industry is constantly exploring alternatives to eliminate or limit the amount of cutting fluid consumption. Added advantage in reducing the consumption of cutting fluids is the huge price and waste savings. From the work of Klocke et al. (1997), it is evident that in some instances the amount of investment in cutting fluids far exceeds the tool costs. The economical and environmental concerns on the usage of cutting fluids led to the development of minimum quantity lubrication (MQL) a long time ago (Heisel 1994).In modern production, importance is given to carefully selecting right cutting fluids taking into consideration health, cost and ecological issues (Sreejith and Ngoi 2000).In this direction, serious efforts have been made to reduce or even eliminate the usage of cutting fluids (Sokovic and Mijanovic 2001). The minimum quantity of lubricant (MQL) notion in machining is an attractive option in contrast to dry or flood lubricating system, for reducing the quantity of lubricant (Diniz et al. 2003).The advantages of minimum quantity lubrication (MQL) are listed below:

MQL saves time and money

- Due to increase in cutting speed, the machining time is reduced, thereby saving manufacturing cost.
- Increase in tool life due to regular cooling, devoid of sudden thermal shock .Hence, reducing the number of tool changes.
- The work pieces remain dry, thus saving on de-greasing
- Chip disposal becomes easier and more cost-efficiently due to drier chips.
- The cost involved in soluble oil maintenance is eliminated.

MQL promotes and enhances quality

- Due to the use of pure lubricants, the surface quality of workpieces is greatly improved.

MQL is environment friendly and safe

- Cleanliness is maintained due to no spreading of cutting fluids.
- Health of workers is safeguarded.
- There are few ecologically harmful residuals

While showing possible benefits for both air quality control and tool performance improvement, minimum quantity lubrication (MQL) has only restricted applications till now. This is due to very few detailed, methodical and quantitative studies on the suitable MQL parameters, such as oil properties, oil flow rate, flow direction and air pressure for different machining processes. An attempt has been made in this research to adopt MQL lubrication mode, during machining of titanium alloy.

1.4 SURFACE QUALITY ENHANCEMENT TECHNIQUES

During turning of hard materials such as refractory metals, hardened steels, nickel based or titanium based alloys, issue of tool wear is a major concern. Increase in tool wear disturbs tool edge geometries. Machining hard metals with worn tools tends to produce a poor surface finish as well as generate tensile residual stress on the surface, which potentially shortens fatigue life and lowers the performance of the functional surface. As a result, it is practical to employ a surface enhancement operation that provides necessary surface modifications (i.e. improving surface finish and converting tensile residual stress to compressive). Advanced industrial applications demand materials with unique surface properties like high corrosion resistivity and wear resistant. But procuring these alloys possessing these properties proves to be costly and eventually their usage will result in a drastic increase in the cost of components. On the other hand, failure or degradation of engineering components due to mechanical and chemical/electrochemical interaction with the surrounding environment is most likely to initiate at the surface because the intensity of external stress and environmental attack are often highest at the surface. As a result, in order to improve the biological, chemical, and mechanical properties, surface modification is the solution and has been successfully applied (Xuanyong Liu et al. 2004).

Several surface treatment techniques are employed to enhance the life of the component. The different surface enhancement techniques are presented in Figure 1.2.The surface enhancement techniques are divided into two types, namely thermal and mechanical surface treatment methods. Thermal techniques involve heating of the material to achieve a microstructure, beneficial towards improving hardness and fatigue life. Few of the widely used thermal surface treatments are nitriding, case

hardening and induction hardening. Nitriding is a metallurgical process which introduces nitrogen in the surface of a material example, for surface-hardening treatment of the steel surface. Case or surface hardening is the practice of hardening the metal surface, usually low carbon steel, by infusing elements into the material's surface and forming a thin layer of a harder alloy. Whereas, induction hardening is a type of heat treatment where a metal component is subjected to induction heating, followed by quenching due to which martensitic transformation takes place resulting in improved hardness and brittleness.

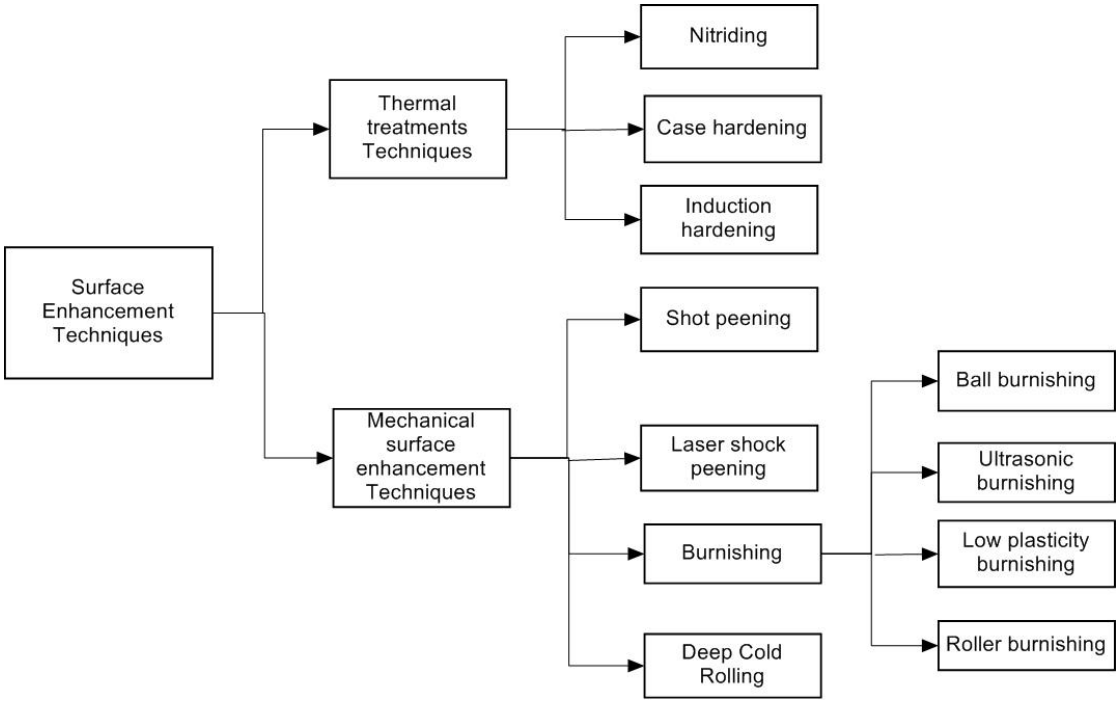

Figure 1.2 Different surface enhancement techniques

Inspite of the advantages of thermal surface treatment techniques such as improvement in the fatigue life of component, hardening, plating etc., they result in a brittle surface after processing. This can lead to damaged or weakened surface grain boundaries resulting in fatigue. As a result, mechanical surface treatment methods are employed to overcome the limitations of thermal treatments. Mechanical surface enhancement techniques such as shot peening, laser shock peening, burnishing and deep cold rolling are used for improving the resistance to wear and stress corrosion, which also enhance the fatigue life of highly stressed components used in variety of

engineering applications (Tolga Bozdana 2005, Tolga Bozdana and Nalla 2003). Shot peening is a cold working process in which a stream of metal, glass or silica particles at high velocity is imparted against the surface of the metallic components in a defined and controlled manner. Shot peening is most commonly used due to its low cost and can be used on small or large areas depending on requirements. However, some of the limitations of shot peening are less coverage, poor surface finish, excessive surface damage. Laser shock peening and ultrasonic peeing are alternative techniques giving better results but their major drawbacks are expensive setup, skilled labor and specially protected environment for treatment. Another popular method is burnishing. Burnishing can be classified as superficial plastic deformation process basically used as surface smoothing and surface enhancements treatment following some machining processes. The result of burnishing is generation of wear resistance and compact surface thereby increasing the life of the component. Burnishing is a cold- working finishing process and the distinct feature that separates it from other cold- working, surface treatment processes such as shot peening, sand blasting etc is the formation of excellent surface finish and generation of residual compressive stresses at the surface layers of the metallic components (Wang 1999).From the investigations carried out by Maawad E et.al (2011), it was proved that ball burnishing produced a deep layer of high compression stresses, compared to shot peening, ultrasonic shot peening and laser shock peening.

1.5 BURNISHING

One of the most well-known mechanical surface treatments is burnishing, which induces a large depth of near surface macroscopic compressive residual stresses as well as work hardening states. Moreover, surface smoothening is also typical in burnishing treatment (Sayahi, M et al. 2013).The demand for superior finish quality is ever increasing. Surface finish quality and hardness of the machined components are the essential requirement owing to their direct effects on the function of the components. Fatigue is one of the major reasons for failure of the engineering components. There are many factors affecting fatigue life, like shape, size, and surface finish of component. The surface quality plays an important role; i.e surface

roughness causes microscopic stress concentrations that lower the fatigue strength. It has been recognized and proven that fatigue occurs due to cracks generally initiated on free surfaces and therefore fatigue life is reliant on the surface finish (Herbert 1927). Tolga Bozdana and Nalla R K (2003) investigated the influence of deep rolling and laser shock peening process on the fatigue behaviour at ambient and elevated temperatures of Ti-6Al-4V work material. They found that deep rolling could be quite effective in retarding the initiation and initial propagation of fatigue cracks at higher temperatures. They also observed that the near surface microstructures consist of a layer of work hardened nanoscale grains which play a critical role in the enhancement of fatigue life by mechanical surface treatment. Altenberger et al. (2012) investigated the thermal stability of near-surface microstructures induced by deep rolling and laser-shock peening in AISI 304 stainless steel (AISI 304) and Ti-6Al-4V using in situ transmission electron microscopy. It is found that, the beneficial effect of deep rolling and laser shock peening on the fatigue life at temperatures as high as 550-600 °C, where almost complete relaxation of residual stresses has occurred, appears to be related to the thermal stability of the work-hardened surface microstructures. In the case of, mechanically surface treated titanium alloys for fatigue failure, within the low stress the high cycle regime is often associated with subsurface (quasi-vacuum) fatigue crack nucleation. This phenomenon may be related to the presence of process-induced tensile residual stresses necessarily present below the mechanically treated surface and required to balance the outer process-induced residual compressive stresses. Since high cycle fatigue (HCF) performance is one of the most important requirements for these applications, it is essential to improve this property by microstructural optimization and by mechanical surface treatments such as shot peening or ball burnishing. The latter improvement is mainly the result of induced near-surface severe plastic deformation which results in work-hardening and the generation of compressive residual stresses that retard fatigue crack propagation (Zay, K et al. 2011). To overcome the surface with inherent irregularities and improve the surface finish, formed during machining processes namely turning and milling, traditional surface finishing methods like lapping, grinding, polishing and honing are generally used. To successfully carry out the burnishing process, the material must be ductile or malleable like steel, stainless, alloys, cast iron, aluminum, titanium alloy,

copper, brass, bronze etc. Another requirement for burnishing is the material should be capable of cold flowing under ball pressure, hardness normally should not be more than 40HRC. Most of the above named traditional finishing processes involve chip removal whereas burnishing is chipless and results in a smooth and work-hardened surface by plastic deformation of surface irregularities. Moreover, the conventional methods induce tensile residual stresses at the surface, whereas the burnishing process induces residual compressive stresses. The burnishing process is characterized by a distinctive combination of elements, namely induction of profound and balanced compressive residual stress, work hardening, decreasing surface roughness as well as micronotches.

To understand the burnishing mechanisms , it can be divided into three major categories, firstly the surface smoothing (geometrical) mechanism, the feature which results in the reduction of surface roughness, secondly surface enhancement (mechanical) mechanism, the characteristics due to which compressive residual stress and cold-work hardening are induced and finally, the microstructural (metallurgical) mechanism, the characteristics resulting in the closure of crack, the change of texture orientation (Zaborski et al. 2000), the elongation and refinement of crystalline grain even to nanocrystallization by severe plastic deformation (Wang et al. 2009). Further, burnishing process is also cost-effective, requires less skill and can be carried out in conventional machine shop environments. Loh and Tam (1988) revealed the fact that plastic deformation process, ball burnishing, is widely accepted as a finishing operation. Hassan and Bsharat (1997) in their experimental work reported that, because of burnishing a large number of variations in the surface features, in the form of enhancement surface hardness, surface roughness, wear resistance, fatigue and corrosion resistance is observed. Grain structure is condensed and refined, resulting in a compacted surface that becomes smooth and hardened than ground or honed surfaces.

Burnishing can be classified as a post-machining forming process where the machined surface is presses against a hard tool usually a multi hardened ball or a roller that is highly polished leading to plastic deformations in cold working environment. The

machined surface consists of a series of peaks and valleys of irregular heights and spacing. The burnishing process is illustrated in Figure 1.3. The work piece is usually driven positively while the burnishing tool rotates as a result of friction. The pressure generated by the ball exceeds the plastic deformation stage and creates a new surface. Plastic flow of the original asperities occurs when the yield point of the work piece material is exceeded and consequently the asperities will also be flattened. The economical benefits of ball burnishing in comparison with the above traditional methods of finishing like grinding, polishing, honing and lapping are illustrated in Figure 1.4.

Optimized process design in burnishing plays an important role in predicting the boundary layer condition. During ball burnishing, when a ball is pressed against the surface of the workpiece to increase the strength of the material, it results in elastic-plastic deformation leading to three physical effects:

- Work hardening
- Surface smoothing
- Induction of residual stresses

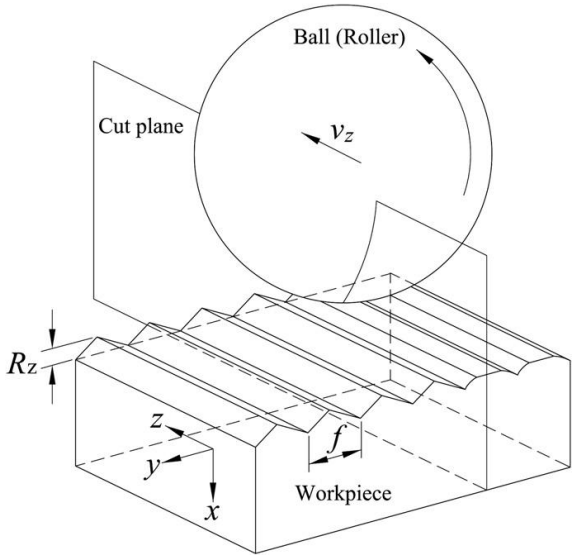

Figure 1.3 Smoothing process during burnishing (Feng, L.L.et al. 2012)

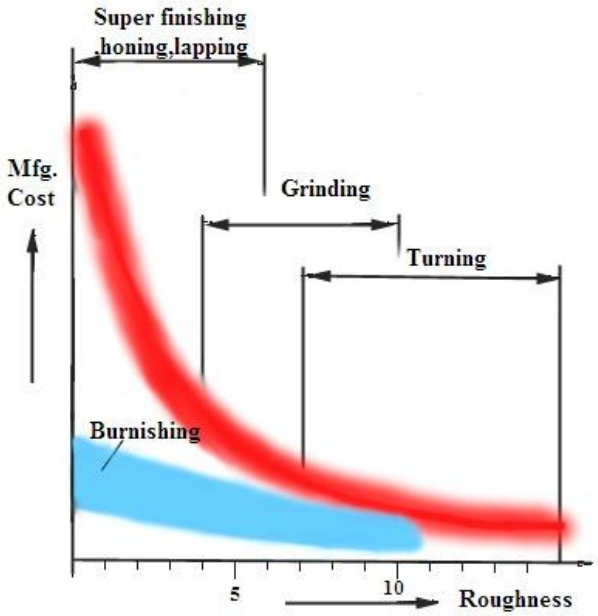

Figure 1.4 Production costs versus surface roughness (ECOROLL AG Germany)

A schematic diagram of the burning process indicating the parameters is shown in Figure 1.5 that summarizes the various factors governing ball burnishing process

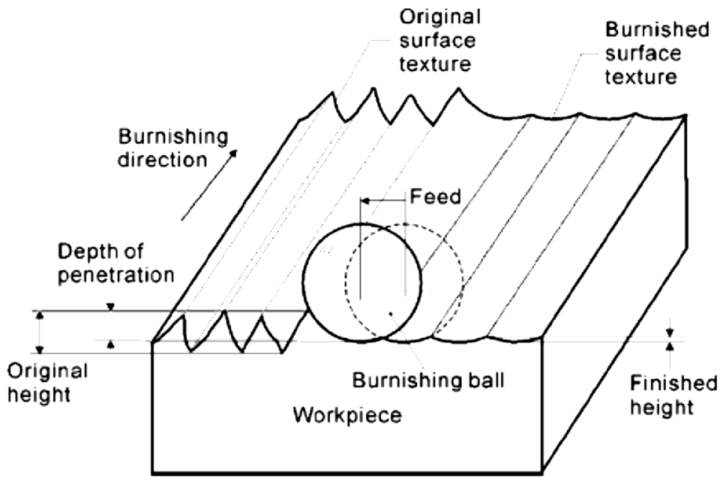

Figure 1.5 Schematic diagram of ball burnishing process (Fang-J and Chuing-H 2010)

Parameters affecting burnishing

Figure 1.6 summarizes the essential variables governing burnishing process which may be classified according to the workpiece, tool, process and device used.

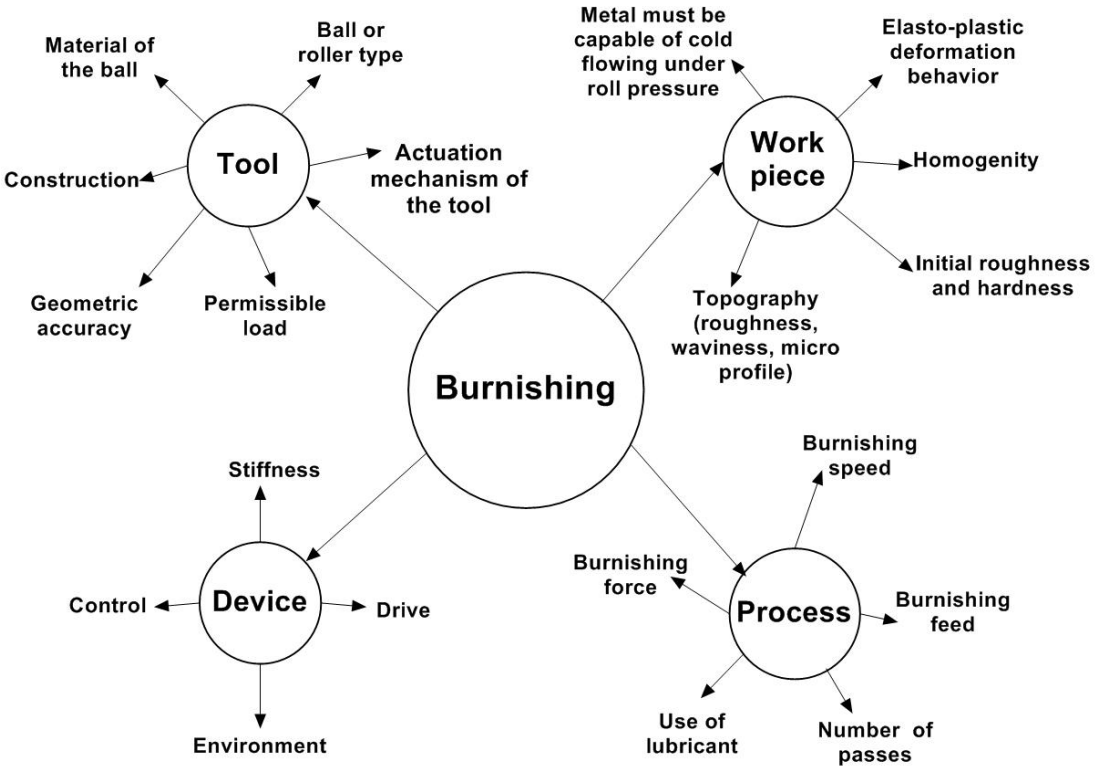

Figure 1.6 Parameters influencing the results of burnishing process

Application of Burnishing

Burnishing helps users to avoid secondary processes resulting in considerable savings of time and being cost effective, apart from enhancing the quality of their product. Burnishing processes are being used in automobile sectors, aircraft, defense, spacecraft, railways, textile, machine tool, motors and pump Industry, hydraulic and pneumatic farm equipment, home appliances etc., and areas where close tolerance and superior surface finish are required. Burnishing is also employed in automotive and heavy equipment components namely construction, agricultural, mining , piston and connecting rod bores, brake system components, transmission parts and torque converter hubs (Boyer 1996,Cui 2011). Burnishing process is also being extensively used in non-automotive applications for a variety of benefits: to produce better and longer-lasting seal surfaces; to improve wear life; to reduce friction and noise levels in running parts; and to enhance cosmetic appearance namely valves, pistons for

hydraulic or pneumatic cylinders, lawn and garden equipment components, shafts for pumps, shafts running in bushings, bearing bores, and plumbing fixtures.

Application of Burnishing in aerospace industries and current trends

A rapid improvement has taken place in burnishing procedure in aero industries. A large number of experimental studies have been conducted. In a recent study Caudill.J et al. (2014), the application of cryogenics during the burnishing process which acts to rapidly cool the burnished work material was conducted. In this research work cryogenic burnishing was performed to produce the severe plastic deformation layer to obtain improved properties in aero space material Ti-6Al-4V alloy. In the severe plastic deformation layer produced by cryogenic burnishing, increased hardness, refined grain structure, and a drastically improved surface finish, along with compressive residual stresses are achieved. The cryogenic burnishing of Ti-6Al-4V alloy was shown to be superior to flood-cooled and dry burnishing in terms of surface integrity and the likely functional performance of components during the service life of such components. Tao Zhang (2015) conducted burnishing on aerospace blade material 17-4 PH stainless steel using hydrostatic ball burnishing tool developed by ECOROLL Ltd. Smoother surfaces of aerospace material modified by ball burnishing have been achieved and significant influences of process parameters on both surface roughness and maximum residual stresses were established. Burnishing also transformed tensile residual stresses into compressive residual stresses during which burnishing pressure played an important factor. An investigation by Zhuang.W et al. (2014) to determine the enhancement of fatigue life of laser clad aircraft aluminium alloy during deep surface rolling was carried out. In this study, aluminium alloy 7075-T651 specimens with a blend-out region were first repaired using laser cladding technology. The surface of the laser cladding region was then treated by deep surface rolling. Fatigue testing was subsequently conducted for the laser clad, deep surface rolled and post-heat treated laser clad specimens. It was found those deep surfaces rolling can significantly improve the fatigue life in comparison with the laser clad baseline repair. The results also demonstrated that beneficial compressive residual stresses induced by deep surface rolling can reach considerable depths (more than1.0

mm) below the laser clad surface. Wong C C, et al (2014) conducted experimental trials on aero space material Titanium (Ti- 6Al-4V).Although deep cold rolling is able to generate a deeper layer of compressive residual stress and good surface finish, one of the challenges in adopting this process for wider application in the aerospace industry is the limitation in applying it to different geometrical profiles. In this study, three cold rolling tool designs were selected to study its feasibility on processing Titanium (Ti-6Al-4V) test coupons of different features. The effect of process variables (pressure, feed rate and overlap) on residual stress profiles were also investigated for one selected tool. Results showed that deep cold rolling is able to generate deep layer of compressive residual stress (up to 1mm depth) and process variables such as rolling pressure played a significant role in affecting the residual stress profiles. Aerospace compressor blade materials used in modern jet aircrafts are fast and relatively quiet based on high reliability of aero engine in service, in which the aerospace compressor blades work in critical conditions and the materials have good ductility, high strength at high temperature, and good corrosion resistance. The failure of compressor blades is one of the common situations for compromising the safety. The first stage compressor blades are so important that many serious accidents involving aero engine indicated that the failure of the first stage compressor blades was the main reason for foreign object damage (FOD), such as impacts of sands and birds. The root causes of the failure of high compressor blades were focused on FOD with a significant effect on fatigue life even though no sudden fracture happened (Silveira,E et al. 2008). Studies have been conducted to show that that ball burnishing applied to compressor blades highly improved fatigue life, especially the first stage blades. Experimental work by Prevey et al. (2004a) on 17-4 PH stainless steel compressor blades proved the benefits of low plasticity burnishing (LPB) to improve fatigue life. LPB imparted highly beneficial compressive residual stresses on the surface, sufficient to withstand pitting and/or surface damage up to a depth of nominally 0.020 in. (0.5 mm) from the surface. LPB provided a 50% increase in corrosion fatigue strength in the absence of surface damage, and a 12x increase in strength for 0.010 in. deep damage. The fatigue strength improvement is attributed to the depth and magnitude of surface compression due to burnishing. The effect of low plasticity burnishing (LPB) on the HCF performance and FOD tolerance of a first

stage Ti-6Al-4V turbine engine vane have been investigated by Prevey et al.(2004b).The fatigue strength for LPB processed blades increased over 4-fold for both vanes and vane-edge feature specimens with foreign object damage 0.020 in. deep. The fatigue and foreign object damage tolerance improvement are shown by linear elastic fracture mechanics modeling to be due to the deep stable compressive layer produced by low plasticity burnishing. The study by Tao Zhang 2013, investigates the effects of ball burnishing on surface integrity of aerospace material 17-4 PH steel. In this research, he demonstrated that improvement in material property 17-4 PH steel can be achieved by hydrostatic ball burnishing applied to 17-4 PH steel, such as smoother surfaces, enhanced surface hardness and impact strength, and high magnitude of compressive residual stresses with a greater depth of layer. The results indicated the potential benefits of the ball burnishing application for the aerospace blade material.

The study of burnishing could be undertaken either analytically or experimentally to assess the effects of these variables and optimize them for better responses. With modern analytical and computational techniques, it is often possible to estimate the effects of various process parameters of burnishing. However, there are numerous parameters to be considered. Importantly, following the above discussion, the effects of each of these parameters are dependent on other variables. This interaction between variables would make the normal approach of a parametric study followed by simple inspection of the results prohibitively more complex for more than two or possibly three variables. Therefore, the methodology of statistical experimental design has been developed to address such problems where multiple, interacting variables with significant experimental variation make interpretation of the data complex and difficult. Design of experiments can be used for planning the experiments so that the data obtained can be analyzed to yield valid and objective conclusions (Ross 1996).The process of burnishing has many varied forms such as low plasticity burnishing (LPB), deep rolling, deep cold rolling and ultrasonic burnishing aimed at diverse purposes and objectives.

1.6 DESIGN OF EXPERIMENTS

Design of experiments (DOE) is a very effective, analytical and economical technique that can be used in an organized way to conduct industrial trials. Multiple product design and/or process variables can be studied at the same time with these efficient designs, instead of trial and error method, providing very satisfactory results (Montgomery 2005). Because of the statistical balance of the designs, large number of potential combinations of numerous factors (at varying levels) can be evaluated for the optimum overall combination, by conducting a small number of trials. Design of experiments (DOE) is an efficient method for planning experiments so that the data obtained can be analyzed to yield valid and objective conclusions. In a trial, purposeful changes to one or more process factors are made in order to examine the interactive effect that those changes have on one or more response factors. The analysis is made using the popular software specifically used for design of experiment applications known as MINITAB 15. The possible interactions between the control factors must be considered before using the application software. To understand a detailed visualization of influence of various factors and their interactions, it is important to develop analysis of variance (ANOVA) table to find out the contribution of each factor on the response as well as their interactions.

After determining which process variables contribute and affect the response, next step is to optimize, that is to find the level of factors that results in the best possible response. Usually, the characteristics of a product quality are related to various process parameters and noise factors through a complicated, nonlinear function. One can determine the various combinations of process parameter values which can give the desired target value of the product's quality characteristic subjected to nominal noise conditions. But because of nonlinearity, these combinations of process parameters result in quite different variations in the quality characteristic, inspite of the noise factor variations being identical. The central objective of the robust design is to study this non linearity to determine a combination of process parameter values that would result smallest variation in the value of the quality characteristics around the

desired target value (Phadke M S 1989).The block diagram representation of a process is shown in Figure 1.7.

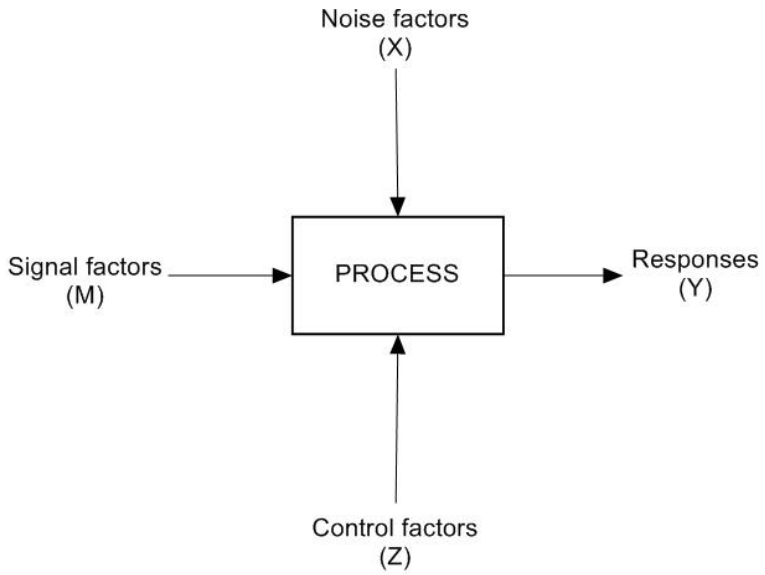

Figure 1.7 Block diagram of a process: P Diagram (Montgomery 2005)

P- Diagram is basically a schematic diagram that includes signal factor, control factor, noise factor and response variable. The response or output of the process is denoted by 'Y' which represents the quality characteristic considered for the purpose of optimization. A number of parameters can influence the quality characteristic or response of a process. These parameters or factors can be classified into the following three classes:

Signal factors (M): These are the parameters which are to be decided by the operator to get the desired value for the response of the process. The signal factors are chosen by the design engineer, considering the knowledge of the process being studied. Sometimes, two or more signal factors are used in combinations to express the desired response.

Noise factors (X): These are the factors which have a significant effect on the design but beyond the control of the engineer. They include environmental factors, customer usage, interfaces with other systems, degradation over time, piece-to-piece variation, among others. If these noise factors are not considered, their design is of no use and it cannot be termed as robust against the expected noise factors. Hence, noise factors cause the response to move away from the target due to change of process parameters from unit to unit and product deterioration.

Control factors (Z): Control Factors are the elements such as design, materials and processes that are controlled and specified freely by the design engineer. In fact, it is the designer's responsibility to determine the best values of these parameters. Each control factor can take multiple values called levels. When the levels of certain control factors are changed, the manufacturing cost does not change; however, when the levels of others are changed, the manufacturing cost also changes.

1.6.1 Taguchi's Method

This method was developed by a Japanese statistician Dr. Genichi.Taguchi. He won the highest award for quality, Deming prize. He developed the techniques to enhance quality using robust design of products and production processes. He pioneered the fractional factorial experimental designs using which the results and the optimization of a process can be determined by conducting minimum number of trials. Taguchi method has been used extensively in engineering design successfully (Ross 1996 and Phadke 1989). Conventional designs of experiments process are tedious and difficult to use. Moreover, to get the results a large number of trials have to be conducted and it becomes complicated when a large number of process parameters are involved. To solve this problem, Taguchi technique uses a unique design of orthogonal arrays to study the effects of process parameters by carrying out minimum number of trials (Taguchi G 1986). Taguchi techniques use parametric design, that is an engineering technique for product or process design that focuses on determining the control factor settings producing the best levels of a quality performance measure with a least noise variation. Taguchi method offers a powerful and efficient technique for designing processes that operates consistently and optimally under a wide variety of conditions.

The central concept of Taguchi's method for quality enhancement is Taguchi's loss function. The loss function specifies that society's loss because of badly performing products is proportional to the square of the deviation of the performance characteristic from its target value. The orthogonal array is finalized by the design engineer taking into consideration the number of control factors, interactions among them and the range of factors. Taguchi has utilized Signal–Noise [S/N] ratio as the quality characteristic of choice. S/N ratio is used as measurable value instead of

standard deviation because as the mean decreases, the standard deviation also decreases and vice versa. That is, the standard deviation cannot be minimized first and the mean brought to the target. Practically, the target mean value may vary during the process development. The S/N ratio characteristics can be divided into three categories given by Equations (1.1) – (1.3), when the characteristic is continuous (Taguchi 1986).

Nominal is the best characteristic $$\frac{S}{N} = 10\log\frac{\bar{y}}{s_y^2} \quad (1.1)$$

Smaller is the best characteristic $$\frac{S}{N} = -10\log\frac{1}{n}\left(\sum y^2\right) \quad (1.2)$$

Larger the better characteristic $$\frac{S}{N} = -\log\frac{1}{n}\left(\sum\frac{1}{y^2}\right) \quad (1.3)$$

where $\bar{y}$ the average of observed data, s_y^2 is the variation of y, n is the number of observations, and y is the observed data.

The earlier developed experimental design methods were not practical and mostly widely used by statisticians rather than practitioners (Phadke 1989). Taguchi's approach to design of experiments is practical and easy to use and execute even with minimum knowledge of statistics. Because of these features, it is accepted and acknowledged method used successfully in the field of engineering and by the scientific community. It is most suitable for optimizing and analyzing metal cutting problems. (Ghani et al 2004). A large number of investigators have successfully applied Taguchi techniques to materials processing for process optimization (Rastee et al. 2014, Khaider et al.2014, Navneet et al. 2015, Venkatesh et al. 2015).

1.6.2 Response Surface methodology

The surface finish of machined materials is significant in manufacturing engineering applications which have substantial effect on some properties such as wear resistance, light reflection, heat transmission, coating and fatigue resistance. During machining,

quality of the parts can be achieved only with the knowledge of proper cutting conditions. To predict the surface quality and dimensional properties, it is essential to employ theoretical models making it realistic to predict in terms of the function of operating conditions (Sahin and Motorcu 2004). Response surface methodology (RSM) is a collection of mathematical and statistical techniques that are helpful for the modeling and analysis of problems in which a response of interest is influenced by several variables and the objective is to optimize this response. The methodology not only reduces the cost and time but also gives the required information about the main and interaction effects (Montgomery 2005).Process modeling by response surface methodology (RSM) using statistical design of experiments is acknowledged to be an efficient modeling tool (Ozel, T and Karpat 2005).

In many engineering fields, there is a relationship between an output variable of interest 'y' and a set of controllable variables $\{x_1, x_2 \ldots .x_n\}$. In some systems, the nature of the relationship between y and x values might be known. Then, a model can be written in the form

$$y = f(x_1, x_2, ..., x_n) + \varepsilon \tag{1.4}$$

Where ε represents noise or error observed in the response *y*. If we denote the expected response be

$$E(y) = f(x_1, x_2, ..., x_n) = \hat{y} \tag{1.5}$$

Then the surface represented by

$$\hat{y} = f(x_1, x_2, ..., x_n) \tag{1.6}$$

is called response surface. The correlation between response and the independent variable is unknown in many of the RSM problems. Therefore, the first procedure in RSM is to determine an appropriate approximation for the exact functional relationship between y and set of independent variables employed. Generally a second order model is used in RSM (Kwak 2005, Montgomery 2005).

$$\hat{y} = \beta_o + \sum_{i=1}^{k} \beta_i x_i + \sum_{i=1}^{k} \beta_{ii} x_i^2 + \sum_i \sum_j \beta_{ij} x_i x_j + \varepsilon \quad (1.7)$$

The β coefficients, utilized in the above model can be determined by using least square method. The second-order model is generally used when the response function is not known or nonlinear. Face-centered central composite design is a useful variation of the central composite design, in which α=1. The choice of α in the central composite design (CCD) is dictated primarily by the region of interest. The experiment includes three controllable process factors (p = 3). The region of interest, coded (−1, 1), is a region determined by lower and upper limits on factor level setting combinations that are of key interest.

1.7 FINITE ELEMENT MODELING

The finite element method (FEM) based simulation techniques assist in predicting results eliminating the need to conduct experimental trials. In addition to experimental studies, predictive models are greatly needed to further understand the mechanisms that drive the surface integrity changes and to find the optimum machining conditions that would lead to desirable surface integrity. The major capability of FEM method is to accurately predict residual stress and white layer formations. Additionally these methods have the ability to vary process parameters and repeat the analysis so as to measure the sensitivity of processes to certain parameters. Residual stress is one of the most commonly studied surface integrity factors in predictive models. The analysis and predictions are in close agreement with the experimentally values, particularly in the measurement of residual stresses, once an accurate material constitutive model is developed. FEM-based simulation models constantly focus on calibrating material constitutive model (often the Johnson–Cook material model) parameters or flow stress data using experimental results and simulation outputs. Due to the improved performance and power of computers, finite element modeling is becoming one of the widely used approaches to predict residual stresses induced by machining. Major advantages of FEM include the application of complex material behavior models which allow flow stress to change with strain, strain-rate and temperature. Also, user subroutines can be easily implemented to capture complex material changes during

the machining process, such as phase transformations, etc., that influence the surface integrity. Obtaining appropriate experimental data as input to calibrate the model is still an essential part of this implementation. FEM-based simulation techniques present a thorough analysis of the physical process variables based on continuum mechanics principles on computational ground; consequently they are reasonably accurate in representing the physical phenomenon that take place during machining processes (Durul and Ozel 2011).The numerical simulation and resulting computations can be performed using a finite element analysis. A typical finite element analysis has three distinct steps building the finite element model, applying loading and obtaining solution and reviewing the results. A large number of authors developed finite element models to study the burnishing process and accordingly analyzed the effect of process parameters on the work piece surface properties. To simulate the multipass LPB process, Zhuang et al. (2004) proposed a three dimensional non-linear moving contact FE model. Beres et al. (2004) used two- and three-dimensional finite element method to model the LPB process numerically. A dependable FE model of burnishing process was also developed by Sartkulvanich et al. (2007). In comparison with experimental data, the outcome obtained by these authors demonstrates that these finite element models were capable of successfully predicting the effect of processing parameters on the residual stress distributions. During the present research, a finite element model of ball-burnishing was used to understand and predict residual stress values and their variation with the burnishing parameters.

1.8 OVERVIEW OF THE DISSERTATION

The organization of the thesis is as follows:

Chapter 1 deals with the introduction to titanium alloy, polycrystalline diamond inserts and the importance of minimum quantity lubrication. The different mechanical surface enhancement techniques highlighting the importance of ball burnishing, design of experiments and finite element modeling are also presented in this chapter.

Chapter 2 deals with the detailed literature review of machining of titanium alloys and associated problems. A detailed survey of the burnishing process, the parameters affecting it and its effect on different materials is studied. The major experimental and numerical studies on surface integrity mainly surface roughness and hardness in burnishing are reviewed. The various numerical, analytical and finite element models for burnishing are studied. Finally, various surface modification techniques to improve the wear resistance of titanium alloy namely physical, mechanical, chemical and electrochemical treatment are studied. Objectives and scope of the present study are presented at the end of this chapter.

Chapter 3 deals with the research methodology and experimentation, employed during machining, burnishing of titanium alloy and development of FEM model. The experimental procedure adopted to find the improvement in wear resistance of ball burnished titanium alloy is also presented. A detailed explanation of the methods used to measure the various response namely surface roughness, hardness and residual stress is provided.

Chapter 4 presents the analysis of surface roughness and hardness in titanium alloy during turning with polycrystalline diamond tool under different lubricating modes namely flood, dry and minimum quantity lubrication (MQL). The optimum conditions for machining were established using Taguchi method. A response surface model (RSM) for surface roughness during finish turning of titanium alloy under minimum quantity lubrication (MQL) was developed. The results from this study provided valuable information about the surface roughness and hardness of titanium alloys during machining, so as to conduct further studies on burnishing.

Chapter 5 deals with the experimental results on the surface integrity resulting from burnishing experiments using titanium alloy and the effect of burnishing parameters like burnishing force, feed, speed and number of tool passes. The surface integrity factors investigated were surface roughness, hardness, residual stresses and microstructure. The optimum conditions of burnishing were established and validated. A FEM model was developed to determine the residual stresses due to burnishing using the software LS-Pre Post. A comparison of residual stresses determined by

FEM model and experimental observations was made. A novel and improved burnishing tool was proposed and burnishing trials were conducted with this tool and the improvement was measured. A comparison of performance of the improved ball and roller burnishing tool was conducted.

Chapter 6 presents an attempt made to determine the improvement in wear resistance of ball burnished titanium alloy. The wear performance of burnished titanium alloy was investigated using pin-on-disk wear testing equipment. The wear volume, wear rate, coefficient of friction, wear appearance and wear debris, before and after burnishing were studied. The effect of burnishing parameters on the specific wear rate and coefficient of friction is also discussed. The results from this study provide valuable information for establishing the relationships among burnishing conditions, surface integrity properties and the wear performance of titanium alloy.

Chapter 7 contains the findings and results of the current work i.e, turning and burnishing are summarized with final remarks and conclusions. The directions and recommendations of the future work are discussed briefly based on the results and observations presented in this dissertation. References and the journal papers published based on the present research work have been listed at the end.

The following chapter focuses on the available literature in the field of machinability of titanium alloys, burnishing process, its modeling, surface treatment and wear resistance of titanium alloy.

Chapter 2

LITERATURE REVIEW

This chapter presents a review of literature on titanium alloy, its machinability, burnishing process and its modeling. Furthermore, a brief introduction to surface treatment and wear resistance of titanium alloy is also provided.

2.1 TITANIUM ALLOY (TI-6AL-4V) AND ITS MACHINABILITY

Titanium alloy with low density, high specific strength, corrosion resistance and good process performance is the ideal structural material, especially for aerospace engineering (Ezugwu and Wang 1997, Arrazola et al. 2009,Cui et al. 2011). However, titanium alloys have often been classified into difficult-to-machine materials because of low thermal conductivity. The lower modulus of elasticity of titanium leads to considerable spring back after deformation under cutting load; causing titanium parts to move away from cutting tool during machining, which leads to high dimensional inaccuracies. The lower hardness of titanium and higher chemical reactivity lead to a tendency for galling of titanium with cutting tool and thus changing the tool geometry.

Properties which have made titanium alloys hard to machine could be summarized as follows(,Komanduri, et al.1981,Hartung et al.1982, Donachie,et al. 1982, Machado 1990, Ezugwu et al. 2003, Ezugwu 2005, Jaffery et al.2008).

- Titanium and its alloys are poor thermal conductors. As a result, the heat generated when machining titanium cannot dissipate quickly; rather, most of the heat is concentrated on the cutting edge and tool face.
- Titanium has a strong alloying tendency or chemical reactivity with the cutting tool material at operating temperatures. This causes galling, welding, and smearing, along with rapid wear or cutting tool failure.

- During machining, titanium alloys exhibit thermal plastic instability which leads to unique characteristics of chip formation. The shear strains in the chip are not uniform; rather, they are localized in a narrow band that forms serrated chips.
- The contact length between the chip and the tool is extremely short (less than one-third the contact length of steel with the same feed rate and depth of cut). This implies that the high cutting temperature and the high stress are simultaneously concentrated near the cutting edge (within 0.5 mm).
- Serrated chips create fluctuations in the cutting force; this situation is further promoted when alpha–beta alloys are machined. The vibrational force, together with the high temperature, exerts a micro-fatigue loading on the cutting tool, which is believed to be partially responsible for severe flank wear.
- High dynamic shear strength and low elastic modulus
- High strain hardening due to their austenitic matrix
- Tendency to adhesion and forming built up edge (BUE)

Xiaoping Yang and C. Richard Liu (1999), in their review paper highlighted three ways to improve the machinability of titanium alloys, namely use of CBN and Diamond tools, designing better cooling systems so that high temperature in machining titanium alloys can be relieved, which could lead to longer tool life, higher cutting speed , better surface integrity and developing a model to optimize the cooling system. They also stressed the need to establish process models and performance models that have predictive power for optimization of machining parameters. Durul and Ozel (2011) in their studies on machining induced surface integrity in titanium alloys revealed that during machining these alloys, the microstructure of the sub-surface of the bulk material is altered due to plastic deformations and white layer formation. The reason for the high surface roughness is due to high temperature, built-up layer created at the cutting location and tool wear. Also during machining, the surface and immediate sub-surface of the material becomes harder due to work hardening occurring because of high mechanical and thermal loads on the workpiece. Zoya and Krishnamurthy (2000) investigated the machining of titanium alloy using CBN tools, and the machining performance was evaluated in terms of cutting force, specific cutting pressure, cutting temperature, chip strain and surface finish. They

concluded that the machining of titanium alloy is a thermally dominant process where a critical temperature of 700^{o}C can be a criterion for better tool life and cutting speed range of 185-220 m/min can be recommended for good surface finish of titanium alloy. Ribeiro et al. (2003) performed turning tests on titanium alloy (Ti–6Al–4V) with conventional uncoated carbides. They observed certain coherence in the behavior of the titanium alloy in relation to variations in cutting parameters on tool wear and roughness produced in the work pieces.

The main problems associated with the machining of titanium , tool wear and the mechanisms responsible for tool failure were studied by Ezugwu and Wang (1997), Xiaoping and Richard (1999) , Ribeiro et al.(2003), Rahman et al.(2006) and Ezugwu (2004). The conventional tools used for machining of titanium alloys include high speed steels and carbide tools. Due to low thermal conductivity of titanium alloys, these tools can only be used at relatively low cutting speeds. When machining at higher cutting speeds, these tools have a relatively short lifetime and hence frequent cutter regrinding is necessary. Oosthuizena et al. (2010) found that the performance of conventional tool materials is poor during machining of titanium alloy (Ti-6Al-4V) at elevated speeds when compared to poly crystalline diamond (PCD) tools. Nabhani (2001) reported that the PCD tools have lowest wear rate and produced better surface quality during titanium alloy machining when compared to the traditionally used tungsten carbide tools. Hence, PCD tool is an alternative to the traditional tungsten carbide grades for Ti-alloy machining. In order to attain higher cutting speeds for titanium alloys during machining, the cutting tool should be able to suppress the heat generated in the cutting process as much as possible, while dissipating it quickly. The higher thermal conductivity of PCD could therefore perhaps allow for higher cutting speeds to be achieved (Narutaki et al. 1985). Brinksmeir et al. (1998) reported that the PCD tools exhibit better tool life than the CBN and tungsten carbide during machining of Ti alloys. Cherukuri et al. (2003) and Ezugwu et al. (2005) found a substantial improvement in tool life during machining of titanium alloy (Ti-6Al-4V) with PCD tools. Mori et al. (1999) also found that the PCD tools have a longer tool life, especially at higher cutting speeds when compared to cemented carbide tools. Michiko et al.2009 explored the possibility of improvement in cutting efficiency using

PCD tool having high thermal conductivity during titanium alloy machining. Emmanuel et al. (2007) reported that surface finish generated during machining titanium alloy(Ti–6Al–4V) with PCD tools is generally acceptable and free of physical damages such as tears, laps or cracks for all cutting conditions investigated. PCD would be the most functionally satisfactory commercial available cutting tool material for machining titanium alloys in comparison to carbide and PCBN tools (Nabhani 2001). Some of the more important features and advantages of polycrystalline diamond are the higher cutting removal rates (self sharpening abrasive), uniform surface finish, more uniform particle size distribution, harder/ tougher particles, hexagonal microcrystallites (equally hard in all directions) and surface area 300% greater than monocrystalline diamond. In view of the above discussion, PCD tool is preferred in our investigations on Titanium alloy machining.

The surface roughness of the workpiece is an important parameter, which influences the quality of components. The surface roughness is an estimate of technological quality of component and also indicator for evaluating the productivity of machine tools and machined parts. Desired value of surface roughness of a product is generally defined to achieve the required fatigue strength, corrosion resistance, precision fits, tribological and aesthetic requirements. Thus, measuring and characterizing the surface finish has been considered as the interpreter of machining performance. Surface roughness prediction model in terms of cutting speed, feed rate and depth of cut using response surface methodology has been widely reported in literature (Dabnun et al.2005,Sahin and Motorcu 2005 , Chauhan SR and Kali Dass 2012). It was found that cutting speed and feed rate are the significant machining parameters affecting surface roughness, while the effect of depth of cut is found to be negligible. The use of higher cutting speed with lower feed rate produces a better surface finish, mainly due to high temperature (Cakir et al. 2009, Bouacha 2010). Azlan Mohd Zain et al. (2010) investigated the effects of radial rake angle of tool, combined with cutting speed and feed on surface roughness. They reported that the cutting conditions should be set at highest cutting speed, lowest feed and highest radial rake angle to achieve the minimal surface roughness. Selvakumar et al. (2012) used cermet inserts for finish turning of titanium alloy and observed remarkable effects of tool type and

feed rate on surface roughness. Ramesh et al. (2012) conducted experiments on turning of titanium alloy (Grade-5) to study the effects of cutting parameters on surface roughness and found that the feed is the most influential factor affecting the surface roughness. Kali Dass and Chauhan (2011) quantified the effects of cutting speed, feed rate, depth of cut and approach angle on surface roughness and tangential force during titanium (Grade-5) alloy machining. The factorial design was utilized to obtain the best cutting conditions for minimization of surface roughness and tangential force.

Poor thermal conductivity of titanium causes concentration of extreme heat near the cutting edge, which in turn leads to premature damage of cutting tool. The situation, thus, demands application of an innovative cooling method that would cause successful removal of heat to make implementation of higher cutting speeds feasible. Shokrani et al. (2012), classified titanium as difficult-to-machine material and stressed the environmental and health hazards associated with the use of conventional cutting fluids together with developing governmental regulations that have resulted in increasing machining costs. The problem associated with machining of titanium alloys are low productivity, poor surface quality and short tool life. They emphasized on the need of reducing and/or eliminating the use of conventional cutting fluids in titanium alloy by using environmentally conscious machining such as dry cutting, minimum quantity lubricant (MQL), cryogenic machining and air cooling to deal with major health and environmental concerns. The experimental research by Machado and Wallbank (1997) indicated that the MQL enables considerable decrease in cutting temperature and dimensional inaccuracy depending upon the levels of cutting speed and feed rate. The results also showed that surface finish, chip thickness and force variation are all affected with low coolant volume when compared to flood cooling. The MQL system has shown encouraging potentials for precision machining at low feed and high speed. Dhar et al. (2006) investigated the role of minimum quantity of lubrication (MQL) on cutting temperature; chip formation and product quality during turning of AISI-1040 steel with uncoated carbide insert and the experimental results were compared with dry flooded machining. Khan et al. (2009) compared the effects of dry, wet and MQL machining of AISI 9310 alloy steel on chip–tool interface

temperature, chip formation mode, tool wear and surface roughness. Their investigation reveals that MQL machining is found to be better when compared to dry and wet machining due to substantial reduction in cutting zone temperature enabling favorable chip formation and chip–tool interaction. Ramana et al. (2011) evaluated the machining performance and optimized the process parameters in turning of Ti-6Al-4V alloy using uncoated carbide tool with different coolant conditions for minimal surface roughness. Klocke and Eisennblatter (2000) reported that the machining efficiency with MQL could be enhanced when compared to dry and conventional flood machining. Ibrahim et al. (2010) optimized the cutting parameters to obtain minimum surface roughness using Taguchi method in titanium alloy (Ti-6Al-4V) turning with coated and uncoated cemented carbide tools under dry cutting condition and high cutting speed.

It is evident from the literature survey on titanium alloy Ti-6Al-4V that it is rightly classified as difficult to machine material. From the detailed study, we can conclude that PCD tool is a promising alternative for machining of titanium alloy because of its numerous advantages as compared to the conventional tools. Further, it is also reviewed that to overcome the environmental and health hazards caused by cutting fluid flood lubrication, an alternative in the form of dry cutting, MQL lubrication and cryogenic machining must be explored. Most of the researchers used the cutting conditions such as cutting speed, feed and depth of cut as input parameters. But as per authors' knowledge, no methodical research work has been reported in the literature to determine the best lubricating mode along with appropriate cutting conditions for achieving better surface quality and surface hardness using poly crystalline diamond (PCD) inserts as the cutting tool. Interestingly, tool nose radius, one of the tool geometry parameters, has not been scientifically investigated, most likely due to its spontaneous effects on part surface finish. Hence, an attempt has been made in this research to find the optimum process parameters namely lubricating mode, cutting speed, feed rate, nose radius and depth of cut during turning of Ti-6Al-4V alloy using PCD tool so as to minimize the surface roughness and maximize surface hardness using Taguchi method.

2.2 BURNISHING PROCESS

Surface modifications and surface treatments play vital roles for increased service life of several critical components and devices that are used for engineering and structural functions. One of the most competent surface engineering methods i.e mechanical treatment, is the burnishing process. Unlike finishing processes, namely grinding, lapping, polishing and honing, which normally depend upon chip removal, the burnishing process is a cold-working chipless process, which effortlessly produces an even and work-hardened surface by plastic deformation of surface irregularities. Burnishing improves the surface characterstics by plastically deforming the surface layers. Loh and Tam (1988), in their review literature discussed the various types of burnishing, important burnishing parameters- force,feed,speed,ball material and diameter,workpiece material, initial roughness on the final surfcae roughness .They concluded that burnishing force ,feed rate are the important factors and a particular surface finish can be obtained by appropriate selection of the burnishing parameters. Many research studies have been conducted to investigate the effects of burnishing feed, speed and force on surface roughness and hardness, during burnishing process.

An experimental analysis was undertaken by Nemat and Lyons (2000) on mild steel and aluminium using a burnishing tool showed that improvement to an extent of 70% in surface roughness can be obtained .Reduction in feed or speed increases the surface hardness of mild steel and aluminium, whereas the increase in the no. of passes or burnishing force leads to an increase in the hardness. Fang-Jung Shiou and Chien-Hua Chen (2003) have studied freeform surface finish of plastic injection mold PDS5 tool steel by using ball-burnishing process. They determined the optimal plane ball-burnishing parameters utilizing the Taguchi's orthogonal array method, wherein the surface roughness improvement of the injection part on plane surface was about 62.9% and that on freeform surface was about 77.8%. The Vickers hardness scale of the tested specimen was improved from about 338Hv to 480 Hv after ball-burnishing process. Luca, L.L. et al. (2005), studied roughness of hardened steel component (64 HRC) using hydrostatic burnishing tool, for different burnishing feeds and pressures. It is reported (Luca et al., 2005) that after burnishing of a hardened steel component

(64 HRC) with a ball of 6.35 mm diameter, a roughness of 0.5 μm was obtained. In particular, when the surface which was turned with a tool of 0.8 mm nose and feed rate of ft = 0.1 mm/rev and subsequently burnished with the pressure of 38 MPa, surface roughness Ra decreased to about 0.2 μm. Their investigations led to the conclusion that the final effect of a smoothing–burnishing process strongly depends on such factors as the initial roughness and the burnishing force. It was found that, when the burnishing feed increases, the roughness increases and roughness comparable to grinding could be obtained through burnishing. Hamadache, H. et al. (2006) studied the characteristics of Rb40 steel superficial layer under ball and roller burnishing. It was found that burnishing force as well as the number of burnishing tool passes played the decisive role during optimization of both surface roughness and hardness. Superficial layers of Rb40 steel treated by roller and ball burnishing behave like ground surfaces and shows an appreciable wear resistance. During roller burnishing of structural Rb40 steel, Hamadache et al. (2006) observed 89% improvement in wear and up to 9% strength improvement in hardness as compared to turning. El-Tayeb et al. (2007) studied the influence of roller burnishing contact width and burnishing orientation on surface quality and tribological behavior of Aluminum 6061.They found that burnishing with smaller roller contact width (1mm) was capable of improving the surface roughness up to 40%. Burnishing force above 220N was capable of decreasing the surface roughness by 35%. In the same study the burnishing speed of 110 rpm yields the highest improvement in hardness, as much as 30% increase. The authors also found that the friction coefficient of burnished surfaces is dependent on the surface roughness.

El-Axir, et al. (2008a) has studied the effect of various burnishing parameters during the inner surface finishing of aluminum alloy 2014 by ball burnishing process. The results have revealed that the effect of burnishing feed is much more pronounced than the effects of burnishing speed on average surface roughness. The specimen could be finished to an average roughness of 0.14μm from an initial roughness of about Ra 4μm, by burnishing. To explore the optimum combination of internal ball burnishing process parameters in an efficient manner, on the basis of the response surface methodology (RSM) a second-order surface profile parameters prediction models has

been developed. Radziejewska and Skrzypek (2009) performed hot and cold burnishing processes on carbon steels alloyed with cobalt stellite. Their results indicated that the burnishing process had caused deformation of grains up to 20-30 μm thick zone and increased microhardness of the surface zone material. Moreover, compressive stresses were generated in surface layer of the alloyed material due to burnishing. Klocke, F et al. (2009) studied the influence of process and geometry parameters on the surface layer after roller burnishing of nickel alloy IN718.The authors reported that the durability and reliability of highly stressed turbine components can be increased by hardening of the surface layer, by roller burnishing. The measurement results showed that the burnishing force significantly influences the amount and depth of induced residual stresses and strain hardening. A clear knowledge of the correlation between process and geometry parameters was developed. El-Taweel and Axir (2009) used Taguchi method to limit the number of trials and reliably determined the optimal parameters during burnishing of brass specimens. The analysis of results shows that the burnishing force with a contribution percent of 39.87% for surface roughness and 42.85% for surface micro-hardness had the dominant effect on both the surface roughness and the micro-hardness, followed by burnishing feed, burnishing speed and then by number of passes.

In their experimental work, Low, K. O. (2010) introduced roller burnishing as a technique to improve the friction and wear characteristic of polymers in such applications. The lowest coefficient of friction value achieved is 0.24 (26.8% decrease) for polyoxymethylene (POM) and for polyurethane (PUR) it is 0.27 (17.7% decrease). The lowest specific wear rate achieved in this work for POM is 0.37×10^{-6} mm^3/Nm (27.8% decrease) and for PUR it is 0.47×10^{-6} mm^3/Nm (25.2% decrease). These findings proved that the roller burnishing process has the capability to improve the surface quality and tribological characteristics of POM and PUR. From the work of Branko, T et al. (2012) during burnishing of aluminum alloy EN AW-6082 (AlMgSi1) T651, it was established that initial surface roughness and surface profile have significant influence on the effects of burnishing process, especially when the primary goal is to achieve high-quality surface finish. They also concluded that burnishing feed significantly affects finish roughness. During the investigations by

Zhang.P et al. (2010), roller burnishing introduced a work-hardened case and compressive residual stresses in the near-surface region of hot-rolled Mg–12Gd–3Y magnesium alloy, which effectively retarded the fatigue-crack nucleation and/or propagation, leading to an improvement in fatigue life. Korzynski et al.(2011)investigated the effects of of burnishing parameters on surface roughness during burnishing of 42CrMo4 alloy steel shafts with a diamond cylindrical-ended tool. They reported a significant improvement in surface roughness, surface microhardness and compressive residual stresses in the burnished surface in comparison with the ground surface .An increase in fatigue strength of 18% was also documented. Travieso-Rodriguez et al. (2011) performed experiments on two different materials, namely, A92017 aluminum and G10380 steel having convex and concave surfaces. They found that smaller curvature radius in convex surface and bigger radius in concave surface could improve surface quality for A92017 aluminum workpieces. The burnishing direction and the curvature radius were found to be the most significant parameters in burnishing of G10380 steel work materials.

From the investigations carried out by Rodríguez et al. (2012) on AISI 1045 mild steel, it was proved that burnishing is an economical and feasible mechanical treatment for the quality improvement of turned parts. The studies determined the influence of burnishing parameters on surface roughness and hardness. Due to burnishing, an improvement in the surface quality (even reaching 0.3 μm Ra), increase in the hardness of the workpiece surface (up to 60% Brinell) and introduction of compressive residual stresses, which are favorable for increasing the fatigue life of the piece and improvement in the wear resistance of the component, were recorded. Grzesik and Zak (2012) compared the surface roughness of 41Cr4 low-alloy steel with conventional cutting, wiper tool cutting and multipass burnishing operations. The results showed that the improvement of the surface roughness through the burnishing process was about 94% over the one from conventional cutting and 40% over Wiper tool cutting. It was also evident from their experimental work that the feed rate and insert geometry (standard versus Wiper inserts) influence the final effects concerning roughness parameters and bearing properties of the machined surfaces. They reported that after burnishing of a hardened steel component (64 HRC)

with a ball of 6.35 mm diameter, a target roughness Ra = 0.5 μm was obtained. Feng Lei Li et al. (2012) carried out turning and burnishing trials on AA 7075 and AISI 5140.They concluded that burnishing can decrease surface roughness at most to about 12.5% to 25.0% as the maximum height of the profile of the machined surface is used as indicator and the lowest surface roughness after burnishing is proportional to the initial surface roughness. The effects of both ball burnishing, electrolytically polished and shot peening surface treatments on AA7075 T73 have been studied by Mansour Mhaede (2012). The most important general conclusions drawn from the obtained results are that, the ball burnishing results in a very smooth surface, comparable to that of electrolytically polished reference conditions, while shot peening leads to the highest surface roughness. Further it was evident that ball burnishing and shot peening induced plastic deformation increases the surface layer hardness and introduced significant levels of residual compressive stresses. Based on the experimental results of Jinlong and Hongyun (2013) during burnishing of 2024 aluminum alloy, it can be concluded that the corrosion property was improved due to grain refining by burnishing. The tensile residual stresses in the surface zone are transformed into compressive stresses after burnishing, thus increasing the fatigue life of the components (Nalla, R.K. et al. 2003 and Douglas, J.H. et al. 2002).

A large number of authors have contributed towards the study of effects of burnishing on titanium alloy. The works of few of the researchers are mentioned below. Nalla.R.K. et al. (2003) investigated the influence of deep rolling and laser shock peening process on the fatigue behaviour at ambient and elevated temperatures of Ti-6Al-4V work material. Their results concentrated on the low cycle fatigue (LCF) and high-cycle fatigue (HCF) behavior of a Ti-6Al-4V alloy with regards to the thermal and mechanical stability of the residual stress states and the near-surface microstructures. They found that at higher temperatures, there was delay in initiation and initial propagation of fatigue cracks, because of cold rolling. The increase in fatigue life by mechanical treatment was recorded because of the layer of work hardened nanoscale grains near the surface microstructure. Altenberger, I et al. (2003) investigated the thermal stability of near-surface microstructures induced by deep rolling and laser-shock peening in AISI 304 stainless steel and Ti-6Al-4V using

transmission electron microscope. Their study revealed that the fatigue life was improved. Bozdana and Gindy (2008) proposed a newly developed technique utilizing ultrasonic vibrations, named ultrasonic deep cold rolling (UDCR) process and presented the experimental results on the treatment of Ti–6Al–4V using conventional deep cold rolling and UDCR processes. They observed an improvement in fatigue life and increased resistance to failure mechanisms. Gill et al. (2008) measured the level of residual stress relaxation during deep cold rolling samples of titanium alloys Ti–6Al–4V and IMI679, caused by low cycle, constant strain amplitude fatigue at both room and elevated temperature. They concluded that residual stress relaxation was limited to a depth of 400–500 μm and thus the depth of compressive residual stress was unaffected by relaxation. Tsuji et al. (2008) employed deep rolling to induce compressive residual stress in plasma-carburized Ti–6Al–4V alloy sample. Plasma surface diffusion processes such as plasma carburizing and nitriding have been used to improve tribological properties of titanium and its alloys. But, the improvement of fatigue strength by these processes has not been successful because of the brittleness introduced in the high hardness surface layer and the disappearance of compressive residual stress and grain growth by heating. You-Li Zhu et al. (2009) developed an ultrasound-aided deep rolling process (UADR) for anti-fatigue applications for surface enhancement of titanium alloy specimens. From their experimental work they concluded that the surface roughness was reduced, a deep layer of residual compressive stress was induced and fatigue strength of the titanium alloy specimens was considerably improved. A comprehensive work was presented by Thamizhmanii et al. (2009) on surface roughness and hardness in burnishing square titanium alloy material, using a multi roller burnishing tool by varying various parameters like burnishing speed, feed and depth of penetration. They reported that, roller burnishing is a constructive process to improve surface quality, hardness and fatigue life.

On review of the burnishing process, it can be seen that burnishing is a promising mechanical surface treatment method, which improves the surface finish, hardness and induces compressive residual stresses thereby improving the fatigue life and wear resistance. Most of the researchers firmly agree that the burnished surface quality has many advantages over machined ones i.e. increase in fatigue life, wear and corrosion

resistance, which leads to improvement in the functional performance of the components. Burnishing process has been successfully employed on various materials of varying hardness and properties namely mild steel, plastic injection mold PDS5 tool steel hardened steel, Rb40 steel , carbon steels, G10380 steel, 41Cr4 low-alloy steel, 42CrMo4 alloy steel, G10380 steel , A92017, aluminum 6061, aluminum alloy 2014 alloyed with cobalt satellite, hot-rolled Mg–12Gd–3Y magnesium alloy aluminum alloy, nickel alloy, IN718 brass, polymers, EN AW-6082 (AlMgSi1) T651 and Ti-6Al-4V.From the above investigations the main burnishing parameters namely, burnishing feed, force, number of passes and speed were identified and their effect on surface finish, hardness, residual stress was analyzed. The review of previous works on burnishing reveals that most of the investigators concentrated on the analysis of ball burnishing process dealing mostly with the surface finish and hardness, but with little focus on the optimization of burnishing parameters. Eventhough quite a few researchers have reported work on titanium alloy, all these works have been on advanced form of burnishing such as low plasticity burnishing, deep rolling, cold rolling and ultrasonic burnishing. To summarize, not much study has been reported on ball burnishing of titanium alloy (Ti–6Al–4V) and the optimization of burnishing parameters.

2.3 MODELING OF BURNISHING PROCESS

Burnishing is a highly nonlinear problem, in which local large strain/ deformation as well as material nonlinearities and unknown boundary conditions in contact area are involved. Thus there is a need to develop a theoretical model to provide a fundamental understanding of burnishing mechanisms and help in optimizing burnishing parameters. Most of the research on burnishing in the past focused on experimental studies and used simplified analytical approaches. Some of the earlier investigators developed several predictive models to understand the burnishing process and consequently analyze the influence of burnishing parameters on the workpiece surface properties. The models in the field of burnishing can be classified into three categories: analytical (Bouzid et al. (2004), Mieczyslaw 2007, Feng Lei Li et al. 2012), statistical (El-Axir, M. H. et al.2008a) and FE models. In the present day,

with the rapid developments of computer technology and numerical calculation, numerical simulations especially those based on Finite Element Method (FEM) modeling became popular. FEM is a very strong and comprehensive technique which can take almost all the burnishing factors into consideration to find out the facts or study the burnishing mechanisms in a way that no other tools can accomplish. Skalski, K. et al. (1995) studied the burnishing indentation process of burnishing ball into workpiece using axisymmetric FEM to analyze the relations between contact pressure, plastic strain depth and burnishing force. The results from Skalski, K. et al. (1995) study showed that the tool force was more influenced by the tool size than by the material yield strength. In addition, a nearly linear relationship exists between the width and depth of the plastic deformation zone.

Röttger (2002) developed a 2Dplane strain FEM model for analysis of ball burnishing on the hardened steel using DEFORM-2D.The predicted surface finish (R_a) and residual stresses of the FEM model agreed reasonably with the experimental values. The simulation is limited to the radial plane of the turned part defined by the axis of the part and the generatrix, followed by the roller. Moreover, the comparisons of residual stress were made based on the effective stress and detailed information on the six stress components (3 normal & 3 shear) was incomplete. Bouzid et al. (2004) investigated the effects of burnishing on the surface roughness of AISI 1042 steel and developed an analytical model to analyze the surface roughness after burnishing. The model was developed taking into consideration the initial surface roughness, burnishing feed and penetration depth. Hertz theory was applied to estimate the penetration depth of the burnishing tool, assuming that the tool and the work piece were supposed to have purely elastic behavior. 2D and 3D finite element modeling of ball burnishing process considering the roughness of the surface has been carried out by Yen et al. (2005) using finite element modeling (FEM) commercial software DEFORM 2D and DEFORM 3D, based on Röttger's (2002) work. The improvement consisted in controlling the position of the rolling element while still invoking the plane strain assumption in the case of a refined 2D model. The penetration depth of the rolling element is previously determined by a fully three-dimensional (3D) simulation of the rolling tool acting on a parallelepiped representing a portion of the

surface layer of the specimen. The residual stresses are compared with the experimental values and the results, unexpectedly, show a greater degree of correlation with the 2D model than with the 3D model. To simulate burnishing process, Zhuang and Wicks (2004) analyzed the residual stress profile in the low plasticity burnishing (LPB) process for IN 718 workpiece using commercial software ABAQUS based on the implicit procedure and proposed a three dimensional non-linear moving contact FE model. Beres et al. (2004) used two- and three-dimensional finite element method to model the LPB process numerically. Bouzid and Sa (2005), developed a 3D FEM model of the burnishing indentation process to analyze the residual stress induced during burnishing. A reliable FE model of burnishing process was also presented by Sartkulvanich et al. (2007). They developed more perfect 2D and 3D FEM models to analyze the influence of burnishing parameters on surface roughness and residual stress based on Rottger's (2002) work. Jiang et al. (2002) simulated rolling contact using 2D and 3D finite element modeling and it was shown that they can differ from each other in terms of profile of residual stress. Surface roughness of the workpiece AISI 1042 steel under ball burnishing process has been analyzed by Bouzid and Sai (2005).

Bougharriou et al. (2010) developed an analytical model and a finite element model to provide a fundamental understanding on the burnishing on an AISI 1042 material. The simulations were devoted to the study of the surface profile, the residual stresses and the influence of burnishing parameters (penetration depth, feed rates, diameter of the ball of burnishing tool and initial surface quality) on surface roughness and the residual stress distribution. These results obtained were successfully compared with experimental data obtained in previous works to prove the model. They concluded that the real workpiece material behaviour should be improved by the incorporation of a largest data base of experimental tests to fit the material parameters and 2D FE model cannot predict precisely the values of the roughness parameters and residual stresses. They recommended the use of the 3D FE model. Maximov and Duncheva (2011) analyzed ball burnishing process of low alloy steel by 2D FEM using ABAQUS/Implicit. Compared with experimental data, the results obtained by these

authors demonstrate that these finite element models were able to predict the effect of process parameters on the residual stress distributions successfully.

2.4 SURFACE TREATMENT AND WEAR RESISTANCE OF TITANIUM ALLOY

Various surface modification techniques pertaining to titanium and titanium alloys namely physical, mechanical, chemical and electrochemical treatment are widely used. Surface modification techniques are very essential for titanium alloys to attain superior biocompatibility, higher wear and corrosion resistance. Through proper surface modification techniques, the use of titanium and its alloys in the biomedical field for long-term implants retaining the excellent properties of substrate material and improving the specific surface properties required by clinical applications has been realized.Ti–6Al–4V alloy is known to possess poor wear resistance that restricts its applications particularly in areas involving wear and friction (Budinski, K.G. 1991; Yerramareddy,S and Bahadur,S 1992). The scope of applications for titanium alloys has been somewhat impeded owing to poor wear resistance under abrasion and erosion conditions (Budinski, K.G. 1991, Grenier, M et al. 1997, Long,M et al. 1998; Agins H.J et al.1988). Molinari et al. (1997) studied the dry sliding wear behavior of Ti–6Al–4V alloy sliding against itself at different sliding velocities and applied loads and confirmed the low wear resistance of the alloy to plastic deformation at low loads and poor protection exerted by the surface oxide. The dominant reason for the poor wear resistance of Ti–6Al–4V alloy is due to low protection exerted by the tribo-oxides. The tribo-layer of Ti–6Al–4V alloy was brittle, tended to be continuously fragmented and did not adhere to the substrate, thus presenting no protective role (Molinari et al. 1997, Straffelini, G. and Molinari, A. 1999). During the investigations carried out by, Alam and Haseeb(2002), on the tribological properties of Ti–6Al–4V and Ti–24Al–11Nb alloys subjected to dry sliding wear against hardened-steel, it was found that the lower wear rate of Ti–6Al–4Valloy alloy was linked to severe delamination wear. An unexpectedly higher wear rate for alumina sliding against Ti–6Al–4V (pin on-disk tests) was reported by Dong and Bell (1999). Qiu et al. (2006) investigated tribological characteristics of Ti–6Al–4V alloy against GCr15 under high

speed and dry sliding and concluded that the low wear resistance of Ti–6Al–4V alloy was attributed to the formation of a loosened oxide layer. Magaziner,R.S. et al. (2009) studied wear of Ti–6Al–4V under reciprocation sliding conditions and reported that the wear was due to the adhesion and abrasion processes without citing the effect of tribo-oxides.

A familiar approach for enhancing the tribological properties of titanium alloys for improved wear resistance is to perform surface modifications for increased hardness and reduction in friction coefficient (Xuanyong et al. 2004, Johnson R et al. 2006; Manisavagam et al. 2009).Surface treatment is the suitable solution for the elevation of the wear resistance of Ti–6Al–4V. Thermal oxidation is a popular process which substantially improves wear resistance (Guleryuz H and Cimenoglu H 2005, Borgioli F et al.2005).A few of the procedures applied are PVD coating (TiN, TiC), ion implantation (N^+), thermal treatments (nitriding, diffusion hardening) (Morton PH and Bell T 1989) or laser alloying with TiC (Chengwei et al.1995).These procedures have limited technical success rate. For example, ion implantation leads to little or substantial improvement in the sliding wear resistance of Ti-6Al-4V with modification of only a thin layer (>10 μm in best cases), which may promote catastrophic wear as the treated surface wears away or becomes discontinuous. Surface modification by oxygen diffusion hardening (ODH) has been considered to enhance the wear resistance of Ti-6Al-7Nb, which provides a gradual increase in the hardness through a relatively thick transformed layer (Streicher et al.1985). A similar approach was taken by Zwicker et al. (1991) for enhanced friction behavior of Ti-5Al-2.5Fe against UHMWPE, using oxide films formation by thermal oxidation. Applying a low-cost approach of thermal oxidation by modifying Ti–6Al–4V surfaces, Johnson R et al. (2006) achieved friction coefficients as low as 0.1, i.e. a reduction of 70% in comparison to the untreated alloy. Nevertheless, this experimental investigation has a limitation that the high thermal stresses produced can lead to torsional twisting of substrates leading to surface roughening, a problem which is also encountered in other thermal processes such as nitriding (Mishra S.C et al.2003), carburization (Luo G Y et al. 2009), boriding (Kartal et al. 2010) and thermal plasma coating techniques (Alves C et al. 2005).Efforts to enhance the tribological performance of Ti–6Al–4V

using SiC or B_4C coatings alone failed as there was no significant improvement on wear performance, despite a noticeable increase in surface hardness (David Flemingt et al.2011).The process of shot peening was employed, which led to an improvement in the wear resistance due to surface hardening of titanium alloy Ti–6Al–4V, but also resulted in an increase in surface roughness (Ganesh B.K.C et al. 2014).

One such acknowledged method of mechanical surface treatment is burnishing to impart specific physical, mechanical and tribological properties. Burnishing process is a post-machining operation in which the surface of the work piece is compressed by the application of a ball or roller to produce a smooth and work-hardened surface by plastic deformation of surface irregularities. Burnishing process is capable of improving the resistance to wear, corrosion and oxidation. These improvements can be extended to minimize friction and reduce adhesion. Many investigators have pointed out that burnishing reduces friction coefficient and improves wear resistance. El-Tayeb (1994) revealed that burnishing process helps to reduce friction up to a critical depth, beyond which cracks are initiated .In another study, El-Tayeb, N.S.M. and Ghobrial (1993) found that burnishing process reduced wear rate by 38% for copper and 44% for St-37 steel whereas an excessive burnishing depth accelerated the response for wear rate and this resulted in surface damage. N.S.M.El-Tayeb et al. (2008) in their study proved that ball burnishing process is capable of improving coefficient of friction by 48% reduction and weight loss by 60–80% reduction of burnished surface of Aluminum 6061. Srinivasa Rao D et al. (2008) studied the effects of burnishing parameters on the surface hardness and wear resistance of HSLA Dual-Phase Steels aluminum alloy and observed that the percentage reduction in weight of the components decreases with increase in burnishing force. Rajasekariah R and Vaidyanathan S (1975) conducted experiment on steel components and observed an increase in wear-resistance of 40% due to burnishing. Low K.O. and Wong, K.J (2011) conducted ball burnishing on polymers under dry sliding conditions and determined that the lowest coefficient of friction value achieved was 0.22 (32.9%decrease) for polyoxymethylene (POM) and 0.24 (28.8% decrease) for polyurethane (PUR) whereas the lowest specific wear rate value achieved was $0.31x10^{-6}$ mm^3/Nm (38.6% decrease) for polyoxymethylene (POM) and $0.41x10^{-6}$

mm^3/Nm (37.9% decrease) for polyurethane (PUR). Thus without compromising the advantageous properties of titanium alloys, suitable surface modification techniques have to be employed to enhance the wear and corrosion resistance of titanium alloys(Geetha, M et al. 2009).

From the above literature review, it can be summarized that titanium alloy has poor wear resistance and hence some form of surface treatment is required to improve its tribological properties. A large number of thermal and mechanical surface treatment process have been carried out by researchers as discussed above. These methods have their own merits and demerits. From the above discussion, the burnishing process emerges out as a promising and economical technique to improve the wear resistance. Burnishing has been applied successfully by earlier investigators to improve the wear resistance of brass, HSLA Dual-Phase Steels aluminum alloy, copper, St-37 steel and polymers. No work as on date has been reported on the improvement in wear resistance of titanium alloy due to burnishing. Thus, it provides a potential to investigate the enhancement of wear resistance of components through burnishing.

2.5 SUMMARY OF LITERATURE SURVEY

Though burnishing has been widely employed, no systematic studies have been conducted or reported till date, which elucidate the effects of all burnishing processing parameters on the surface finish, surface residual stress, micro structure and micro hardness. Very few authors have conducted burnishing trials to determine the optimum parameters. After carrying out a literature review on titanium alloy and its machinability, burnishing process and wear resistance of Ti-6Al-4V, the following conclusions have been drawn:

- From the literature review, it is established that titanium alloy Ti-6Al-4V is rightly classified as difficult to machine material.
- Compared to the various conventional tools used for machining of Ti-6Al-4V, polycrystalline diamond tool is the best alternative because of longer tool life, high thermal conductivity and being economical

- No methodical research work has been reported in the literature for titanium alloy, to determine the best lubricating mode along with appropriate cutting conditions for achieving better surface quality and surface hardness using poly crystalline diamond (PCD) inserts as the cutting tool. Interestingly, tool nose radius, one of the tool geometry parameters, has not been scientifically investigated, most likely due to its spontaneous effects on part surface finish.
- To date, research related to the machining of Ti-6Al-4V has mostly been experimental. There is hardly any evidence of quantitative analysis of machining process.
- Although the application of MQL has a tremendous effect on the machining of Ti-6Al-4V, little research has been devoted to this aspect. From the literature review, it is evident that no systematic research work has been reported in the literature to determine the optimum quantity of lubricant with appropriate cutting conditions for achieving better surface finish during machining of Ti-6Al-4V.
- The review of literature on machining of Ti-6Al-4V reveals that surface roughness and hardness have been given relatively little attention during the machining studies.
- Studies have been conducted on advanced forms of burnishing such as low plasticity burnishing, deep rolling, deep cold rolling and ultrasonic burnishing of Ti-6Al-4V.But no study has been reported related to the ball burnishing of titanium alloy (Ti-6Al-4V). There is hardly any evidence of quantitative analysis of burnishing process of Ti-6Al-4V.
- Although few studies have been conducted on burnishing of titanium alloy, till date there is no report on optimization of burnishing parameters. The analysis and effect of burnishing parameters namely burnishing feed, force, speed, number of pass on the output surface hardness and roughness has not been studied in detail.
- It is evident from the literature review that Ti-6Al-4V has poor wear resistance and some form of surface treatment is essential to improve its functional properties. So there is ample scope to explore the potential of burnishing as a mechanical surface treatment process to enhance the wear resistance of titanium alloy.

- A large number of studies have been reported on the improvement of fatigue life due to burnishing, but no such work on the effect of improvement in wear resistance of burnished components of titanium alloy (Ti-6Al-4V) has been reported.
- Data for an optimization process is needed in order to find the optimal combination of surface integrity properties for achieving the most desirable wear performance of the titanium alloy.

2.6 OBJECTIVES OF THE CURRENT RESEARCH WORK

A large number of surface treatment techniques have been successfully adopted to improve the functional properties of components. Most of these techniques are expensive and require skilled labour. In India, importing these sophisticated machinery will add up to the cost of manufacturing. Most of the automobile and aerospace industries in India sub-contract their jobs to small and medium scale industries which cannot afford to invest large amounts on these machines performing surface treatments like laser burnishing, ultrasonic burnishing etc. One such promising and cost effective alternative to the above stated problem is burnishing. As mentioned earlier, investigations on burnishing process are primarily involving improvement in surface finish and hardness with hardly any emphasis on optimization of the process. Literature review also indicates that burnishing of Ti-6Al-4V has not received due attention despite its wide usage in aerospace, automotive and biomedical industry. As explained earlier, burnishing involves many parameters crucial in obtaining the desired improvement in surface hardness and finish. Thus, need for such a study in the ball burnishing of Ti-6Al-4V exists. There is a need to carry out research in this field so as to gain a better understanding of the machining conditions that result in improved machinability and burnishing of Ti-6Al-4V. Development of an economical turn-assisted ball burnishing process and its optimization to obtain enhanced wear resistance coupled with good surface finish and hardness is the goal of present research work with the following clearly defined objectives.

Following are the objectives of the proposed research investigation:

- To develop optimal performance measures for turning of titanium alloy (Ti-6Al-4V) as a pre-machining process to obtain best quality finish.
- To optimize the process parameters during ball burnishing of titanium alloy (Ti-6Al-4V) such as burnishing speed, burnishing feed, burnishing force and number of passes with the objective to minimize the surface roughness and maximize the hardness.
- To study and analyze the effects of burnishing parameters on surface integrity factors such as surface topography, microhardness, roughness, microstructure and residual stresses of titanium alloy (Ti-6Al-4V).
- To develop an improved ball burnishing tool and analyze its performance.
- To study the improvement in wear resistance and effect of burnishing parameters on specific wear rate, coefficient of friction during ball burnishing of Ti-6Al-4V.

The brief literature survey on machining and burnishing is provided in the beginning of this chapter followed by summary of the literature review, objectives and scope identified for the present research.

The following chapter discusses research methodology adopted for machining trials, burnishing, developing a modified burnishing tool, set-up to measure wear rate, different response measurement methods, and the design of experiments along with the finite element modeling for proposed ball burnishing process.

Chapter 3

EXPERIMENTAL METHODOLOGY

To achieve objectives of the proposed work as defined in chapter two, the turning and burnishing process are carried out. The main objective is to carry out the burnishing experiments on titanium alloy (Ti-6Al-4V) and study the effect of burnishing parameters on surface roughness and hardness. From the literature survey, it is evident that the final effect of smoothing during burnishing process depends heavily on the initial roughness (Luca et al. 2005, Korzynski 2007). Feng Lei Li et al. (2012) carried out turning and burnishing trials on AA 7075 and AISI 5140 and revealed that lowest surface roughness after burnishing is proportional to the initial surface roughness. Hence, understanding the machining characteristic of titanium alloy and determining the finish cutting parameters is important. The turning process is carried out to identify the optimal condition of process parameters for the best surface finish. Turning is carried out under the optimal parameter combination obtained and the specimens are prepared to further undergo the process of burnishing. A ball burnishing tool is developed to be fitted on a CNC lathe for burnishing set up. The important burnishing parameters, namely burnishing speed, feed, force and number of passes, with their range and levels are selected. The different responses identified for studies are surface roughness, surface hardness and residual stress. The response measurement techniques, finite element modeling, the design and conduction of experiments and detailed study are presented in this chapter. An innovative ball and roller burnishing tool is also developed and experiments are conducted to analyze the effect of surface roughness, hardness and observe their relative improvement. Finally, wear tests are conducted on the burnished titanium alloy to determine the improvement in wear resistance due to burnishing. The steps adopted in this study which give an overview of the investigations are shown in Figure 3.1.

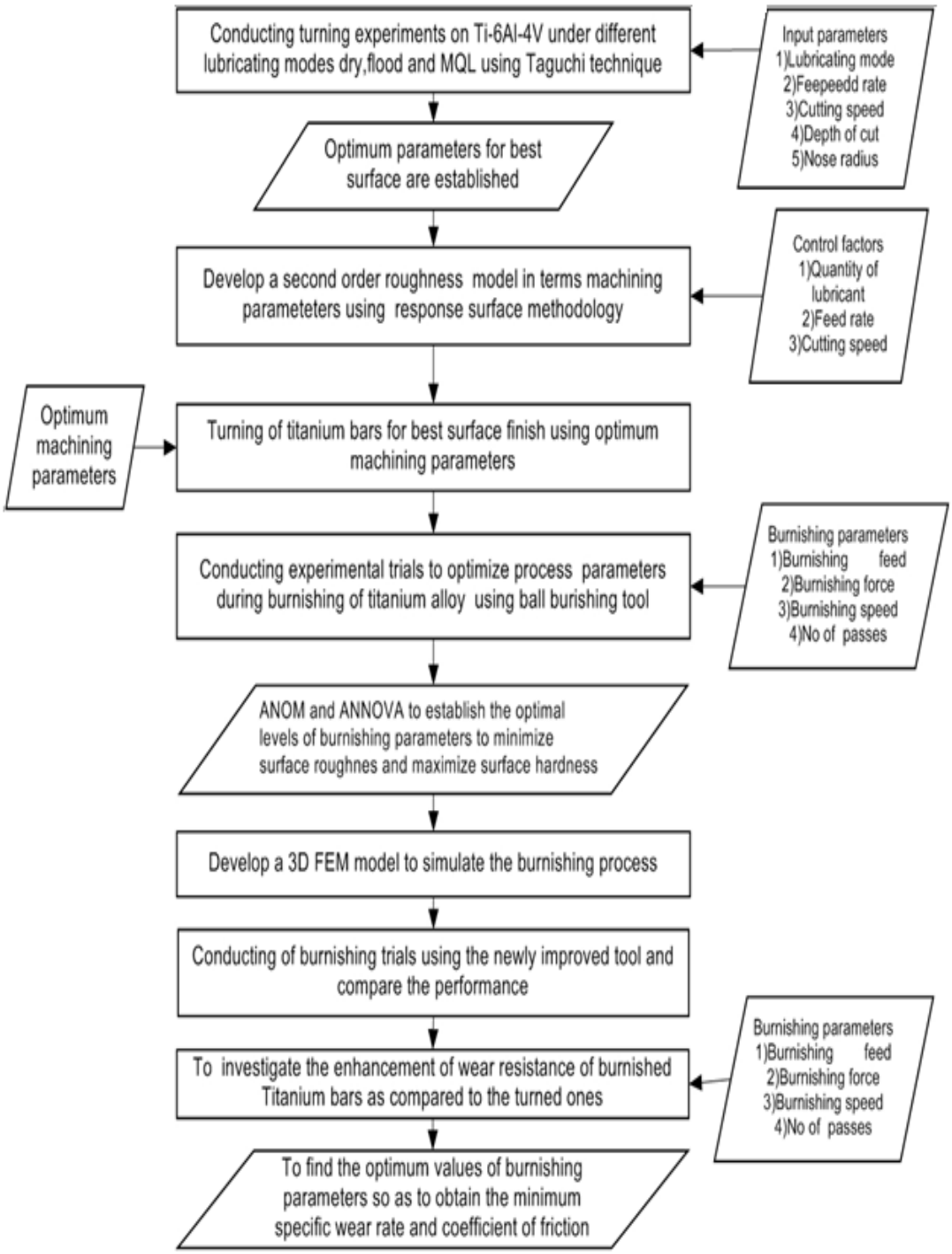

Figure 3.1 Process flow for studying turning and burnishing process

3.1 MACHINING OF TITANIUM ALLOY

Titanium alloy Ti-6Al-4V, is an (α+β) alloy of aerospace Grade 5, is selected as the work material and its chemical composition is given in Table 3.1.The titanium round

bars were supplied by Baoji Yongshegtai Titanium Industry Co., Ltd China and procured through Hindustan Aeronautics Ltd. , Bangalore. The mechanical properties of the specimen at room temperature are shown in Table 3.2. The microstructure of the α and β-phase on the cross sections of the titanium alloy Ti-6Al-4V is shown in Figure 3.2.

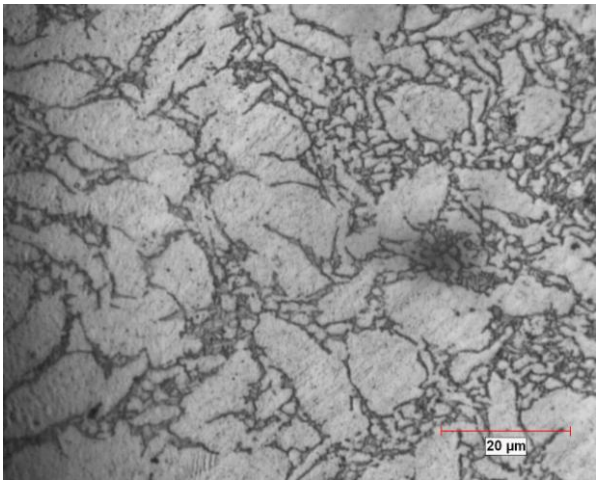

Figure 3.2 Microstructure of titanium specimen

Titanium alloy (Ti-6Al-4V) bars of 25 mm diameter were used as work material (Figure 3.3).

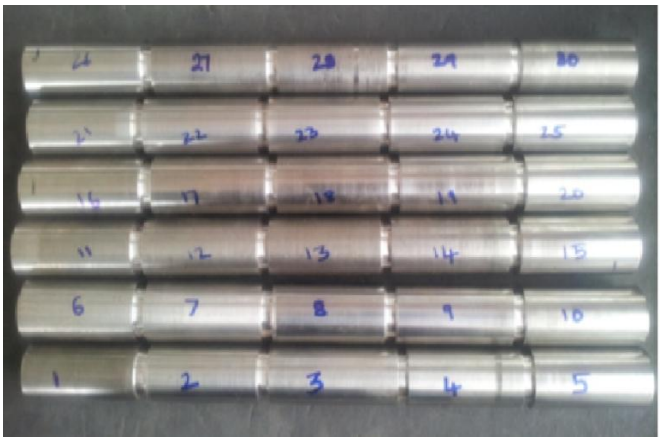

Figure 3.3 Titanium work pieces for turning experiments

Table 3.1 Chemical composition (Wt %) of titanium alloy (Ti-6Al-4V) used in the current investigation

Element	Al	V	Fe	O	C	N	Y	H	Ti
Wt (%)	6.1	4	0.16	0.11	0.02	0.01	0.001	0.001	Bal

Table 3.2 Mechanical properties of titanium alloy Ti-6Al-4V

Property	Typical Value
Hardness, Rockwell	30
Ultimate Tensile Strength (MPa)	955
Yield Tensile Strength(MPa)	900
Modulus of Elasticity (GPa)	113.8
Poisson's ratio	0.342
Density(g/cm^3)	4.51
Elongation in 4D (%)	18
Reduction of area (%)	42
Fatigue Strength(MPa) (at 1E+7 cycles .K_t stress concentration factor-3.3)	240

In the current study for turning operation, five parameters namely, lubricating mode, cutting speed, feed rate, nose radius and depth of cut were identified. The range of values for feed rate and depth of cut were selected based on the recommendations given by the insert manufacturer. The highest value of the cutting speed and the ranges of other parameters were selected after preliminary tests. Each parameter was investigated at three levels to study the non-linearity effect of the process parameters. The identified control factors and their levels are given in Table 3.3. According to Taguchi quality design concept, for three levels and five factors, a standard L_{27} orthogonal array (OA) was selected as shown in Table 3.4.

Table 3.3 Control factors and levels

Control Factors	Levels		
	1	2	3
Lubricating Mode (A_t)	Flood	MQL	Dry
Cutting Speed(B_t), m/min	50	100	150
Feed rate (C_t), mm/rev	0.15	0.25	0.35
Nose radius(D_t), mm	0.2	0.4	0.6
Depth of Cut(E_t), mm	0.25	0.5	0.75

The turning tests were performed as per OA, on '*Ace Turn mill CNC Fanuc lathe*', which is equipped with 11 kW spindle power and a maximum spindle speed of 4000 rpm. The polycrystalline diamond (PCD) insert and tool holder with an ISO designation of CCMT09T304 was used to machine the Ti-6Al-4V work pieces. The image of tool holder and PCD insert is shown in Figure 3.4(a) and the tool geometry of the PCD insert are shown in Figure 3.4(b).

Figure 3.4 (a) Tool holder and PCD insert

Table 3.4 Control factor settings as per L_{27} orthogonal array

Trial No.	Lubricating mode (A_t)	Cutting speed (B_t)	Feed rate (C_t)	Nose radius(D_t)	Depth of cut(E_t)
1	1	1	1	1	1
2	1	1	1	1	2
3	1	1	1	1	3
4	1	2	2	2	1
5	1	2	2	2	2
6	1	2	2	2	3
7	1	3	3	3	1
8	1	3	3	3	2
9	1	3	3	3	3
10	2	1	2	3	1
11	2	1	2	3	2
12	2	1	2	3	3
13	2	2	3	1	1
14	2	2	3	1	2
15	2	2	3	1	3
16	2	3	1	2	1
17	2	3	1	2	2
18	2	3	1	2	3
19	3	1	3	2	1
20	3	1	3	2	2
21	3	1	3	2	3
22	3	2	1	3	1
23	3	2	1	3	2
24	3	2	1	3	3
25	3	3	2	1	1
26	3	3	2	1	2
27	3	3	2	1	3

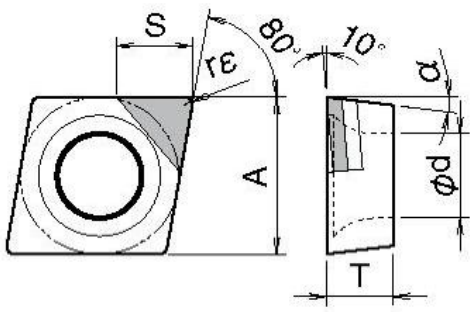

CCMT09T304 Geometry (mm)					
A	T	Ød	Nose radius (rε)	S	A
9.525	3.97	4.4	0.2,0.4,0.6	3.9	7°

(b)

Figure 3.4(b) Tool geometry of the PCD insert

Different lubrication systems have been introduced, to regulate the temperature during turning for better surface finish. Three different types of lubricating modes used in the present study are dry, flooded and minimum quantity lubrication (MQL). Palm oil (viscosity index of 190) having density 0.91 gm/cm^3 and viscosity of 40 mm^2/s at 40°C is used as lubricant in MQL lubricating mode. Palm oil was used as the lubricant during MQL, as it facilitates more effective lubrication and cooling at the tool-work interface especially when high cutting temperature are generated thus allowing the chips to flow away from the cutting zone (Rahim and Sasahara 2011). Rahim and Sasahara (2010) reported that the high viscosity of palm oil resulted in better penetration in the cutting zone especially at elevated cutting temperature. For flood cooling, 5% water emulsion of vasco 1000, a commercially available water miscible, vegetable oil based cutting fluid was used. This fluid is free from phenol, chlorine and other additives. In MQL application, the experiments were conducted using a thin-pulsed jet nozzle and controlled by a variable speed control drive. The MQL setup employed in the current investigation is shown in Figure 3.5. It consists of a reservoir of 2 liters capacity and a pneumatic piston pump to inject oil. A filter regulator is fitted in air line to regulate air used in the MQL set up and an oil filter cum air breather to filter oil with 149 micron.

Figure 3.5 Minimum quantity lubrication (MQL) set up

A pressure switch is used to make sure that required air pressure is maintained in the system. The solenoid valve is used for working of pneumatic piston pump and an air regulator is used to control air pressure in both the lines. The electronic timer B1DCA-X is a cyclic ON-OFF adjustable timer with time range from 0.6 seconds to 60 minutes (8 ranges) to control the frequency of oil piston pump. The discharge from the pump is at the rate of 0.40cc/stroke. The intervals between two strokes and duration of stroke can be adjusted to get the desired discharge. There is a provision in the form of a portable fixture at the machining center spindle to attach the nozzle. This flexibility in design makes it easy to place the injection nozzle at any desired position without interfering with the tool or work piece during the machining process. The schematic diagram of the MQL set up is presented in Figure 3.6.

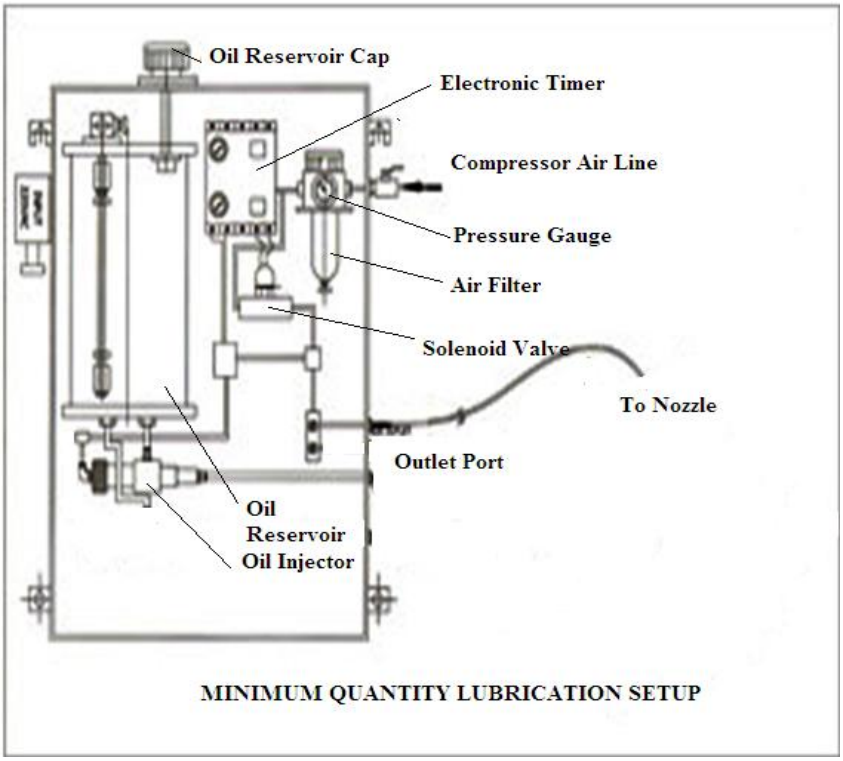

Figure 3.6 Schematic diagram of MQL Set up

Figure 3.7 Dry cutting

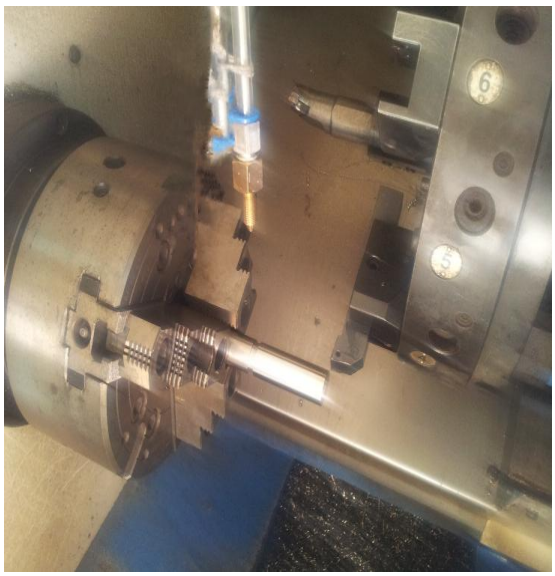

Figure 3.8 MQL cutting

The diameter of nozzle orifice is 1 mm and the delivery pressure is set at 4 kgf/ cm^2. During MQL mode the fluid nozzle is positioned opposite to the feed direction. In the flood type application, the flood fluid was discharged through two nozzles around the tool at the rate of 8,000 ml/min.The various lubricating modes, namely, dry, MQL and flood lubrication employed for turning Ti-6Al-4V are shown in Figures 3.7-3.9 respectively.

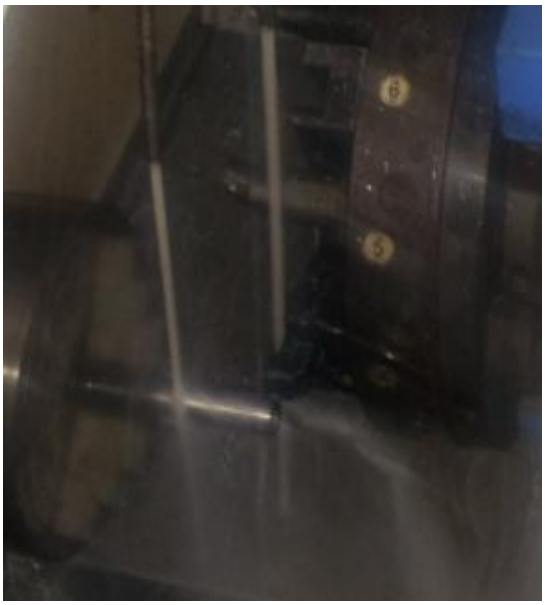

Figure 3.9 Flood lubrication

3.1.1 Experimental plan to develop response surface model for surface roughness during finish turning of titanium alloy under minimum quantity lubrication (MQL)

Planning for experimentation is necessary to develop the RSM based surface roughness model. Based on earlier experiments conducted, under various lubricating modes, namely, dry, MQL and flood lubrication employed for turning Ti-6Al-4V for better surface finish, the optimum parameter for lubrication mode, MQL was selected. Palm oil was used as the lubricant during MQL. In the current study, the quantity of lubricant (Q), cutting speed (v) and feed rate (f) are selected as the process parameters. The range of depth of cut for finishing is typically between 0. 25 to 0.5 mm. Based on the results of the experimental trials conducted earlier, the depth of cut was kept constant at 0.25mm and nose radius of PCD insert at 0.6mm. The shape of the insert is not so vital because the depth of cut is in general below the nose radius. More important is the ratio between the depth of cut and radius, since as this ratio changes the entry angle varies and subsequently the maximum chip thickness. Therefore for higher productivity, the largest nose radius of 0.6mm was selected. The ranges of the cutting conditions under MQL mode were determined from the previous investigations carried out by the author. The nozzle exit pressure is one of the significant factors which directly influences the machinability. High nozzle exit pressure of 0.6 Mpa was selected because of the relative benefits of increasing the pressure. By increasing the pressure, the cutting force is reduced , there will be decrease in the friction at the tool chip interface, thereby causing the cutting force, contact length and the chip thickness to reduce (Vikramkumar et al.2007) and moreover a decrease in droplet size leads to effective lubrication of contact zones (Nageswara Rao and Vamsi Krishna 2008).

In the present work, the experiments are planned as per Taguchi's orthogonal array (Phadke, M.S. 1989). Each parameter was investigated at three levels to study the non-linearity effect of the process parameters. The identified parameters and their levels are given in Table 3.5. According to Taguchi design, L_{27} orthogonal array (Phadke, M.S. 1989, Ross P.J.1996) is employed for the experimentation, which

requires 27 trials to be conducted. Table 3.6 shows the planning for experimental design considered for the current investigation. The first, second and third column of L_{27} array refer to quantity of lubricant (Q), cutting speed (v) and feed rate (f), respectively.

Table 3.5 Control factors and levels for MQL

Control Factors	Levels		
	1	2	3
Quantity of lubricant ,Q(ml/hr)	50	100	150
Cutting Speed, v (m/min)	125	150	175
Feed rate, f (mm/rev)	0.05	0.10	0.15

The turning tests were performed on '*Ace Turn mill CNC Fanuc lathe*' as shown in Figure 3.10.

Figure 3.10 CNC lathe and MQL setup used for turning and burnishing experiments

The trials were conducted as per L_{27} orthogonal array as shown in Table 3.6.

Table 3.6 Experimental conditions as per L_{27} orthogonal array

Tr.No	Levels		
	Quantity of lubricant Q(ml/hr)	Cutting Speed v(m/min)	Feed rate f(mm/rev)
1	1	1	1
2	1	1	2
3	1	1	3
4	1	2	1
5	1	2	2
6	1	2	3
7	1	3	1
8	1	3	2
9	1	3	3
10	2	1	1
11	2	1	2
12	2	1	3
13	2	2	1
14	2	2	2
15	2	2	3
16	2	3	1
17	2	3	2
18	2	3	3
19	3	1	1
20	3	1	2
21	3	1	3
22	3	2	1
23	3	2	2
24	3	2	3
25	3	3	1
26	3	3	2
27	3	3	3

An electronic timer B1DCA-X which is a cyclic ON-OFF adjustable timer with time range from 0.6 seconds to 60 minutes (8 ranges) is provided in the set up to control the frequency of oil piston pump. The discharge from the pump is at the rate of 0.40cc/stroke. The intervals between two strokes and duration of stroke can be adjusted to get the desired discharge. By setting the electronic timer, different discharge rates of 50, 100 and 150 ml/hr can be attained to conduct the different trials as per the orthogonal array (Table 3.6).

3.2 BALL BURNISHING OF TITANIUM ALLOY (TI-6AL-4V)

Turning operation on the titanium alloys is followed by burnishing, as the next operation. Based on the literature review, in the current research four control factors namely burnishing speed, burnishing feed, burnishing force and number of passes were considered. Taking into considerations the work piece hardness and machine tool capacities, low speed range burnishing was preferred in our investigation. It is advisable not to increase the burnishing force as it results in increase of surface roughness, due to the distortion of the micro profile and excessive work hardening (Loh and Tam 1988). In the present investigation, the burnishing tool has been designed for the maximum permissible force of 400 N. From the preliminary investigation it was evident that higher burnishing force caused shear failure in the subsurface layers, resulting in flaking. Taking this factor into considerations, the burnishing force is varied from 150 to 350 N. Each factor was examined at five levels to explore the non-linearity effects. The selected control factors and their levels are illustrated in Table 3.7.

Table 3.7 Control factors and their levels for burnishing trials

Code	Control factor	Level				
		1	2	3	4	5
A	Burnishing Speed(m/min)	15	30	45	60	75
B	Burnishing Feed (mm/rev)	0.05	0.10	0.15	0.20	0.25
C	Burnishing Force (N)	150	200	250	300	350
D	No of passes	1	2	3	4	5

According to Taguchi method, L_{25} orthogonal array with 4 columns and 25 rows was selected; each control factor is assigned to a column and twenty five distinct factor combinations are offered (Phadke, M.S. 1989, Ross P.J.1996). Thus, twenty five experiments are enough to analyze the entire burnishing experimental design space using L_{25} orthogonal array .The experimental layout plan used for the present research is given in Table 3.8.

The same CNC 'Ace *Turn mill Fanuc'*, lathe used for conducting turning trials was used to perform the burnishing experiments. The work material used in this study is the turned bars of 25 mm diameter. From the results of the turning experiments conducted, the following optimal parameters were identified for turning namely minimum quantity lubrication (MQL) condition using palm oil as the lubricant with a flow rate of 150 ml/hr, finish cutting parameters with cutting speed of 175 m/min, depth of cut of 0.25 mm and feed of 0.05 mm/rev. A polycrystalline diamond (PCD) insert with a nose radius 0.6 mm was used as the cutting tool.

The average roughness of the turned specimen was found to be in the range 0.40 - 0.45 μm and the hardness obtained was around 340 Hv. In the present investigations, external ball burnishing tests were performed as per the experimental plan (Table 3.8) under lubricated conditions using SAE 40 oil. The workpiece to be burnished was clamped by the chuck. Both cutting tool and burnishing tool were mounted on the CNC tool holder .The burnishing process was carried out after turning without releasing the workpiece from the lathe chuck, to keep the same turning alignment and to overcome the roundness error.

The workpieces were prepared with four recesses such that each sample could be used for five different burnishing conditions as shown in Figure 3.3. Figure 3.11 depicts a specifically designed ball-burnishing tool, which consists of two steel parts. The foremost part of square cross section is a shank held on the lathe tool post, while the supplementary part is a mandrel of material EN 31 to hold an active ball (8 mm in diameter), which is made up of carbide material. The type of carbide used as the constituent of the balls used for burnishing is tungsten carbide (WC). Loh N.H.et.al (1993) conducted experimental work on a vertical machining center to establish the

Table 3.8 Orthogonal array for conducting the turning trials

Trial No.	Burnishing Speed, A	Burnishing Feed, B	Burnishing Force, C	Number of Passes , D
1	1	1	1	1
2	1	2	2	2
3	1	3	3	3
4	1	4	4	4
5	1	5	5	5
6	2	1	2	3
7	2	2	3	4
8	2	3	4	5
9	2	4	5	1
10	2	5	1	2
11	3	1	3	5
12	3	2	4	1
13	3	3	5	2
14	3	4	1	3
15	3	5	2	4
16	4	1	4	2
17	4	2	5	3
18	4	3	1	4
19	4	4	2	5
20	4	5	3	1
21	5	1	5	4
22	5	2	1	5
23	5	3	2	1
24	5	4	3	2
25	5	5	4	3

effects of various burnishing parameters on the surface finish of ASSAB XW-5 steel (high-carbon, high-chrome steel), with different burnishing ball materials, namely tungsten carbide, ball bearing steel, silicon carbide and zirconia, to conclude that

tungsten carbide ball gave the best and most consistent surface finish. The hardness of the ball is 90 HRA. High hardness and dimensional stability make tungsten carbide balls the preferred choice for burnishing. Tungsten carbide balls are ideal for applications where extreme hardness must be accompanied by high resistance to wear and impact. They are well-suited to elevated temperatures, corrosion, humidity, abrasion, and poor lubrication conditions.

The preliminary analysis and literature survey reveal that large diameter balls are found to be more effective in improving the surface finish, whereas small diameter balls seem to be more efficient in enhancing the surface hardness. Hence, 8 mm diameter ball was selected in the present investigation, which was found to be having a considerable augmentation in both surface finish and hardness.

The ball holder i.e. the mandrel is elastically supported by a helical spring. This ball is additionally supported by three small carbide balls of 4 mm diameter. With this setup, during the burnishing process the active bill is free to rotate, in contact with the rotation of the work piece because of the frictional forces developed.

a) Assembled burnishing tool

b) Dissembled parts

Figure 3.11 Ball burnishing tool a) assembled tool b) dissembled tool

The ball is easily detachable from the tool for changing, readjusting or cleaning by unscrewing the ball guide cage. When the burnishing force is applied, the head of burnishing tool moves resulting in compression of the spring which has been calibrated to measure the burnishing force.

The sectional view of the burnishing tool is shown in Figure 3.12.The burnishing force is measured with help of spring of known stiffness and dial gauge. Keeping the spring inside the tool and placing the dial gauge at the end of the tool shank, the deflection of dial gauge is noted down for determining the burnishing force. During burnishing trials, it is very important to prevent the hard particles from entering the contact surface between the tool and the work piece. These hard particles usually leave profound scratches which damage the burnished work piece surface. To overcome this, workpiece was regularly cleaned with alcohol before burnishing and during the trials. The experimental set up employed for the burnishing experiments is presented in Figure 3.13.

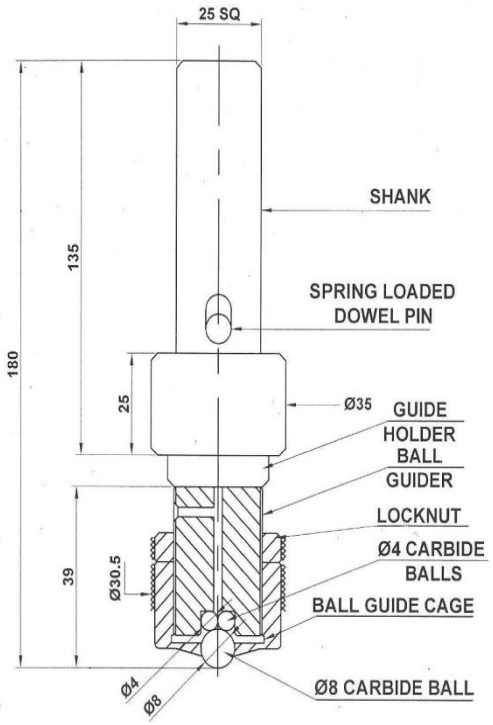

Figure 3.12 Sectional view of ball burnishing tool

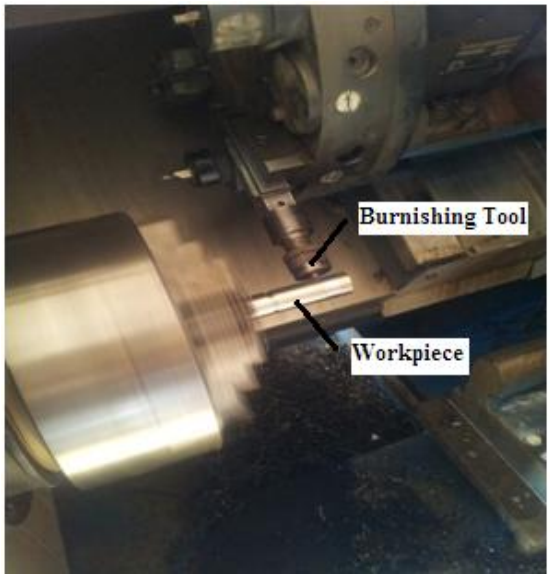

Figure 3.13 Experimental set up of burnishing experiments

3.2.1 Experimental trials with improved burnishing tool

The objective is to conduct the experimental trials using the improved burnishing tool. During the experimental trial, four parameters, namely, burnishing speed, burnishing feed, burnishing force and number of passes were identified and the range for each of the process parameters was determined through the results of preliminary experiments. Each process parameter was investigated at three levels to study the non-linearity effects of process parameters. The identified process parameters and their levels in the current investigation of burnishing process are summarized in Table 3.9.

Table 3.9 Ball burnishing process parameters and their identified levels

Code	Parameter	Level		
		1	2	3
A	Burnishing speed (m/min)	2.5	6.9	11.7
B	Burnishing feed (mm/rev)	0.10	0.13	0.15
C	Burnishing force(N)	250	300	350
D	Number of passes	1	2	3

Using Taguchi design concept (Phadke, M.S. 1989, Ross P.J.1996), L_9 orthogonal array (OA) with 4 columns and 9 rows was selected. Each burnishing process parameter is assigned to a column and nine different process parameter combinations are available. Thus using L_9 OA, the number of trials were reduced to only nine so as to, study the complete burnishing process. The experimental layout for the current investigation using L_9 OA is shown in Table 3.10. In the present study, external ball burnishing tests were performed under lubricated conditions as per the experimental plan of Table 3.10. The bars were turned to proper dimensions and work specimens were prepared as shown in Figure 3.14. The work pieces were prepared with one recess such that each work piece could be used in two different burnishing conditions. Similar turning conditions as conducted earlier were used to prepare the workpieces. The titanium bars were turned under minimum quantity lubrication (MQL) condition using palm oil as the lubricant with a flow rate of 150 ml/hr, finish cutting parameters with cutting speed of 175 m/min, depth of cut of 0.25 mm and feed of 0.05 mm/rev. A polycrystalline diamond (PCD) insert with a nose radius 0.6 mm was used as the cutting tool. After turning trials the average roughness and hardness obtained were in the range from 0.45 to 0.65 μm (R_a) and 340 (Hv), respectively

Figure 3.14 Work specimens used in the ball burnishing experiments

Table 3.10 L_9 Orthogonal array for burnishing

Trial No.	Levels of process parameters			
	Burnishing Speed A	Burnishing Force B	Burnishing Feed C	Number of passes D
1	1	1	1	1
2	1	2	2	2
3	1	3	3	3
4	2	1	2	3
5	2	2	3	1
6	2	3	1	2
7	3	1	3	2
8	3	2	1	3
9	3	3	2	1

A 12 mm diameter ball was selected in the burnishing tool. Figure 3.15 presents a specially designed ball burnishing tool (MECH-INDIA SRL 32 HR), which consists of two steel parts.

Figure 3.15 Improved ball burnishing tool

The first part of rectangular cross section is a shank held on the lathe tool post, whereas the other part is a mandrel of material EN 31 to hold 12 mm diameter ball made of carbide material. The ball holder, that is the mandrel was elastically supported by a belleville springs (disc spring). The sectional view of the ball burnishing tool is shown in Figure 3.16. The movement of the mandrel due to the applied burnishing force will cause compression of the spring. This compression has been calibrated to measure the burnishing force.

The newly developed burnishing tool used in the current investigation has the following advantages:

- Ball assembly and spring loaded cushion mechanism cannot be accommodated in the regular burnishing tool shank of 32 mm, but can be accommodated comfortably in our designed tool.
- A long cushion spindle can be used and the attachment to CNC will be easier because of extra grip provided in our designed tool.
- Moreover, a square shank tool has a larger overhang, whereas the newly designed tool used in the present investigation has a smaller overhang with a better reach.
- Unlike the conventional tool, belleville springs (disc springs) are used instead of coil springs, which facilitate better stiffness and use of number of belleville springs in different direction leads to an increase in the force induced. Moreover, the ability to change the force characteristic, by way of varying the cone height to thickness ratio, is a particularly useful feature of the belleville spring.

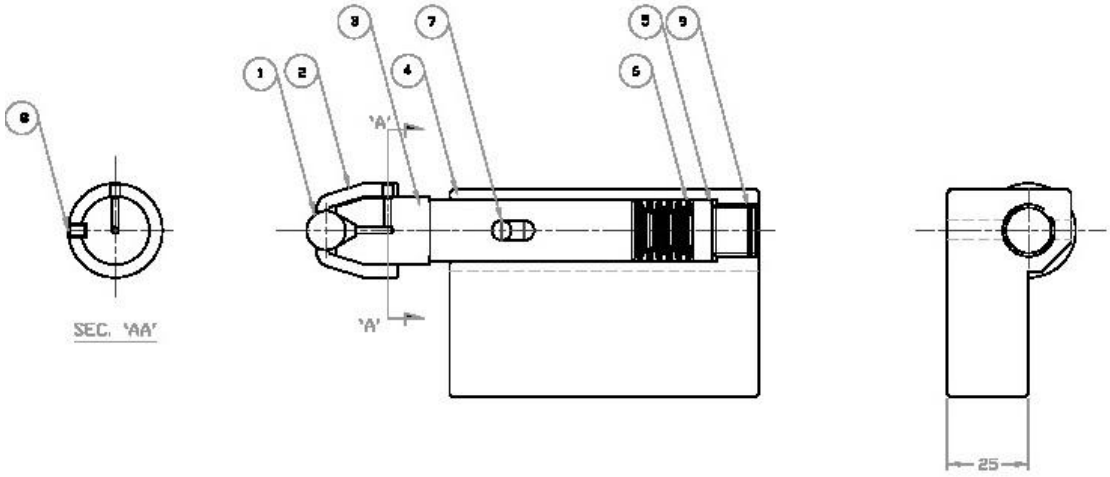

1	Ball- 1Nos	6	Belleville Spring- 14 Nos
2	Cage	7	Dowel pin
3	Mandrel	8	Set screw
4	Shank	9	SOC Set screw
5	Washer		

Figure 3.16 Sectional view of improved ball burnishing tool

3.2.2 Experimental Trials to compare the performance of improved ball burnishing tool with that of roller burnishing tool

To compare the performance of the ball burnishing with that of a roller burnishing tool, the above design was modified by replacing the ball holding arrangement with that of the flat roller. The roller burnishing tool and its sectional view are shown in Figure 3.17(a-b).

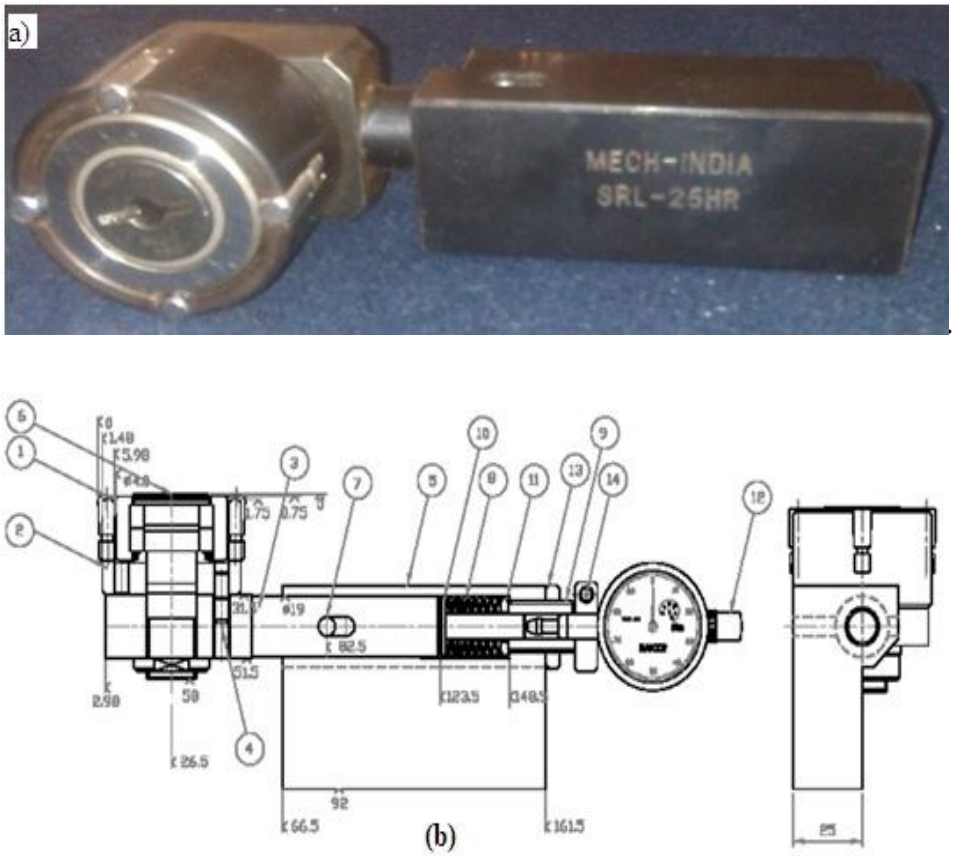

1	Roller- 4Nos	8	Belleville Spring- 14 Nos
2	Cage	9	Holder
3	Holder	10	Plunger
4	Screw	11	Washer
5	Shank	12	Pressure dial gauge
6	Stud type track roller	13	Hex. lock nut
7	Split Dowel pin	14	Screw

Figure 3.17 (a) Roller burnishing tool and (b) Sectional view

The construction of the improved roller burnishing tool is exactly similar to that of the ball burnishing tool, except for the roller attachment. The first part of rectangular cross section is a shank held on the lathe tool post, whereas the other part is a mandrel of material EN 31 to hold the stud type track roller. Around this roller four rollers, are fitted as shown in Figure 3.17. These small four rollers made of carbide material are made to rotate freely, having rolling contact around the stud type track roller. This

facilitates free movement of rollers. It consists of belleville spring to give the elastic support. The movement of the mandrel due to the applied burnishing force will cause compression of the spring. This compression can be measured with the help of the pressure dial gauge and the burnishing force can be computed. To compare the performance of ball burnishing and roller burnishing, with regards to surface roughness and hardness, the experimental trials were conducted varying one burnishing parameter, whereas keeping all the other burnishing parameters constant. Based on the earlier trials, the variable burnishing parameters selected for the experimental work are given in Table 3.11.

Table 3.11 Ball burnishing process parameters for comparative performance analysis of ball and roller burnishing tool

Parameter	**Range**
Burnishing speed(m/min)	10
Burnishing feed(mm/rev)	0.10,0.15,0.20
Burnishing force (N)	250,300,350
Number of passes	1,2,3
Lubrication	SAE 40 oil

3.3 WEAR TEST OF BURNISHED SAMPLES

12 mm diameter bars of titanium alloy (Ti-6Al-4V) were used as work materials .The bars were turned to proper dimensions i.e. 12 mm diameter and work specimens were prepared as shown in Figure 3.18. The work pieces were prepared with one recess such that each work piece could be used for two different burnishing conditions. The turned average roughness and hardness obtained were in the range from 0.40 to 0.45 μm (R_a) and 340 (*Hv*), respectively.

Figure 3.18 Titanium bars used in the ball burnishing experiments for wear tests

The identified process parameters and their levels in the current investigation of burnishing process are summarized in Table 3.12. According to Taguchi design concept, L_9 orthogonal array (OA) with 4 columns and 9 rows was selected (Phadke, M.S. 1989, Ross P.J.1996).Each burnishing process parameter is assigned to a column and nine different process parameter combinations are available. Thus, nine experiments are required to study the complete burnishing process parameter space using L_9 OA.The experimental layout for the current investigation using L_9 OA as shown in Table 3.10.

Table 3.12 Ball burnishing process parameters and their identified levels for wear tests

Code	Parameter	Levels		
		1	2	3
A	Burnishing Speed (m/min)	15	30	45
B	Burnishing Feed (mm/rev)	0.05	0.10	0.15
C	Burnishing Force (N)	150	200	250
D	No of passes	1	2	3

In the present study, external ball burnishing tests were performed under lubricated conditions using SAE 40 oil, as per the experimental plan given in Table 3.10, for wear test. The ball-burnishing tool, as show in Figure 3.11 is employed to carry out

the burnishing process. The surface roughness and hardness of the turned and burnished surfaces was measured. After turning and burnishing, cylindrical specimen was cut of 12mm diameter and 5mm thickness for each trial, as per experimental layout shown in Table 3.10. The specimen for wear tests were cut for 5mm thickness using wire electro discharge machining (EDM).Wire EDM was used because it is relatively faster and accurate way of preparing specimen from the turned bars without inducing unwanted residual stresses in the surface.

Dry sliding wear tests were conducted on all the burnished cylindrical specimens, on a pin-on-disc wear testing machine (Model: TR-20, DUCOM) shown in Figure 3.19 as per ASTM: G99-95 (ASTM 1995).The counterpart disc was made of quenched and tempered EN-32 steel having a surface hardness of 65HRC and surface roughness Ra=1.60µm. The cylindrical wear specimens of size Ø12×5 mm thickness cut from the burnished bar, were clamped in such a way that the burnished surface comes in contact with the counterpart disc as shown in Figure 3.20.The specimens were cleaned with acetone before conducting the test. The wear tests were conducted under uniform condition at a constant load of 10 N at a sliding velocity of 2.68 m/s and a sliding duration of 180sec as shown in Table 3.13.

Table 3.13 Parameters for friction and wear test.

Parameter	Value
Sliding Velocity , Vs (m/s)	2.68
Test Duration, t (sec)	180
Load , F_N (N)	10
Lubrication	Dry

All the tests were conducted in ambient air conditions with temperature and humidity in the range of 18–22°C and 52–62%, respectively (Bressan, J.D. and E Hesse, R 2001). The data collected from wear tests reflected the average value and standard deviation of 3 wear tests. Good repeatability was obtained in both friction and wear results. To determine the mass loss of the pin specimen for the evaluation of wear, an

electronic balance with an accuracy of 0.01mg was used. At the end of each test, the specimen was weighed again on the same balance after cleaning with acetone.

Figure 3.19 Wear testing machine

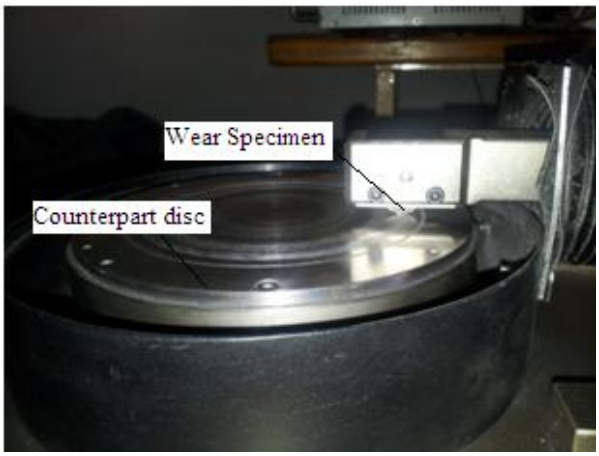

Figure 3.20 Experimental set up for wear tests with specimen

To measure slide mass loss, the difference between the initial and final weights was taken and was divided by the sliding distance to calculate the wear rate. The friction force was monitored by a load cell-based force measurement system. The micrograph of the burnished surface of titanium work-piece was obtained for each sample by

using scanning electron microscope. The micrograph of each burnished sample at other magnifications was also obtained in order to perform a detailed study. The residual stresses of turned and burnished parts were measured by X-ray diffraction method. The worn surfaces after wear testing were examined under scanning electron microscope.

3.4 RESPONSE MEASUREMENT TECHNIQUES

The samples of the machined and burnished specimen are mounted as shown in Figure 3.21 for microstructure analysis. The microstructure of machined and burnished surfaces of titanium work-piece was obtained for each sample by using scanning electron microscope (SEM). The microstructure of machined and burnished samples at other magnifications was also obtained to carry out a detailed study of the machined and burnished surfaces. The test samples were assessed for surface topographies and sub-surface micro-hardness.

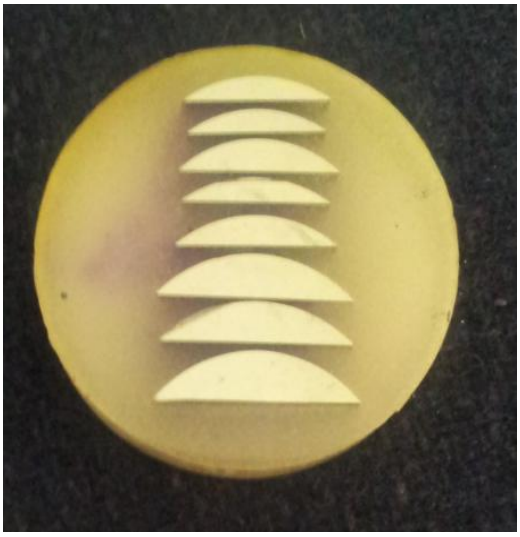

Figure 3.21 Specimen for sub surface hardness and SEM analysis

3.4.1 Measurement of surface finish

The surface roughness was measured to evaluate the quality of the turned and burnished surface. The Surf test model '*SJ-40*' (Mitutoyo make) surface roughness tester was used to measure the surface roughness of pre-machined, turned as well as burnished surfaces. Mitutoyo Surftest SJ-400 Series Portable Surface Roughness

Tester was used for measurement of surface roughness. A wide range, high-resolution detector and an ultra-straight drive unit provide class-leading accuracy. A high quality, high-speed thermal printer prints out measured results. It can also print a BAC curve or an ADC curve as well as calculated results and assessed profiles. These results and profiles are printed out in landscape format, just as they appear on the LCD, in easy-to-understand form. The level of accuracy for a measuring range of 800 μm, resolution was 0.01 μm and the straightness/traverse length was 0.3 μm/.98"(25mm).The surface roughness measurements were performed with a cutoff length of 0.8 mm and an average of five readings was taken as a process response. Figures 3.22 depicts surface roughness measuring device used in the present work.

Figure 3.22 Surface roughness tester

3.4.2 Measurement of surface hardness

Figure 3.23 shows Vickers hardness tester used in the present work. The hardness of each specimen was measured using computerized microvickers hardness testing machine (Model '*VM50 50PC'*) along the length as well as around the periphery. The instrument used for testing hardness used "State of the Art" image processing technology. This tester is suitable for measuring the hardness of precision metallic parts with wide testing range - from soft to hard and their accurate results are widely acclaimed. The tester strictly confirmed to IS 1754 - 2002.Vickers micro-hardness

Figure 3.23 Vickers hardness device

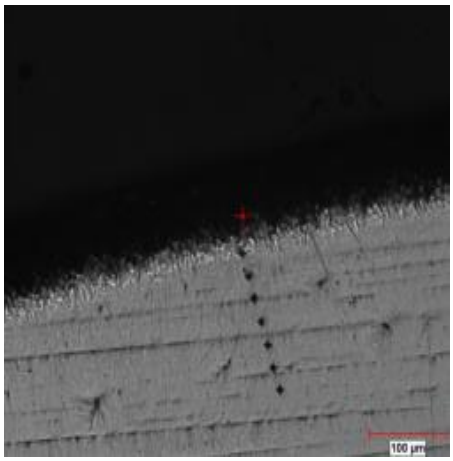

Figure 3.24 Optical image of indentation markings for microhardness measurement of burnished surface

measurements are carried out using an indentation load of 300 g and allowing a dwell time of 15 seconds for each indentation. Each micro-hardness value reported in the present work is an average value of three measurements for each specimen. The optical image of the indentation marking beneath for microhardness measurement is shown in Figure 3.24.

3.4.3 Residual stress measurement

The residual stress values of burnished parts were measured by X-ray diffraction method. Residual stress measurements were performed by X-ray diffraction using synchrotron radiation from Bruker. The characteristic of the used beam line EDDI offers a white X-ray beam with an energy range of 10–80 keV. The primary beam cross section was set to 0.5 mm×0.5 mm. The angular divergence in the diffracted beam was restricted to $\Delta\theta \leq 0.005^{\circ}$ by a double slit system with apertures of 0.03 mm × 5 mm. The scattering angle was chosen to be 8° considering the energy of X-ray. Energy-dispersive X-ray diffraction (EDXRD) gives complete diffraction spectra for a fixed detector position. Any Bragg reflection was obtained by a different X-ray energy (wavelength), i.e. the signal of any reflection belongs to a different depth in the specimen. Due to the limited usable energy range provided by the 7 T multipole wiggler which extends from about 10–80 keV, the maximum information depth for titanium accessible in reflection mode experiments is about 100µm. In order to get a stress distribution in deeper region, two or three specimens were prepared for each condition. For one or two of them, layer removal in a step of 100‑150 µm was applied by electro polishing. The correction on the measured residual stress was made for the electro polished specimens. Residual stresses were evaluated by means of the $\sin^2\psi$ method, where ψ is the tilting angle, in steps of $\Delta = 4^{\circ}$ up to 80°. A modified multi-wavelength approach for any energy line $E_{(h\,k\,.l)}$ gives an average penetration depth $\tau_{(h\,k\,.l)}$. $\tau_{(h\,k\,.l)} = (\tau_{(h\,k\,.l)}\,\min + \tau_{(h\,k\,.l)}\,\max) / 2$. Where $\tau_{(h\,k\,.l)}\,\min$ and $\tau_{(h\,k\,.l)}\,\max$ are the minimum and the maximum penetration depths corresponding to the maximum (ψ_{max}) and minimum (ψ_{min}) tilting angles, respectively. The X-ray diffraction elastic constants of α and β phases were calculated by the Kroner-Model. Residual stresses at the surface were determined using laboratory X-ray diffraction (D-5000) using Cu-Ka1 radiation with a wavelength of 1.54 A^{o}. The {2 1 .3}-Bragg peak was used with diffraction elastic constants of $S_1 = -2.564 \times 10^{-6}\ MPa^{-1}$ and $1/2S_2 = 1.083 \times 10^{-5}\ MPa^{-1}$.The $\sin^2\psi$ method was used to evaluate the surface residual stresses with tilting angle range of -45^{o} to $+45^{o}$ in steps of $\Delta\sin^2\psi = 0.125$. Ball burnishing, results in plastic deformation on the part surface leading to a significant modification of the residual stress state. X-ray diffraction (XRD) techniques were used for the residual

stress measurement. XRD allows measuring the stress field on the surface or close to the surface. Thus, electro-polishing the specimen surface was a feasible option to obtain deep measurements; other methods could change the stress state of the specimen.

3.4.4 SEM Micrograph

The micrograph of burnished surface specimens and worn surface of wear test samples are examined on a field emission scanning electron microscope (Model: JEOL JSM-6480LV) using secondary electron (SE) and backscattered electron (BSE) imaging modes, whereas chemical compositions of the constituent phases are examined using an energy dispersive X-ray (EDX) micro analyzer. The SEM is operated at an acceleration voltage of 10-30 kV. For examination by optical microscope or in SEM by SE-signal mode, polished samples were submerged in Kroll's reagent for 15 seconds. After etching, they were immediately rinsed in ethanol and then water. The Kroll's reagent with composition 92ml distilled water, 6 ml nitric acid and 2ml HF was used as macro- and micro etchant**.** After mechanical polishing and etching for some specimen, thorough rinsing in ultrasonic acetone bath was performed. Samples were then flushed with ethanol. All the samples were cleaned in plasma cleaner as a final step, before insertion into SEM. Samples where handled with rubber gloves after this final cleaning stage.

3.4.5 Electron back-scattered diffraction (EBSD)

Electron back-scattered diffraction (EBSD) analyses were performed on burnished specimens. EBSD has been used for materials characterization including characterization of grain boundary types, characterizing texture and its changes during deformation process burnishing, establishing links between grain size and texture components during deformation. The sample is prepared to carry out EBSD analysis by electro polishing. The viable option to obtain deep measurements was electro-polishing, as other methods could change the stress state of the piece. Electro polishing is a chemical surface finishing technique by which metal is electrolytically removed ion by ion, from the surface of the metal object .Since electro polishing

involves no mechanical, chemical or thermal impact, small mechanical parts can be treated. To carry out the process of electro polishing, three operations were carried out metal preparation, electro polishing and post treatment. The instrument Struers Electropol 5 as shown in Figure 3.25 is used for electro polishing. The paper of 400, 1000, 2500 Grade were used for diamond polishing with 1 micron diamond paste.

Figure 3.25 Struers ElectroPol-5 polishing and etching cell.

Figure 3.26 FEI Quanta 3D FEG

The electro-polishing solution used was an equal volume mixture of 80% mass fraction methanol and 20% percloric acid solution. The operating conditions were current densities of 15V and operation time is of 45 sec. The image of microstructure was reconstructed by creating grain boundary maps from the EBSD pattern measurements. The image of the set up used for EBSD analysis is given in Figure 3.26. Automatic generation and indexing of EBSD patterns were carried out on SEM of FEI Company produced by TSL Technology Inc., which was equipped with a back-scattered electron detector and OIM software (Version-7.O.1) for analysis. The experimental software used is TSL OIM data collection. Beam scan mode was adapted with a step spacing of 0.8 mm.

3.5 FINITE ELEMENT MODELING

3.5.1 Finite Element Model description

The main objective of this study is to present a FE model for ball burnishing. Here, the geometry and the mesh were created using LS-PrePost. This is an advanced pre and post-processor tool from Livermore Software technology corporation (LSTC). Due to large variation in the stress components throughout the layers beneath the contact zone, small elements should be assigned to this region. From the study conducted by Liu, Y et al. 2011, it is revealed that proportion of the smallest size to the diameter of dimple generated in the contact zone is recommended to be about 1/10th in the ball burnishing process. The geometric workpiece model considered in the 3D FEM simulations is shown in Figure 3.27. The workpiece is modelled by a portion of a cylindrical part. The choice of workpiece size in 3D FEM simulations takes into account the real dimensions of the treated piece, the presented boundary conditions and the optimization of computational time. The external radius is equal to the rod bar radius which is utilized in experimental work. The mesh generated of the ball tool and the workpiece in the 3D ball burnishing simulation are shown in Figure 3.27.

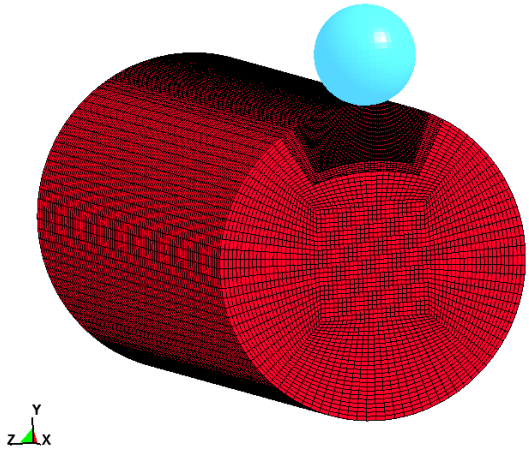

Figure 3.27 Meshing of the ball tool and the workpiece in the 3D ball burnishing simulation

As described, in the contact zone, fine elements should be used. However, in the regions, which are far away from the contact zone, course elements can be generated to decrease the number of degrees of freedom and computational costs. Smooth transition between the fine and coarse elements should be provided using intermediate elements. In this study, linear tetrahedral elements are used to discretize the work piece and ball. Taking these facts into consideration the mesh for the specimen was created such that at the area of contact the element size was very fine and gradually the mesh was coarsened out. This helped to minimize the number of element count. FEM analysis was carried out with sufficient mesh density in the region of burnishing and lesser density elsewhere. Initially, to determine the effect of the mesh density on computational accuracy, processing time and program convergence, different types of FE mesh were prepared and studied for the 3D model. Finally, a FE model with 283,550 eight-node C3D8R elements and 300,456 nodes was prepared with increased mesh density in the area close to the surface, as shown in Figure 3.28.

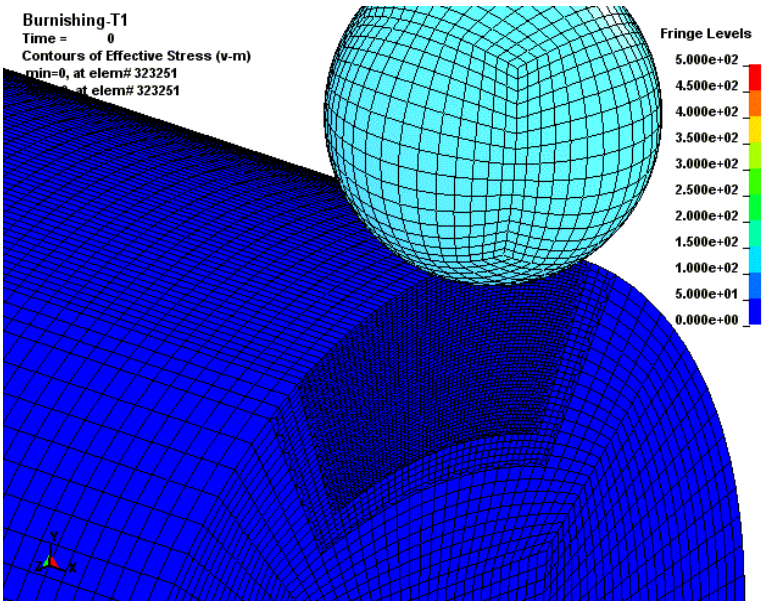

Figure 3.28 Discretization of the ball and the workpiece in the 3D ball burnishing simulation

Rotating quads were used in order to achieve transition of mesh. Solid brick element having Elform 2 (Fully integrated elements) were used. The nodes are shown in Figure 3.29.The spherical indenter was modelled with rigid shell elements having properties of tungsten carbide material and the Ti-6Al-4V workpiece was modeled considering as kinematic plastic material. The properties of both material models are given in Table 3.14.

The FE model is based on the following assumptions:

1. The ball tool is considered rigid and is modelled by an analytically rigid part.
2. The work piece is considered as kinematic plastic material.
3. The surface roughness profile is neglected.
4. The ball burnishing speed effect is neglected.

A number of different empirical constitutive models based on the isotropic hardening behavior have been previously developed for Ti–6Al–4V material such as Sellars–Tegart model (Sellars and Tegart 1966), Johnson– Cook model (Johnson and Cook 1985) and polynomial relation model (Westman 2003). The Johnson–Cook model has been widely used in the literatures to characterize Ti–6Al–4V.

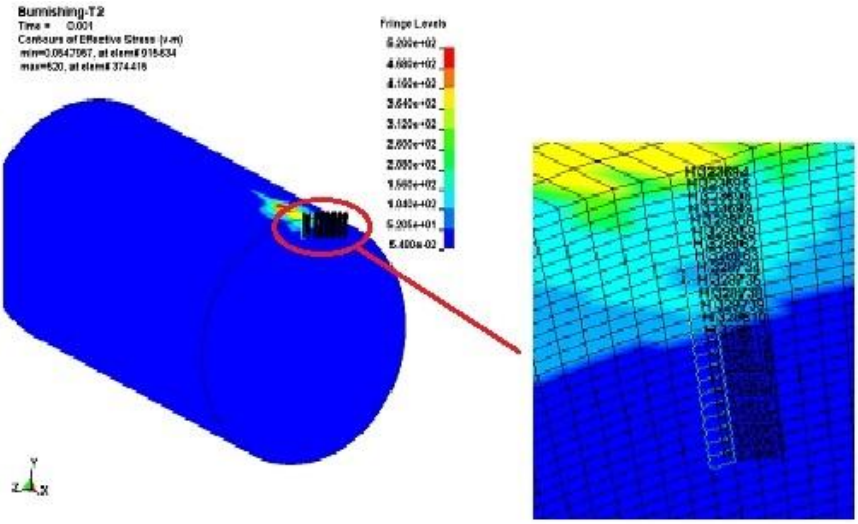

Figure 3.29 Magnified view of the nodes

In this model, the material properties not only depend on the strain, but also depend on the temperature and strain rate. Johnson–Cook constitutive model for Ti–6Al–4V is a simple numerical material model developed for isotropic material. In this material model, it is assumed that elastic strains are negligible in comparison to plastic strain. The elastic domain is defined by means of the Von-Mises yield criterion, and it is assumed that isotropic strain hardening is sufficient to describe the evaluation of the yield surface during plastic deformation.

Table 3.14 Material properties used for finite element simulation

a) Ball	
Material	Tungsten Carbide
Density (kg/m^3)	15800
Elastic Modulus (GPa)	700
Poisson's ratio	0.24
b) Workpiece	
Material	Titanium Alloy (Ti-6Al-4V) Grade 5
Density (kg/m^3)	4510
Elastic Modulus (GPa)	113.8
Poisson's ratio	0.31
Yield Strength (MPa)	900
Tangent Modulus (GPa)	10

Strain hardening is thus described in terms of the damage accumulated plastic strain. It is further assumed that the elastic and visco-plastic properties of the material depend on the temperature generated by adiabatic heating under high strain rate loading conditions, while any thermo-mechanical coupling with the surrounding is not included in the formulation. The parameters given in Table 3.15, which provide better agreement with experimental data, are utilized in the Johnson– Cook material model here.

Table 3.15 Set of parameters for the Johnson-Cook model

Properties	Symbol	Value	Properties	Symbol	Value
Density	ρ	7850 kg/mm^3	Johnson Cook Thermal softening parameter	M	0.0
Young's Modulus	E	200GPa	Critical damage parameter	DC	0.3
Poisson's Ratio	PR	0.3	Damage threshold	PD	0
User defined strain rate normalization factor	E0DOT	5E-4	Fracture parameter 1	D1	0.0705
Room temperature	Tr	293K	Fracture parameter 2	D2	1.732
Melt temperature	Tm	1800K	Fracture parameter 3	D3	-0.54
Initial temperature	To	293K	Fracture parameter 4	D4	-0.015
Johnson Cook yield stress	A	900Mpa	Fracture parameter 5	D5	0
Johnson Cook hardening parameter	B	380Mpa	Critical temperature parameter	TC	2000
Johnson Cook hardening Parameter	n	0.73	Critical shear stress parameter	TAUC	2000
Johnson Cook Strain rate sensitivity parameter	C	0.0114			

3.5.2 Finite element simulations

The movement of the ball with respect to workpiece can be controlled by the displacement of tool. This method would require information on the ball penetration depth for the given process settings. This depth value, involving plastic deformation, changes from one cycle to another. It cannot be solved analytically due to the nonlinearity of the workpiece properties and is usually very difficult to measure during ball burnishing experiments. The relationship between the force and ball penetration depth is obtained from series ball burnishing simulations as shown in Figure 3.30. To apply the required burnishing force during simulation, the corresponding penetration depth is calculated from a 3D indentation simulation test results given in Figure 3.30. The movement of the ball in the simulation can be controlled, by using two different ball movement controls, that is, displacement control and force control. In the force control, the ball presses on the work piece until the maximum applied load is reached for every indentation cycle. This type of loading does not strictly reflect the real load applied to the part during cylindrical rolling. Indeed, the real contact is a sphere/cylinder one, whereas the 2D model simulates a cylinder/plane contact.

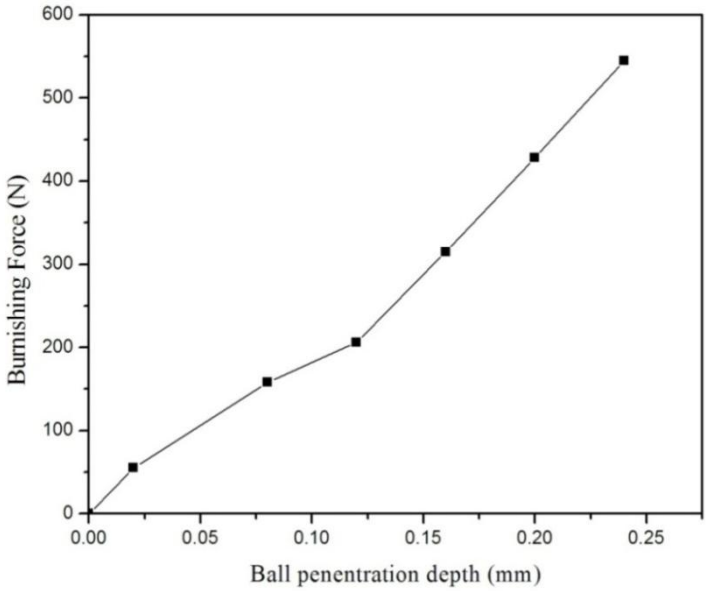

Figure 3.30 Burnishing force versus penetration depth obtained from 3D ball burnishing simulations

For these reasons, it is preferred to use the displacement control method in the 3D FEM. This load is a succession of three repetitive movements.

To attain a sufficient simulation area, eight cycles of the burnishing process were carried out .The load stages of each cycle are given below:

Stage 1: the ball traverses down vertically applying the corresponding burnishing force related to the phase of penetration into the material (loading)
Stage 2: the ball traverses to the initial position (unloading)
Stage 3: the ball traverses horizontally with a displacement value of burnishing feed (feed per revolution)

The specimen was fixed axially at one end in translation DOF. To reduce the analysis time, it was assumed that the same effect of experiment would be achieved if the specimen was not rotated and if the indenter moved axially on the surface of specimen. Nodes to surface contact were evoked in order to get a better correlation of the results. Considering the fact that sliding between analytical rigid ball and deformable workpiece is inevitable, the simulation has been conducted so that the friction has been introduced in order to avoid sliding between the ball and workpiece as assumed in the study given by Fischer-Cripps (2007). A friction parameter of μ=0.3, was assumed for the contact between the tool and the workpiece during modeling as per the classical Coulomb law. The spring-back analysis was conducted after ball burnishing, in order to achieve the steady state of residual stress profile. However, it was found that this analysis was not practical to be simulated, since long time is required to reach the steady state. Thus implicit method was used to simulate the spring-back analysis , since after removing the ball there is no complexity due to contact between the parts and consequently different nonlinearities are not involved in the spring- back problem.

In conducting the simulations, the following burnishing conditions were used:

- Burnishing ball diameter = 8 mm
- Burnishing force (N) =150,200,250,300 and 350
- Burnishing feed rate (mm/rev) = 0.05, 0.10, 0.15, 0.20 and 0.25
- Number of passes=1

In this chapter, the experimental details for turning of Ti-6Al-4V as a pre-machining process are explained in detail. The experimental process and settings to carry out the burnishing trials are also presented. The newly developed ball and roller burnishing tool is put on trial to study its performance. Important process parameters, their levels, range and responses are identified. The design of experimental plan for conducting the experiments, the response measurement methods, finite element modeling of the burnishing process and the trials conducted to measure the improvement in wear resistance of burnished components are also presented in this chapter.

The following chapters discuss in detail on the results of turning and burnishing experiments, design of experiments, finite element analysis of burnishing process and enhancement in wear resistance.

Chapter 4

ANALYSIS OF SURFACE ROUGHNESS DURING MACHINING OF TITANIUM ALLOY WITH PCD TOOL

4.1. OBJECTIVE

This chapter deals with the investigation on machining of difficult-to-machine material titanium alloy (Ti–6Al–4V) using poly crystalline diamond (PCD) tool under different coolant strategies, namely dry, flooded and minimum quantity lubrication (MQL), as pre-machining for burnishing operation. Taguchi technique has been employed to arrive at the optimum results. As seen from the literature, most of the researchers used the cutting conditions namely cutting speed, feed and depth of cut as input parameters. But as per author's knowledge, no methodical research work has been reported in the literature to determine the best lubricating mode along with appropriate cutting conditions for achieving better surface quality using poly crystalline diamond (PCD) inserts as the cutting tool. Interestingly, tool nose radius, one of tool geometry parameters, has not been scientifically investigated, most likely due to its spontaneous effects on part surface finish. An attempt has been made in this chapter, to determine the optimum process parameters namely lubricating mode, cutting speed, feed rate, nose radius and depth of cut during turning of Ti-6Al-4V alloy using PCD tool so as to obtain the best surface finish using Taguchi method.

4.2. EXPERIMENTAL WORK

In the current study, five parameters, namely, lubricating mode, cutting speed, feed rate, nose radius and depth of cut were identified. The ranges for feed rate and depth of cut were selected based on the recommendations given by the insert manufacturer. The highest value of the cutting speed and the ranges of other parameters were selected after preliminary tests. Each parameter was investigated at three levels to study the non-linearity effect of the process parameters. The identified control factors and their levels are given in Table 4.1

Table 4.1 Control factors and levels for turning

Control Factors	Levels		
	1	2	3
Lubricating Mode (A_t)	Flood	MQL	Dry
Cutting Speed(B_t), m/min	50	100	150
Feed rate (C_t), mm/rev	0.15	0.25	0.35
Nose radius(D_t), mm	0.2	0.4	0.6
Depth of Cut(E_t), mm	0.25	0.5	0.75

The measured values of surface roughness and hardness with the corresponding signal noise ratio are summarized in Table 4.2.

4.3 RESULTS AND DISCUSSION

4.3.1. Analysis of means and variance

In the present work, the objective is to minimize the surface roughness and maximize the surface hardness. Hence, "smaller the better type" category is used for surface roughness and "larger the better type" category for surface hardness have been selected (Phadke.M.S. 1989). The S/N ratios associated with the objective functions for each trial of the OA are given by:

$$\eta_1 = -10\log_{10}(R_a^{\,2}) \tag{4.1}$$

$$\eta_2 = -10\log_{10}(H^{-2}) \tag{4.2}$$

The corresponding S/N ratios for each trial of L_{27} orthogonal array were determined using Equations (4.1) and (4.2) for surface roughness and surface hardness respectively and are presented in Table 4.2 which gives the combinations of experimental machining parameters and parameter levels in the L_{27} orthogonal array (OA). A total of 27 experiments were conducted in accordance with the parameter level of each factor and observed values of surface roughness and surface hardness

Table 4.2 Control factor settings as per L_{27} OA, with the measured responses and the corresponding signal to noise ratios for turning

Trial No.	A_t	B_t	C_t	D_t	E_t	Surface roughness (R_a), µm	Hardness, *H* (Hv)	S/N ratio for surface roughness, η_1 (dB)	S/N ratio for hardness, η_2 (dB)
1	1	1	1	1	1	1.02	311	-0.1720	49.8552
2	1	1	1	1	2	1.04	312	-0.3407	49.8831
3	1	1	1	1	3	0.99	315	0.0873	49.9662
4	1	2	2	2	1	2.05	316	-6.2351	49.9937
5	1	2	2	2	2	2.45	318	-7.7833	50.0485
6	1	2	2	2	3	2.8	319	-8.9432	50.0758
7	1	3	3	3	1	2.65	318	-8.4649	50.0485
8	1	3	3	3	2	2.15	320	-6.6488	50.1030
9	1	3	3	3	3	2.43	321	-7.7121	50.1301
10	2	1	2	3	1	1.35	323	-2.6067	50.1841
11	2	1	2	3	2	1.75	325	-4.8608	50.2377
12	2	1	2	3	3	1.65	326	-4.3497	50.2644
13	2	2	3	1	1	3.85	327	-11.7092	50.2910
14	2	2	3	1	2	3.65	328	-11.2459	50.3175
15	2	2	3	1	3	3.49	329	-10.8565	50.3439
16	2	3	1	2	1	0.91	331	0.8192	50.3966
17	2	3	1	2	2	0.89	332	1.0122	50.4228
18	2	3	1	2	3	0.92	334	0.7242	50.4749
19	3	1	3	2	1	3.25	337	-10.2377	50.5526
20	3	1	3	2	2	3.27	338	-10.2910	50.5783
21	3	1	3	2	3	3.26	341	-10.2644	50.6551
22	3	2	1	3	1	1.75	342	-4.8608	50.6805
23	3	2	1	3	2	1.85	346	-5.3434	50.7815
24	3	2	1	3	3	1.89	347	-5.5292	50.8066
25	3	3	2	1	1	2.12	336	-6.5267	50.5268
26	3	3	2	1	2	1.97	339	-5.8893	50.6040
27	3	3	2	1	3	2.15	345	-6.648	50.7564

were noted, which were further converted to corresponding S/N ratio. Table 4.3 and 4.4 help to find the optimal combination level of the machining parameters and the extent to which the machining parameters affect the observed values were evaluated. The analysis of means (ANOM) based on S/N ratio was carried out to determine the optimal levels of control factors**.** The results of ANOM for surface roughness and hardness are represented in Tables 4.3 and 4.4 respectively.

Table 4.3 ANOM for surface roughness based on S/N ratio for turning

Factor code	Levels			Optimum level
	1	2	3	
A_t	-5.1347	-4.7859	- 7.2879	2
B_t	-4.7817	-8.0563	-4.3706	3
C_t	-1.5115	-5.9826	-9.7145	1
D_t	-5.9224	-5.6888	-5.5974	3
E_t	-5.5549	-5.7101	-5.9436	1

Table 4.4 ANOM for surface hardness based on S/N ratio for turning

Factor code	Levels			Optimum level
	1	2	3	
A_t	50.0116	50.3259	50.6602	3
B_t	50.2418	50.3710	50.3848	3
C_t	50.3630	50.2990	50.3356	1
D_t	50.2827	50.3554	50.3596	3
E_t	50.2810	50.3307	50.38599	3

The level of a parameter with the highest value of S/N ratio is the best combination level. The optimal parameter setting is found to be MQL lubricating mode (A_t2), high cutting speed of 150 m/min (B_t3), lowest feed rate of 0.15 mm/rev (C_t1), higher nose radius of 0.6mm (D_t3) and lowest depth of cut 0.25mm (E_t1) for minimum surface roughness. Whereas, for maximum surface hardness dry mode (A_t3), high cutting

speed of 150 m/min (B_t3), lowest feed rate of 0.15 mm/rev (C_t1), higher nose radius of 0.6mm (D_t3) and highest depth of cut 0.75 mm (E_t3) are the optimum parameter settings. The results of the ANOM table are also shown in the main effect plots shown in Figures 4.1 and 4.2, for surface roughness and hardness respectively. The main effect plots (Figures 4.1 and 4.2) are generated using *MINITAB* statistical software for exploring the effects of control factors on surface roughness and hardness.

To examine the effects of control factors quantitatively, the analysis of variance (ANOVA) based on S/N ratio has been performed (Phadke.M.S.1989). The ANOVA is accomplished by separating total variability of S/N ratio, which is measured by sum of squared deviations from total mean of S/N ratio into contributions by each of the factors and the error. The summary of ANOVA results for surface roughness and surface hardness are shown in Table 4.5 and Table 4.6 respectively. It can be seen from the ANOVA (Table 4.5) that the feed rate (72.32%) and cutting speed (17.49%) have major contributions, whereas lubricating mode (7.87%) has a less significant role in minimizing the surface roughness. On the other hand, nose radius and depth of cut have the least effects in minimizing the surface roughness.

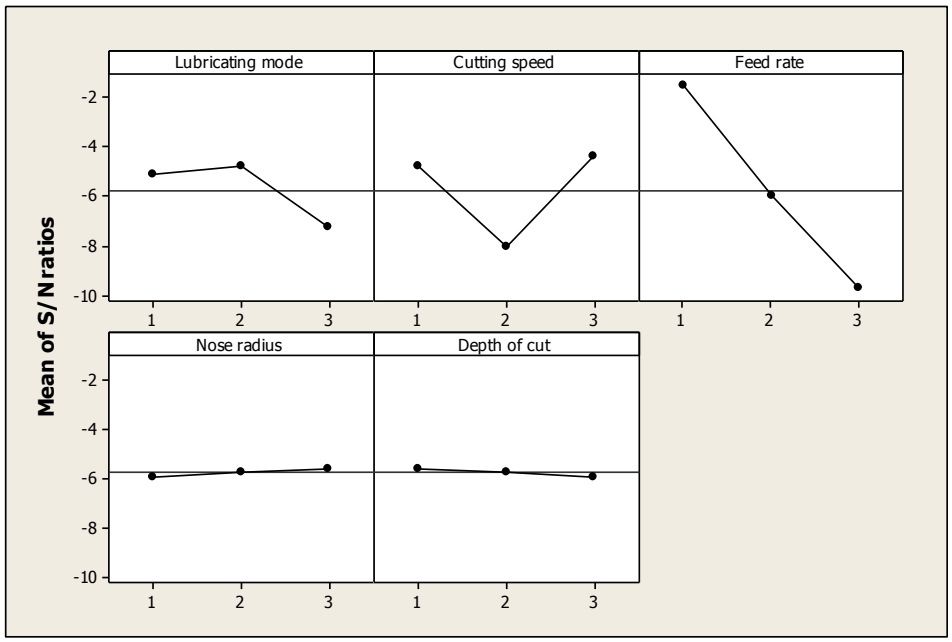

Figure 4.1 Main effect plots of surface roughness based on S/N ratio for turning

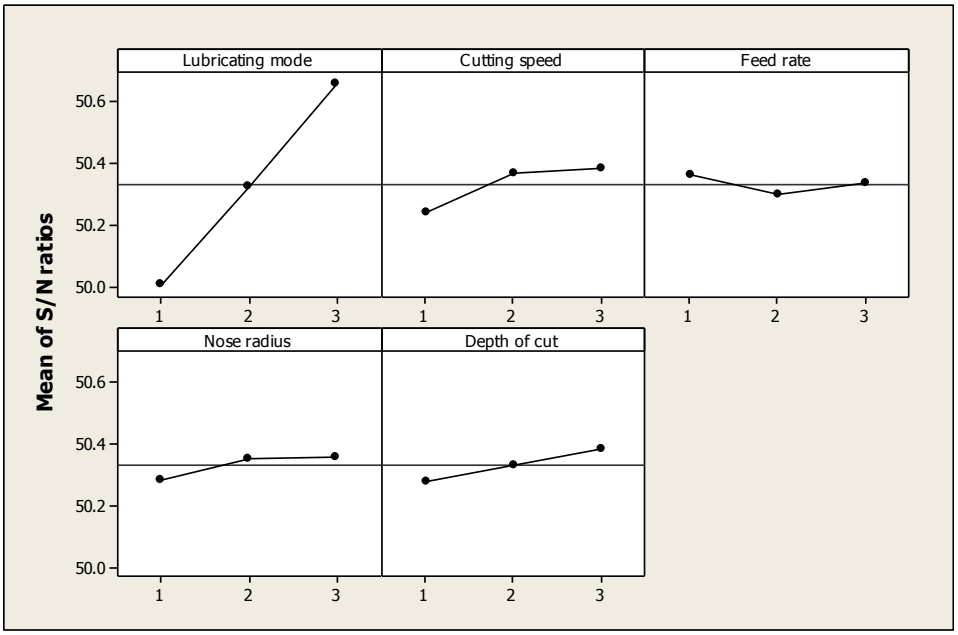

Figure 4.2 Main effect plots of surface hardness based on S/N ratio for turning

It is clear from ANOVA results of Table 4.6 that the lubricating mode (89.27%) and cutting speed (5.28%) are the major contributors, whereas feed rate, nose radius and depth of cut play less significant roles in maximizing the surface hardness.

Table 4.5 ANOVA for surface roughness based on S/N ratio for turning

Factor code	Degrees of freedom	Sum of squares	Mean square	% contribution
A_t	2	33.0537	16.5268	7.87
B_t	2	73.4293	36.7147	17.49
C_t	2	303.6227	151.8113	72.32
D_t	2*	0.5058	0.2529	0.12
E_t	2*	0.6891	0.3446	0.17
Error	16	8.5342	0.5334	2.03
Total	26	419.8348	16.1475	100
(Error)	(20)	(9.7291)	(0.4865)	

***** Factors D_t and E_t are pooled.

Table 4.6 ANOVA for surface hardness based on S/N ratio for turning

Factor code	Degrees of freedom	Sum of squares	Mean square	% contribution
A_t	2	1.8938	0.9469	89.27
B_t	2	0.1119	0.0560	5.28
C_t	2	0.0186	0.0093	0.87
D_t	2	0.0337	0.0168	1.59
E_t	2	0.0496	0.0248	2.34
Error	(16)	(0.0138)	0.0009	0.65
Total	26	2.1214	0.0816	100

Validation experiments were performed at the optimal levels of the control factors and the prediction error is found to be within the 95% confidence limit; indicating the adequacy of the additivity of the proposed surface roughness and hardness models. The best combinations of the control factors for minimizing the surface roughness and maximizing the hardness along with the corresponding optimal values are presented in Table 4.7.

Table 4.7 Optimal control factor settings and the corresponding optimal values of surface roughness and surface hardness for turning

Response	Optimal process parameter setting					Optimal value
	Lubricating mode	Cutting speed (m/min)	Feed (mm/rev)	Nose Radius (mm)	Depth of Cut (mm)	
Surface roughness	MQL	150	0.15	0.6	0.25	0.81 µm
Surface hardness	Dry	150	0.15	0.6	0.75	349 Hv

4.3.2 Analysis of Surface Roughness for turning

4.3.2.1 Effect of lubricating mode

From Figure 4.1, it is evident that, the surface roughness is low for MQL machining in contrast to dry and flooded conditions. The cutting fluid which is supplied at high pressure and velocity penetrates minute particles into tool-chip and tool-work piece surfaces, during flooded lubricant conditions, reduces the friction thereby resulting in lower surface roughness. In contrast, MQL machining provides both cooling and lubrication effectively. The cooling provides convective as well as evaporative heat transfer and hence lower surface roughness is obtained during MQL machining when compared to flooded lubrication (Machado and Wallbank J 1990). Moreover, during flooded condition, an effective penetration of the cutting fluid into tool-chip as well as tool- work surface is not possible along with convective heat transfer. Therefore, surface roughness is more in flooded when compared to MQL condition. On the other hand, during dry machining, as no cutting fluid is supplied, it results in high friction, high tool wear and low heat transfer, which in turn lead to higher surface roughness. Similar results were obtained by Dhar et al. (2006) during turning of AISI 1040 steel. Their results of study showed that MQL machining is better than conventional flood coolant system. The benefit over flood condition is obtained by reducing the cutting temperature. Finally, it can be concluded that MQL machining provides better performance in terms of reduction in surface roughness as compared to dry and flooded lubricant condition (Diniz et al. 2003). Hence, it is recommended to implement MQL machining in order to improve surface finish, reduce the quantity of lubricant, cost and prevent environmental pollution. My results agree with the study. Domnita and Cristian (2012) concerning the use of MQL to AISI 1045 turning with carbide insert under finishing conditions, which confirmed that the environmental-friendly techniques, particularly MQL, can be successfully implemented without affecting the process results, in this case by meaning of surface quality.

4.3.2.2 Effect of cutting speed

From ANOVA analysis (Table 4.5), it is evident that cutting speed has noticeable contribution (17.49%) in minimizing the surface roughness. From Figure 4.1, it is clear that the surface roughness of the machined component decreases with increase in cutting speed. The reduction in surface roughness can be attributed to the increase in cutting temperature, which increases the softening of the work piece material and hence reduces the cutting forces, leading to better surface finish. A similar result was also reported by Che-Haron and Jawaid (2005) during machining of Ti-6Al-4V alloy with 883 inserts under dry cutting conditions where low surface roughness was obtained with an increase in cutting speed. Besides this, with the increase in spindle speed the chip will break away with less material deformation at the immediate tool tip region, which in turn maintains the machined surface properties resulting in minimal surface roughness. Furthermore, the spindle speed should be controlled at an optimum value, as the influence of high temperature would significantly have an effect on the chip formation mode, cutting forces and tool life. The surface roughness could be improved by increasing cutting speed, though the improvement is very limited at higher cutting speed (100-150 m/min). The surface finish is also related to the formation of built up edge at different cutting speed. With the increase in cutting speed, the possibility of formation of BUE is eliminated, thereby resulting in improvement of surface finish. During my current investigations on Ti-6Al-4V alloy machining, the cutting speeds are higher than those favoring BUE formation. From the experimental works of Chen (2000) and Bouacha et al. (2010), it is reported that the deformation velocity depends on the properties of metals i.e., higher the velocity, less important is the plastic behavior. If the material exhibits less plasticity by increasing the cutting speed and hence deformation velocity, the surface finish can be enhanced, because of less significant lateral plastic flow and consequently less additional increase in the peak-to-valley height of the machined surface roughness. One of the reasons for poor surface finish at low cutting speed is due to the development of grooves on the tool wear face. With the increase in development of the grooves, the surface finish further deteriorates.

4.3.2.3 Effect of feed rate

From ANOVA (Table 4.5), it is seen that feed rate has the major contribution (72.32%) in minimizing the surface roughness. These results agree with the results of the study by Nikos (2010) using Response Surface Methodology (RSM) and fuzzy logic system through the Adaptive Neuro-Fuzzy Inference System (ANFIS), who verified that feed rate was the most important parameter affecting the surface roughness of Ti-6Al-4V. From the main effect plots of surface roughness based on S/N ratio in Figure 4.1, it is evident that as feed rate increases, the surface roughness also increases. My results agree with the earlier investigations by Cakir et al. (2009) that among the cutting parameters, feed rate had the greatest impact on surface roughness followed by cutting speed. Their work also established that, increase in feed rates led to higher surface roughness values. From the experimental trials conducted by Ramesh et al. (2012) on turning of titanium alloy (Grade-5) it was confirmed that the feed was the factor which influenced surface roughness followed by cutting speed. The surface roughness increased with increase in feed but decreased with increase in cutting speed. Moreover as the feed rate increases, the surface roughness also increases because of less available time to carry out the heat from the cutting zone, high amount material removal rate and an accumulation of chip between the tool-work piece zones. As a result of rise in temperature at tool-chip interface, the tool wear increases and hence surface roughness increases. The mathematical relation between theoretical surface roughness and feed rate given by Boothroyd and Knight (1989) and Davim, J.P (2001) in equations (4.3) and (4.4) further establishes the fact that , surface roughness increases with the increase in feed rate.

$$R_{at} = f^2 / 32r \times 1000 \quad (4.3)$$

$$R_{tt} = f^2 / 8r \times 1000 \quad (4.4)$$

However, MQL shows reduction in surface roughness when compared to dry and flooded condition under different feed rates due to the MQL delivery pressure applied, which in turn will remove chips (debris) from the cutting zone.

4.3.2.4 Effect of nose radius

It is evident from the main effect plots of surface roughness based on S/N ratio (Figure 4.1) that the surface roughness decreases with increased tool nose radius.As tool nose radius increases, the contact length between tool and work piece increases, diminishing the height of feed marks and therefore, reducing the surface roughness. As predicted theoretically (R_{th}= f ^{2}/8r), surface roughness decreases with increased tool nose radius (Boothroyd and Knight 1989). However, it was also noticed that at low feed rates, there was a deviation from the theoretical prediction. The reason attributed to this is the ploughing action caused by smaller uncut chip thickness. Tools with larger nose radius perform better with regards to surface finish in contrast to smaller nose radius tools during cutting (Escalona and Cassier 1998). My results agree with the work of Ashvin et al. (2013) during turning of AISI 410 steel that the surface roughness decreases with the increase in tool radius. The tool nose radius plays an important role in producing the finished surface, because if the nose is made to a sharp point, the surface finish deteriorates and tool life decreases.

4.3.2.5 Effect of depth of cut

From ANOVA analysis (Table 4.5), it is evident that depth of cut has minimum contribution (0.17%) in minimizing the surface roughness and has no significant effect on the surface roughness. It is quite evident from Figure 4.1 that the surface roughness increases with increased depth of cut, mainly due to increase in thermal load and vibration of the machine tool. Further, due to more contact area between tool and work piece, high friction and tool wear exist and hence leading to higher surface roughness. Colafemina et al. (2007) conducted several experiments on Ti-6Al-4V alloy machining and established relationship between depth of cut and roughness. They recommended low depth of cut to reduce the chatter, which in turn subsequently leads to good surface finish. My findings also closely agree with the experimental results reported in the above literature.

4.3.3 Analysis of hardness for turning

During turning, the surface and immediate sub-surface of the material become harder due to work hardening. The hardness values are averaged over 7-8 indents per specimen (Figure 3.24). As compared to the bulk material hardness, the hardness value of the surface is much higher. This increase in hardness is recorded till about 200 µm deep from the surface, after which values approached the hardness of the base material. The hardness of titanium material before machining was 300 Hv and after carrying out the machining for different trials, the hardness varied between 311 Hv (minimum) to 347 Hv (maximum). The higher surface hardness after turning as compared to the average hardness of the base material is due to work hardening of deformed layer below the machined surface up to 200 µm deep. The top layer of the machined surface experiences work hardening process. But, the material below the top layer is softer because of over-aging of titanium alloy due to the very high cutting temperature produced at the local surface. Additionally, poor low thermal conductivity of titanium alloy caused the temperature beneath the machined surface to be retained. It is revealed from the investigations of Ezugwu and Tang (1995) that the combination of high compressive stresses and pressure at the cutting edge during machining contributed to the occurrence of the work hardening effect.The engagement of tool for cutting the workpiece material results in internal work hardening accumulation for heating and accumulation for cooling takes place with the disengagement of tool from the workpiece material. Additionally, rapid heating and cooling may have contributed to the work hardening effect during machining (Chou,Y.K. 2002). From the experimental work of Ramakrishna and Shunmugam (1987), it is seen that the depth of the work hardening layer varies depending on the type of mechanical and thermal interaction. According to Zou et al. 2009 the evolution of microhardness of the machined surfaces was influenced by cutting speed, feed rate and depth of cut during turning of NiCr20TiAl nickel-based alloy.

4.3.3.1 Effect of lubricating mode

From Figure 4.2, it is noticed that hardness is highest at the surface level for dry machining due to large amount of heat generated when compared to MQL and dry

machining. From ANOVA (Table 4.5), it is evident that lubricating mode has the major contribution (89.27%) on surface hardness. During dry machining as the workpiece material is subjected to high cutting temperature and high cutting pressure, a competing process between work hardening and thermal softening takes place and affects the fundamental behavior of the workpiece material. Furthermore, from the experimental work of Lapin et al. (2000) it is concluded that the softening process of the sub-surface region can be characterized by the effect of ageing on microhardness.The turned surface subjected to high cutting temperature during machining process is comparable to the ageing process. From this discussion it can be inferred that, because of the high temperature during dry machining there is instability or alteration of microstructure in the form of plastic deformation resulting in softening of the titanium alloy sub-surface (metallurgical alteration). Ezugwu et al. (2007) during finish turning of Ti-6Al-4V using PCD tool revealed that, the hardening effect is due to high plastic flow rate combined with the heat generation at the primary shear zone . However, the MQL is seen to induce lower softening at the outer layers of the ground surfaces. Softening of the machined surface implies improved ductility and yield strength of the Ti-6Al–4V alloy, thereby improving process ability. Flood lubrication increases the access of the coolant to the chip-tool interface and contributes to reducing friction coefficient and the resistance to primary shear stress (Ezugwu et al.2007). Heat generation is decreased and consequently lower temperatures and plastic flow, resulting in lesser hardening effect and micro structural damage (Narutaki and Murakoshi 1985).

4.3.3.2 Effect of cutting speed

It is observed from main effect plot of Figure 4.2 that, as the cutting speed increases the surface hardness increases. This may most likely be due to increase in the cutting force that occurs for increased cutting speeds. There is a considerable amount of increase in cutting temperature with the increase in cutting speed, thereby increasing the temperature on the machined surface. Because of these changes a sticking friction is generated between the tool-work interfaces; thus contributing to an increase in subsurface plastic flow, giving a higher hardness value. Similar observation was

reported by, Grzegorz et al. 2013 during machining of duplex stainless steel. As reported by Ezugwu et al. (2005) during the machining of nickel-base, Inconel 718 alloy with ceramic tools under finishing conditions, increasing the cutting speed increased the hardness and depth of the affected layer.

4.3.3.3 Effect of feed rate

From Figure 4.2, it is clear that the hardness value does not vary much with the feed rate. Again from ANOVA (Table 4.6), it is also seen that the contribution of feed rate towards hardness is almost negligible for maximizing hardness. Hence, it can be concluded the hardness value is almost independent of feed rate. From the study conducted by Ezugwu et al. (2005) during the machining of nickel-base, Inconel 718 alloy with ceramic tools under finishing conditions, it was reported that increasing feed rate increased the hardness and depth of the affected layer.

4.3.3.4 Effect of nose radius

From ANOVA Table 4.6, it is observed that nose radius has minor contribution effect of about 2.34% on surface hardness. The increase in nose radius (Figure 4.2) has a direct effect on cutting forces; leading to a significant increase in the ploughing effect in the cutting zone. Increasing the ploughing force leads to more material flow on the machined surface thereby increasing the surface hardness. Increasing the ploughing effect leads to more material side flow on the machined surface. A large nose radius results in generation of compressive residual stress beneath the machined surface (Sasahara and Obikawa 2004).

4.3.3.5 Effect of depth of cut

It is clear from Figure 4.2 that, the surface hardness value increases with the increase in depth of cut because of increased cutting forces. The ANOVA analysis from Table 4.6 also reveals that the depth of cut is a significant parameter affecting the surface hardness.

4.3.4 SEM micrograph

The SEM micrograph of the machined surface of titanium work-piece was obtained for each sample with the help of scanning electron microscope (SEM). The micrograph of each machined sample was obtained in order to perform a detailed study of the machined surface. Figures 4.3-4.5 show the SEM images of Ti-6Al-4V under different lubricant conditions. Figure 4.3 depicts the surface generated under dry mode with cutting speed of 50 m/min, feed of 0.35 mm/rev, nose radius of 0.4 mm and depth of cut of 0.25 mm. The measured surface roughness is 3.25 µm. The higher surface roughness is due to dry cutting mode and higher feed rate of 0.35 mm/rev (Cakir et al. 2009).

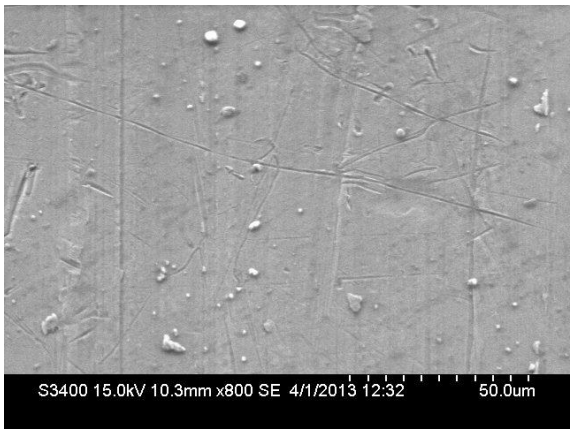

Figure 4.3 SEM image of the surface generated during turning of titanium alloy (Ti-6Al-4V) with PCD insert under dry mode (cutting speed: 50 m/min, feed: 0.35 mm/rev, nose radius: 0.4 mm and depth of cut: 0.25 mm)

The surface roughness measured for the sample shown in Figure 4.4 which is machined under flood lubrication, with cutting speed of 150 m/min, feed of 0.35 mm/rev, nose radius of 0.6 mm and depth of cut of 0.25 mm is 2.65 µm.The higher surface roughness generated during machining under flood lubrication, shown in Fig.4.4, is due to high feed rate and high nose radius (Escalona and Cassier ,1998). Figure 4.5 shows the surface generated with a better surface finish of 0.89 µm under MQL condition with cutting speed of 150 m/min, feed of 0.15 mm/rev, nose radius of 0.4 mm and depth of cut of 0.5 mm. The better surface finish is attributed due to MQL condition, low feed and high cutting speed (Machado and Wallbank J. 1990).

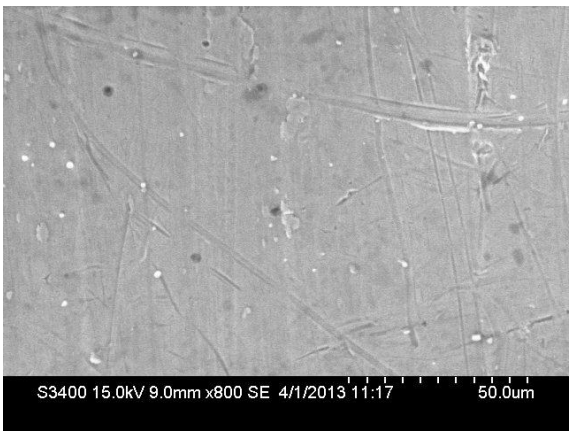

Figure 4.4 SEM image of the surface generated during turning of titanium alloy (Ti-6Al-4V) with PCD insert under flood lubrication (cutting speed: 150 m/min, feed: 0.35 mm/rev, nose radius: 0.6 mm and depth of cut: 0.25 mm)

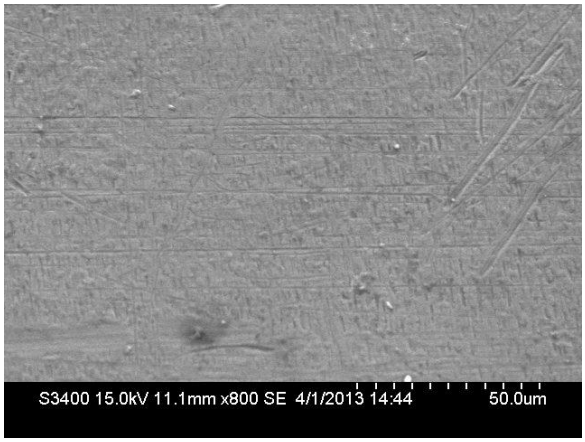

Figure 4.5 SEM image of the surface generated during turning of titanium alloy (Ti-6Al-4V) with PCD insert under MQL condition (cutting speed: 150 m/min, feed: 0.15mm/rev, nose radius: 0.4 mm and depth of cut: 0.5 mm)

A large number of defects were observed on the surface during the experimental trials conducted which is evident from Figures 4.3 to 4.5. The SEM images of the machined surfaces reveals that micro-pits and re-deposited work material cause damages to the surfaces. However, damage like tears, laps or cracks were not observed on the surface when machining Ti–6Al–4V with PCD tools. The examinations of the machined surfaces reveal no plastic deformation after finish machining at the cutting conditions.

4.4 RESPONSE SURFACE MODEL FOR SURFACE ROUGHNESS DURING FINISH TURNING OF TITANIUM ALLOY UNDER MINIMUM QUANTITY LUBRICATION CONDITION

4.4.1 Experimental plan

The developing concept of minimum quantity of lubrication (MQL) in machining is considered as one of the solutions to reduce the amount of lubricant to deal with the environmental, economical and ecological issues. As discussed earlier in this chapter, from the experimental investigations it was concluded that MQL is the best lubricating mode to obtain best surface finish as compared to dry and flood cooling. This study further investigates the influence of cutting speed, feed rate and different amount of lubricant during turning of titanium alloy (Ti–6Al–4V) using poly crystalline diamond (PCD) inserts. The experimental trials have been designed as per Taguchi's orthogonal array and the second order surface roughness model in terms of machining parameters was generated using response surface methodology (RSM). The parametric analysis has been carried out to analyze the interaction effects of process parameters on surface roughness. In the present work, the experiments are planned as per Taguchi's orthogonal array (Taguchi, G. 1986). The identified parameters and their levels are given in Table 4.8.

Table 4.8 Control factors and levels for MQL turning

Control Factors	Levels		
	1	2	3
Lubricant (Q), ml/hr	50	100	150
Speed(v) ,m/min	125	150	175
Feed(f) ,mm/rev	0.05	0.10	0.15

Each parameter was investigated at three levels to study the non-linearity effect of the process parameters (Table 4.8). According to Taguchi design, L_{27} (3^{13}) orthogonal array is employed for the experimentation, which requires 27 trials to be conducted.

Table 4.9 shows the planning for experimental design considered for the current investigation along with the measured response surface roughness. The first column, second column and third column of L_{27} (3^{13}) array were assigned to quantity of lubricant (Q), cutting speed (v) and feed rate (f), respectively.

Table 4.9 Experimental conditions as per L_{27} orthogonal array and surface roughness (Ra)

Tr.No.	Levels			Surface Roughness R_a (µm)
	Quantity Q (ml/hr)	Speed v (m/min)	Feed,f (mm/rev)	
1	1	1	1	0.42
2	1	1	2	0.61
3	1	1	3	0.92
4	1	2	1	0.55
5	1	2	2	0.75
6	1	2	3	0.95
7	1	3	1	0.31
8	1	3	2	0.48
9	1	3	3	0.97
10	2	1	1	0.57
11	2	1	2	0.66
12	2	1	3	0.87
13	2	2	1	0.47
14	2	2	2	0.62
15	2	2	3	0.92
16	2	3	1	0.45
17	2	3	2	0.79
18	2	3	3	0.86
19	3	1	1	0.36
20	3	1	2	0.56
21	3	1	3	0.91
22	3	2	1	0.39
23	3	2	2	0.76
24	3	2	3	0.88
25	3	3	1	0.29
26	3	3	2	0.64
27	3	3	3	0.97

4.4.2 Results and Discussion

Turning, done under MQL condition shows a considerable reduction in surface roughness. During MQL mode, as there is a significant reduction in temperature it results in a uniform and gradual tool wear. The foremost benefit of MQL is the atomization of cutting fluid into very fine tiny globules or particles whose size is inversely proportional to the pressure of injection of the cutting fluid. These high velocity particles of the cutting fluid penetrate into the tool-chip interface leading to reduced friction. Furthermore, micro channels present at the tool chip interface act as capillaries and hence cutting fluid can access, cutting zone due to capillary action. This phenomenon eventually results in reduction in temperature of cutting zone, as the heat generated during cutting is transferred through evaporation. This mode of heat transfer is more effective in comparison with conduction heat transfer during flood lubrication. This phenomenon, keeps chip-tool interface cool and hence the tool maintains the cutting edge in MQL conditions which contributes to improved surface roughness.

4.4.2.1 RSM -based surface roughness model

Multiple regression analysis has been performed to develop the RSM based, second order mathematical model of surface roughness by utilizing the experimental results of Table 4.10.

Table 4.10 Summary of ANOVA for RSM-based surface roughness model

Sum of squares		Degrees of freedom		Mean square		F-ratio
Regression	Residual	Regression	Residual	Regression	Residual	
1.146	0.12160	9	17	0.12741	0.00715	17.81

The mathematical model to predict surface roughness in turning of titanium alloy (Ti–6Al–4V) using poly crystalline diamond (PCD) tool is given by equation (4.5):

$$Ra = - 0.969259 - 0.000244Q + 0.0204v - 1.022222f - 0.000016 Q^2 - 0.000084 v^2 + 7.111111 f^2 + 0.000017Qv + 0.005333Qf + 0.026667vf. \quad (4.5)$$

where, Q represents quantity of lubricant in ml/hr, v represents cutting speed in m/s, f represents feed in mm/rev and Ra represents surface roughness in microns.

The statistical testing of the developed quadratic surface roughness model has been performed by Fisher's statistical test for ANOVA (Montgomery 2003) at 95% confidence interval. The ANOVA table consists of sum of squares and degrees of freedom. The sum of squares is usually performed into contributions from regression model and residual error. The mean square is the ratio of sum of squares to degrees of freedom. F-ratio is the ratio of mean square of regression model to mean square of the residual error. As per this technique, the calculated value of F-ratio of the developed model should be more than tabulated value of table (F-table, see Table 4.10) for the model to be adequate at 95% confidence interval. The results of ANOVA for surface roughness model are presented in Table 4.10 and are found to be adequate at 95% confidence level.

The goodness of fit of the models was also tested by the coefficient of determination (R^2) and adjusted coefficient of determination (R^2_{adj}). R^2 provides a measure of variability in the observed response and can be explained by the process parameters along with their interactions. On the other hand, R^2_{adj} is the coefficient of determination adjusted for the number of independent variables in the regression model. The R^2 and R^2_{adj} values are found to be 0.904 and 0.853, which clearly indicate the significance of non-linear regression model. The developed surface roughness model is then used to test the accuracy and the % prediction error is calculated. The average prediction error of the developed models with the experimental data of an orthogonal array was found to be 5.99%. The comparison of the predicted and experimental values as per orthogonal array is shown in Figure 4.6.

The analysis of parametric influences on surface roughness has been carried out through the developed RSM based model by generating 3D response surface plots using Minitab statistical software.

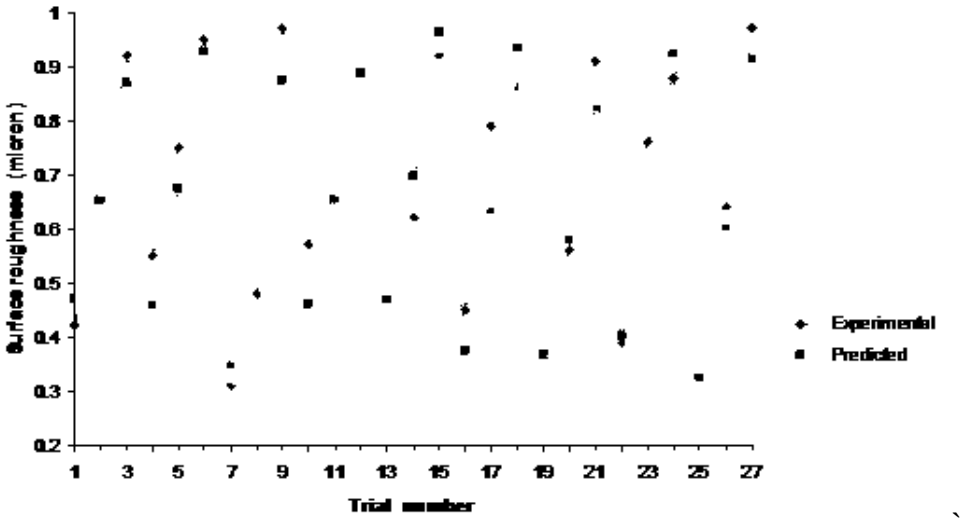

Figure 4.6 Experimental and RSM predicted values for surface roughness

Figure 4.7 exhibits the interaction effect of quantity of lubricant (Q) and cutting speed (v) on surface roughness (Ra) with feed rate (f) held at 0.1mm/rev. At high values of Q, the sensitivity of surface roughness with variations in v is large as compared to low values of Q.

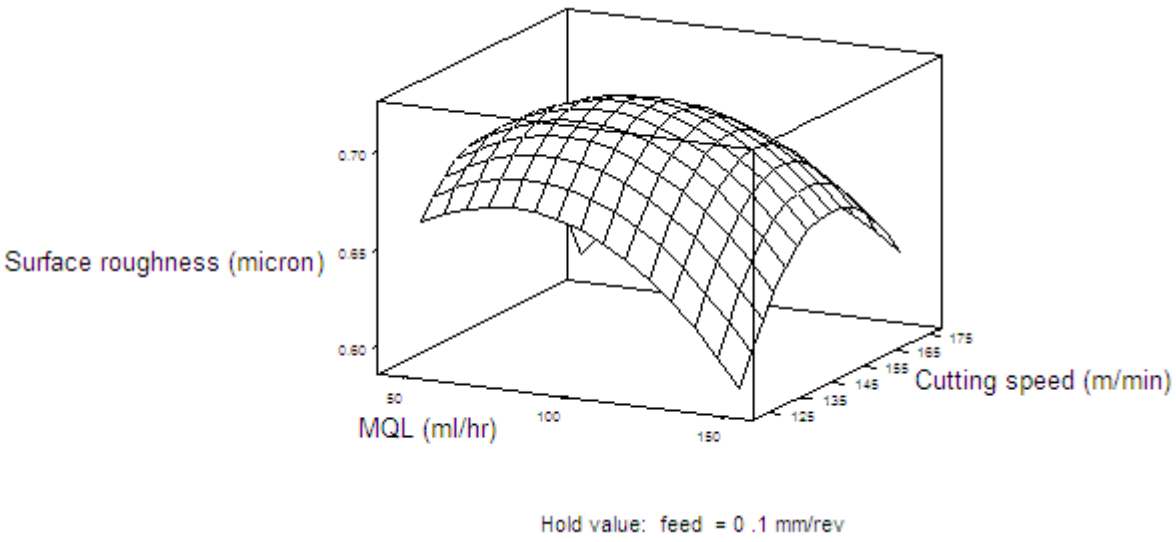

Figure 4.7 The response surface plot of surface roughness (Ra) according to change of quantity of lubricant(Q) and cutting speed (v)

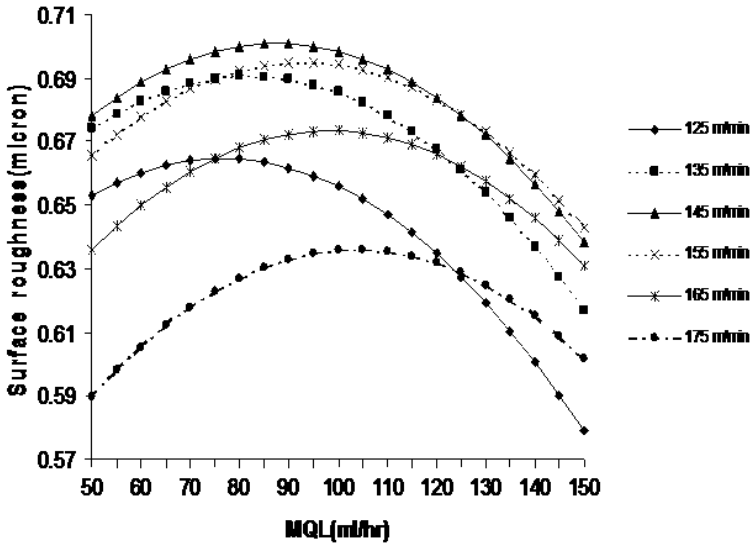

Figure 4.8 Variation of surface roughness(Ra) with quantity of lubricant (Q) under different cutting speeds(v)

Higher the value of quantity of lubricant Q, minimum is the surface roughness.The reason might be, the thinner chips produced at higher cutting speed are pushed by high MQL due to capillary effect, which enables the chips to come closer to hot tool-chip zone to remove the heat more effectively and hence surface roughness decreases (Gaitonde et al. 2012). It is further evident from the Figure 4.8 that as quantity of lubricant (Q) increases, the surface roughness decreases, at different cutting speed.Figure 4.9 depicts the interaction effect due to quantity of lubricant (Q) and feed rate (f) on surface roughness (Ra) with cutting speed (v) held at 150m/min.

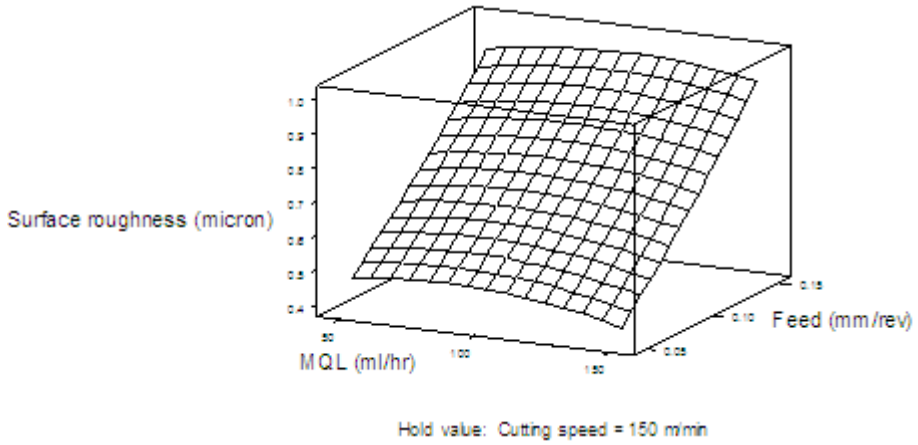

Figure 4.9 The response surface plot of surface roughness (Ra) according to change of quantity of lubricant(Q) and feed rate(f)

It can be seen from Figure 4.9 that, the value of surface roughness sharply increases with feed rate (f) irrespective of quantity of lubricant (Q). As the feed rate increases, the surface roughness also increases because of less available time to carry out the heat from the cutting zone, high material removal rate and accumulation of chip between tool-work piece zones. This may be due to the fact that, at higher feed rate more amount of heat is generated due to high material removal rate(MRR) and hence increase in temperature at tool-chip interface. Due to rise in temperature at tool-chip interface, the tool wear increases and hence surface roughness increases (Gaitonde et al. 2012). The poor surface roughness is obtained when a higher feed rate is employed, due to pronounced feed marks on the machined surface (Ezugwu et al. 1999). It is also further revealed from Figure 4.10 that, variations in surface roughness (Ra) is minimal with the variations in quantity of lubricant (Q) for all values of feed rate (f).The minimum surface roughness results in high MQL in the range 140–150 ml/h with low feed rate.

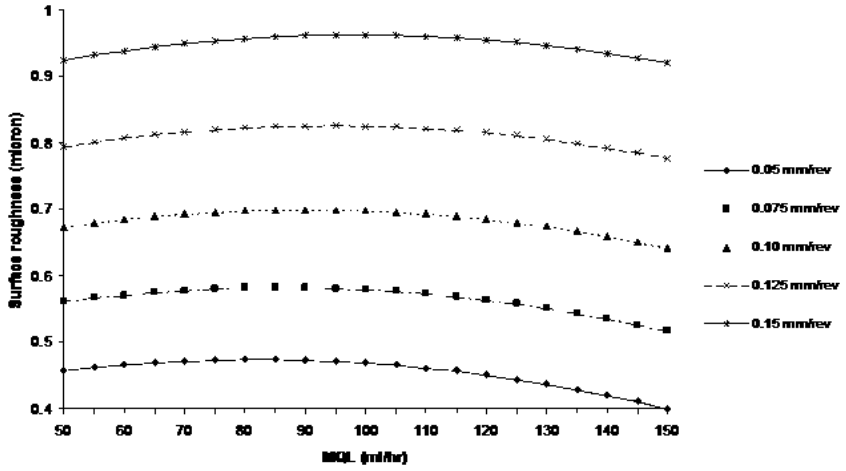

Figure 4.10 Variation of surface roughness (Ra) with quantity of lubricant(Q) under different feed rate (f)

Figure 4.11 shows the variation of cutting speed (v) and feed rate (f) on surface roughness with quantity of lubricant (Q) at 100 ml/hr.

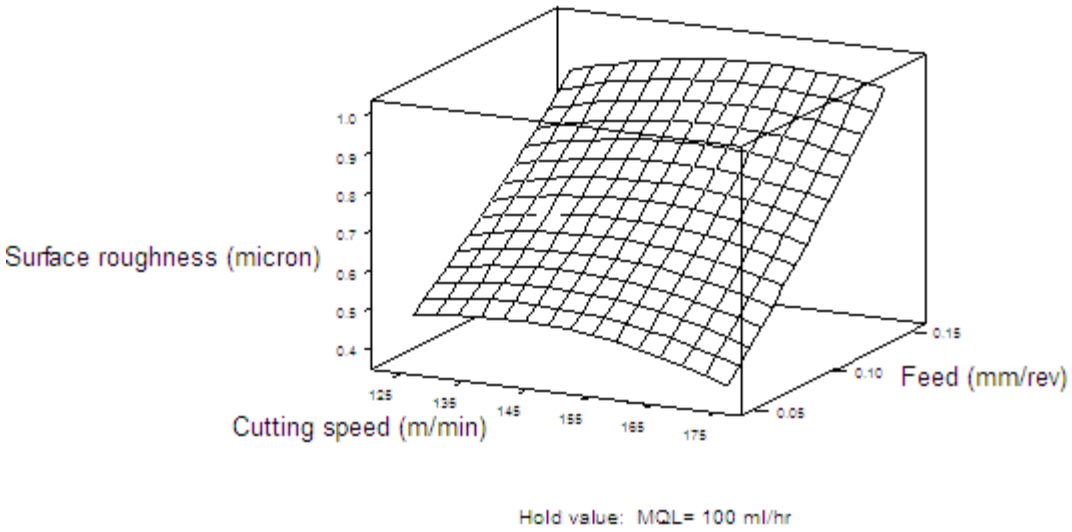

Figure 4.11 The response surface plot of surface roughness (Ra) according to change of cutting speed(v) and feed rate(f)

From Figure 4.11 it is clear that the surface roughness of the machined component decreases with increase in cutting speed. The surface roughness increases with feed rate (f), irrespective of cutting speed (v) and it clear that the variations in surface roughness, with the variations in feed rate (f) are less at all values of cutting speed (v). Because, as the feed rate increases a large amount of material has to be taken out per revolution, which demands excess amount of energy thereby increasing the cutting forces and temperature. As a result of the collective effect of effect of increase in temperature and cutting forces, tool wear rate is very high eventually leading to increase in surface roughness (Gaitonde et al. 2012). It is further confirmed from Figure 4.12 that as the cutting speed increases the surface roughness decreases.

The results here agree with the experimental investigations conducted by different authors. Yuan et al. (2011) conducted experimental trials on the influence of different coolant strategies such as dry, wet, minimum quantity lubrication (MQL) and MQL with cooling air on the parameters of milling Ti–6Al–4V alloy with uncoated cemented carbide inserts. The results showed that minimum quantity lubrication (MQL) with cooling air significantly reduces cutting force, tool wear and surface roughness.

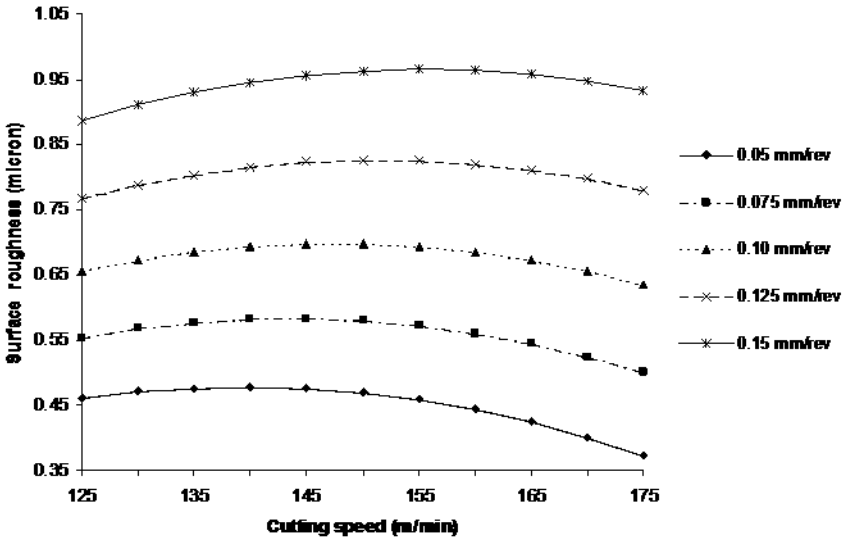

Figure 4.12 Variation of surface roughness (Ra) with cutting speed(v) under different feed rate (f)

In the study conducted by Zoya.Z.A and Krishnamurthy.R (1998) during machining of titanium alloy using CBN tools, the machining performance was evaluated in terms of cutting force, specific cutting pressure, cutting temperature, chip strain , surface finish and concluded that a cutting-speed range of 185 to 220 m/min can be recommended for the machining of titanium alloy. My results also indicate that the best surface finish can be obtained at a cutting speed of 175m/min. Nalabant, et al.(2009) have extensively studied the effects of uncoated, PVD and CVD coated cutting inserts and various cutting process parameters on surface roughness and it was found that the best average surface roughness values were obtained at cutting speed of 200 m/min with a feed of 0.25 mm/rev using a 2.3 μm thickness PVD coated TiAlN-coated cutting tool. They conducted experimental trials with different feed rates of 0.25, 0.30, 0.35, 0.40 and 0.45 mm/rev and concluded that the lowest feed of 0.25mm/rev is suitable for best surface finish. It is also evident from the present results that the as the feed decreases the surface roughness also decreases.

4.5 CHAPTER CONCLUSIONS

Taguchi optimization method for machining titanium alloy (Ti-6Al-4V) machining with poly crystalline diamond (PCD) tool for minimizing the surface roughness and

maximizing surface hardness is presented in this chapter. The results indicate the substantial benefit of the minimum quantity of lubrication (MQL) and justify PCD inserts to be the most functionally satisfactory commercially available cutting tool material for machining titanium alloys for better surface finish. Based on the analysis of the experimental results, the following conclusions are drawn:

- A combination of MQL lubricating mode, high cutting speed, low feed rate, high nose radius with low depth of cut is helpful for achieving minimal surface roughness during turning of titanium alloy.
- The cutting speed (72.32%) and feed rate (17.49%) have major effects on minimizing surface roughness. The lubricating mode also plays vital role in minimizing the surface roughness.
- Reduced surface roughness is obtained for MQL turning when compared to dry and flooded conditions.
- The surface roughness decreases with increased cutting speed and nose radius, whereas the surface roughness increases with increased feed rate and depth of cut.
- Work hardening of deformed layer below the turned surface up to 200 μm caused higher hardness than the average hardness of the base material.
- The lubricating mode (89.27%) and cutting speed (5.28%) have key roles on maximizing the surface hardness**.**
- The hardness is more at the surface level in dry lubrication due to large amount of heat generated when compared to MQL and flooded lubrication.
- The second order surface roughness model based on RSM was developed using the experimental database obtained from Taguchi's orthogonal array.
- Second-order response surface model can be effectively used to predict the surface roughness on machining of titanium under different conditions of MQL, cutting speed and feed rate at 95% confidence interval.
- Response surface analysis indicates that at high values of quantity of lubricant, the sensitivity of surface roughness with the variations in cutting speed is larger as compared to low values of the quantity of lubricant.

- The surface roughness sharply increases with feed rate irrespective of the amount of quantity of lubricant.
- PCD insert was successfully used as a cutting tool material for machining titanium alloys for better surface finish.

The turned specimens are then analysed for the surface roughness and hardness during ball burnishing, the details of which are presented in the next chapter.

Chapter 5

ANALYSIS OF SURFACE ROUGHNESS AND HARDNESS DUE TO BALL BURNISHING OF TITANIUM ALLOY

5.1 OBJECTIVE

Ball burnishing is a popular post-machining metal finishing operation. An attempt has been made in this study to optimize the process parameters during burnishing of titanium alloy (Ti-6Al-4V). Ball burnishing process parameters such as burnishing speed, burnishing feed, burnishing force and number of passes were considered to minimize the surface roughness and maximize the hardness. The lubricated ball burnishing experiments were planned as per L_{25} orthogonal array and signal to noise (S/N) ratio was applied to measure the proposed performance characteristics. The validation tests with the optimal levels of parameters were performed to illustrate the effectiveness of Taguchi optimization. The review of previous works on burnishing reveals that only a few investigators concentrated on the analysis of ball burnishing process dealing mostly with the surface finish and hardness, but with little focus on the optimization of burnishing parameters. Furthermore, not much study has been reported on burnishing of titanium alloy (Ti-6Al-4V). The current study is aimed at optimizing and analyzing the burnishing parameters using Taguchi method. The influence of burnishing parameters on output responses i.e., surface roughness and surface hardness is also discussed in this study.

5.2 EXPERIMENTAL DETAILS

The experiments are conducted based on Taguchi's method which is a tool used to determine the best combination levels of the control factors to build the product/process insensitive to noise factors (Phadke 1989 and Ross 1996). Taguchi optimization is based on orthogonal arrays (OA), which permits simultaneous attainment of many control factors to be investigated effectively (Phadke 1989 and Ross 1996). The purpose of conducting an orthogonal experiment is to decide the

optimum level for each of the control factors and to establish the relative implication of individual factor on the response (Phadke 1989 and Ross 1996). The ball burnishing tool used is shown in Figure 3.11 and the experimental set up is shown in Figure 3.13.

The usual traditional methods are multifarious, time consuming and besides not straight forward to use. A huge number of experiments have to be conducted when the number of factors is more. Taguchi advocates the use of orthogonal arrays to investigate the whole parameter space with merely a small number of experiments. Taguchi proposed signal to noise (S/N) ratio as the objective function for orthogonal matrix experiments (Phadke 1989 and Ross 1996), which indicates the degree of expected performance in the presence of noise factors. Taguchi categorized the S/N ratio into smaller the better type, larger the better type and nominal the best type based on the kind of objective function. The analysis of means (ANOM) based on S/N ratio is used to decide the best combination levels of the control factors and the optimum level for a factor is the level that has the highest S/N ratio in the experimental zone. The analysis of variance (ANOVA) ascertains the comparative magnitude of control factors and is executed on S/N ratio to achieve the contribution of each factor (Phadke 1989 and Ross 1996). In the current research, four control factors such as burnishing speed, burnishing feed, burnishing force and number of passes were considered based on preliminary investigation. Each factor was examined at five levels to explore the non-linearity effects. The selected control factors and their levels are illustrated in Table 5.1.

Table 5.1 Control factors and their levels for burnishing

Code	Control factor	Level				
		1	2	3	4	5
A	Burnishing Speed, m/min	15	30	45	60	75
B	Burnishing Feed ,mm/rev	0.05	0.10	0.15	0.20	0.25
C	Burnishing Force , N	150	200	250	300	350
D	Number of passes	1	2	3	4	5

Table 5.2 Orthogonal array, measured responses and corresponding S/N ratios for burnishing

Trial No.	A	B	C	D	Surface roughness, R_a (μm)	Hardness, H (Hv)	S/N ratio for surface roughness, η_1 (dB)	S/N ratio for hardness, η_2 (dB)
1	1	1	1	1	0.15	372	16.4782	51.4109
2	1	2	2	2	0.17	375	15.3910	51.4806
3	1	3	3	3	0.19	388	14.4249	51.7766
4	1	4	4	4	0.25	392	12.0412	51.8657
5	1	5	5	5	0.31	396	10.1728	51.9539
6	2	1	2	3	0.13	365	17.7211	51.2459
7	2	2	3	4	0.24	401	12.3958	52.0629
8	2	3	4	5	0.29	406	10.7520	52.1705
9	2	4	5	1	0.20	387	13.9794	51.7542
10	2	5	1	2	0.30	370	10.4576	51.3640
11	3	1	3	5	0.16	391	15.9176	51.8435
12	3	2	4	1	0.18	390	14.8945	51.8213
13	3	3	5	2	0.17	395	15.3910	51.9319
14	3	4	1	3	0.14	358	17.0774	51.0777
15	3	5	2	4	0.19	376	14.4249	51.5038
16	4	1	4	2	0.20	377	13.9794	51.5268
17	4	2	5	3	0.26	386	11.7005	51.7317
18	4	3	1	4	0.22	373	13.1515	51.4342
19	4	4	2	5	0.27	376	11.3727	51.5038
20	4	5	3	1	0.30	358	10.4576	51.0777
21	5	1	5	4	0.19	399	14.4249	52.0195
22	5	2	1	5	0.32	373	9.8970	51.4342
23	5	3	2	1	0.22	370	13.1515	51.3640
24	5	4	3	2	0.24	360	12.3958	51.1261
25	5	5	4	3	0.29	390	10.7520	51.8213

According to Taguchi method, L_{25} orthogonal array with 4 columns and 25 rows was selected; each control factor is assigned to a column and twenty five distinct factor combinations are offered (Phadke 1989 and Ross 1996). Thus, twenty five experiments are enough to analyze the entire burnishing experimental design space using L_{25} orthogonal array. The experimental layout plan used for the present research is given in Table 5.2.

5.3 RESULTS AND DISCUSSION

5.3.1 Analysis of mean and variance

In the current study of burnishing process, the surface roughness is to be minimized and the hardness is to be maximized. Thus, '*smaller the better*' type category for surface roughness and '*larger the better*' type category for hardness have been chosen. The S/N ratio for each trial of the OA is given by:

$$\eta_1 = -10\log_{10}(R_a^{\,2}) \tag{5.1}$$

$$\eta_2 = -10\log_{10}(H^{-2}) \tag{5.2}$$

The subsequent S/N ratios for each trial of L_{25} are summarized in Table 5.2.The analysis of means (ANOM) based on S/N ratio was performed to decide the optimal levels of control factors; the summary is presented in Tables 5.3 and 5.4 respectively. The level of a control factor with the highest S/N ratio is the optimal level. The best combination control factor setting is A3, B1, C2 and D3 for minimal surface roughness and A2, B3, C5 and D5 for maximum hardness. The analysis of variance (ANOVA) based on S/N ratio has been performed to know the relative importance of each of the control factors (Phadke 1989 and Ross 1996). Tables 5.5 and 5.6 present the results of ANOVA for surface roughness and hardness respectively.

From ANOVA Table 5.5, it is observed that burnishing feed (40.13%) and burnishing speed (31.49%) play significant roles in minimizing the surface roughness; while burnishing force and number of passes have the slightest effects. In contrast, number of passes (48.95%) and burnishing force (19.80%) play significant roles in

maximizing the hardness, whereas burnishing speed and burnishing feed do not have visible effects in maximizing the hardness (Table 5.6).

Table 5.3 ANOM for surface roughness based on S/N ratio for burnishing

Parameter code	Levels					Optimum level
	1	2	3	4	5	
A	13.7016	13.0612	15.5411	12.1324	12.1243	**3**
B	15.7042	12.8558	13.3742	13.3733	11.2530	**1**
C	13.4123	14.4123	13.1183	12.4838	13.1337	**2**
D	13.7922	13.5230	14.3352	13.2877	11.6224	**3**

Table 5.4 ANOM for hardness based on S/N ratio for burnishing

Parameter code	Levels					Optimum level
	1	2	3	4	5	
A	51.6975	51.7195	51.6356	51.4548	51.5530	**2**
B	51.6093	51.7061	51.7355	51.4655	51.5441	**3**
C	51.3442	51.4196	51.5774	51.8411	51.8783	**5**
D	51.4856	51.4859	51.5306	51.7772	51.7812	**5**

Table 5.5 ANOVA for surface roughness based on S/N ratio for burnishing

Parameter code	Degrees of freedom	Sum of squares	Mean square	% contribution
A	4	39.9296	9.9824	31.49
B	4	50.8910	12.7227	40.13
C	4	9.8790	2.4697	7.79
D	4	20.8868	5.2217	16.47
Error	8	5.2245	0.6531	4.12
Total	24	126.8109	5.2838	100

Table 5.6 ANOVA for hardness based on S/N ratio for burnishing

Parameter code	Degrees of freedom	Sum of squares	Mean square	% contribution
A	4	0.2381	0.0595	9.99
B	4	0.2509	0.0627	10.53
C	4	1.1667	0.2917	48.95
D	4	0.4720	0.1180	19.80
Error	8	0.2559	0.0320	10.73
Total	24	2.3837	0.0993	100

To predict and confirm the proposed responses using the best combination of the control factors, the predicted S/N ratio (η_{opt}) is computed by (Phadke 1989 and Ross 1996):

$$\eta_{opt} = m + \sum_{j=1}^{p} [(m_{i,j})_{max} - m] \tag{5.3}$$

where, $(m_{i,j})_{max}$ is the S/N ratio of the best combination level i of factor j and p is number of main design factor. The confidence interval (CI) is calculated to witness the closeness of the observed S/N ratio (η_{obs}) value with that of predicted value (η_{opt}) and is determined by (Ross 1996):

$$CI = \sqrt{F_{(1,\upsilon_e)} V_e \left(\frac{1}{n_{eff}} + \frac{1}{n_{ver}}\right)} \tag{5.4}$$

where, $F_{(1,\upsilon_e)}$ is the F value for 95% CI

υ_e is the degrees of freedom for error

V_e is the variance of error

$n_{eff} = \frac{N}{1+\upsilon}$; N = Total no. of trials in OA and

υ = Degrees of freedom of *p* factors

n_{ver} is the validation test trial number.

At the optimal values of the control factors, the work pieces of the identical lots were machined. The observed value of S/N ratio (η_{obs}) was then compared with the predicted value (η_{opt}). Table 5.7 presents the validation test results and it is found that the prediction error i.e., (η_{opt} - η_{obs}) is within the *CI* value, undoubtedly demonstrating the adequacy of the surface roughness and hardness additive models.

Table 5.7 Results of validation tests for burnishing

Performance measure	Surface roughness	Hardness
Optimum levels (A, B, C, D)	A3, B1, C2, D3	A2, B3, C5, D5
S/N predicted (η_{opt}), dB	20.0565	52.2781
Observed value	0.10 µm	416 Hv
S/N observed (η_{obs}), dB	20	52.3819
Prediction error, dB	0.0565	0.1038
Confidence Interval value (*CI*), dB	± 6.1769	± 0.3026

The optimal values of control factors for minimizing surface roughness and maximizing hardness are given in Table 5.8.

Table 5.8 Optimal factor settings and corresponding best combination values of surface roughness and hardness for burnishing

Response	Optimal process parameter setting				Optimal value
	Burnishing Speed(A) (m/min)	Burnishing Feed(B) (mm/rev)	Burnishing Force(C) (N)	Number of Passes(D)	
Surface roughness	45	0.05	200	3	0.10 µm
Hardness	30	0.15	350	5	416 Hv

5.3.2 Effects of Burnishing Parameters

The main effect plots are generated using Minitab software, for investigating the influence of burnishing process parameters on surface roughness and hardness.

5.3.2.1 Analysis of Surface roughness

Surface profiles of cylindrical turned and burnished surfaces are shown in Figure 5.1 for Trial No.3 as per the experimental plan (Table 5.2). It can be seen that a significant decrease in surface roughness of the topography height of the work piece is obtained due to the burnishing process. The variation in surface roughness of the turned and burnished sections of the workpiece is shown in Figure5.2.

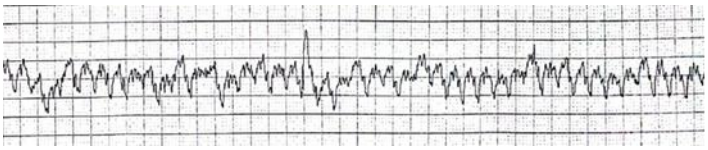

a) Turning

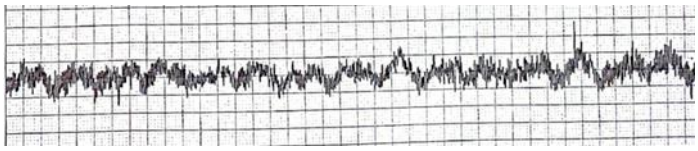

b) Burnishing

Figure 5.1 Surface profile a) Turning R_a-0.43µm b) Burnishing R_a-0.19 µm for Trial No. 3 under burnishing conditions of cutting speed-15m/min, feed -0.15 mm/rev, burnishing force -250N and no. of passes-3

From the main effect plot of surface roughness (Figure 5.3), it is observed that when the cutting speed is increased from 15 m/min to 30 m/min, the surface roughness increases a bit, while it reduces when the speed is increased to 45 m/min. Because, with the increase in burnishing speed, the burnishing ball has more opportunity to settle down the abnormalities of the burnished surface and hence decreased surface roughness. Further as the burnishing speed increases from 45 m/min to 75 m/min, the surface roughness again increases. In this stage because of increased speed the temperature at the interface increases. Thus, consecutively increasing the material

transformation between burnishing ball-work piece interfaces and hence an enhanced surface roughness (El-Axir,M.H. 2000, El-Taweel, T.A. and El-Axir, M.H. 2009).

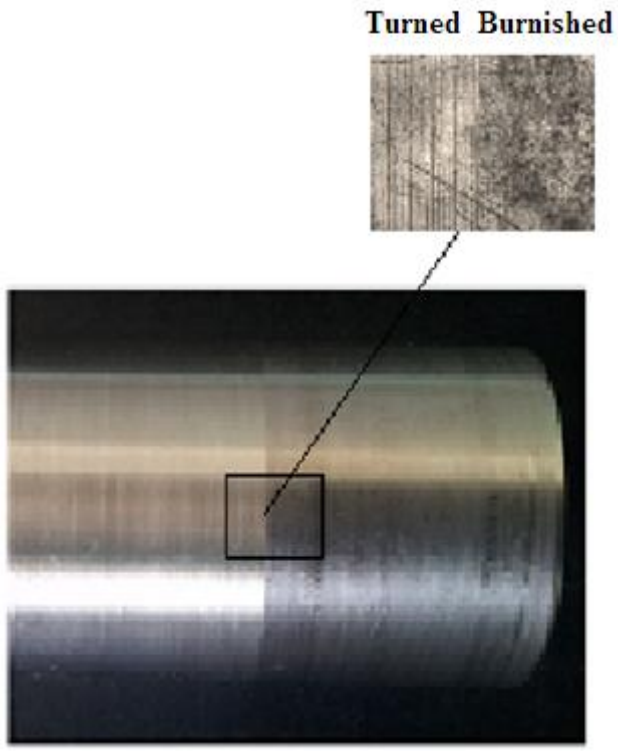

Figure 5.2 Images of turned and burnished surfaces

Moreover , at higher speeds, mainly due to the presence of chatter and reduced amount of deformation time being offered for the burnishing tool to smooth out more irregularities, an increase in surface roughness is observed (Nemat, M. and Lyons, A.C. 2000).The change in surface roughness with respect to feed (Figure 5.3) reveals that the at low feed i.e. 0.05 mm/rev , the distances between the consecutive traces of the burnishing ball will be little, moreover the ball will have more opportunity to smooth out the bulged edges of the previous traces as the tool passes slowly all along the workpiece. This leads to a decrease in surface roughness. At higher feed ranges .i.e. 0.20-0.25 mm/rev, the surface roughness drastically increases. As the feed is progressively increased, the distance between the successive burnishing ball traces increases; resulting in a reduction in likelihood for the burnishing ball to even out all the bulged edges of the former traces and therefore an enhanced surface roughness(El-Axir,M.H. et al.2008, El-Taweel,T.A.and El-Axir,M.H. 2009).

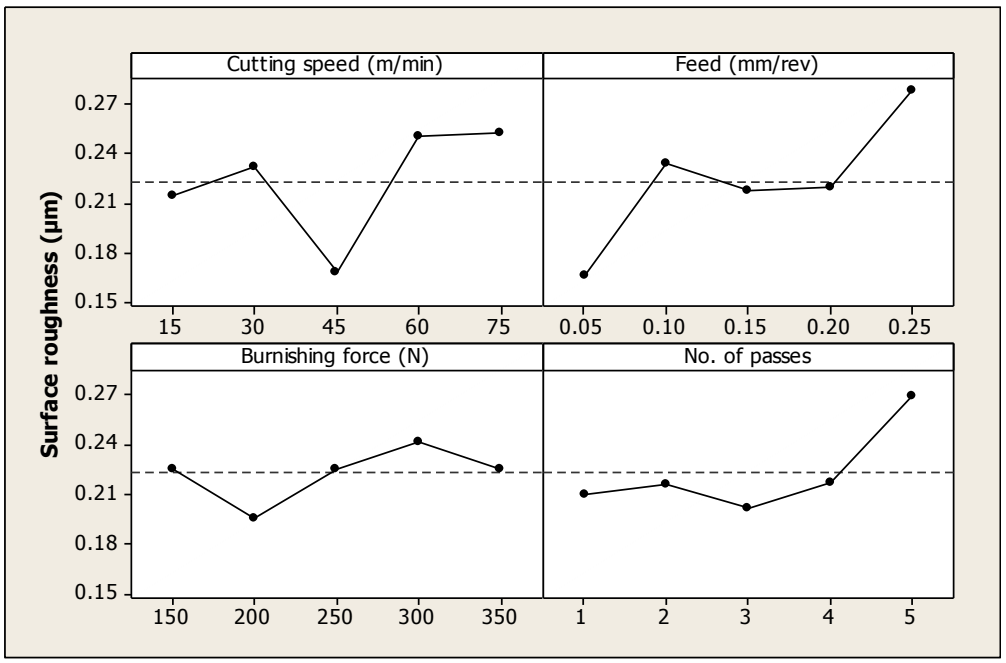

Figure 5.3 Main effect plots of surface roughness for burnishing

Also at higher feeds, the burnishing ball produces larger feed marks with a centre-line distance between two succeeding indentations and hence raised surface roughness (Nemat, M. and Lyons, A.C. 2000).As indicated in Figure 5.3 low feeds are advantageous for minimizing the surface roughness because the deforming action of the burnishing tool is greater and metal flow is regular at low feed. As illustrated in Figure 5.3, the surface roughness appreciably decreases for low range of forces from 150 to 200 N and further the surface roughness increases further for higher range of 200-300 N. This is due to the fact that at the commencement, the burnishing ball penetrates a little distance into a work surface, causing a little or incomplete deformation of the asperities and thus resulting in reduced surface roughness. When the force is slowly increased, the protrusion of work in front of the burnishing tool becomes large and the plastic deformation region broadens that in turn spoils the formerly burnished surface resulting in an enhanced surface roughness (Klocke, et al.1997; Nemat, M. and Lyons, A.C.2000). El-Taweel, T.A. and El-Axir, M.H. (2009), also reported that when the burnishing ball advances further along the work piece, the repeating plastic deformation action on the work surface leads to increased work-hardening of the earlier exaggerated layers of the deformed surface; which in turn produces flaking on the surface and hence, surface roughness increases. The

diminished surface roughness noticed at higher force ranges may be probably due to increased ball pressure on work piece surface resulting in condensing most of the asperities and increasing the metal flow that leads to filling of more voids and/or valleys that were exited in subsurface layer due to burnishing operation. Our experimental results closely agree with the results obtained by López de Lacalle, L.N. et al. (2007) and Branko, T. et al. (2012). As exhibited in Figure 5.3, the surface roughness decreases when the number of passes is increased and reaches a minimum value when the number of passes is 3. However, with the further increase in the number of passes, the surface roughness increases considerably. The increase in surface roughness with more number of passes is fairly understandable because of over hardening and consequently flaking of the surface layers due to more repeated ball burnishing of the work surface (Nemat, M. and Lyons, A.C. 2000, El-Taweel, T.A. and El-Axir, M.H. 2009).

5.3.2.2 Analysis of hardness

Figure 5.4 illustrates the main effect plots of burnishing parameters on surface hardness.

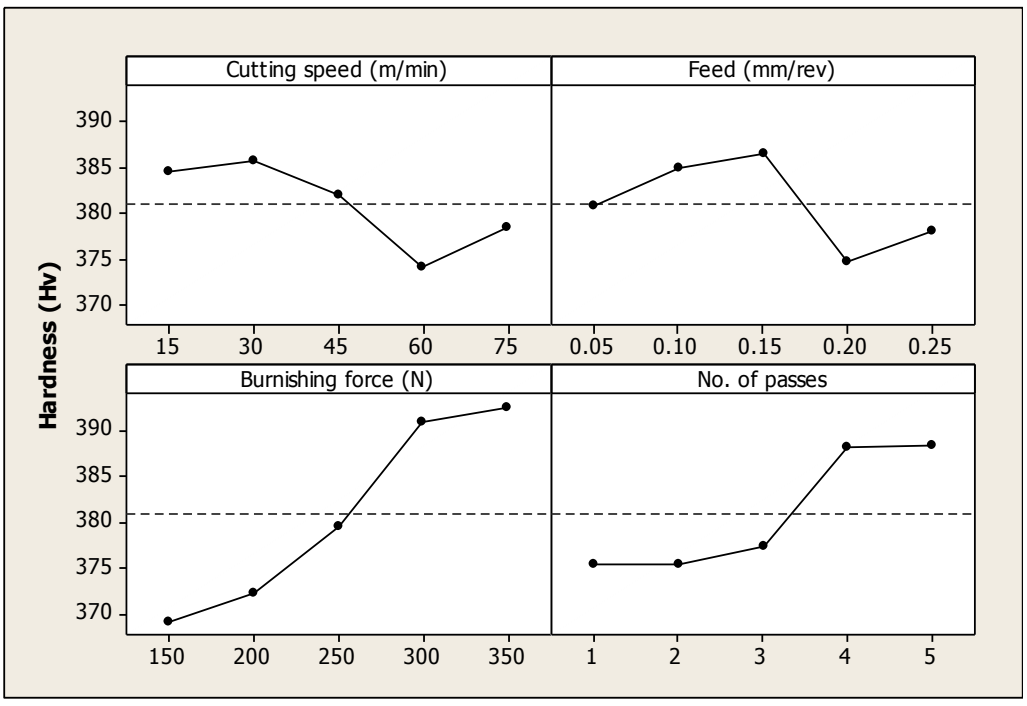

Figure 5.4 Main effect plots of surface hardness for burnishing

During initial range of burnishing speed (15-30 m/min), the hardness increases. Because at low speed, due to more time of penetration of the burnishing tool into the burnished surface, the plastic deformation is more and hence subsequently an added amount of work hardening occurs on the burnished surface. However, with a further increase in cutting speed in the range 30-60 m/min, the hardness decreases. The reason for this may be attributed to the increase in recovery of the work-hardening on the surface as a result of rise in temperature between the workpiece and the burnishing ball, leading to the increase in the rate of surface deformation with the increase in burnishing speed. Also the increase in speed leads to instability of burnishing tool across the work piece surface and there will be incoherent deforming action of the tool, which in turn decreases hardness (Klocke, et al. 1997, El-Taweel, T.A.and El-Axir,M.H. 2009). In our present investigation, especially at higher speeds, insufficient burnishing was observed and probably due to this reason, the surface hardness might be low. In our study, the burnishing speed of 30 m /min was found to be better for improved surface hardness.

It can be observed from Figure 5.4 that surface hardness initially increases for a feed of 0.05 to 0.15 mm /rev and then constantly decreases with increase in feed from 0.15 to 0.25 mm /rev. The reason for greater increase in hardness at lower feed is due to more rigorous plastic deformation. Additionally at lower feed, the probability that the number of times a ball deforms over the same spot is more than at higher feed. Furthermore, the work hardening impact on the burnished surface is enhanced at lower feed and diminishes with increased feed. Study by El-Taweel, T.A. and El-Axir, M.H. (2009), reveals that increase in feed leads to decrease in surface hardness because of less work-hardening on the surface due to smaller surface area of the work piece subjected to plastic deformation.

The main effect plot of burnishing force versus hardness (Figure 5.4) reveals that the surface hardness increases with increased burnishing force constantly from 150 to 350 N. Due to increased burnishing force, both the surface deformation and work hardening increases, thereby resulting in an increase of the surface hardness(El-Taweel, T.A. and El-Axir, M.H. 2009). The present results (Figure 5.4) show that,

with the increase in the number of passes, the surface hardness also increases, due to condensed grain structure and increased structural homogeneity (Hassan,A.M. et al. 1998, El-Axir, M.H. et al. 2008,El-Taweel, T.A. and El-Axir, M.H. 2009).

During the burnishing experiments, the hardness varied from 360 Hv to 406 Hv. The hardness of the titanium work piece material before burnishing was 340 Hv. Due to burnishing, the surface and immediate sub-surface of the material turned harder as a result of work hardening, due to mechanical and thermal load on the work piece. It is apparent that, when a metal/alloy is continually moving over a surface, plastic deformation takes place, which in turn produces work hardening effect and creates harder surface .The micro hardness depth distribution of titanium material for Trial no.8 as per the experimental plan (Table 5.2), after burnishing is shown in Figure5.5.

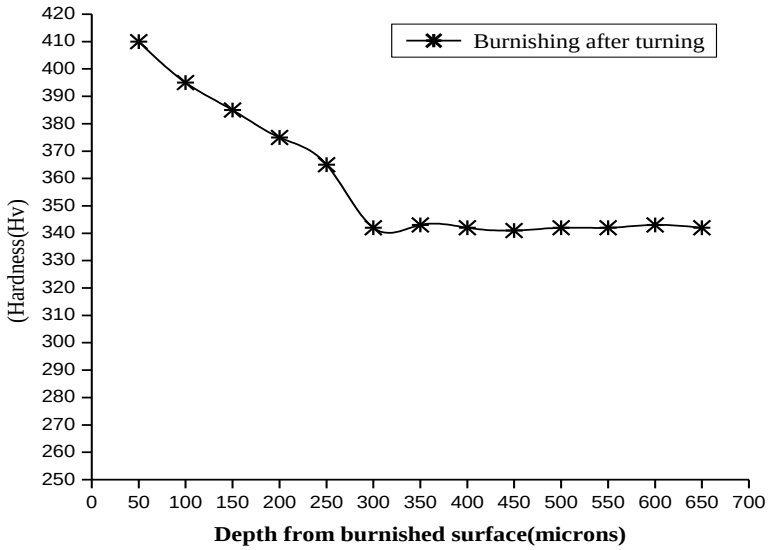

Figure 5.5 Results of surface layer micro hardness tests on burnished surface for Trial No. 8 under burnishing conditions of burnishing speed-30m/min, feed -0.15 mm/rev, burnishing force – 300N and no. of passes-5.

The hardness value of the surface is much higher than the bulk material hardness. It was observed that the micro hardness induced by ball burnishing had a steep fall, close to the surface. This is due to slight shearing between the ball and the sample surface, as well as lower strain rate by ball burnishing. At a depth of 210 μm beneath

the burnished surface, the difference in hardness was very small and the hardness values approached the hardness of the base material as the depth beneath the burnished surface increased. The top layer of the burnished surface experiences work hardening process and hence the hardness is higher than the average hardness of the work piece material. On the other hand, due to the very high cutting temperature produced at the local surface, the material below the top layer is softer as a result of over-aging of titanium alloy. Furthermore, the temperature beneath the burnished surface is retained because of low thermal conductivity of titanium alloy. From the above discussion on surface hardness during burnishing of titanium alloy it is evident that the surface hardness of the material increases with the increase in the burnishing force and number of passes due to work hardening.

5.3.2.3 Effect of Residual Stresses

To evaluate the degree of residual stress induced in the near surface layers by ball burnishing, X ray diffraction measurements were performed on the turned and burnished components. It was observed that in the turned surface, tensile residual stresses are produced close to the surface, whereas after burnishing, large axial compressive macro stresses occur in the surface layer and in the near-surface regions. After analyzing the results, it was observed that compressive stresses occur in the surface layers of all the burnished surfaces. Figure 5.6 shows the profiles of the residual stresses, as a function of depth into the surface for turned and burnished surface for Trial 17 as per experimental layout plan of our investigation (Table 5.2). It is obvious that after ball burnishing, compressive residual stress as high as 955 MPa was noticed immediately below the surface and this compressive stress decays over a depth of approximately 600 μm. However, the smallest compressive stress value of 255 MPa was obtained for a workpiece Trial No. 1, subjected to a burnishing force of 150 N, speed of 15 m/min, feed of 0.05 mm/rev and one pass. Residual stress distribution can be affected by the burnishing parameters such as burnishing force, speed, feed and number of passes. Burnishing force has a major influence on the residual stresses.

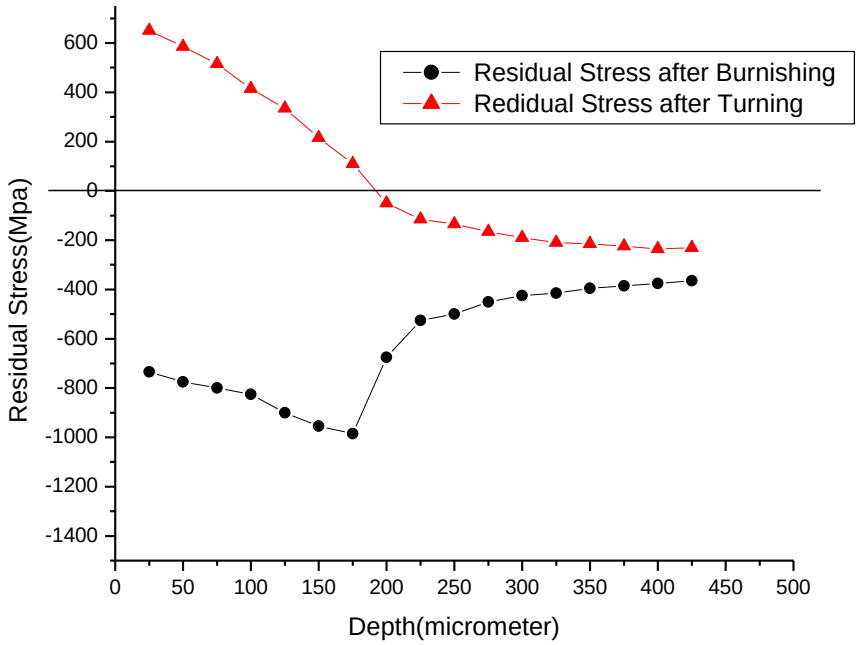

Figure 5.6 Residual stress-depth profile in Ti–6Al-4V after turning and ball burnishing (a) Initial turned surfaces under MQL conditions with a flow rate of 150ml / hr, speed of 175m/min, cutting depth of 0.25mm and a feed of 0.05mm/rev (b) Burnishing for Trial No.17 under burnishing conditions of burnishing speed-60m/min, feed -0.10 mm/rev, burnishing force -350N and no. of passes-3.

The amount of plastic deformation in the work piece increases with the burnishing pressure and hence the magnitude of compressive residual stresses increase with increased burnishing force. The compressive residual stresses competently retard the formation and growth of cracks when subjected to cyclic loading and thus enhance the fatigue resistance and vice versa for the residual tensile stresses (Prevéy, P.S.et al. 2002, Nalla, R.K. et al. 2003, Maawada, E. et al. 2012).Hence, the residual stress on the burnished surface plays an important role, in determining the performance and fatigue strength of components.

5.3.2.4 Effect of Lubricant

The influence of lubricant on surface hardness and roughness is found to be extremely important (Loh, N. H. and Tam, S.C. 1989). From the earlier investigations by Shirsat, U.M. and Ahuja, B.B (2005) it was found that SAE 30 base oil has a

noteworthy effect on the surface finish when compared to kerosene, 5% and 10% graphite in weight in SAE 30 base oil as a lubricant. In the present analysis, the burnishing experiments were performed under lubricated conditions using SAE 40 oil. For the selected burnishing conditions at a speed range of 15-75 m/min, it is seen that the lubrication was found to be essential. Without lubrication, the surface gets deteriorated and it was also observed that there was no rolling effect of the ball used in burnishing tool. Generally, lubricant reduces the force of cutting and forming by reducing the friction. In burnishing also, lubricants assist in easy deformation of surface layer with an applied burnishing force by providing constructive friction conditions between burnishing tool and the work material.

Some of my experimental results were compared with the earlier reported works in the literatures. During the previous studies on burnishing of non-ferrous metals (Luo, H.Y et al. 2005), brass (El-Taweel, T.A. and El-Axir, M.H. 2009) , mild steel, aluminum (Nemat, M. and Lyons, A.C. 2000) and polymers (Low and Wong .2011) it was noticed that the surface roughness reduces with increased speed until the occurrence of the optimum speed, beyond which the surface roughness increases. My investigation on burnishing of titanium alloy also supports these findings. The reduction in hardness was observed with increased speed during burnishing of brass (El-Taweel, T.A. and El-Axir, M.H. 2009), mild steel and aluminum (Nemat, M. and Lyons, A.C. 2000) materials, which closely concur with my results on titanium alloy. It was found by many researchers that feed, plays an important role in minimizing the surface roughness during burnishing experiments (Nemat, M. and Lyons, A.C.2000, Shiou, F.J. and Chen, C.H. 2003a, Luo, H.Y et al. 2005, El-Tayeb,N.S.M et al. 2008, El-Taweel, T.A. and El-Axir, M.H. 2009, El-Tayeb, N.S.M et al. 2009, Afef, B. et al. 2010, Low and Wong . 2011). The increase in feed during burnishing of mild steel and aluminum materials, lead to the increase in surface roughness whereas the surface hardness decreased (El-Tayeb, et al. 2009). The surface roughness decreased with the increase in feed up to certain limit and on further increase beyond this limit, the surface roughness decreased during burnishing of several materials (Luo, H.Y et al. 2005; El-Taweel, T.A. and El-Axir, M.H. 2009; Low and Wong . 2011). However, in all the burnishing investigations, low feeds were recommended mainly due to regular

flow of the material and better deforming action of the burnishing tool. In the present investigation also, low feeds are recommended for the reduction in surface roughness during burnishing of titanium alloy. In the current investigation, I found that during burnishing of titanium alloy, the surface roughness decreases fairly at low burnishing force, whereas the surface roughness started to increase at higher burnishing force. Previous studies (Hassan,A.M. et al. 1998, Nemat, M. and Lyons, A.C. 2000, Luo, H.Y et al. 2005, Shiou, F.J. and Chen, C.H. 2003a, Shiou, F.J. and Chen, C.H. 2003b, El-Taweel, T.A. and El-Axir, M.H. 2009, Low and Wong .2011) also support my findings with regard to influence of burnishing force on surface roughness. Further, my research outcome on surface hardness also strongly agrees with the earlier studies of burnishing on different materials ((Nemat, and Lyons 2000, Luo, H.Y et al. 2005, El-Taweel, T.A. and El-Axir, M.H. 2009, Low and Wong 2011) i.e. hardness is directly related to the applied force under all the experimental conditions tested. The present study on burnishing of titanium alloy demonstrates that in general, surface roughness reduces with increased number of passes, reaching a least value and later with further increase in number of passes the surface finish deteriorates. Conversely, the surface hardness increases with increased number of tool passes. Earlier researchers also obtained, similar results during burnishing of ferrous and non ferrous metals (Nemat, M. and Lyons, A.C. 2000, El-Taweel, T.A. and El-Axir, M.H. 2009).Further, the experimental research findings on roughness, hardness and residual stresses, are in agreement with that of other authors (Nalla, R.K. et al. 2003 and Maawada, E. et al. 2012).

5.3.3 SEM micrographs of machined surface and subsurface characterizations

The effect of the burnishing process on the machined surface of titanium alloy was studied. Figure 5.7 shows the SEM micrograph of the surface turned under MQL conditions with a flow rate of 150ml / hr, speed of 175m/min, cutting depth of 0.25mm and a feed of 0.05mm/rev. Figure 5.8 (a-f) shows SEM images of surfaces produced by ball burnishing under different machining conditions. Figure 5.9(a-d) depicts SEM images of the subsurface cross section at the topmost machined surfaces under different conditions. The obtained results confirm that the sub-surface is

affected by the burnishing process. A comparison between the SEM images of turned and the burnishing surface under different experimental trials was made. Figures 5.8 show the SEM images of the burnished surfaces. It is evident from these figures that the marks caused by turning are removed by burnishing (Figure 5.7). Burnishing eliminates scars leading to reduced roughness and smoother surface texture as evident from Figure 5.8(a-f) (El Tayeb N S M 2009). The SEM micrograph of turned component, shown in Figure 5.9(a) exhibits the elongated grains just below the top surface. The examination of the subsurface of the burnished components in Figure 5.9 (b-d) reveals the grain structure just beneath the top burnished surface and a zone of depth of few micrometers in which the microstructure appears to be disturbed is observed (Balland,P.et al.2013). The grains in the layer disturbed by the influence of burnishing shows re-crystallized fine grains. It is also evident that the grains below the disturbed surface are elongated.

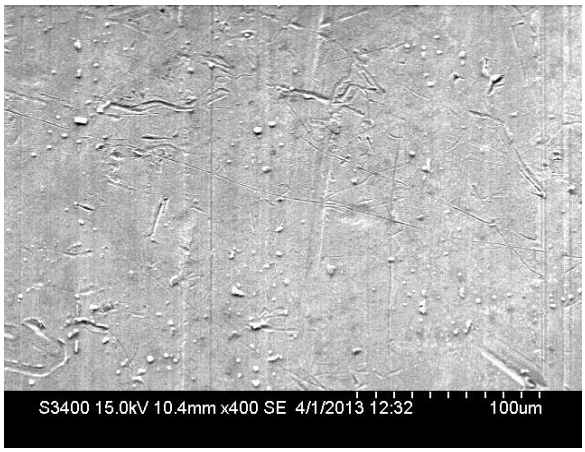

Figure 5.7 SEM image of surface turned under MQL conditions with a flow rate of 150ml / hr, speed of 175m/min, cutting depth of 0.25mm and a feed of 0.05mm/rev.

Wu et al. (2005) have reported that the burnished sub surface shows the features of fine grains, elongated sub grains with stacking faults and heavy twinnings. The disturbed layer just below the top surface may be due to larger forces in tangential and radial directions. Larger forces will induce more severe plastic deformation to the surface and the subsurface as reported by Pu,Z et al. (2012).From the SEM images

(Figure 5.7) of initial turned surfaces before burnishing, it is observed that there is typically rough texture characterized by marks, profound grooves, sharp ridges and the feed marks. When these turned surfaces were burnished, the sharp asperities were plastically deformed resulting in a smoother and uniform surface as depicted in Figure 5.8. The burnishing process removes these scars, leading to reduced roughness and smoother surface texture. The surface cracks and delamination were not observed on further examination of cross section of burnished surface [Figures 5.9(b-d)].

The cross-sectional microstructures, just beneath the topmost surface regions, of turned and burnished surfaces under different burnishing conditions are shown in Figure 5.9. The direction of arrow in these figures indicates the top surface. It is evident from the comparisions between Figure.5.9 (a) and Figures 5.9 (b-d) that the grains were elongated and condensed in a very small layer close to the surface of the workpiece in the burnished region than the turned region. The turned surface displays no change in the grain size near the surface .However, due to burnishing process, owing to the application of the burnishing force and friction force introduced between specimen and burnishing tool, the grains become sheared and grain size decreases dramatically. It is evident from these figures that , adjoining to the burnished surface, a layer is present where the grain boundaries were not discernable under the current observation method.

This featureless layer has no identifiable grain structure and indiscernible grain boundaries were also reported after deep rolling of Ti-6Al-4V (Nalla, R.K et al.2013). The layer influenced by burnishing is described as a layer where the microstructure exhibits the features of recrystallized grains, elongated sub grains, and/or grains with heavy twinnings and stacking-faults (Wu, X et al. 2005). A different microstructure is observed after deformation due to burnishing, no nanocrystallites were formed.

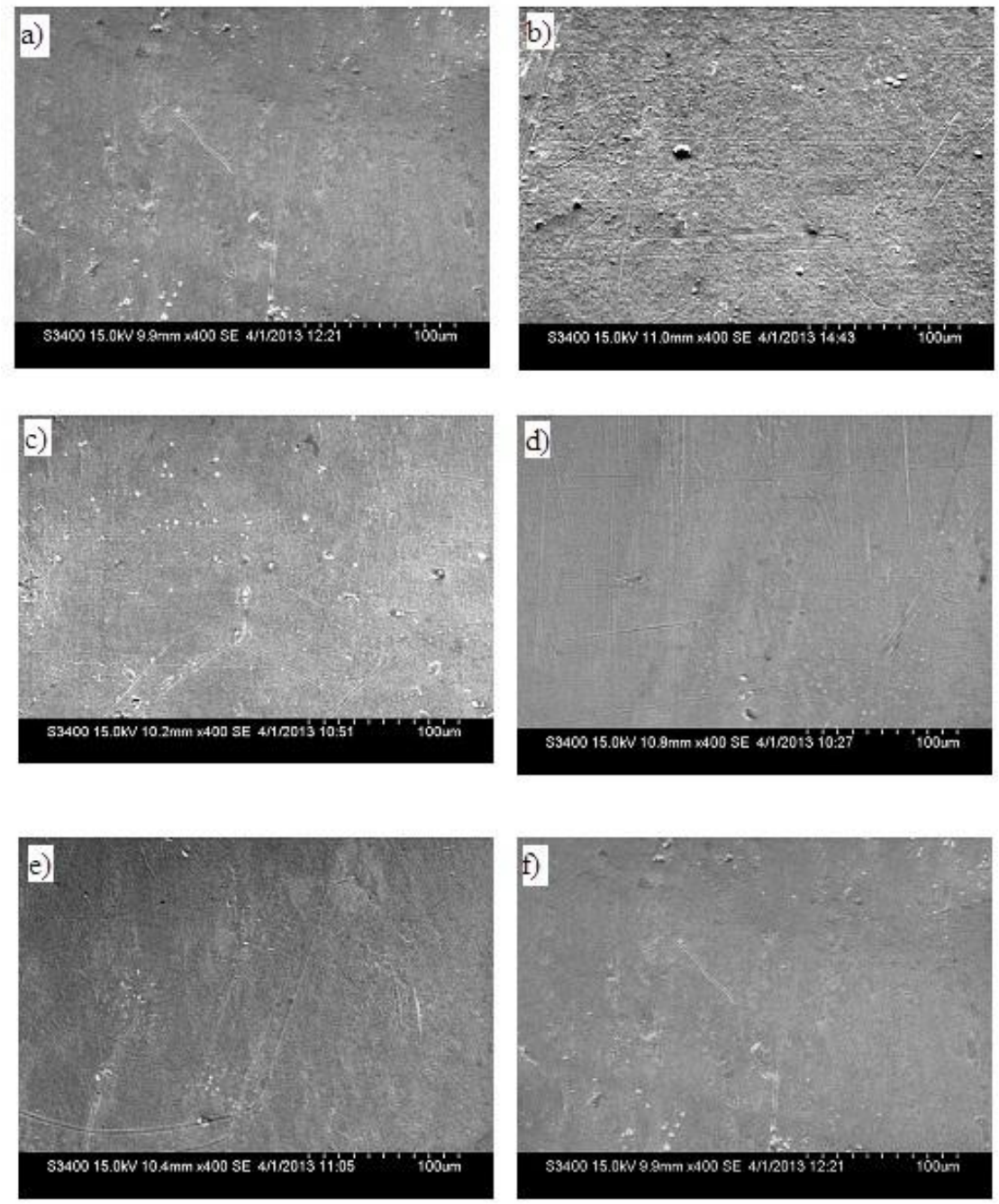

Figure 5.8 SEM images of surfaces produced by ball burnishing at a) At burnishing speed = 15 m/min, feed=0.20 mm/rev, force=300 N, No. of passes = 4 (Tr.No-4) b) At burnishing speed = 15 m/min, feed = 0.25 mm/rev, force= 350 N, No. of passes =5(Tr.No-5) c) At burnishing speed= 45 m/min, feed=0.10 mm/rev, force = 300 N, No. of passes =1(Tr.No-12) d) At burnishing speed= 60 m/min, feed=0.10 mm/rev, force= 350N, passes = 3(Tr.No-17) e) At burnishing speed= 75 m/min, feed= 0.05 mm/rev, force= 350N, No. of passes= 4. f) At burnishing speed = 75 m/min, feed =0.10 mm/rev, force = 150 N, No. of passes = 5.(Tr.No-21)

Altenberger, I et al. (2012) have reported that cell formation was not observed, and the dislocation arrangement was almost entirely planar. This gives rise to significant increase in dislocation density . and lattice distortion in near sub surface.Bulk microstructure appears after this layer, which is considered as the end of burnishing influenced layer.

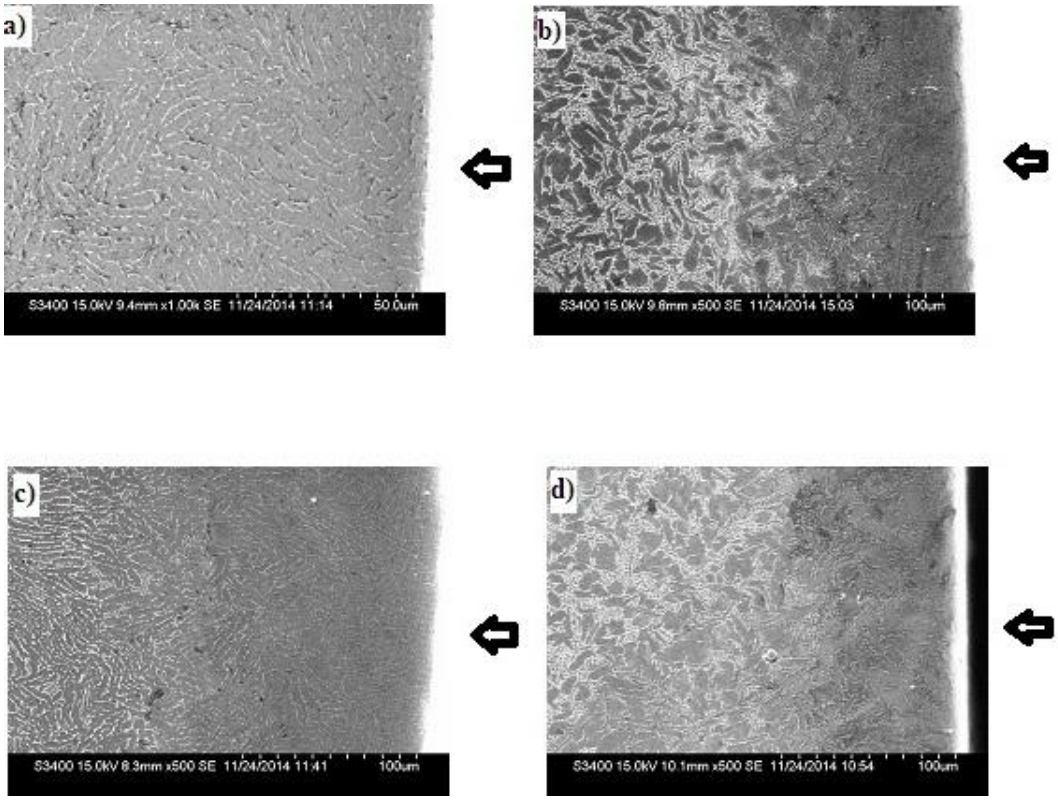

Figure 5.9 SEM images of the subsurface cross section at the topmost surfaces under different burnishing conditions a) Turned surface b) Burnished at burnishing speed = 15 m/min, feed=0.10 mm/rev, force = 200N, No. of passes = 2 (Tr.No-2) c) Burnished at burnishing speed = 15 m/min, feed =0.15mm/rev, force = 250 N, No. of passes = 3(Tr.No-3) d) Burnished at burnishing speed = 45 m/min, feed =0.15 mm/rev, force = 200N, No. of passes = 1(Tr.No-13) (Direction of arrow indicates the top surface)

5.3.4 EBSD ANALYSIS

Electron backscattered diffraction (EBSD) observation in the present study was performed at a depth of 100 µm from the top surface owing to the ultrafine grains in

the top surface of burnished samples. The orientation EBSD images of the titanium alloy before and after deformation are shown in Figure 5.10.

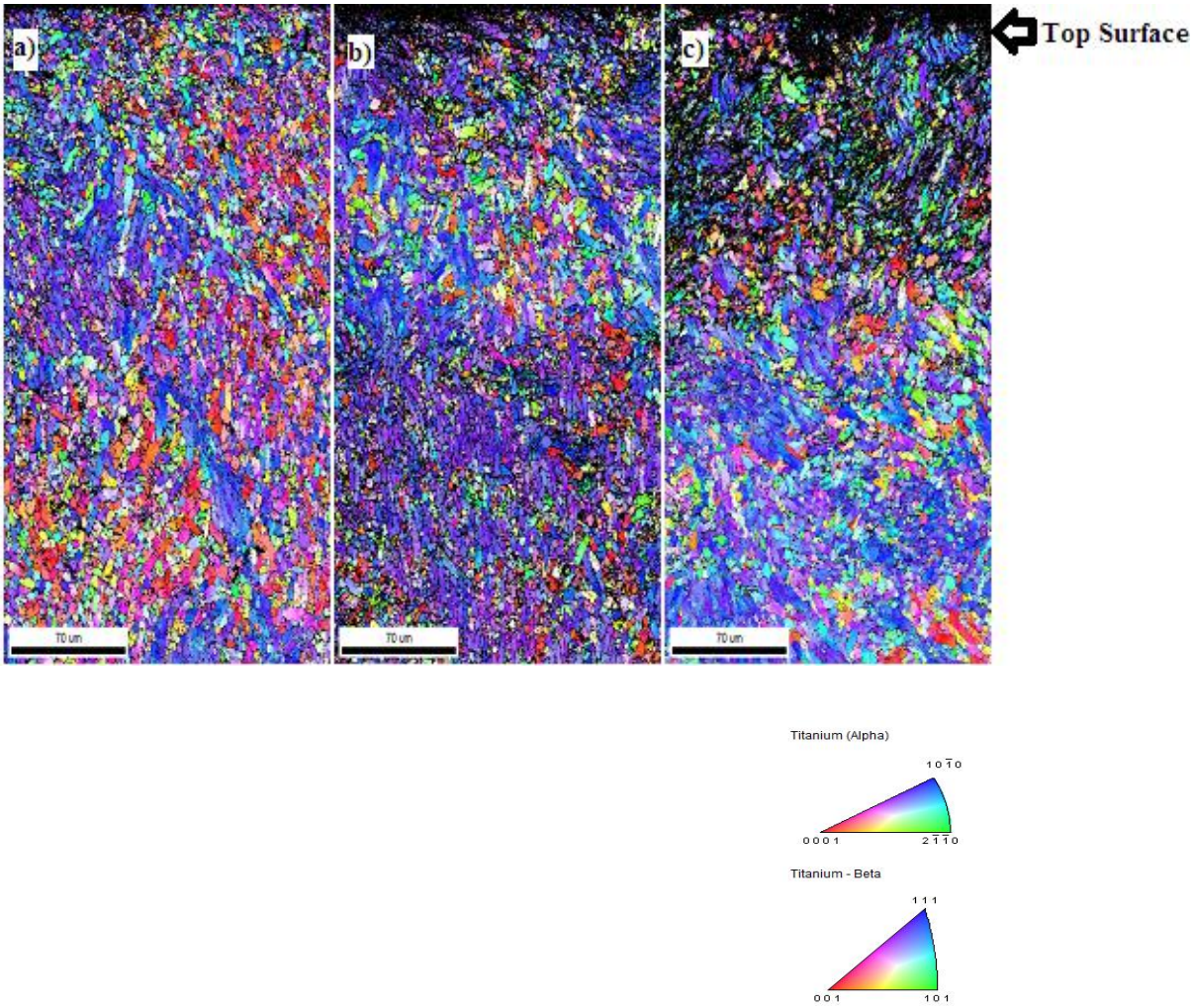

Figure 5.10 EBSD image morphology of turned and burnished surfaces of Ti–6Al–4V alloy specimens a) Turned specimen under MQL conditions with a flow rate of 150ml/hr, speed of 175m/min and a feed of 0.05mm/rev. b) Burnished at speed = 15 m/min, feed =0.10 mm/rev, force = 200N, No. of passes = 2(Tr.No.-2) c) Burnished at speed = 15 m/min, feed =0.15mm/rev, force = 250 N, No. of passes = 3 (Tr.No.-3)

As shown in the figure, the color of the grains indicates the different orientation and the similar color means the grains have similar orientation. Figure 5.10 (a) shows the image before deformation i.e. after turning. Some grains were elongated in the specimen deformed as shown in Figure 5.10 (b). On being further deformed by increasing the burnishing force, the dislocations can be observed as shown in Figure

5.10(c). EBSD examinations disclose that the density of sub-grain boundaries and high angle grain boundaries increased during deformation, clearly signifying that dislocation sliding and climbing are the significant processes during deformation (Tan, M.J. and Zhu, X.J. 2006).The experimental results indicate that the superplastic deformation is controlled by grain boundary sliding and dislocation motion.

5.3.5 FEM simulation results and discussions

In order to obtain reasonable representative residual stress distributions from 3D simulations, the residual stress distributions over the depths along five points at the middle of the burnished zone were extracted and the average residual stresses were computed. Stresses in X -direction represent axial stress while stresses in Y-direction represent tangential stress. The residual stresses in the radial direction (Z- direction) are small and negligible as shown in Figure 5.11. To obtain stress distribution, a central region of the simulation was selected, indicating the beginning and end of the tool traverse. Five depth lines in an intermediate simulation area were selected in order to obtain the arithmetic mean of five values of stress at each depth.

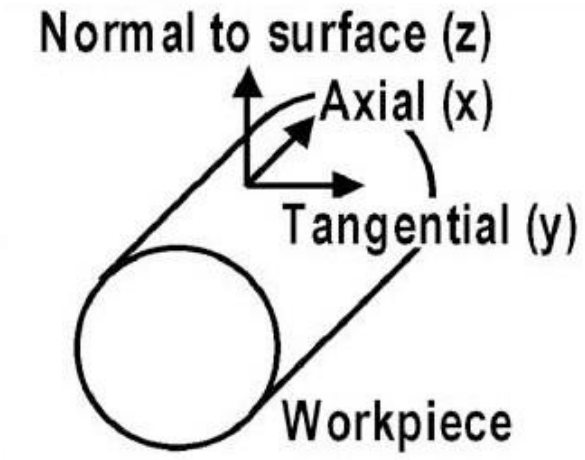

Figure 5.11 Measurement of residual stresses along various axes

Figure 5.12 depicts various stages of contact interactions during simulations. The ball is brought into contact with the surface of the workpiece and no residual stress is observed (Figure 5.12 (a)).

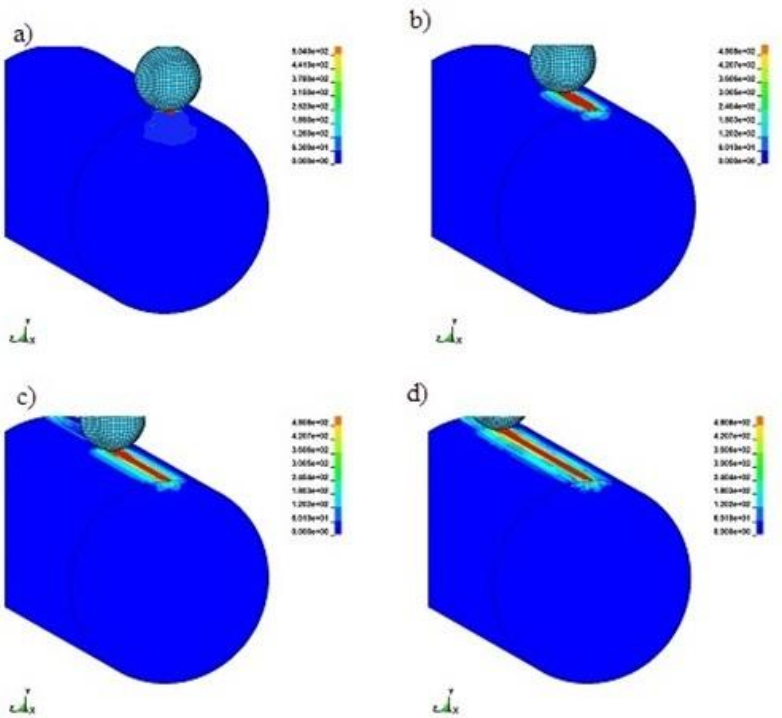

Figure 5.12 Various stages of finite element simulations

Then, the ball is pressed against the surface of the workpiece by applying required force and then rolled all along the surface as shown in Figures 5.12 (b), (c) and (d). Residual stress distribution could be observed on the surface and subsurface of the workpiece. Finally, the ball is withdrawn from the surface of the workpiece and moved to the original position.

Residual stress profile and the maximum residual stress obtained by finite element analysis of burnishing are compared with the experimentally obtained data as shown in Figures 5.13 and 5.14.

5.3.5.1 Effect of burnishing feed on residual stress

To study the distribution of the residual stresses using different values of burnishing feed (f=0.05, 0.10, 0.15, 0.20 and 0.25 mm/rev) with a burnishing force of 200N, FEM simulations were carried out. Figure 5.13 shows the effect of burnishing feed on the experimental and simulated residual stress distribution.

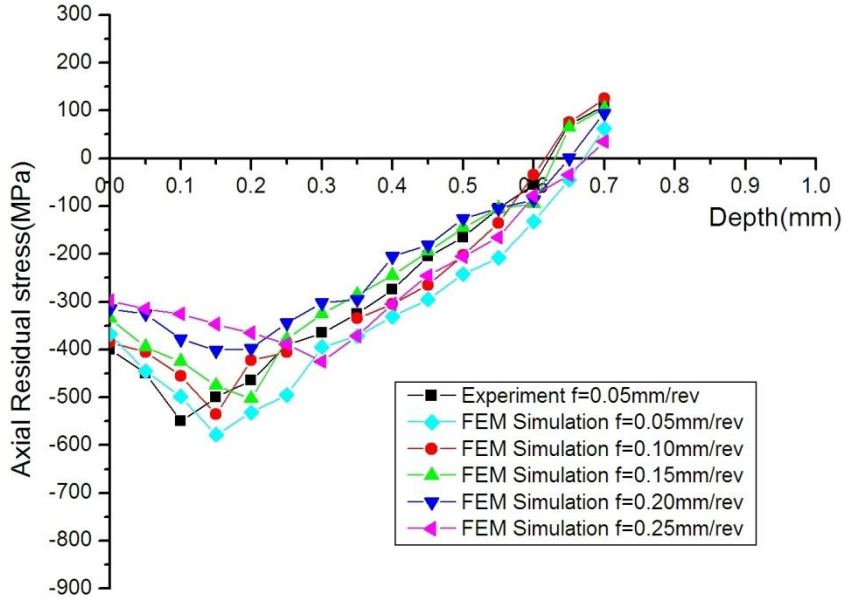

(a)

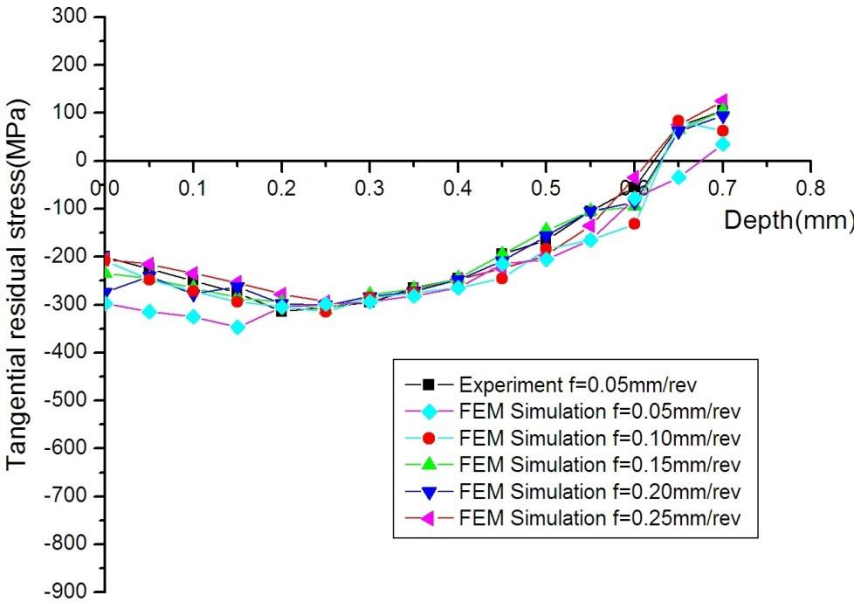

(b)

Figure 5.13 Simulation of the axial (a) and tangential (b) residual stress state after burnishing using different burnishing feed (f=0.05,0.10,0.15,0.20 and 0.25 mm/rev) and F= 200N

It is evident from Figure 5.14 that the predicted values of axial and tangential residual stress, under different feed rate are in good agreement with the experimental values. The effect of feed rate on residual stress is consistent with experimental observations. From the FEM simulation results in Figure 5.13, it is clear that a decrease in the burnishing feed slightly raises the magnitude of the compressive residual stresses in both axial and tangential directions. This can be explained by the fact that a small feed indicates shorter distance between ball traces. As a result, the workpiece surface was subjected to greater amount of plastic deformation and residual stresses due to more repetitive compression by the ball tool. Simulations showed greater influence of burnishing feed rate on tangential residual stresses i.e., more variation of residual stresses in tangential direction due to change in burnishing feed. However it was found that the magnitudes of the residual stresses are weak, for different values of feed. Thus, it can be concluded from FEM simulations that the axial and the tangential residual stresses are not significantly influenced by the feed (Afef Bougharriou et al. 2010).

5.3.5.2 Effect of burnishing force on residual stress

To study the distribution of the residual stress under different burnishing pressures (F=150,200,250,300 and 350N) with a burnishing feed rate of 0.05 mm/rev, various FEM simulations were carried out. Figure 5.14 shows the effect of burnishing pressure on the experimental and simulated residual stress distribution. Because of burnishing, compressive residual stresses were obtained in both axial and tangential direction. It was also evident that with the increase in burnishing pressure, higher residual stresses were generated at a greater depth. It is evident from Figure 5.14 that the predicted values of axial and tangential residual stress, under different values of burnishing force with a feed rate of 0.05mm/rev are in good agreement with the experimental values. The residual stress gradually increases upto a certain depth from the surface and achieves maximum value in the sub-surface and then decreases as we go deep into the surface. As the Figure 5.14 indicates, both FEA and experimental results show similar variations with respect to depth. To further study the effect of

burnishing force on residual stress, different simulations were tried out under different magnitudes of burnishing force, keeping the feed rate constant.

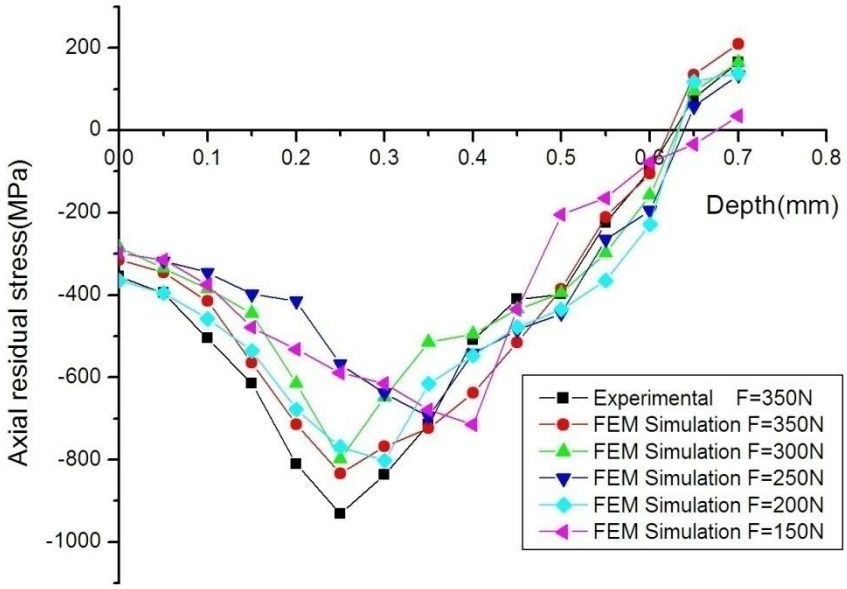

(a)

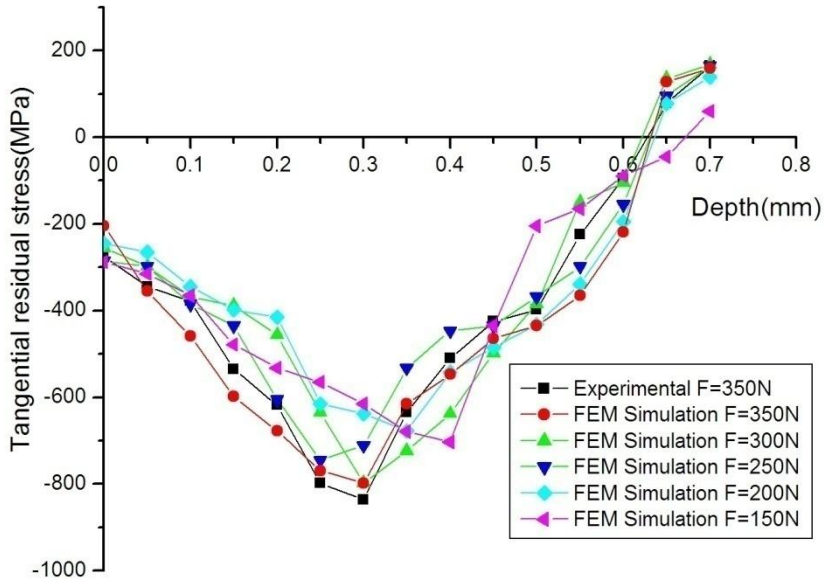

(b)

Figure 5.14 Simulation of the axial (a) and tangential (b) residual stress state after burnishing using different burnishing force (F=150, 200, 250,300,350 N) and burnishing feed (f=0.05 mm/rev.

The results qualitatively agree with the experimental results. Higher burnishing pressures generate more compressive residual stress near the surface and produce a deeper effective compressive stress layer. The occurrences of maximum residual compressive stress, its magnitude and depth at which it occurs follow similar trend in both techniques. The induced residual compressive stress values obtained from FEA are compared with the experimental X-ray diffraction results and the deviation is found to be less than 16%. As the burnishing force increases the compressive residual stresses also increase. The increase of applied burnishing force leads to an increase in the amount of plastic deformation as more roughness valleys are filled, during the process. It is established from the Figure 5.14 that the depth and maximum values of the residual stresses considerably increases with the increase in burnishing force. These results also agree with experimental study by Farough M et al.(2014) during low plasticity burnishing process of titanium alloy. From my study, it is evident that, with the increase in penetration depth, an increase in the burnishing force applied to the surface is observed which leads to increase in the surface hardness and compressive residual stresses (Klocke and Liermann, 1998). These results are qualitatively in agreement with the results of Sartkulvanich et al. (2007), Afef Bougharriou et al. (2010) and Sayahi M et al. (2013).Therefore, it can be concluded from the results that, if the only objective of surface treatment is to generate high residual stresses, the best choice is to burnish with the maximum pressure. But, increasing the burnishing pressure can result in increase of surface roughness and geometrical error, which has to be monitored.

5.4 ANALYSIS AND OPTIMIZATION IN BALL BURNISHING OF TITANIUM ALLOY (TI-6AL-4V) USING TAGUCHI METHOD USING IMPROVED BURNISHING TOOL

Based on the earlier experimental trials an attempt was made to develop a new burnishing tool and study its performance. The constructional details of the improved tool with its potential advantages have been explained in section 3.2.1.The burnishing trials were conducted using the improved burnished tool and its performance was analyzed for optimized burnishing process parameters.

5.4.1 Experimental details

In the present study, four parameters, namely, burnishing speed, burnishing feed, burnishing force and number of passes were identified and the range for each of the process parameters was determined through the preliminary experiments. Each process parameter was investigated at three levels to study the non-linearity effects of process parameters. The identified process parameters and their levels in the current investigation of burnishing process are summarized in Table 5.9.

Table 5.9 Ball burnishing process parameters and their identified levels for burnishing with improved tool

Code	Parameter	Level		
		1	2	3
A	Burnishing speed, m/min	2.5	6.9	11.72
B	Burnishing feed, mm/rev	0.1	0.13	0.15
C	Burnishing force, Newton	250	300	350
D	Number of pass	1	2	3

Table 5.10 L_9 Orthogonal array with the measured responses and corresponding S/N ratios for burnishing with improved tool

Trial No.	Levels of process parameters				Surface roughness, R_a (µm)	Hardness, H (Hv)	S/N ratio for surface roughness, η_1 (dB)	S/N ratio for hardness, η_2 (dB)
	A	B	C	D				
1	1	1	1	1	0.132	345	17.5885	50.7564
2	1	2	2	2	0.231	372	12.7278	51.4109
3	1	3	3	3	0.320	412	9.8970	52.2979
4	2	1	2	3	0.151	392	16.4205	51.8657
5	2	2	3	1	0.203	363	13.8501	51.1981
6	2	3	1	2	0.181	351	14.8464	50.9061
7	3	1	3	2	0.162	402	15.8097	52.0845
8	3	2	1	3	0.190	382	14.4249	51.6413
9	3	3	2	1	0.261	354	11.6672	50.9801

According to Taguchi design concept (Phadke, 1989 and Ross, 1996), L_9 orthogonal array (OA) with 4 columns and 9 rows was selected. Each burnishing process parameter is assigned to a column and nine different process parameter combinations are available. Thus, only nine experiments are required to study the complete burnishing process parameter space using L_9 OA. The experimental layout for the current investigation using L_9 OA is shown in Table 5.10. The pre-machined average roughness and hardness obtained were in the range from 0.63 to 0.78 μm (R_a) and 340 (*Hv*), respectively.

5.4.2 Results and discussion

5.4.2.1 Analysis of means and variance

In the present work, the objective is to minimize the surface roughness and to maximize the hardness of burnishing process. Hence, "smaller the better type" category for surface roughness and "larger the better type" category for hardness has been selected. The S/N ratios associated with the objective functions for each trial of the orthogonal array are calculated for surface roughness and hardness by using Equations (5.1) and (5.2) respectively. The corresponding S/N ratios for each trial of L9 orthogonal array are presented in Table 5.10

Table 5.11 ANOM for surface roughness based on S/N ratio for burnishing with improved tool

Parameter code	Levels			Optimum level
	1	2	3	
A	13.4044	15.0390	13.9673	2
B	16.6062	13.6676	12.1369	1
C	15.6200	13.6051	13.1856	1
D	14.3686	14.4613	13.5808	2

The analysis of means (ANOM) based on S/N ratio was carried out to determine the optimal levels of process parameters**;** the results of ANOM for surface roughness and hardness are represented in Tables 5.11 and 5.12 respectively. The level of a

parameter with the highest value of S/N ratio is the best combination level. The optimal parameter setting is found to be A2, B1, C1 and D2 for minimum surface roughness and A3, B1, C3 and D3 for maximum hardness.

Table 5.12 ANOM for hardness based on S/N ratio for burnishing with improved tool

Parameter code	Levels			Optimum level
	1	2	3	
A	51.4884	51.3233	51.5686	3
B	51.5689	51.4168	51.3947	1
C	51.1013	51.4189	51.8602	3
D	50.9782	51.4672	51.9350	3

Table 5.13 ANOVA for surface roughness based on S/N ratio for burnishing with improved tool

Parameter	Degrees of freedom	Sum of squares	Mean square	% contribution
A	2	4.1372	2.0686	8.87
B	2	30.9538	15.4769	66.34
C	2	10.1617	5.0808	21.78
D	2	1.4045	0.7023	3.01
Error	0	0	-	-
Total	8	46.6571	5.8321	100

To investigate the effects of burnishing process parameters quantitatively, the analysis of variance (ANOVA) based on S/N ratio has been employed (Phadke, 1989; Ross, 1996). Tables 5.13 and 5.14 give the summary of ANOVA results of surface roughness and hardness respectively. It can be seen from the ANOVA tables that burnishing feed (66.34%) and burnishing force (21.78%) have major contributions in minimizing the surface roughness; whereas burnishing speed and number of passes have least effects in minimizing the surface roughness. The number of passes (57.40%) and burnishing force (36.43%) play major roles in maximizing the hardness,

whereas burnishing speed and burnishing feed do not show noticeable effects in controlling the hardness.

Table 5.14 ANOVA for hardness based on S/N ratio for burnishing with improved tool

Parameter	Degrees of freedom	Sum of squares	Mean square	% contribution
A	2	0.0938	0.0469	3.92
B	2	0.0540	0.0270	2.25
C	2	0.8716	0.4358	36.43
D	2	1.3734	0.6867	57.40
Error	0	0	-	-
Total	8	2.3928	0.2991	100

Table 5.15 Results of confirmatory tests for burnishing with improved tool

Performance measure	Surface roughness	Hardness
Optimum Levels (A, B, C, D)	A2, B1, C1, D2	A3, B1, C3, D3
S/N predicted (η_{opt}), dB	18.9914	52.4436
Observed value	0.105 µm	422 Hv
S/N observed (η_{obs}), dB	19.5762	52.5063
Prediction error, dB	0.5848	0.0627
Confidence Interval value (*CI*), dB	± 23.0979	± 1.776

Here, the best combination values of the process parameters obtained through Taguchi optimization were set and the work pieces of the same batches were machined. The observed value of S/N ratio (η_{obs}) is compared with that of the predicted value (η_{opt}). Table 5.15 gives the confirmatory test results and it is observed from the table that the prediction error i.e., (η_{opt} - η_{obs}) is within the *CI* value indicating the adequacy of the surface roughness and hardness additive models. The best combinations of process parameters for minimizing surface roughness and for maximizing hardness along with the corresponding optimal values are given in Table 5.16. The main effect plots were

generated using *MINITAB* software (Minitab Inc., 2011) for analyzing the effects of process parameters on surface roughness and hardness.

Table 5.16 Optimal process parameter setting and the corresponding optimal values of surface roughness and hardness for burnishing with improved tool

Response	Optimal process parameter setting				Optimal value
	Burnishing speed (rpm)	Burnishing feed (mm/rev)	Burnishing force (Newton)	Number of passes	
Surface roughness	88	0.10	250	2	0.105 µm
Surface hardness	150	0.10	350	3	422 Hv

5.4.2.2 Analysis of surface roughness

The main effect plots of surface roughness are shown in Figure 5.15.

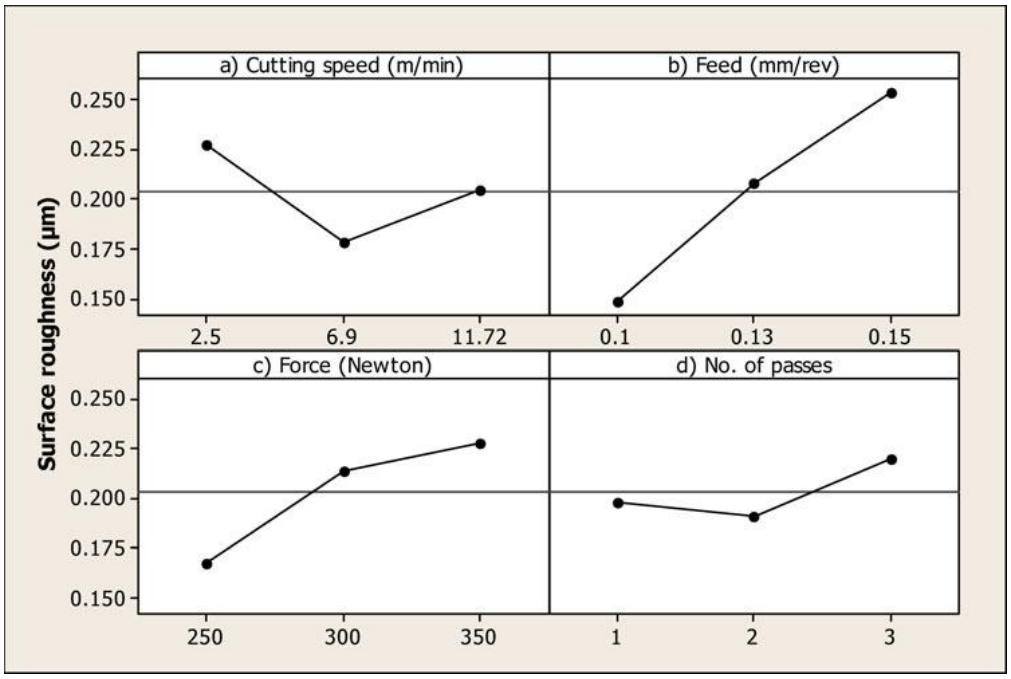

Figure 5.15 Main effect plots of surface roughness for burnishing with improved tool

The trends exhibited by the plots with regards to the effect of burnishing parameters on surface roughness are similar as explained in section 5.3.2.1 of the thesis. Hence, based on main effect plots of surface roughness, it is observed that a combination of medium burnishing speed, small feed, low burnishing force and medium pass is desirable to obtain the least rough surface during burnishing of titanium alloy.

5.4.2.3 Analysis of Hardness

The main effect plots of burnishing process parameters on mean values of surface hardness are depicted in Figure 5.16. The trends exhibited by the plots with regards to the effect of burnishing parameters on surface hardness are similar as explained in section 5.3.2.2 of the thesis. Hence, based on main effect plots of surface hardness, it is noticed that the increased burnishing force as well as the number of passes increase the surface hardness.

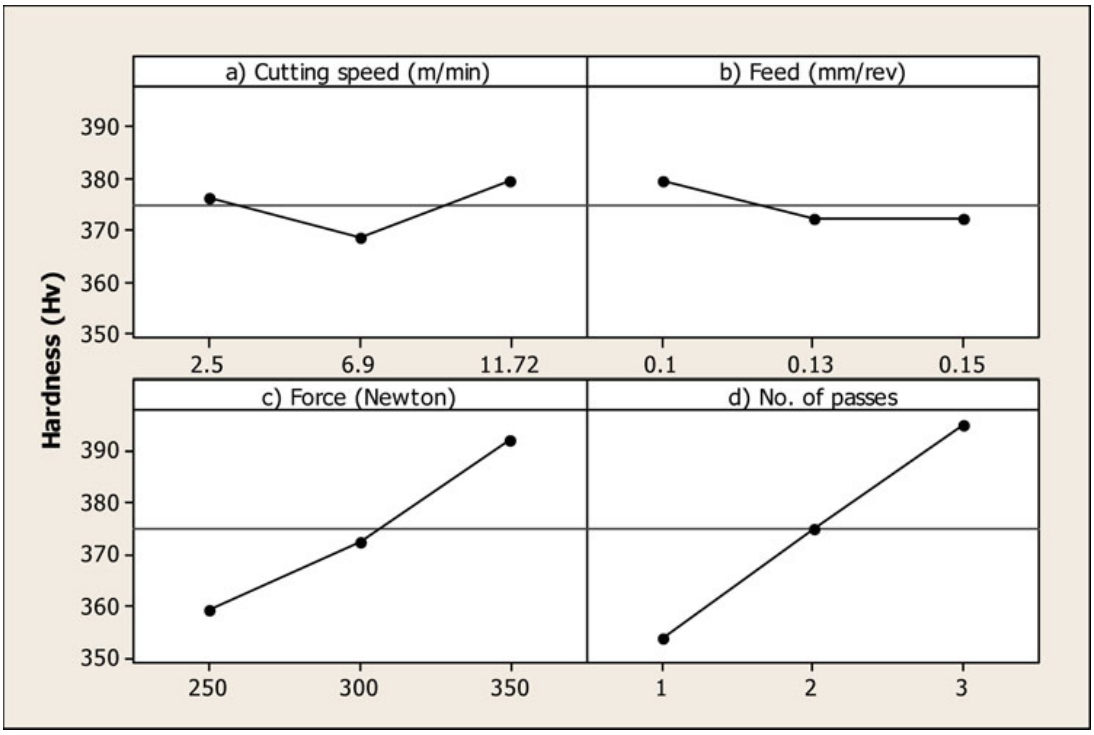

Figure 5.16 Main effect plots of hardness for burnishing with improved tool

The potential advantages of the improvised tool have been explained in section 3.2.1 of the thesis. Comparing the performance of this improvised tool with that of conventional tool, a marginal improvement of 1.5% in surface hardness was measured while the surface roughness remained about the same.

5.5 COMPARISION OF PERFORMANCE OF IMPROVED BALL BURNISHING AND ROLLER BURNISHING TOOLS

The present work is an attempt is an attempt to study the effects of both the ball and roller burnishing tool on the surface roughness and hardness of titanium alloy. The selected parameters for burnishing are shown in Table 3.11.The results and discussions of the experimental trials are presented below.

5.5.1 Analysis of surface roughness

The effect of burnishing parameters with respect to the surface roughness for both the ball and roller burnishing tool was studied. From the Figure 5.17, it is evident that the surface roughness decreases initially with the increase in force, then it starts increasing for both ball and roller burnishing tool. This is caused by flaking of the surface as the burnishing force increases.

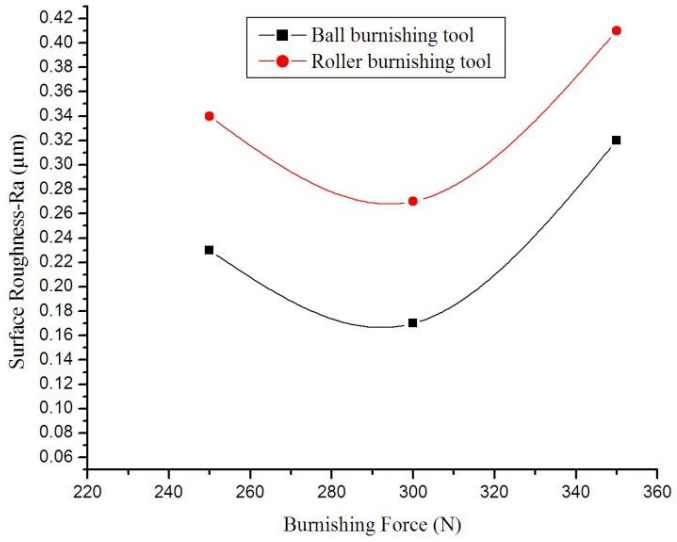

Figure 5.17 Effect of burnishing force on the surface roughness. Burnishing conditions: burnishing feed=0.10 mm/rev, burnishing speed=10m/min and number of passes=1

Minimum surface roughness is obtained for ball burnishing tool as compared to roller burnishing tool. The contact surface area between the tool and specimen is smaller in ball burnishing tool as compared to roller burnishing tool subjected to the same burnishing force. This means that the ball will penetrate inside the metallic surface deeper than the penetration of the roller.

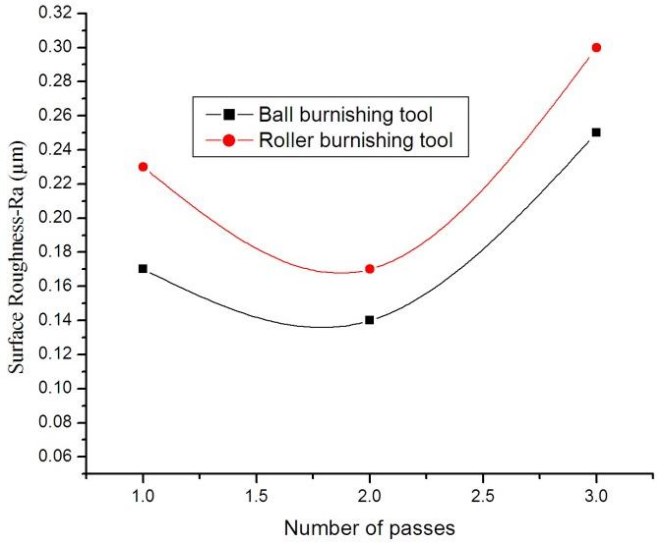

Figure 5.18 Effect of number of passes on the surface roughness. Burnishing conditions: burnishing feed=0.10 mm/rev, burnishing speed=10m/min and burnishing force =300N

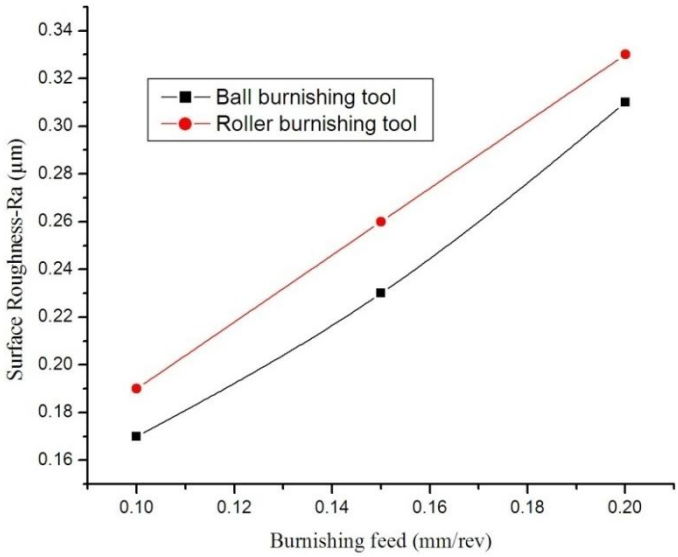

Figure 5.19 Effect of burnishing feed on the surface roughness. Burnishing conditions: number of passes = 1, burnishing speed=10m/min and burnishing force =300N

It is evident from the curves of Figure 5.18 that the surface roughness initially decreases with the increase in number of passes, but with further increase, the surface finish deteriorates. It is also evident that lower surface roughness was observed for ball burnishing tool in comparison with roller burnishing tool for all the number of passes. It is clear from Figure 5.19 that as the feed increases the surface roughness increases for both ball and roller burnishing tools. This phenomenon has been explained in section 5.3.2.1.

5.5.2 Analysis of surface hardness

The effect of burnishing parameters with respect to the surface hardness for both the ball and roller burnishing tool was studied. The bulk hardness of the surface before burnishing was 340Hv.After burnishing, the surface hardness varied between the ranges 355-405 Hv under different burnishing conditions. From the Figure 5.20, it is evident that, performance of ball burnishing tool with respect to surface hardness was better for the entire range of forces as compared to roller burnishing tool.

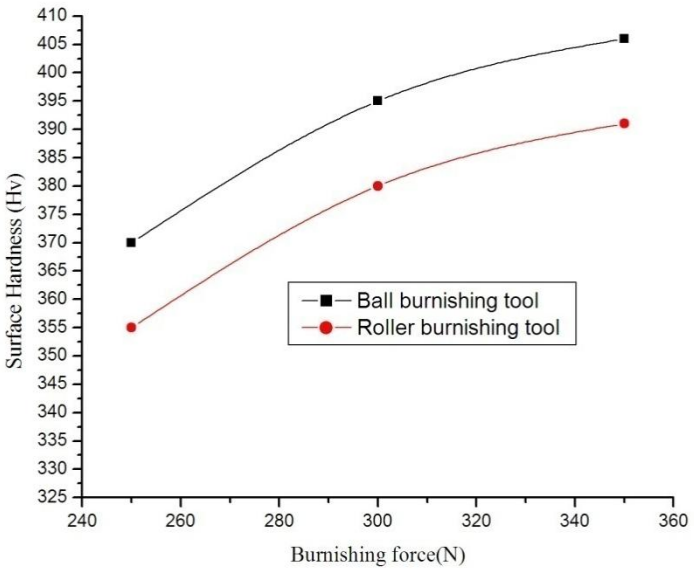

Figure 5.20 Effect of burnishing force on the surface hardness. Burnishing conditions: number of passes = 1, burnishing speed=10m/min and burnishing feed =0.10mm/rev.

Similarly the trend for number of passes and burnishing feed as shown in Figure 5.21 and Figure 5.22, respectively show that the ball burnishing tool fared better, resulting

in higher hardness, as compared to the roller burnishing tool under similar burnishing conditions .

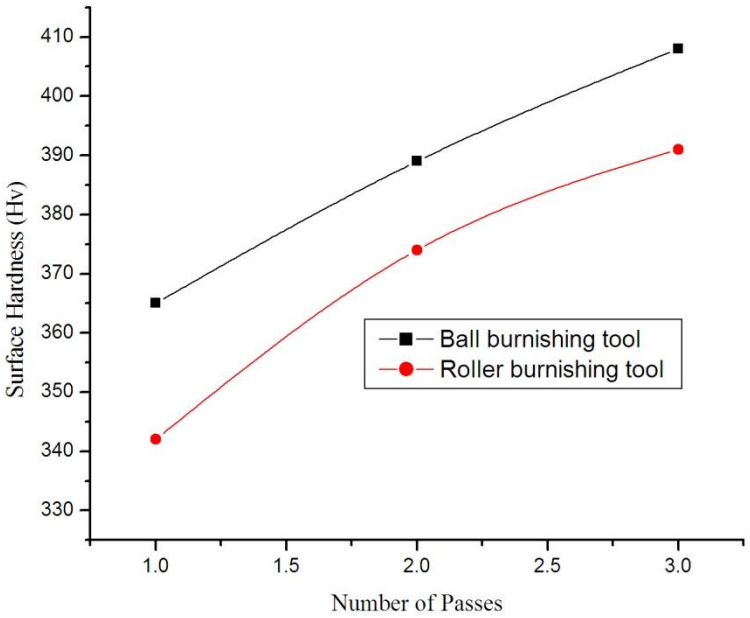

Figure 5.21 Effect of number of passes on the surface hardness. Burnishing conditions: burnishing force=300 N, burnishing speed=10m/min and burnishing feed =0.10mm/rev.

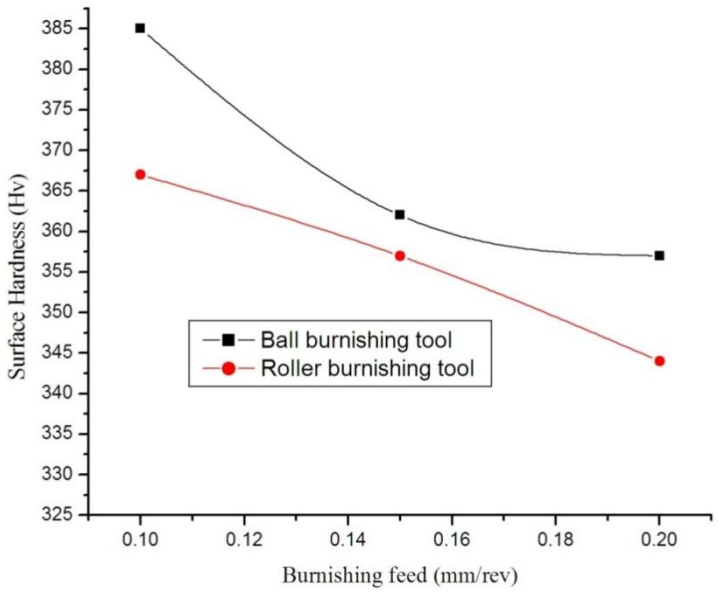

Figure 5.22 Effect of burnishing feed on the surface hardness. Burnishing conditions: burnishing force=350 N, burnishing speed=10m/min and number of passes =1.

The reason for this can be explained based on the ability of the ball to penetrate deeper into the metallic surface as compared to the roller (Hassan, A.M 1997).Thus based on the burnishing condition considered here it can be concluded that in both ball and roller burnishing, the surface roughness decreases to a minimum value with the increase in burnishing force and number of passes, after which it starts to increase. As illustrated in Figure 5.17, the surface roughness appreciably decreases for low range of forces and surface roughness increases further for higher range forces. This is due to the fact that at the commencement, the burnishing ball penetrates a little distance into a work surface, causing a little or incomplete deformation of the asperities and thus resulting in reduced surface roughness. When the force is slowly increased, the protrusion of work in front of the burnishing tool becomes large and the plastic deformation region broadens that in turn spoils the formerly burnished surface resulting in an enhanced surface roughness (Klocke, et al.1997; Nemat, M. and Lyons, A.C.2000). El-Taweel, T.A. and El-Axir, M.H. (2009), also reported that when the burnishing ball advances further along the work piece, the repeating plastic deformation action on the work surface leads to increased work-hardening of the earlier exaggerated layers of the deformed surface; which in turn produces flaking on the surface and hence, surface roughness increases. The diminished surface roughness noticed at higher force ranges may be probably due to increased ball pressure on work piece surface resulting in deforming most of the asperities and increasing the metal flow that leads to filling of more voids and/or valleys that were exited in subsurface layer due to burnishing operation. Our experimental results closely agree with the results obtained by López de Lacalle, L.N. et al. (2007) and Branko, T. et al. (2012). As shown in Figure 5.18, the surface roughness decreases when the number of passes is increased and reaches a minimum value. However, with the further increase in the number of passes, the surface roughness increases considerably. The increase in surface roughness with more number of passes is fairly understandable because of over hardening and consequently flaking of the surface layers due to more repeated ball burnishing of the work surface (Nemat, M. and Lyons, A.C. 2000, El-Taweel, T.A. and El-Axir, M.H. 2009). It is evident from Fig.5.19 that lower the burnishing feed better lower is the surface roughness and as the feed increases the surface roughness increases. At low feed, the distances between the consecutive traces of the

burnishing ball will be little; moreover the ball will have more opportunity to smooth out the bulged edges of the previous traces as the tool passes slowly all along the workpiece. This leads to a decrease in surface roughness. Low feeds are advantageous for minimizing the surface roughness because the deforming action of the burnishing tool is greater and metal flow is regular at low feed. With the increase in feed, the surface roughness drastically increases. As the feed is progressively increased, the distance between the successive burnishing ball traces increases, resulting in a reduction in likelihood for the burnishing ball to even out all the bulged edges of the former traces and therefore an enhanced surface roughness (El-Axir,M.H. et al.2008, El-Taweel,T.A.and El-Axir,M.H. 2009). Also at higher feeds, the burnishing ball produces larger feed marks with a centre-line distance between two succeeding indentations and hence raised surface roughness (Nemat, M. and Lyons, A.C. 2000).In both the tools, the surface hardness increases with the increase in burnishing force and number of passes. Overall , the ball burnishing tool results in lower surface roughness and higher surface hardness than the roller burnishing tool.

5.5 CHAPTER CONCLUSIONS

The application of Taguchi optimization for burnishing of titanium alloy (Ti-6Al-4V) to minimize the surface roughness and maximize the hardness using conventional and improvised ball burnishing tool is presented in this paper. The burnishing speed, feed, force and number of passes were considered as the input process parameters. Based on the analysis of the experimental results, the following conclusions can be drawn in the present investigation.

- A combination of burnishing speed in the medium range, small feed, low burnishing force with three passes is helpful for reduced surface roughness. However, burnishing with medium speed and feed, higher force and more number of tool passes could improve the surface hardness.
- The burnishing feed and burnishing speed with contribution of 40.13% and 31.49% have major effects in minimizing the surface roughness. On the contrary, the burnishing force and number of passes with contribution of 48.95% and 19.80% have key roles in maximizing the hardness.

- In general, the surface roughness increases with increased feed and burnishing force. But, the roughness decreases with increased speed and number of tool passes until it reaches a minimal value and then with further increased speed and number of tool passes, the roughness increases.
- The surface hardness increases with burnishing force and number of tool passes. However, hardness increases with increased speed and feed only in the low ranges specified and beyond this range, the hardness starts decreasing.
- Taguchi optimization in our investigation, showed greater improvements in surface finish (77%) and visible improvements in hardness (17%) when compared to pre-machined surfaces.
- Our investigation reveals that, particularly at higher feeds, micro-cracks were developed, due to which the burnishing parameters could not be increased beyond certain limits.
- The compressive residual stresses were developed in axial and tangential directions after burnishing. The higher residual stresses were observed at higher feeds with increased burnishing force and at more number of tool passes. Even though our experimental findings confirm that the best option is to burnish titanium alloy with the maximum force for improved hardness; but with the introduction of residual stresses, the surface roughness increases.
- Predictions of residual stress distributions beneath the burnished surfaces with the developed 3D FEM model are in good agreement with the experimental measurements obtained using x-ray diffractions.
- The impact of burnishing feed on residual stress is less. The results of FEM simulations indicate that increasing burnishing feed rate causes a slight decrease in residual stress.
- The burnishing force has the maximum influence on the residual stresses. As the amount of plastic deformation in the workpiece increases, the magnitude of compressive residual stresses increase with increasing burnishing force. From the results of FEM simulations it is evident that with an increase of burnishing force, the compressive residual stresses also increases.

- During the study on the effect of burnishing parameters on surface roughness and hardness the improved tool showed similar trends as the earlier one.
- A marginal improvement of 1.5% in the surface hardness with the improvised tool was obtained, with reference to conventional tool, while the surface roughness remained almost the same.
- The improved ball burnishing tool performed better as compared to roller burnishing tool with respect to surface roughness and hardness under similar burnishing conditions.

The next chapter focuses on the viability of ball burnishing process for improving the tribological characteristics of titanium alloy, i.e. friction and wear performance.

Chapter 6

WEAR RESISTANCE ENHANCEMENT OF TITANIUM ALLOY (TI–6AL–4V) BY BALL BURNISHING PROCESS

6.1 OBJECTIVE

Titanium alloys have good biocompatibility and hence widely used as implant materials, but they suffer from poor wear resistance. In this chapter, an attempt is made to study the improvement in the wear resistance of titanium alloys potentially for implant applications. Titanium alloy Ti–6Al–4V was subjected to burnishing process to study the wear behavior. Ball burnishing process parameters such as burnishing speed, burnishing feed, burnishing force and number of pass were considered to minimize the specific wear rate and coefficient of friction. Burnishing is an acknowledged method of improving the resistance to wear, corrosion and oxidation. Further, these improvements can be widened to minimize friction and reduce adhesion. A large no of investigators have concluded that burnishing reduces coefficient of friction and enhances wear resistance. The aim of the present work is to investigate the wear resistance of burnished titanium alloy specimen by ball burnishing under different burnishing conditions, using the pin-on-disc testing in accordance with the ASTM G99-95 standard, in comparison with the turned specimen.

6.2 EXPERIMENTAL DETAILS

From the initial turning experiments conducted in the present work, the titanium bars were turned using poly crystalline diamond (ISO designation of CCMT09T304) tool under MQL conditions with a flow rate of 150ml / hr, speed of 150 m/min and a feed of 0.15mm/rev. After turning, the average roughness and hardness obtained were in the range from 0.40 to 0.45 μm (R_a) and 340 (Hv), respectively. In the present study, four parameters, namely, burnishing speed, burnishing feed, burnishing force and number of passes were identified and the range for each of the process parameters was determined through the preliminary experiments. The identified process parameters

and their levels in the current investigation of burnishing process are summarized in Table 6.1. Thus as per Taguchi method , nine experiments are required to study the complete burnishing process parameter space using L_9 orthogonal array .The experimental layout for the current investigation using L_9 orthogonal array along with the experimental results are shown in Table 6.2 and Table 6.3.

Table 6.1 Ball burnishing process parameters and their identified levels for wear tests

Code	Parameter	Levels		
		1	2	3
A	Burnishing Speed, (m/min)	15	30	45
B	Burnishing Feed ,mm/rev	0.05	0.10	0.15
C	Burnishing Force, N	150	200	250
D	Number of passes	1	2	3

Wear tests were conducted, on a pin-on-disc wear testing machine (Model: TR-20, DUCOM) as per ASTM: G99-95. The wear tests were conducted under uniform condition at a constant load of 10 N at a sliding velocity of 2.68 m/s and a sliding duration of 180sec. At the end of each test, the specimen was weighed again on the same balance after cleaning with acetone. To measure slide mass loss, the difference between the initial and final weights was taken and was divided by the sliding distance to calculate the wear rate. To convert, mass based wear rate to volumetric wear rate, the density of the titanium alloy (0.00451g/mm^3) was taken. The specific wear rate, W_r (mm^3/Nm) was calculated using the following equation:

$$W_r = \Delta m / (\rho \times t \times Vs \times F_N) \quad (6.1)$$

where , Δm is the mass loss of the pin samples (g), ρ is the density of the test sample (g/mm^3), t is the test duration (s), Vs is the sliding velocity (m/s) and F_N is the average normal load (N).

Table 6.2 Orthogonal array, measured responses and corresponding S/N ratios for hardness and surface roughness during wear tests

Tr. No.	A	B	C	D	Hardness (Hv)	S/N ratio for Hardness	Surface Roughness (μm)	S/N ratio for Surface Roughness (dB)
1	1	1	1	1	378	51.5498	0.13	17.7211
2	1	2	2	2	371	51.3875	0.16	15.9176
3	1	3	3	3	405	52.1491	0.27	11.3727
4	2	1	2	3	400	52.0412	0.12	18.4164
5	2	2	3	1	395	51.9319	0.23	12.7654
6	2	3	1	2	388	51.7766	0.25	12.0412
7	3	1	3	2	398	51.9977	0.19	14.4249
8	3	2	1	3	385	51.7092	0.18	14.8945
9	3	3	2	1	382	51.6413	0.26	11.7005

Table 6.3 Orthogonal array, measured responses and corresponding S/N ratios for specific wear rate and coefficient of friction during wear tests

Tr. No.	A	B	C	D	Specific wear rate , W_r (mm^3/Nm)x 10^{-4}	S/N ratio for Specific wear rate (dB)	Coefficient of friction	S/N ratio for Coefficient of friction (dB)
1	1	1	1	1	4.72621	66.5097	0.20	13.9794
2	1	2	2	2	4.97496	66.0642	0.21	13.5556
3	1	3	3	3	3.31664	69.5860	0.32	9.8970
4	2	1	2	3	3.77268	68.4670	0.19	14.4249
5	2	2	3	1	3.95924	68.0478	0.25	12.0412
6	2	3	1	2	4.51892	66.8993	0.28	11.0568
7	3	1	3	2	3.91778	68.1392	0.24	12.3958
8	3	2	1	3	4.85059	66.2841	0.27	11.3727
9	3	3	2	1	4.74694	66.4717	0.31	10.1728

6.3. RESULTS AND DISCUSSION

6.3.1 Analysis of mean and variance for wear tests

In the present work, the objective is to minimize the specific wear rate and coefficient of friction during burnishing process. Hence, "smaller the better type" category for the specific wear rate ($W_{r)}$ and coefficient of friction (μ) has been selected. Moreover, to study the effect of burnishing parameters on hardness(H) and surface roughness(Ra), "larger the better type" category for hardness and "smaller the better type" category for surface roughness have been selected The S/N ratio associated with the objective functions for each trial of the orthogonal array are given by:

$$\eta_1 = -10 \log_{10}(Wr^2) \quad (6.2)$$

$$\eta_2 = -10 \log_{10}(\mu^2) \quad (6.3)$$

$$.\eta_4 = -10 \log_{10}(Ra^2) \quad (6.4)$$

$$\eta_3 = -10 \log_{10}(H^{-2}) \quad (6.5)$$

The corresponding S/N ratios for each trial of L_9 orthogonal array were determined using Eqs. (3) to Eqs.(5) and are presented in Table 6.2 and Table 6.3. The analysis of means (ANOM) based on S/N ratio was carried out to determine the optimal levels of process parameters**;** the results of ANOM for specific wear rate and coefficient of friction are represented in Tables 6.4 and 6.5 respectively. The level of a parameter with the highest value of S/N ratio is the best combination level. The optimal parameter setting is found to be A2, B1, C3 and D3 for minimum specific wear rate and the optimal parameter setting for minimum coefficient of friction is found to be A2, B**1**, C2 and D2.

It can be seen from the ANOVA Table 6.6 that the burnishing force (57.77%) and number of passes (20.13%) play major roles in minimizing the specific wear rate, whereas burnishing speed (13.15%) and burnishing feed (8.95%) do not show noticeable effects in controlling the specific wear rate.

Table 6.4 ANOM for specific wear rate based on S/N ratio for wear tests

Parameter code	Levels			Optimum level
	1	2	3	
A	67.3867	67.8047	66.9650	2
B	67.7053	66.7987	67.6524	1
C	66.5644	67.0010	68.5910	3
D	67.0097	67.0342	68.1124	3

Table 6.5 ANOM for Coefficient of friction based on S/N ratio for wear tests

Parameter code	Levels			Optimum level
	1	2	3	
A	12.4773	12.5077	11.3138	2
B	13.6000	12.3232	10.3755	1
C	12.1363	12.7178	11.4447	2
D	12.0645	12.3361	11.8982	2

To investigate the effects of burnishing process parameters quantitatively, the analysis of variance (ANOVA) based on S/N ratio has been employed (Phadke 1989 and Ross 1996). Table 6.6 give the summary of ANOVA results of specific wear rate. Similarly, Table 6.7 gives the summary of ANOVA results of coefficient of friction. It can be seen from the ANOVA Table 6.7 that the burnishing feed (74.17%) and burnishing speed (13.03%) play major roles in minimizing the coefficient of friction, whereas burnishing force (11.43%) and number of passes (1.37%) do not show noticeable effects in controlling the coefficient of friction.

Here, the best combination values of the process parameters obtained through Taguchi optimization were set and the work pieces of the same batches were machined. The observed value of S/N ratio (η_{obs}) is compared with that of the predicted value (η_{opt}).

Table 6.6 ANOVA for specific wear rate based on S/N ratio for wear tests

Parameter	Degrees of freedom	Sum of squares	Mean square	% contribution
A	2*	1.0576	0.5288	8.95
B	2	1.5535	0.7768	13.15
C	2	6.8259	3.4130	57.77
D	2	2.3788	1.1894	20.13
Error	0	0	-	-
Total	8	11.8158	-	100
(Error)	(2)	(1.0576)	(0.5288)	

***** Factor A is pooled

Table 6.7 ANOVA for coefficient of friction based on S/N ratio for wear tests

Parameter	Degrees of freedom	Sum of squares	Mean square	% contribution
A	2	2.7802	1.3901	13.03
B	2	15.8211	7.9105	74.17
C	2	2.4373	1.2186	11.43
D	2*	0.2931	0.1466	1.37
Error	0	0	-	-
Total	8	21.3317	-	100
(Error)	(2)	(0.2931)	(0.1466)	

Table 6.8 gives the confirmatory test results and it is observed from the table that the prediction error i.e., (η_{opt} - η_{obs}) is within the *CI* value indicating the adequacy of the surface roughness and hardness additive models. The best combinations of process parameters for optimum specific wear rate and coefficient of friction, along with the corresponding optimal values are given in Table 6.9.

Table 6.8 Results of confirmatory trials for wear tests

Performance measure	Specific wear rate	Coefficient of friction
Optimum Levels (A, B, C, D)	A2, B1, C3, D3	A2, B1, C2, D2
S/N predicted (η_{opt}), dB	69.6378	14.6263
Observed value	0.000329 mm^3/Nm	0.1856
S/N observed (η_{obs}), dB	69.6561	14.6284
Prediction error, dB	-0.0183	-0.0021
Confidence Interval value (CI), dB	±3.7601	±1.9797

Table 6.9 Optimal process parameter setting and the corresponding optimal values of Specific wear rate and coefficient of friction for wear tests

Response	Optimal process parameter setting				Optimal Value
	Burnishing speed (m/min)	Burnishing feed (mm/rev)	Burnishing force (Newton)	Number of passes	
Specific wear rate (mm^3/Nm)	30	0.05	250	3	3.29×10^{-4}
Coefficient of friction	30	0.05	200	2	0.18

6.3.2 Analysis of Surface hardness and Roughness for wear tests

It is evident from the findings in Table 6.2 that the hardness of the burnished specimen was in the range of 371-405 Hv as compared to the turned specimen whose hardness was recorded as 340Hv. The analysis of hardness has revealed the influence of burnishing force on the formation of the cold worked zone leading to plastic deformation, thus providing wear resistance improvement for the sliding components. Also, the extent of this plastic deformation influences the magnitude of the compressive residual stresses with the increased burnishing force.

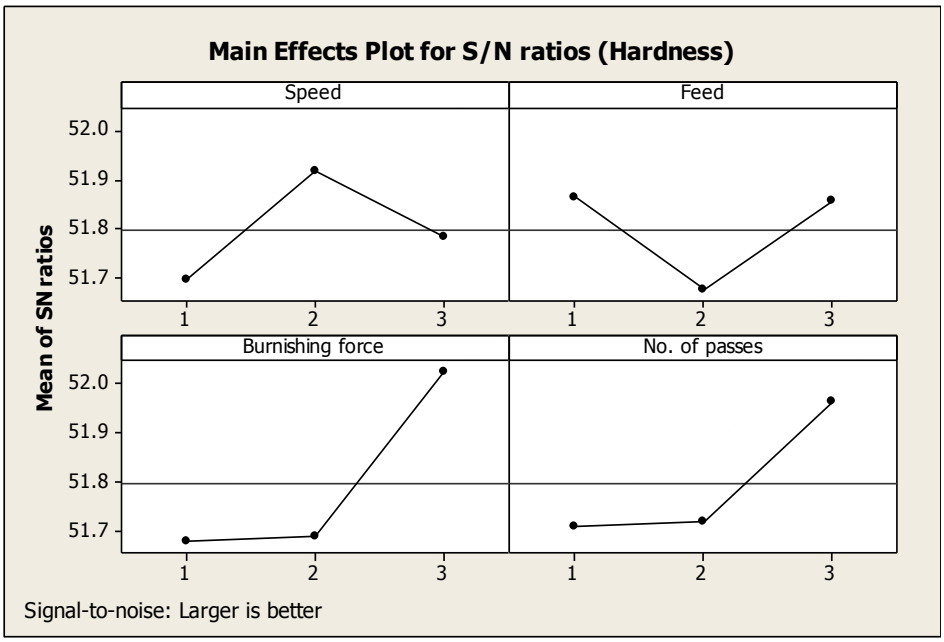

Figure 6.1 Main effect plots of surface hardness based on signal to noise ratio

From the main effects plot in Figure 6.1 on surface hardness during burnishing of titanium alloy, a similar trend as explained in section 5.3.2.2 of this thesis was observed. From Table 6.2, it is evident that the surface roughness of the burnished surface varied in the range of 0.12-0.27 µm as compared to the turned surface whose surface roughness was 0.5 µm. In general, the obtained enhancement of surface quality (Ra) can be explained in terms of the elimination of surface irregularities that occurred by the pressing of the ball which slides along the cylindrical surfaces with pressing burnishing force. The effect of the burnishing parameters on the surface

roughness can be studied from the main effects plot in Figure 6.2. A similar trend as explained in section 5.3.2.1 of this thesis was observed for surface roughness.

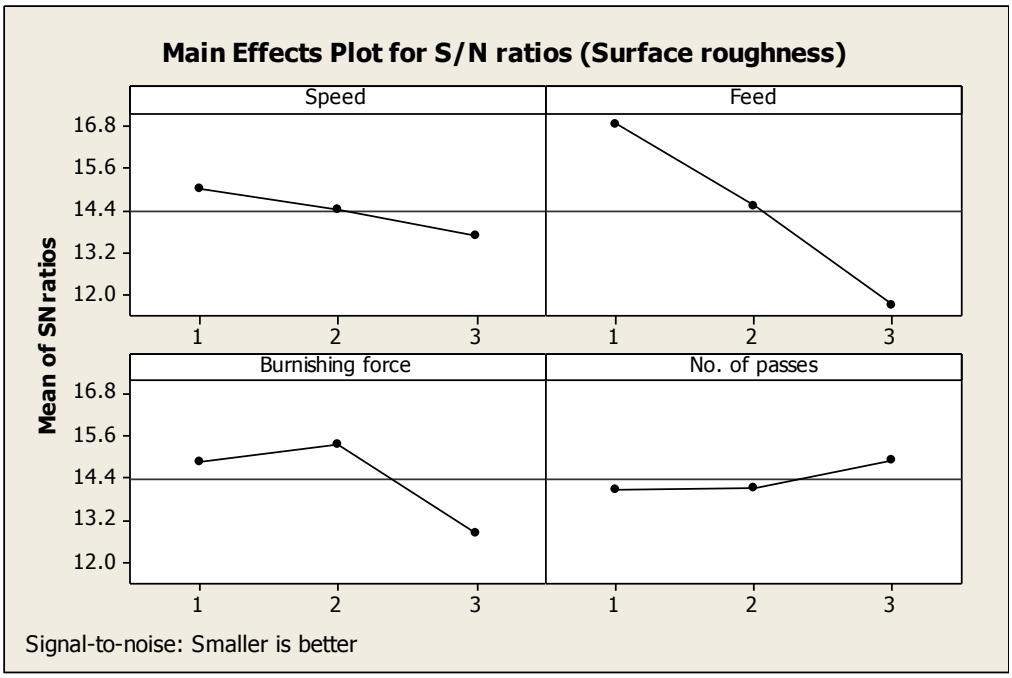

Figure 6.2 Main effect plots of surface roughness based on signal to noise ratio

6.3.3 Analysis of Specific Wear Rate for wear tests

From the ANOVA analysis in Table 6.6, it is evident that the strongest influence on specific wear rate was exerted by the burnishing force (57.77%) and number of passes (20.13%).Figure 6.3 illustrates the main effects plot of burnishing parameters on specific wear rate. From Figure 6.3 it is evident that the specific wear rate is reduced or an increase in wear resistance is observed with the increase in burnishing force, feed and no of passes whereas the specific wear rate decreases with the increase in burnishing speed. This is due to the fact that as the burnishing force increases from 150 N to 250 N, hardness of the surface is increased. The surface hardness increases rapidly with increase in burnishing force resulting in the improvement of wear resistance. Further, burnishing force increases the compressive residual stress at the surface layers, thus hindering the growth of cracks and wear delamination. On the other hand, low burnishing force leads to less improvement because the insufficient pressure results in incomplete deformation action.

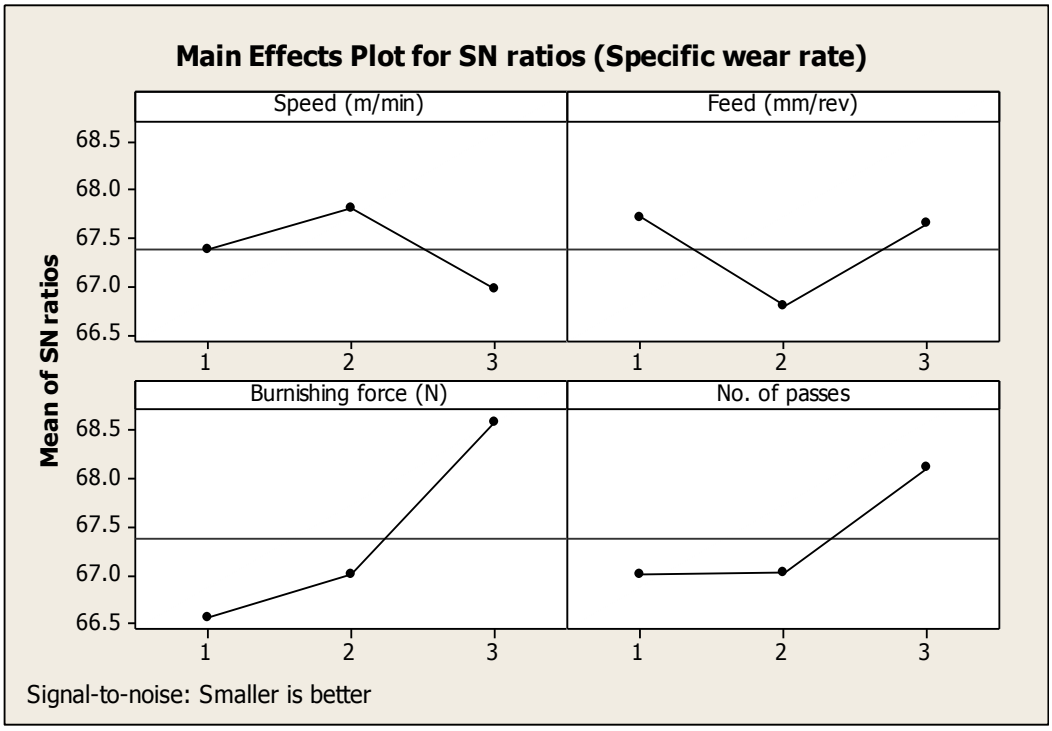

Figure 6.3 Main effect plots of specific wear rate based on signal to noise ratio

The variation of the specific wear rate with respect to hardness is shown in Figure 6.4. The equation for linear fit correlating the specific wear rate (Wr) and Hardness (Hv) is formulated, and given below (Eqn. 6.6)

$$Wr=0.00234-4.91751x10^{-6}Hv \qquad (6.6)$$

The best fit line indicates a linear relationship for decrease of wear rate with hardness. Some of the results of our investigations are compared with the previously published works. The study conducted by Yasuhiro, M and Kei, D. (2011) on surface age hardening and wear properties of beta-type titanium alloy revealed that the wear amount of the titanium alloy decreased with the increase in hardness. Titanium has low wear and abrasion resistance because of its low hardness (Freese,H et al.2001). Because of the increase in burnishing force, the surface deformation and work hardening also increased, thus resulting in increase of surface hardness(Yasuhiro, M and Kei, D. 2011).The wear resistance of titanium has been related to the sub surface deformation behavior (Long, M. and Rack, H. 1998,Ohkubo, C et al.2003 and Chan, K.S et al.2007). From the experimental findings of Chan, K.S et al. (2007) it has

been demonstrated that wear resistance of Ti-based alloys increases with increasing hardness. It is reported in the literature that blasting of metals/metal alloys with particulate material can lead to work hardening and that this increased hardness can give rise to enhanced surface wear resistance (Gil, F.J. et al. 2007). Similar observation was reported from the studies of Srinivasa Rao, D et al. (2008) that the wear resistance of HSLA Dual-Phase Steels improved with increase in burnishing force due to the plastic deformation of surface of the components by obtaining highest hardness.

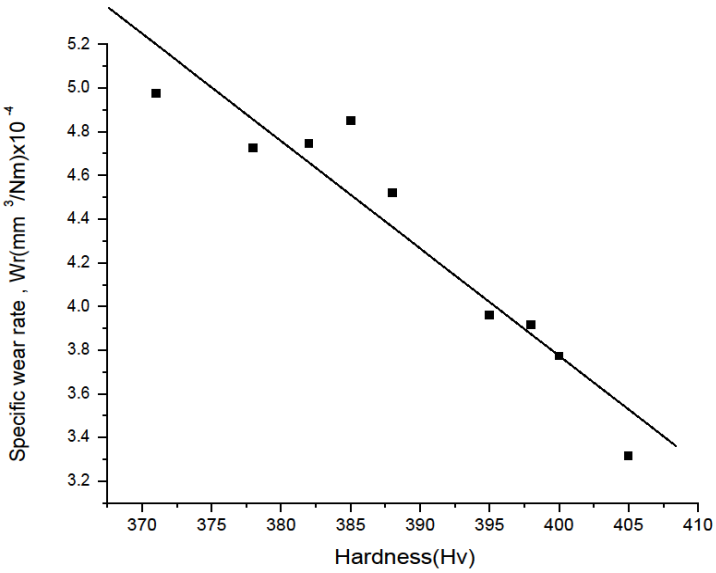

Figure 6.4 Plot showing the variation of wear rates with hardness of the burnished Ti-6Al-4V alloy component

The present results (Figure 6.3) show that, with the increase in number of passes, the specific wear rate decreases. As the number of passes increase, the surface hardness also increases, due to deformed grain structure and increased structural homogeneity (Nemat, M. and Lyons, A.C. 2000, El-Taweel, T.A.and El-Axir, M.H. 2009) . It can also be observed from the main effect plot that the specific wear rate decrease with the decrease in feed. At lower feed the surface hardness is high and hence lower specific wear rate. This can be explained by the fact that, at lower feed, the plastic deformation is more rigorous causing a greater increase in surface hardness. In

addition at lower feed, the number of times a ball deforms over the same spot is greater than at higher feed. The work hardening influence on the burnished surface is also greater at lower feed and decreases with increased feed. Study by El-Taweel, T.A.and El-Axir, M.H. (2009) reveals that increase in feed leads to decrease in surface hardness because of less work-hardening on the surface due to smaller surface area of the work piece subjected to plastic deformation. The area subjected to plastic deformation is smaller because at higher feeds, the distances between the consecutive traces of the burnishing ball will be large ; hence the ball will have less opportunity to cover as the tool passes all along the work piece. The disadvantage of high feeds is the lower deforming action of the burnishing tool .This leads to a decrease in surface hardness. From Figure 6.3 the effects of burnishing speed on specific wear rate can be analyzed. It is observed that at low speed, the specific wear rate decreases and worsens with the rise of burnishing speed. During initial range of burnishing speed (15-30 m/min), the hardness increases which tend to enhance the wear resistance. Because at low speed, due to more time of penetration of the burnishing tool into the burnished surface; the plastic deformation is more and hence subsequently an added amount of work hardening into the burnished surface. However, with a further increase in cutting speed in the range 30-60 m/min, the hardness decreases. As the speed increases there is a rise in temperature of the work piece and the burnishing ball, resulting in the increase in recovery of the work-hardening on the surface, which is associated with the increase in the rate of surface deformation. Moreover, at higher speed, greater frictional heat is generated as lubricant loses its effect due to limited time to interpose between the burnishing ball and work piece surface. This frictional heating promoted a temperature rise in the burnishing zone and subsequently softening of the surfaces. The increase in burnishing speed leads to instability of burnishing tool across the work piece surface resulting in insufficient burnishing and hence surface hardness is low (Srinivasa Rao, D et al. 2008, El-Taweel, T.A.and El-Axir, M.H. 2009). During my present study, it was observed that higher speeds led to insufficient burnishing and probably due to which, the surface hardness might be low hence decreased wear resistance. In my study, the burnishing speed of 30 m /min was found to be suitable for improved surface hardness. An attempt has been made to examine the depth beneath the surface, upto which plastic deformation occurs. Due to

burnishing, the surface and immediate sub-surface of the material turned harder as a result of work hardening, due to mechanical and thermal load on the work piece. It is apparent that, when a metal/alloy is continuously moving over a surface, plastic deformation takes place, which in turn produces work hardening effect and creates harder surface .The micro hardness depth distribution of titanium material for Trial no.8 as per the experimental plan (Table 5.2), after burnishing is shown in Figure5.5 and the optical image of indentation markings for micro hardness is shown in Figure 3.24. The hardness value of the surface is much higher than the bulk material hardness. It was observed that the micro hardness induced by ball burnishing had a steep fall, close to the surface. This is due to slight shearing between the ball and the sample surface, as well as lower strain rate by ball burnishing. At a depth of 210 μm beneath the burnished surface, the difference in hardness was very small and the hardness values approached the hardness of the base material as the depth beneath the burnished surface increased. The top layer of the burnished surface experiences work hardening process and hence the hardness is higher than the average hardness of the work piece material. On the other hand, due to the very high cutting temperature produced at the local surface, the material below the top layer is softer as a result of over-aging of titanium alloy. Furthermore, the temperature beneath the burnished surface is retained because of low thermal conductivity of titanium alloy. From the above discussion on surface hardness during burnishing of titanium alloy, it is evident that the surface hardness of the material increases with the increase in the burnishing force and number of passes due to work hardening. Plastic deformation produced by the application of a high burnishing force to the material surface creates a localized cold worked zone. The thickness of the consolidated metal layer formed after the compression of the surface will be greater as the burnishing force is increased. This layer provides a corrosion resistance enhancement and also a wear resistance improvement of sliding component. When a hardness increase is essential, burnishing force is a critical parameter. Using high burnishing force, hardness increase can be up to 60% (Brinell scale). Microstructure, affected layer and micro-hardness for turned and burnished surfaces shows that when the surface is turned, the sub-surface hardness is approximately constant whereas a deformation of the surface grains due to the cold-work process takes place during burnishing. This deformation is only

appreciable near the surface (20–30 μm). However, the hardness increase due to the deformation process extends to over 300 μm from the surface. Results show that the hardness improvement was higher with higher burnishing force values (Rodriguez A et al. 2012).

From the ANOM results as shown in Table 6.4 , the optimal burnishing parameters for minimum specific wear rate are burnishing speed(level 2) of 30m/min, feed (level 1) of 0.05 mm/rev, force (level 3) of 250 N and 3 no of passes (level 3). The minimum wear rate obtained under the optimum experimental condition was 3.29 $x10^{-4}mm^3/Nm$ when compared to its initial turned surface, where the corresponding value was $6.85x10^{-4}mm^3/Nm$ Therefore specific wear rate decreased by 52% in comparison with turned surface. The burnished surfaces in general, show better wear resistance compared to the initial turned surfaces.

Further burnishing trials were conducted under different burnishing to study the effect of burnishing parameters on specific wear rate. One burnishing parameter was varied whereas the other parameters were kept constant. The Figures 6.5-6.8, show the effect of burnishing parameters on specific wear rate under different burnishing conditions

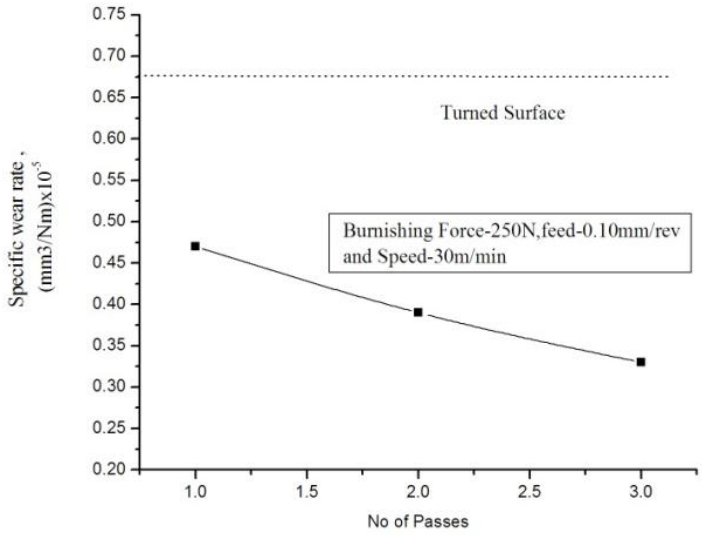

Figure 6.5 Effect of number of passes on the specific wear rate. Burnishing conditions: burnishing force=250 N, burnishing speed=10m/min and burnishing feed=0.10mm/rev.

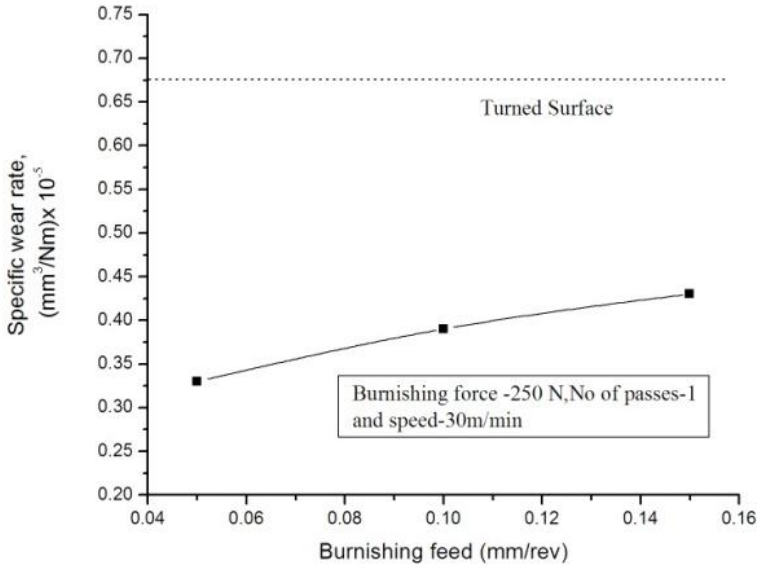

Figure 6.6 Effect of burnishing feed on the specific wear rate. Burnishing conditions: burnishing force=250 N, burnishing speed=10m/min and number of passes = 1.

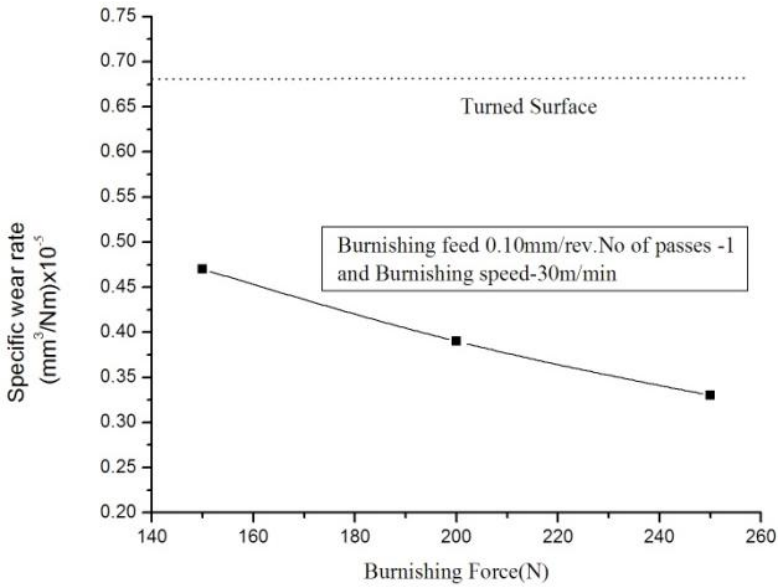

Figure 6.7 Effect of burnishing force on the specific wear rate. Burnishing conditions: number of passes =1, burnishing speed=30m/min and burnishing feed=0.10mm/rev.

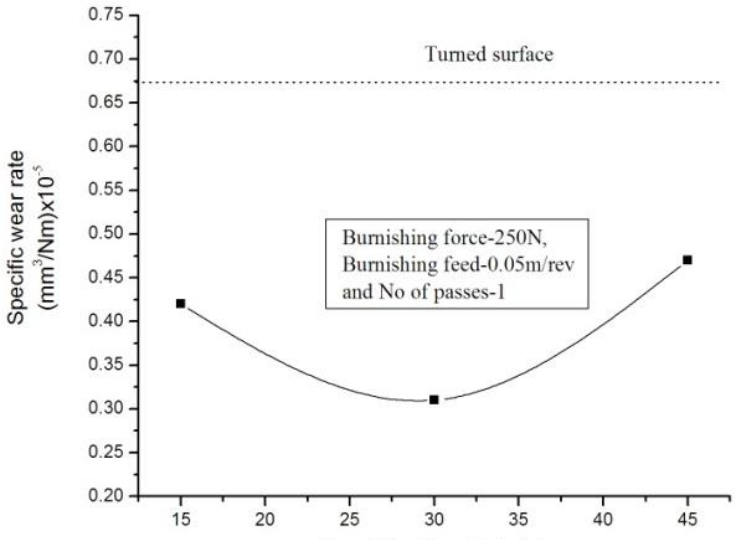

Figure 6.8 Effect of burnishing speed on the specific wear rate. Burnishing conditions: burnishing force=250 N, number of passes =1 and burnishing feed=0.10mm/rev.

From the Figures we can further verify experimentally that the trends shown by the burnishing parameters, agree very well with discusions presented in this section .Thus we can conclude that the specfic wear rate decreases with increase in burnishing force and number of passes.With the increase in burnishing feed and speed the , the specfic wear rate increases.

6.3.4 Analysis of coefficient of friction for wear tests

From the ANOVA analysis as shown in Table 6.7, it is evident that the strongest influence on coefficient of friction was exerted by the burnishing feed (74.17%) and burnishing speed (13.03%). The friction characteristics are evaluated in terms of coefficient of friction of the titanium alloy sliding against quenched and tempered EN-32 steel. These findings revealed that the burnished surfaces with low surface roughness assisted in a way to reduce coefficient of friction as compared to the turned surface (Low, K.O. and Wong, K.J. 2011). From the ANOM results as shown in Table 6.5 , the optimal burnishing parameters for minimum coefficient of friction are burnishing speed(level 2) of 30m/min, feed (level 1) of 0.05 mm/rev, force (level 2) of 200 N and 2 number of passes (level 2). The coefficient of friction for the turned surface was recorded as 0.5 whereas lowest coefficient of friction for the burnished

surface under optimum condition was 0.18 that is a reduction of 64%. The variation of coefficient of friction with respect to surface roughness is shown in Figure 6.9.

This trend supports the fact that lower surface roughness leads to lower friction coefficient. This is because burnishing action caused the sharp and serrated tip of asperities to deform. As a result, lesser interlocking between the asperities led to abridged ploughing action and resulted in the decrease of friction force, whose magnitude is determined by the energy to overcome deformation. Figure 6.10 illustrates the main effects plot of burnishing parameters on coefficient of friction. It is evident from the figure that as burnishing feed increases, the coefficient of friction also increases. The variation of coefficient of friction with respect to feed (Figure 6.10) reveals that the at low feed of 0.05 mm/rev, the distances between the successive traces of the burnishing ball will be small, and also the ball will have more chance to smooth out the bulged edges of the previous traces as the tool passes slowly along the workpiece. This leads to a decrease in surface roughness and hence reduced coefficient of friction. At higher feed ranges .i.e. 0.10-0.25 mm/rev, the coefficient of friction drastically increases.

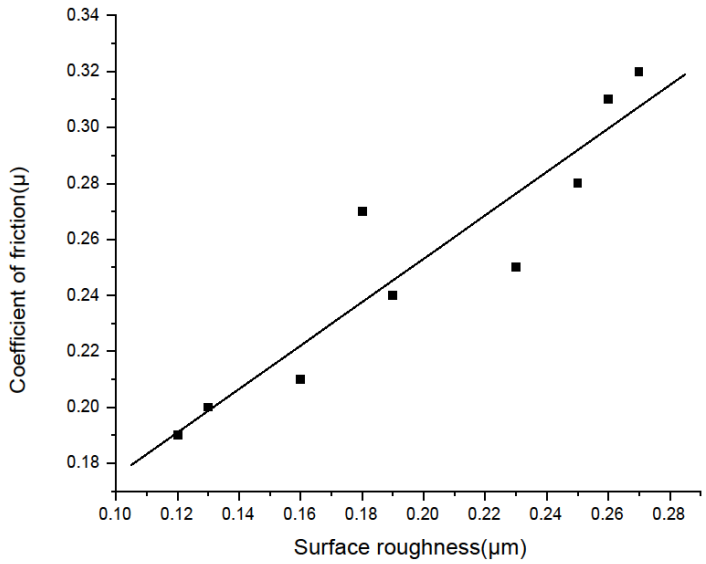

Figure 6.9 Plots showing the variation of coefficient of friction as a function of surface roughness for Ti-6Al-4V alloy component subjected to burnishing

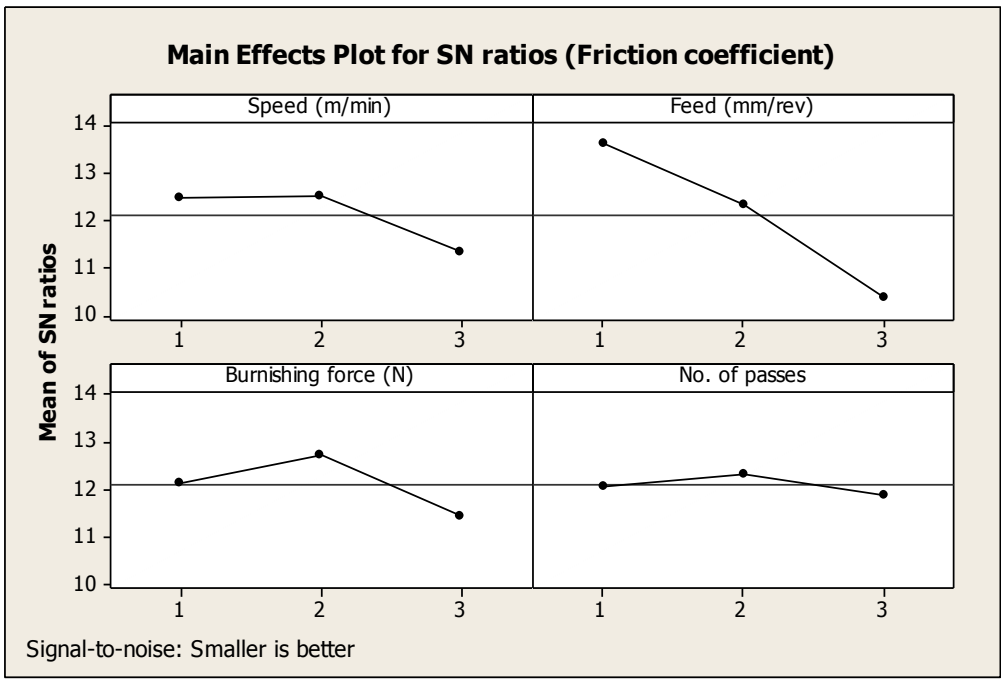

Figure 6.10 Main effects plot of coefficient of friction for wear tests

With the progressive increase in feed, the distance between the successive burnishing ball traces increases; resulting in a reduction in likelihood for the burnishing ball to even out all the bulged edges of the former traces and therefore leading to increased surface roughness (El-Tayeb et al.2008, El-Taweel, T.A.and El-Axir, M.H. 2009). Also at higher feeds, the burnishing ball produces larger feed marks with a centre-line distance between two succeeding indentations and hence raised surface roughness (Hassan,A.M. et al. 1998).As indicated in Figure 6.10 low feeds are advantageous for minimizing the surface roughness and coefficient of friction because the deforming action of the burnishing tool is greater and metal flow is regular at low feed.`

From the direct plot of coefficient of friction (Figure 6.10), it is observed that when the cutting speed is 15 m/min, the coefficient of friction is reduced due to reduction in surface roughness. The results revealed that less reduction in coefficient of friction was attained at lower burnishing speed 15 m/min. In the beginning, when burnishing speed is gradually increased, the work piece and burnishing ball temperature increase due to unsuitability of the burnishing tool crossing the work piece surface,

consecutively increasing the material transformation between burnishing ball-work piece interfaces and hence less reduction in surface roughness(El-Taweel, T.A.and El-Axir, M.H. 2009). With further increase in burnishing speed, from 15 m/min to 30 m/min the burnishing ball has more opportunity to settle down the abnormalities of the burnished surface and hence decreased surface roughness leading to reduced coefficient of friction. Further as the burnishing speed increases from 30 m/min to 45 m/min, the coefficient of friction increases. The reduced lubrication effect at the burnishing zone at high speed caused a rise in temperature, leading to higher coefficient of friction. Moreover, at higher speeds mainly due to the presence of chatter and reduced amount of deformation time being offered for the burnishing tool to smooth out more irregularities, an increase in surface roughness is observed (Hassan,A.M. et al. 1998). However, it can be seen that at all burnishing speed, a reduction in coefficient of friction was achieved.

As illustrated in Figure 6.10, the coefficient of friction appreciably decreases for low range of forces from 150 to 200 N and the coefficient of friction increases further for higher range 200-250 N. This is due to the fact that at the commencement, the burnishing ball penetrates a little distance into a work surface, causing a little or incomplete deformation of the asperities and thus resulting into reduced coefficient of friction. When the force is slowly increased, the protrusion of work in front of the burnishing tool becomes large and the plastic deformation region broadens that in turn spoils the formerly burnished surface resulting in an enhanced surface roughness (Hassan,A.M. et al. 1998,Srinivasa Rao, D et al. 2008). El-Taweel, T.A.and El-Axir, M.H. 2009 also reported that when the burnishing ball advances further along the workpiece, the repeating plastic deformation action on the work surface leads to increased work-hardening of the earlier exaggerated layers of the deformed surface; which in turn produces flaking on the surface and hence, surface roughness increases. The diminished surface roughness noticed at higher force ranges may be probably due to increased ball pressure on work piece surface resulting in condensing the most asperities and increasing the metal flow that leads to filling of more voids and/or valleys that were exited in subsurface layer due to burnishing operation. Our experimental results closely agree with the results obtained by López de Lacalle, L.N.

et al. (2007).The surface roughness decreases when the number of passes is increased and reaches a minimum value when the number of passes is 2. However, with the further increase in the number of passes increases, the surface roughness considerably increases thereby resulting in increase of coefficient of friction. The increasing surface roughness with more number of passes is mainly due to the repeated over pressing of the surface by the burnishing ball which causes an increase in the surface hardness and consequently, flaking of the surface layers due to more repeated ball burnishing on the work surface (Hassan,A.M. et al. 1998, El-Taweel, T.A.and El-Axir, M.H. 2009).

Further burnishing trials were conducted under different burnishing to study the effect of burnishing parameters on coefficient of friction. One burnishing parameter was varied whereas the other parameters were kept constant. The Figures 6.11-6.14, show the effect of burnishing parameters on coefficient of friction under different burnishing conditions From the trend depicted in Figures 6.11-6.14, we can further verify experimentally that the trends shown by the burnishing parameters with respect to coefficient of friction , agree very well with discusions presented in this section.

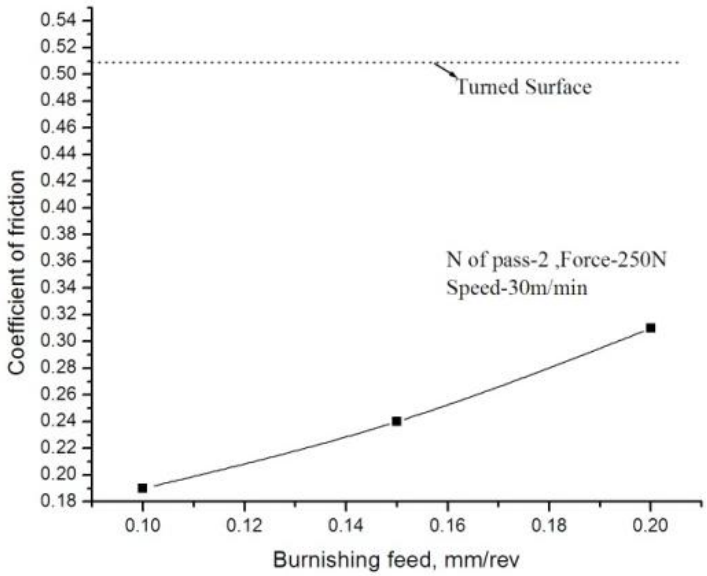

Figure 6.11 Effect of burnishing feed on the coefficient of friction. Burnishing conditions: burnishing force=250 N, number of passes =2 and burnishing speed=30 mm/rev.

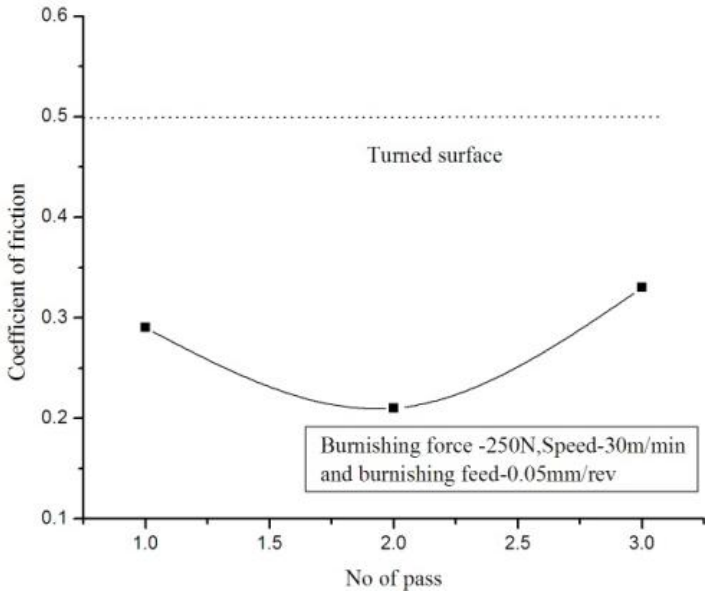

Figure 6.12 Effect of number of passes on the coefficient of friction. Burnishing conditions: burnishing force=250 N, burnishing feed =0.05mm/rev and burnishing speed=30 mm/rev.

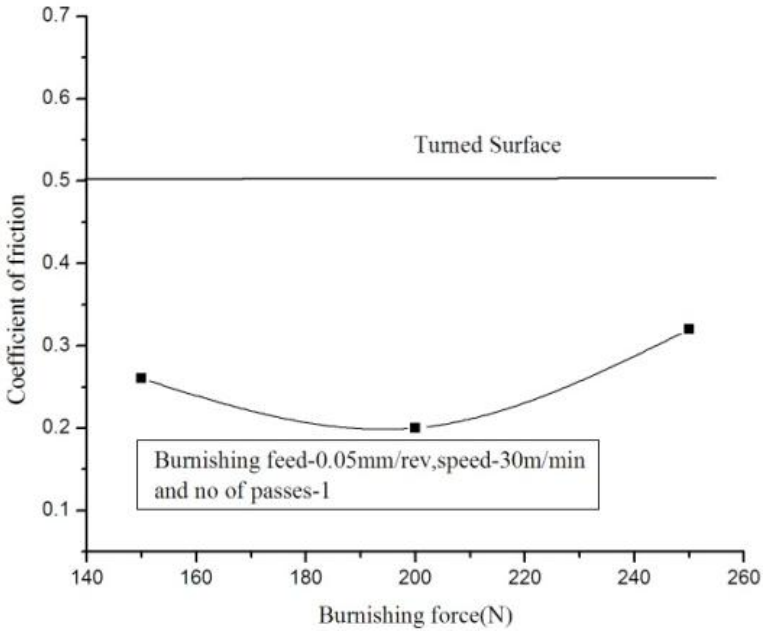

Figure 6.13 Effect of burnishing force on the coefficient of friction. Burnishing conditions: number of passes=1, burnishing feed =0.05mm/rev and burnishing speed=30 mm/rev.

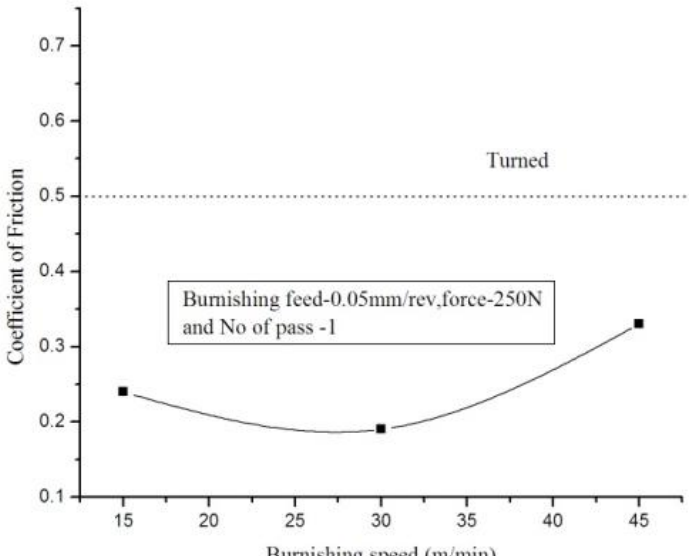

Figure 6.14 Effect of burnishing speed on the coefficient of friction. Burnishing conditions: number of passes=1, burnishing feed =0.05mm/rev and burnishing force=250N.

Thus we can conclude that the coefficient of friction increases with increase in burnishing feed.Whereas the coefficient of friction decreases initially with the increase in burnishing speed, number of passes and burnishing force , after which further increase in these parameters will result in increase of coefficient of friction.

6.3.5 Wear surface and wear debris

Morphology of worn surfaces generated during wear test on turned specimen is presented in Figure 6.15 (a-b) and that of burnished specimen of Ti–6Al–4V alloy under various burnishing conditions are presented in Figure 6.16 (a–f). Irrespective of turning or burnishing, the surfaces generated through wear, show a pattern of grooves and ridges running parallel to each other in the sliding direction, caused by deformation. It is evident from Figure 6.15(a-b) that the worn surface of turned specimen shows signs of excessive wear as compared to that of burnished specimen [Figures 6.16 (a-f)]. The presence of vestiges with plastic deformation and fracture was observed on the worn surfaces. The furrow and ridge were noticed along the sliding direction, through continuous squashing and ploughing by the counter face. All the wear surfaces show a typical abrasive wear. From the study of worn surfaces

and sub surfaces, a tribo oxide layer was always found to form on worn surfaces and there were no traces of delaminated regions on worn surfaces.

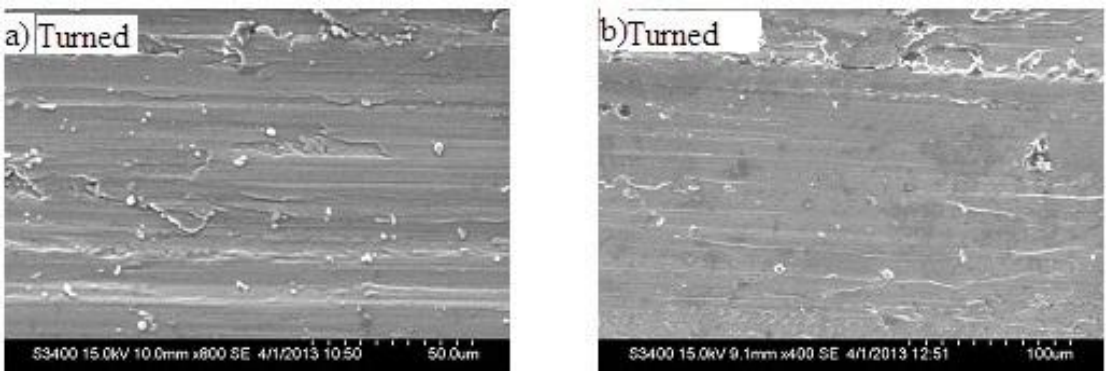

Figure 6.15 a- b SEM micrographs showing morphology of worn surfaces of turned Ti–6Al–4V (Alloy being turned under MQL conditions with a flow rate of 150ml / hr, speed of 150 m/min and a feed of 0.15mm/rev)

Rigney, D.A (1992) confirmed by experimental observations that the sliding of metals can be described by the following basic wear sequence: surface and sub-surface plastic deformation, formation of debris and material transfer, reaction with the environment, mechanical mixing and formation of tribological layer.

During sliding of Ti–6Al–4V alloy, tribo-layer is supposed to be formed through metal debris being produced and/or transferred, ground, mixed, compacted and even sintered on worn surfaces. In this procedure, metal debris would react with oxygen. Thus oxygen enters the tribo-layer.Based on the XRD result of wear debris during wear of Ti–6Al–4Valloy, Straffelini and Molinari. (1999) have identified two wear mechanisms for Ti–6Al–4V alloy, irrespective of the counterface and applied load. Oxidation wear prevailed at the lowest sliding velocities (0.3–0.5m/s)and delamination wear occured at the highest speed range (0.6–0.8m/s). According to experimental study by Hsu,S.M. et.al (1997), plastic deformation and its accumulation on the contacting asperities control the wear process when the ambient temperature and sliding speed are not high.

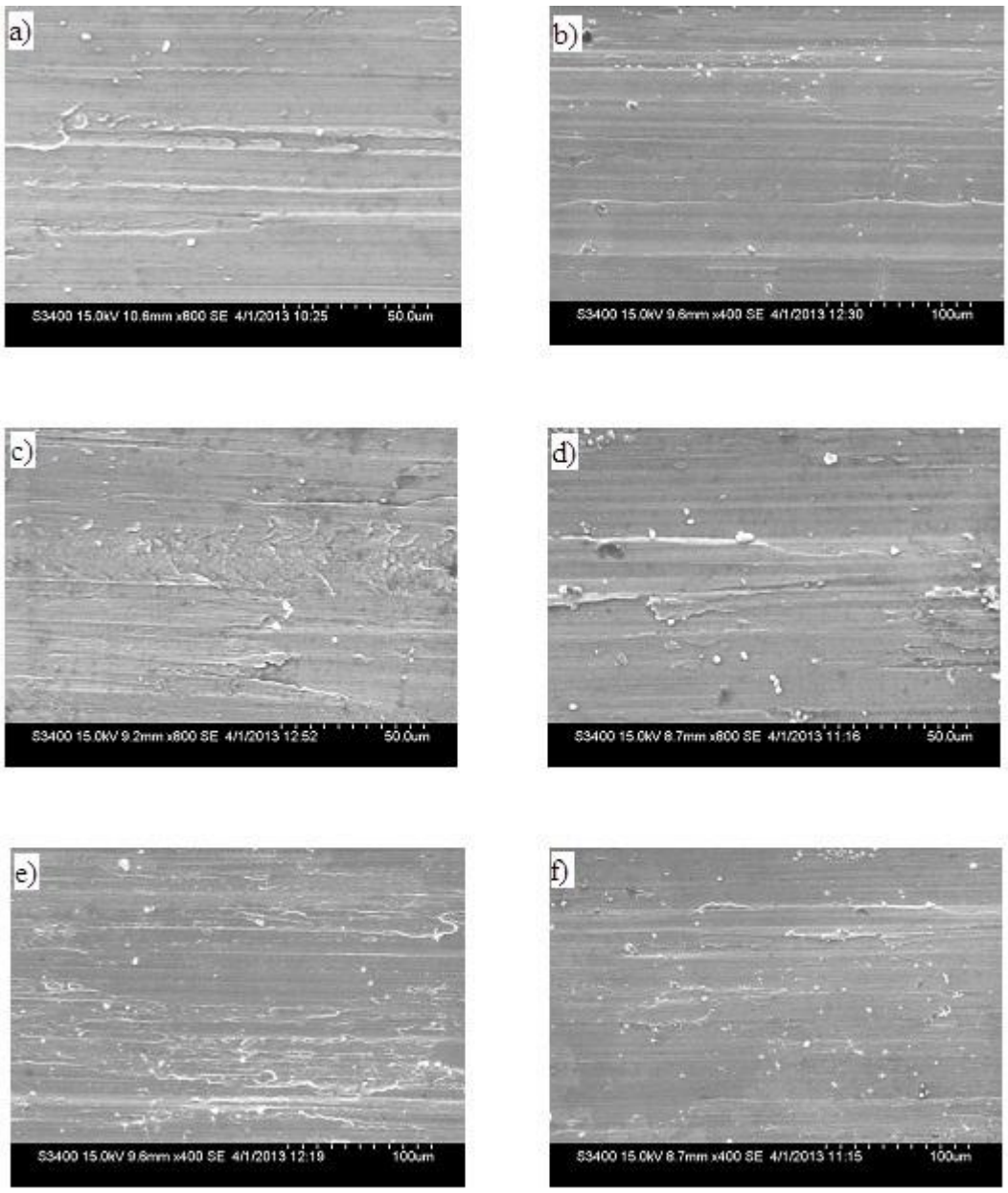

Figure 6.16 (a-f) Morphology of worn surfaces of burnished Ti–6Al–4V alloy (alloy being burnished under different burnishing conditions a) At speed = 30 m/min, feed=0.05mm/rev, force=200 N, No. of passes= 3 b) At speed = 30 m/min, feed = 0.10mm/rev,force = 250 N, No. of passes =1. c) At speed = 45 m/min, f=0.10 mm/rev, force = 150 N, No. of passes =3. d) At speed = 15 m/min, feed =0.10 mm/rev, F= 200N, No. of passes = 2. e) At v= 15 m/min, feed =0.15mm/rev, force = 250 N, n= 3. f) At speed = 15 m/min,feed = 0.05 mm/rev, force = 150N,No.of passes= 1.

Because of relatively higher strength of Ti–6Al–4V alloy it is subjected to a lower load during wear test and hence plastic deformation and fracture were considered to occur first on worn surface. As a result, under a low load, adhesive wear was considered to be the predominant wear mechanism.But delamination wear prevailed under high load, where plastic deformation and fracture occurred at subsurface. Because of high hardness of steel counter- face and traces of tribo-oxides, the contacting asperities of counterface and oxidized wear debris would plough the surface of Ti–6Al–4V alloy, producing furrow and ridges on worn surfaces. Hence, it is suggested that adhesive wear and delamination wear prevailed at 25–200°C, accompanying abrasive wear. Under the experimental conditions, even though the sliding speed is high at 2.68m/s, delamination wear was not observed contrary to the views of Straffelini and Molinari. (1999). However, since the load is low at 10N, there was no presence of delamination wear, which is consistent with the work of Hsu, S.M et al. (1997). Wear debris can act as a very useful diagnostic tool for finding out the mechanism of wear. In my work, the wear debris obtained was in the form of a powder, unlike flake-like metallic wear particles which is an indication of delamination that occurs during wear (Suh, N P.1973). Titanium alloy commonly transfers to the counterface when rubbing against other metals or ceramics (Budinski, K.G. 1991, Molinari, A. et al.1997, Dong, H. and Bell,T. 1999).The steel counterpart surfaces typically exhibited minor micro-ploughing wear scars aligned parallel to the reciprocating-sliding direction together with a high density of heavily flattened patches and smeared metal prows aligned in the sliding direction.

6.4 CHAPTER CONCLUSIONS

The results obtained from the surface quality and tribology studies indicate that ball burnishing process has good prospect to be introduced as a new surface treatment method for titanium alloy. Based on the analysis of the experimental results, the following conclusions can be drawn in the present investigation.

- After burnishing, surface micro hardness increased from 340 HV to 405 HV, whereas surface roughness decreased from 0.45 μm to 0.12 μm and compressive residual stress as high as 955 MPa was noticed immediately below the surface.
- A combination of burnishing speed in the medium range, low feed, high burnishing force with three passes is helpful to minimize specific wear rate. However, burnishing with medium speed, low feed, medium force and two numbers of passes could minimize the coefficient of friction.
- It is evident that the specific wear rate is reduced with the increase in burnishing force, feed and no of passes. However, specific wear rate decreases with the increase in burnishing speed.
- It is observed that the coefficient of friction decreases with the increase in burnishing feed, speed and number of passes however it increases with the increase in burnishing force.
- The burnishing force and number of passes with contribution of 57.77% and 20.13% respectively have major effects in minimizing the specific wear rate. On the contrary, the burnishing feed and burnishing speed with contribution of 74.17% and 13.03% have key roles in minimizing the coefficient of friction.
- Taguchi optimization in our investigation, showed greater improvements in specific wear rate 3.29 $x10^{-4}mm^3/Nm$ (52% decrease) and coefficient of friction 0.18 (64% decrease) when compared to turned surfaces.
- The surface quality and tribological characteristics of titanium alloy Ti-6Al-4V can be improved by ball burnishing, showing improved friction and wear performance.

Chapter 7

CONCLUSIONS AND SCOPE FOR FUTURE WORK

In this chapter, the findings and results of the current research are summarized with final remarks and conclusions. The concluding remarks are given in the order of appearance in the chapters. The directions and recommendations of the future work are discussed briefly based on the results and observations presented in this dissertation.

7.1 CONCLUSIONS

- The optimum combination of MQL lubricating mode, high cutting speed, low feed rate, high nose radius with low depth of cut is determined to obtain best surface finish during turning of titanium alloy. From the ANNOVA analysis, it is evident that the cutting speed (72.32%) and feed rate (17.49%) have major effects on minimizing surface roughness, whereas the lubricating mode (89.27%) and cutting speed (5.28%) play key roles in maximizing surface hardness. A second-order response surface model was developed to predict the surface roughness during machining of titanium alloy under different conditions of MQL, cutting speed and feed rate with a 95% confidence interval. The experimental and predicted values of surface roughness are almost similar.
- Using Taguchi technique, it was found that a combination of burnishing speed in the medium range, lower feed rate, low burnishing force with three number of passes is optimal for reduced surface roughness. From ANNOVA analysis, it was established that the burnishing feed and burnishing speed with contribution of 40.13% and 31.49% respectively, have major effects in minimizing the surface roughness. The burnishing force and number of passes with contribution of 48.95% and 19.80% respectively, play key role in maximizing the hardness. The optimal results obtained are tabulated below

Optimal factor settings and corresponding best combination values of surface roughness and hardness for burnishing

Response	Optimal process parameter setting				Optimal value
	Burnishing Speed(A) (m/min)	Burnishing Feed(B) (mm/rev)	Burnishing Force(C) (N)	Number of Passes(D)	
Surface roughness	45	0.05	200	3	0.10 µm
Hardness	30	0.15	350	5	416 Hv

- From the experimental results, it was observed that the surface roughness increases with increased feed and burnishing force. But, roughness decreases with increased speed and number of tool passes until it reaches a minimal value and then with further increased speed and number of tool passes, the roughness increases. The surface hardness increases with burnishing force and number of tool passes. However, hardness increases with increased speed and feed only in the low ranges specified and beyond this range, the hardness starts decreasing. It was found that greater improvements in surface finish (77%) and an improvement in hardness of 17% was recorded when compared to pre-machined surfaces. The results of FEM simulations indicate that the effect of burnishing feed rate has a lower influence on residual stress whereas an increase in burnishing force leads to increased residual stresses.
- The newly developed burnishing tool showed similar trends with regards to the effect of burnishing parameters on surface roughness and hardness as the earlier tool. The performance of the newly developed tool was comparatively better as indicated by the fact that the surface hardness as high as 422Hv was obtained and the lowest surface roughness of 0.105 µm was recorded. This tool is more compact, holds more rigidly to the CNC tool post and can withstand higher burnishing force because of its structure. The comparison of the performance between ball and roller burnishing tool shows that under similar burnishing conditions, the ball burnishing tool performed better.

- From ANNOVA analysis, it is revealed that the burnishing force and number of passes with contribution of 57.77% and 20.13% respectively, have major effects in minimizing the specific wear rate. On the other hand, the burnishing feed and burnishing speed with contribution of 74.17% and 13.03% respectively, play key roles in minimizing the coefficient of friction. Taguchi optimization method here showed greater improvements in specific wear rate at 3.29 $x10^{-4}$ mm^3/Nm (52% reduction) and coefficient of friction 0.18 (64% reduction)in the burnished surface when compared to turned surfaces.

Thus it can be concluded that the surface quality and tribological characteristics of titanium alloy Ti-6Al-4V can be improved by ball burnishing, resulting in improved friction and wear performance.

7.2 FUTURE RESEARCH DIRECTIONS

- Burnishing process is an emerging, hot topic in the manufacturing field and the benefits of this process are vast. Hence, further works can be carried out related to improvement in fatigue performance of burnished titanium alloy (Ti-6Al-4V) components.
- Further studies can be made, to study the evolution mechanisms of the ultrafine grain and texture in the burnished surface layer of titanium alloy (Ti-6Al-4V alloy).
- One of the drawbacks of burnishing process is that it is more suitable for regular shapes and not for irregular shapes. So there is ample scope to design burnishing tools and new techniques may be developed to burnish irregular shapes.

REFERENCES

Afef, B., Wassila, B.S. and Kacem, S. (2010). " Prediction of surface characteristics obtained by burnishing." *Int. J. Adv Manuf. Technol*., 51, 205-215.

Agins,H.J., Alcock, N.W., Bansal, M., Salvati, E., Wilson, P.O., Pellicci, P.M. and Bullough, P.G. (1988)."Metallic wear in failed titanium-alloy hip replacements." *J Bone Joint Surg. Am*.,70A (3) , 347-356.

Alam and Haseeb. (2002). "Response of Ti-6Al-4V and Ti-24Al-11Nb alloys to dry sliding wear against hardened steel." J of Tribology Int., 35,357-362.

Altenberger,I., Stach, E. A., Liu, G., Nalla R. K. and Ritchie R. O.(2003)."An in situ transmission electron microscope study of the thermal stability of near-surface microstructures induced by deep rolling and laser-shock peening." *Scripta Materialia* 48, 1593-1598.

Altenberger, I., Nalla, R.K., Sano, Y., Wagner. L.and Robert, O. R. (2012). "On the effect of deep-rolling and laser-peening on the stress-controlled low- and high-cycle fatigue behavior of Ti–6Al–4V at elevated temperatures up to 550 °C." *Int. J. of Fatigue*, 44, 292–302.

Ashvin J. Makadia J.I. Nanavati(2013). "Optimisation of machining parameters for turning operations based on response surface methodology." *Measurement*, 46, 1521‑1529

Alves, Jr. C., Guerra, Neto, C., Morais, G., da Silva C. and Hajek, V.(2005)."Nitriding of titanium disks and industrial dental implants using hollow cathode discharge." *Surf.Coat.Technol*., 194 ,196-202.

Arrazola, P.J.,Garay,A., Iriarte, Armendia, L.M., Marya, M. and Le Maître, F. (2009). "Machinability of titanium alloys (Ti6Al4V and Ti555.3)."*J.Mater. Process.Technol*., 209(5), 2223-2230.

ASTM,(1995). Designation: G99-95; Standard Test Method for Wear Testing with a Pin-on-Disk Apparatus,.336–390.

Autret, R. and Liang, S.Y. (2003).“ Minimum quantity lubrication in finish hard turning.” HNICEM ’03.

Azlan, M.Z., Habibollah, H. and Safian, S.(2010).“Simulated annealing to estimate the optimal cutting conditions for minimizing surface roughness in end milling Ti-6Al-4V.”*Mach.Sci. and Technol*., 14(1), 43-62.

Bakon, A. and Szymanski.(1993).*Practical Uses of Diamonds*. Ellis Horwood Ltd. and Polish Scientific Publishers PWN Ltd., 57-60.

Balland,P., Tabourot,T., Degre, F. and Moreau,V.(2013). “ An investigation of the mechanics of roller burnishing through finite element simulation and experiments.” *Int. J. of Mach. Tools and Manuf*., 65 , 29–36.

Belov V A .(1966). “ Technical and Economic aspects of ball burnishing.” *Russian Eng. J*. XLVI,79–81.

Beres, W., Li, J. and Patnaik, P.C.(2004).“Numerical Simulation of the Low Plasticity Burnishing Process for Fatigue Property Enhancement.”ASME Turbo Expo 2004: *Power for Land, Sea, and Air*,4 ,809-818.

Borgioli, F., Galvanetto, T. E., Iozzelli, F. and Pradelli, G.(2005).“ Improvement of wear resistance of Ti–6Al–4V alloy by means of thermal oxidation.” *Mater. Lett*. 59, 2159–2162.

Boothroyd, G., Knight W.(1989).*Fundamentals of Machining and Machine Tools*,Marcel Dekker, New York, 155–173.

Bouacha, K., Yallese, M.A., Mabrouki, T. and Rigal, J.F.(2010).“Statistical analysis of surface roughness and cutting forces using response surface methodology in hard turning of AISI 52100 bearing steel with CBN tool.”*Int. J. Refrac. Metals Hard Mater*., 28(3),349-361.

Bougharriou, A., Sai,W. B. and Sai, K. (2010). “Prediction of surface characteristics obtained by burnishing.” *Int. J. Adv. Manufac. Technol*., 51(1-4), 205-215.

Bouzid,W., Tsoumarev, O.and Sai, K. (2004).“An investigation of surface roughness of burnished AISI 1042 steel. ” *Int. J. Adv. Manufac. Technol*., 24(1-2), 120-125.

Bouzid,W. and Sai, K. (2005). “Finite element modeling of burnishing of AISI 1042 steel.” *Int J. Adv. Manuf .Technol*., 25, 460–465.

Boyer, R.R.(1996). “An overview on the use of titanium in the aerospace industry. ”*Mater. Sci. Eng.A*,, 213,103–114.

Bozdana, A.T. and Gindy, N.Z. (2008). “Comparative experimental study on effects of conventional and ultrasonic deep cold rolling processes on Ti–6Al–4V.” *Mater. Sci. Technol.*, 24, 1378–1384.

Branko, T., Petar, M.T., Ognjan, L., Dragomir, M., Branislav, M.J., Bojan, B. and Djordje,V. (2012). “Using specially designed high-stiffness burnishing tool to achieve high-quality surface finish. ” *Int. J. Adv. Manuf. Technol*., 67, 601-611.

BRESSAN, J.D. e Hesse, R., Construction and validation tests of pin-on-disc equipment. In.:XVI Congresso Brasileiro de Engenharia Mecânica, COBEM 2001, Uberlândia/MG, December 2001.

Brinksmeier, E. and Riemer O.(1998). “Measurement of optical surfaces generated by diamond turning. ”*Int.J.Mach.Tools . Manuf*., 38(5-6), 699-705.

Budinski, K.G. (1991). “Tribological properties of titanium alloys.” *Wear*, 151, 203–217.

Cakir, M.C., Ensarioglu, C. and Demirayak, I.(2009).“Mathematical modeling of surface roughness for evaluating the effects of cutting parameters and coating material.”*J. Mater.Process. Technol.*, 209(1), 102-109.

Caudill, J,Huang, . B. Arvin, C. Schoop, J. Meyer, K and Jawahir I.S. (2014). “Enhancing the surface integrity of Ti-6Al-4V alloy through cryogenic burnishing.” *Procedia CIRP* ,13 , 243- 248.

Chan, K.S., Koike, M. and Okabe, T.(2007). “Modeling wear of cast Ti alloys.” *Acta. Biomate.*, 3 ,383–389.

Chauhan. S.R. and Kali, D.(2012). “Optimization of machining parameters in turning of titanium (Grade-5) alloy using response surface methodology.” *Mater. and Manufac.Process.* , 27(5), 531-537.

Che-Haron, C.H. and Jawaid, A.(2005). “The effect of machining on surface integrity of titanium alloy Ti-6Al-4V.” *J. Mater. Process.Technoly.,* 166,188–192.

Cherukuri, R. and Molian, P.(2003). “Lathe Turning of Titanium Using Pulsed Laser Deposited, Ultra-Hard Boride Coatings of Carbide Inserts.” *Mach. Sci. and Technol: An Int.J.,* 7,119 – 135.

Chen, W.Y. (2000). “Cutting forces and surface finish when machining medium hardness steel using CBN tools.” *Int J. Mac. Tools and Manufac.*, 40 (3), 455-466.

Chengwei, C., Zhiming, Z., Xitang, T., Wang, Y. and Sun, X.T.(1995).“Influence of rapidly solidifed structures on wear behavior of Ti-6Al-4V laser alloyed with TiC.”*Tribol. Trans.*, 38(4), 875-878.

Chou, Y.K.(2002). “Surface hardening of AISI 4340 steel by machining: a preliminary investigation.” *J. Mater.Process. Technol.,* 124, 171–177.

Colafemina, J.P., Jasinevicius, R.G and Duduch, J.G. (2007).“Surface integrity of ultra-precision diamond turned Ti (commercially pure) and Ti alloy (Ti-6Al-4V).” *Proc. of Ins. of Mech. Eng., J. of Eng. and Manufac. Part B*, 221 (6), 999–1006.

Cui,Chunxiang, Hu BaoMin, Zhao, Lichen, L. and Shuangjin.(2011).“Titanium alloy production technology, market prospects and industry development.”*Mat.Des.*, 32, 1684-1691.

Dabnun, M.A., Hashmi, M.S.J. and El-Baradie, M.A.(2005).“Surface roughness prediction model by design of experiments for turning machinable glass-ceramic (Macor).”*J.Mater. Process.Technol.,* 164, 1289-1293.

David, F.,Liam, O.,Greg, B.,Nicholas, B. and Denis, P. D. (2011). "Wear resistance enhancement of the titanium alloy Ti–6Al–4V via a novel co-incident micro blasting process." *Surf. Coat. Technol*., 205, 4941–4947.

Davim, J.P.(2001). "A note on determination of optical cutting conditions for surface finish obtained in turning using design of experiments." *J.Mater. Process.Technol.,* 116, 305–308.

Davim, J.P., Sreejith, P.S. and Silva, J.(2007)."Turning of brasses using minimum quantity of lubricant and flooded lubricant conditions." *Mater. and Manufac. Process.,* 22, 45-50.

Dhar, N.R., Islam, M.W., Islam, S. and Mithu, M.A.(2006)." The influence of minimum quantity of lubrication (MQL) on cutting temperature, chip and dimensional accuracy in turning AISI-1040 steel. "*J.Mater. Process.Technol*., 171(1), 93- 99.

Diniz, A.E., Ferreira, J.R. and Filho, F.T.(2003). "Influence of refrigeration and lubrication condition on SAE 52100 hardened steel turning at several cutting speeds. " *Int.J.of Mac. Tools and Manufac.,* 43,317–326.

Domnita Frăţilă & Cristian Caizar (2012). "Investigation of the influence of process parameters and cooling method on the surface quality of AISI-1045 during turning." *Mat. and Manufac. Processes*, 27(10), 1123-1128.

Donachie, J.M.J.(2000).Titanium—A Technical Guide, 2nd ed., ASM International, 2000.79–84.

Dong, H. and Bell,T.(1999). "Tribological behavior of aluminium sliding against Ti6Al4V in unlubricated contact. "*Wear*, 225,874–84.

Douglas,J.H., Paul, S.P. and Edmund, F.L.(2002). "Application of low plasticity burnishing (LPB) to improve the fatigue performance of Ti-6Al-4V Femoral Hip Stems."*J.of Test. Eval.*, 20(10) , 1-14.

Durul, U. and Tugrul, O.(2011). "Machining induced surface integrity in titanium and nickel alloys: A review." *Int. J. Mach. Tools Manuf*., 51, 250–280.

Ecoroll Werkzeugtechnik, , 2005 Celle, Germanywww.ecoroll.de

El-Axir,M.H. (2000). "An Investigation into roller burnishing."*Int.J.Mach.Tools Manuf*., 40, 1603-1617.

El-Axir, M.H., Othman .O.H. and Abodiena.A.M. (2008a). "Study on the inner surface finishing of aluminum alloy 2014 by ball burnishing process." *J. Mater.Process.Technol*., 202, 435-442.

El-Axir, M.H., Othman .O.H. and Abodiena.A.M. (2008b). "Improvements in out-of-roundness and microhardness of inner surfaces by internal ball burnishing process." *J.of Mater. Process Technol*., 196,120-128.

El-Tayeb, N.S.M.(1994). "Frictional behavior of burnished copper surfaces under dry contact conditions. *Eng. Res. Bulletin*, HU, Cairo, 171–184

El-Tayeb, N.S.M. and Ghobrial, M.I.(1993). "The mechanical wear behaviour of burnishing surfaces." *Proc. 4th Int. Conf. on Prod. Eng. and Design for Dev*., Cairo, 198–209.

El-Tayeb, N.S.M., Low, K.O. and Brevern, P.V. (2007). "Influence of roller burnishing contact width and burnishing orientation on surface quality and tribological behavior of Aluminum 6061." *J.Mater. Process. Technol*., 186 272-278.

El-Tayeb,N.S.M., Low, K.O. and Brevern, P. V.(2008). "Enhancement of surface quality and tribological properties using ball burnishing process. " *Mach. Sci. Technol*., 12, 234–248.

El-Tayeb,N.S.M., Low, K.O. and Brevern, P.V. (2009). "On the surface and tribological characteristic of burnished cylindrical Al-6061." *Tribol. Int*., 42, 320-326.

El-Taweel, T.A. and El-Axir, M.H.(2009). "Analysis and optimization of the ball burnishing process through the Taguchi technique."*Int. J. Adv. Manuf. Technol*., 41, 301-310.

Emmanuel, O., Ezugwu, John, B., Rosemar, Da Silva, and Akir, O.C.(2007). "Surface integrity of finished turned Ti–6Al–4V alloy with PCD tools using conventional and high pressure coolant supplies."*Int. J.Mach.Tools & Manuf.,* 47,884–891.

Escalona, P.M., and Cassier,Z.(1998). "Influence of critical cutting speed on the surface finish of turned steel." *Wear*, 218, 103–109.

Ezugwu, E.O. and Tang, S.H.(1995). "Surface abuse when machining cast iron (G-17) and nickel-Base superalloy (Inconel 718) with ceramic tools." *J.Mater.Process.Technol.,* 55,63–69.

Ezugwu, E.O. and Wang, Z.M.(1997). "Titanium alloys and their machinability- a review." *J. Mater. Process Technol*., 68(3), 262-274.

Ezugwu, E.O., Wang, Z.M. and Okeke, C.I.(1999). "Tool life and surface integrity when machining Inconel 718 with PVD and CVD coated tools." *Tribo. Trans*., 42(2), 353–360.

Ezugwu, E.O.(2004). "High speed machining of aero-engine alloys." *J Brazilian Society of Mech. Sci.and Eng*., 26(1), 1-11.

Ezugwu, E. (2005). "Key improvements in the machining of difficult-to-cut aero-space superalloys." *Int. J. Mach. Tools and Manuf*., 45, 1353–1367.

Ezugwu, E., Bonney, J. and Yamane, Y. (2003). "An overview of the machinability of aeroengine alloys. " *J. Mater. Process Technol*., 134, 233–253.

Ezugwu, E.O., Bonney. J., Sales, W.F. and Da Silva, R.B.(2005). "Observations of tool life and wear mechanisms in high speed machining of Ti- 6Al-4V with PCD tools using high pressure coolant."In: *Proc. of WTC2005 World Trib. Congress III*, Washington, D.C., USA.

Ezugwu, E.O.,Bonney, J., Fadare, D.A.and Sales, W.F. (2005). "Machining of nickel-base, Inconel 718, alloy with ceramic tools under finishing conditions with various coolant supply pressure." *J. of Mat. Process. Techn*., 162–163, 609–614.

Ezugwu, E.O., Bonney, J., Silva, R. and Çakirc, O. (2007). "Surface integrity of finished turned Ti–6Al–4V alloy with PCD tools using conventional and high pressure coolant supplies." *Int. J.Mach. Tools & Manufac*., 47(6),884- 891

Fang-Jung, S. and Chien-Hua C. (2003). "Freeform surface finish of plastic injection mold by using ball-burnishing process."*J. Mater. Process Technol*.,140, 248-254.

Fang-Jung S. and Chuing-Hsiung C.(2010). "Precision surface finish of the mold steel PDS5 using an innovative ball burnishing tool embedded with a load cell." *Prec. Engg.,* 34, 76-84.

Farough Mohammadi & Ramin Sedaghati & Ali Bonakdar.(2014). "Finite element analysis and design optimization of low plasticity burnishing process." *Int. J. Adv. Manuf. Technol.*, 70, 1337–1354

Feng, L.L., Wei, X., Zhao, Y. Z., Jing, Z. and Zheng Q. T. (2012). "Analytical prediction and experimental verification of surface roughness during the burnishing process." *Int.J.of Mac. Tools & Manufac*., 62,67–75.

Fischer-Cripps AC (2007). " Introduction to contact mechanics", 2nd edn. *Springer*, New York, 137–150.

Fowler, D.(1988). "Milling with Polycrystalline Diamond." *Carbide Tool J*., 20 (5), 23-25.

Freese, H. Volas, M.G. Wood, J.R, Brunette, D.M. Tengvall, P Textor, M. Thomsen P. (Eds.),(2001). " Titanium in Medicine", Springer, Berlin, 2001.

Gaitonde, V. N. Karnik S. R. & Paulo Davim J. (2012). "Optimal MQL and cutting conditions determination for desired surface roughness in turning of brass using genetic algorithms." *Mach. Sci. and Techn.: An Int. J*., 16(2) , 304-320

Ganesh, B.K.C., Sha, W., Ramanaiah, N. and Krishnaiah, (2014). "A Effect of shot peening on sliding wear and tensile behavior of titanium implant alloys."*Mater Des*.,56, 480–486.

Geetha, M., Singh, A.K., Asokamani, R.and Gogia A.K. (2009). “Ti based biomaterials, the ultimate choice for orthopaedic implants – A review.” *Prog. in Mater. Sci*., 54, 397–425.

Ghani, J.A., Choudhury, I.A. and Hassan,H.H. (2004). “Application of Taguchi method in the optimization of end milling operations. ” *J.of Mater.Process. Technol*., 145, 84–92

Gil, F.J., Planell, J.A., Padrós, A. and Aparicio**.** C.(2007). “Effect of shot-blasting and heat treatment on fatigue fracture of titanium dental implants.” *Dental Mater*., 23, 486-491

Gill, C.M., Fox, N. and Withers, P.J. (2008). “Shakedown of deep cold rolling residual stresses in titanium alloys.” *J. Phys. D: Appl. Phys.*, 41(174005), 1-5.

Grenier, M., Dubé, D., Adnot, A. and Fiset, M.(1997). “Microstructure and wear resistance of CP titanium laser alloyed with a mixture of reactive gases.” *Wear*, 210, 127-135.

Grzegorz, K., Stanislaw, L and Antun, S.(2013). “Influence of cutting parameters and conditions onto surface hardness of duplex stainless steel after turning process .” *Tech. Gazette*, 20(6), 1077-1080.

Grzesik, W. and Zak, K.(2012). “Modification of surface finish produced by hard turning using superfinishing and burnishing operations. ”*J. Mater. Process Technol*., 212(1), 315-322.

Guleryuz, H. and Cimenoglu, H.(2005). “Surface modification of a Ti–6Al–4V alloy by thermal oxidation. ” *Surf. Coat. Technol*., 192, 164–170.

Guo, Y.B., Li, W. and Jawahir, I.S.(2009). “Surface integrity characterization and prediction in machining of hardened and difficult-to-machine alloys; a state-of-the-art research review and analysis.” *Mach. Sci and Technol*., 13, 437–470.

Hamadache, H., Laouar, L., Zeghib, N.E.and Chaoui, K. (2006). "Characteristics of Rb40 steel superficial layer under ball and roller burnishing." *J. Mater.Process. Technol*., 180, 130-136.

Hartung, P.D. and Kramer, B.M. (1982). "Tool wear in titanium machining."*Ann. CIRP 31*, 75–80.

Hassan, A.M.(1997). "The effects of ball and roller burnishing on the surface roughness and hardness of some non-ferrous metals." *J. Mat. Process Tech*. 72, 385-391.

Hassan,A.M., Al-Jalil,H.F. and Ebied, A.A.(1998). "Burnishing force and number of tool passes for the optimum surface finish of brass components. "*J. Mater. Process Technol*., 83, 176-179.

Hassan,A.M. and A.S Al- Bsharat (1997). "Improvement in some properties of non-ferrous metals by the application of ball and roller burnishing processes."*J. Mater. Process. Technol*.59(3), 250- 256.

Heisel, U., Lutz, M., Spath, D. and Wassmer, R.(1994). "Application of Minimum Quantity Cooling Lubrication Technology in Cutting Process." *Prod. Eng*., II/1, 49-54.

Herbert, E. G.(1927). " The work hardening of steel by abrasion, with an appendix on the "cloudburst" test and super hardening." *J.of Iron and Steel* 11, 265-282.

Hsu, S.M., Shen, M.C. and Ruff, A.W. (1997). "Wear prediction for metals." *Tribol. Int.* , 30 , 377–383.

Ibrahim, G.A., Che Haron, C.H., Ghani, J.A. and Arshad, H.(2010). "Taguchi optimization method for surface roughness and material removal rate in turning of Ti-6Al-4V. " *Int. Rev. of Mech. Eng.* 4(3), 216-221.

Jaffery, S.I. and Mativenga, P.T.(2008). "Assessment of the machinability of Ti–6Al–4V alloy using the wear map approach."*The Int. J. Adv. Manuf. Technol*., 40, 687–696.

Jiang, Y. XB. and Sehitoglu, H. (2002). “Three-dimensional elastic-plastic stress analysis of rolling contact.”*J Tribol. Trans. ASME*., 124, 699–708.

Jinlong, L. and Hongyun,L.(2013). “Effect of surface burnishing on texture and corrosion behavior of 2024 aluminum alloy. ” *Surf. Coat. Technol*., 235, 513–520

Johnson, R. and Eberhardt, J.(2006). “Thermal Oxidation: a Promising Surface Treatment for Titanium Engine Parts.” Transportation Program Oak Ridge National Laboratory.

Johnson GR, Cook WH (1985). “Fracture characteristics of three metals subjected to various strains, strain rates, temperatures and pressures.” *Eng. Fract. Mech*., 21:31–48

Joshi, V. A.(2006). “Titanium Alloys: An Atlas of Structures and Fracture Features.”*CRC Press*.

Kali, D. and Chauhan, S.R.(2011). “Machinability study of titanium (Grade-5) alloy using design of experiment technique.” *Engg*., 3(6),609-621.

Kamata, Y. and Obikawa, T.(2007). “High speed MQL finish-turning of Inconel 718 with different coated tools.”*J. of Mater. Prorcess. Technol*., 192, 281-286.

Kartal, G., Timur, S., Urgen, A. and Erdemir, A.(2010). “Electrochemical boriding of titanium for iImproved mechanical properties.” *Surf. Coat. Technol*., 204, 3935-3939.

Khaider,B.M., Amane, Y., Samir, K. and Salim, B.(2014). “Analysis and optimization of hard turning operation using cubic boron nitride tool.”*Int. J. of Refrac. Metals and Hard Mater*., 45, 160-178,

Khan, M. A., Mithu M. A. and Dhar, N. R.(2009). “Effects of minimum quantity lubrication on turning AISI 9310 alloy steel using vegetable oil-based cutting fluid.” *J.Mater.Process. Technol*., 209(15-16), 5573-5583.

Klocke,F. and Eisenblaetter,G.(1997). “Dry Cutting." CIRP Annals. *Manufac. Technol*., 46(2), 519-526.

Klocke, F.,Beck, T., Eisenblatter, G., Fritsch, R., Lung. D. and Pohls, M. (2000). "Applications of minimal quantity lubrication (MQL) in cutting and grinding." In: *Proc. of the 12th Int.Colloquium Ind. Auto.e Lub., Esslingen. Technische Akademie*, 11-13.

Klocke, F., and Liermann, J., (1998). "Roller Burnishing of Hard Turned Surfaces." *Int. J. Mach. Tools Manuf*., 38(5-6), 419–423.

Klocke, F., Backer, V., Wegner, H., Feldhaus, B., Baron, H. and Hessert , R.(2009). "Influence of process and geometry parameters on the surface layer state after roller burnishing of IN718." *Prod. Eng. Res.and Dev*., 3, 391-399.

Komanduri, R. and Turkovich, B.F. (1981). "New observation on the mechanism of chip formation when machining titanium alloys." *Wear*, 69, 179–188.

Korzynski, M. (2007). "Modeling and experimental validation of the force-surface roughness relation for smoothing burnishing with a spherical tool." *Int. J. of Mac. Tools and Manufac*., 47, 1956–64.

Korzynski, M., Lubas, J., Swirad, S. and Dudek, K. (2011). "Surface layer characteristics due to slide diamond burnishing with a cylindrical-ended tool." *J.Mater.Process. Technol*., 211(1), 84-94.

Kotiveerachari.B and Murty,R.L.(1989). "Study of optimum force in burnishing, Proc." *llth AIMTDR Conf,. lIT,* Madras,408-414.

Kukielka,L.(1989). "Designating the field areas for the contact of a rotary burnishing element with the rough surface of a part, providing a high-quality product." *J.of Mech. Work.Tech*., 19, 319–356.

Kwak,J.S.(2005). "Application of Taguchi and response surface methodologies for geometric error in surface grinding process." *Int. J. of Mac.Tools and Manufac*., 45, 327–334.

Lapin,J., Pelachova,T.and Bajana, O.(2000). "Microstructure and mechanical properties of a directionally solidified and aged internetallic Ni-Al-Cr-Ti alloy with β-γ-γ^{l}-α structure." *Intermetallics,* 8 (12), 1417-1427.

Liu Y, Wang L, Wanga D. (2011). "Finite element modeling of ultrasonic surface rolling process." *J. Mater. Process Technol*., 211, 2106– 2113

Loh, N. H. and Tam, S.C. (1988). "Effects of Ball Burnishing Parameters on surface finish - A Literature survey and discussion." *Prec. Engg*., 10, 215-220.

Loh, N. H. and Tam, S.C.(1989). "A study of the effects of ball burnishing parameters on surface roughness using factorial design." *Prec. Engg*., 18, 53-61.

Loh N.H., Tam S.C and Miyazawa,S.(1993). "Ball burnishing of tool steel ." *Prec. Eng*.,15(2),100–105.

Long, M. and Rack, H.(1998). "Titanium alloys in total joint replacement—a materials science perspective."*Biomaterials*, 19, 1621-1639.

López de Lacalle, L.N., Lamikiz,A., Sanchez,J.A. and Arana, J.L.(2007). "The effect of ball burnishing on heat-treated steel and Inconel 718 milled surfaces." *Int. J. Adv Manuf.Technol*., 32, 958-968.

Low, K. O. (2010). "Surface Characteristics Modification of Polyoxymethylene and Polyurethane Using Burnishing."*Tribol.Transac*., 54(1), 96-103.

Low, K.O. and Wong, K.J.(2011). "Influence of ball burnishing on surface quality and tribological characteristics of polymers under dry sliding conditions." *Tribol.Int*. 44, 144–153.

Luca, L.L., Neagu,S.V. and Marinescu, I.(2005). "Effects of working parameters on surface finish in ball-burnishing of hardened steels." *Prec. Eng*., 29, 253–256.

Luo, H.Y., Liu, J.Y., Wang, L.J. and Zhong, Q.P.(2005). "Investigation of the burnishing process with PCD tool on non-ferrous metals." *Int. J. Adv.Manuf.Technol*., 25 , 454 -459.

Luo, Y., Ge, S., Liu, H. and Jin, Z.(2009). "Microstructure analysis and wear behavior of titanium cermet femoral head with hard TiC layer." *J. Biomech*., 42, 2708-2711.

Low, K.O. and Wong, K.J.(2011). "Influence of ball burnishing on surface quality and tribological characteristics of polymers under dry sliding conditions." *Tribol.Int*. 44, 144–153.

Maawad,E., Brokmeier,H.G., Wagner,L.,Sano,Y. and Genzel, Ch.(2011). "Investigation on the surface and near-surface characteristics of Ti–2.5Cu after various mechanical surface treatments." *Surf. Coat. Technol*., 205, 3644–3650.

Maawada, E., Sanob, Y.,Wagnera, L., Brokmeiera, H.G. and Genzelc, C. (2012). "Investigation of laser shock peening effects on residual stress state and fatigue performance of titanium alloys." *Mater.Sci.Eng.A*. 536, 82– 91.

Machado,A.R. and Wallbank, J. (1990). "Machining of Titanium and its Alloys:A Review." *Proc. of the Inst. of Mech. Eng., Part B: Manag. and Eng. Manufac*., 204(1),53-60.

Machado, A.R. and Wallbank, J.(1997). "The effect of extremely low lubricant volumes in machining."*Wear*, 210(1-2), 76-82.

Magaziner, R.S., Jain, V.K. and Mal, S. (2009). "Investigation into wear of Ti–6Al–4V under reciprocating sliding condition."*Wear*, 267, 368–373.

Manisavagam, G., Amritpreet, K. S., Rajamanickam, A. and Ashok K. G.(2009). "Ti based biomaterials, the ultimate choice for orthopaedic implants - A review."*Prog. in Mater. Sci*., 54(3), 397-425.

Mansour,M.(2012). "Influence of surface treatments on surface layer properties, fatigue and corrosion fatigue performance of AA7075 T73." *Mater. Des*., 41 , 61–66.

Maximov, J.T. and Duncheva, G.V.(2011). "Finite element analysis and optimization of spherical motion burnishing of low-alloy steel." *Proc. I. Mech. E. C. J. Mech. Eng. Sci*., 226,161–176.

Michiko, O., Junya, O., Takashi, H., Naohiro, T.and Hitoshi S. (2009). “High speed cutting of titanium alloy with PCD tools.” *Key Eng. Mater.*, 389, 157-162.

Mieczyslaw, K.(2007). “Modeling and experimental validation of the force–surface roughnessrelation for smoothing burnishing with a spherical tool.”*Int. J.Mach. Tools Manufac*., 47, 1956–1964.

Minitab Inc., Minitab User Manual Version 16, Quality Plaza, 1829 Pine Hall Road, State College, PA 16801–3008, USA, 2011.

Mishra, S.C., Nayak, B.B., Mohanty, B.C. and Mills, B.(2003). “Surface nitriding of titanium in arc plasma.”*J. Mater.Process. Technol*., 132, 143-148.

Molinari, A., Straffelini, G., Tesi, B. and Baccai T. (1997). “Dry sliding wear mechanism of the Ti6Al4V alloy.” *Wear*, 208, 105–112.

Montgomery, D.C,(2005). *Design and Analysis of Experiments*,sixth edition, John Wiley & sons, Inc.

Mori, M. , Furuta, M., Nakai, T. and Fukaya, T.(1999). “High-Speed Machining of Titanium by New PCD Tools.” *SAE Tech. Paper* -2296.

Morton, P.H. and Bell,T.(1989).“Surface engineering of titanium.”*Me«moireset E¨ tudes ScientiÞques Revue deMe« tallurgie*, 86(10), 639-646.

M’Saoubi, R.., Outeiro, J.C., Chandrasekaran, H., Dillon Jr, O.W. and Jawahir, I.S. (2008). “A review of surface integrity in machining and its impact on functional performance and life of machined products.” *Int. J. of Sustain- able Manufac*., 1(1–2), 203–236.

Nabhani, F.(2001). “Machining of aerospace titanium alloys.” *Robotics and Comp. Integ. Manuf.*, 17 (1-2), 99–106.

Nalbant,M.,Hasan G., Toktaş,I and Sur.,G. (2009). “The experimental investigation of the effects of uncoated, PVD- and CVD-coated cemented carbide inserts and cutting parameters on surface roughness in CNC turning and its prediction using artificial neural networks.” *Robotics and Comp. Integ. Manuf*., 25(1), 211-223.

Nageswara Rao D. and Vamsi krishna P.(2008). “The influence of solid lubricant particle size on machining parameters in turning.” *Int. J.of Mach.Tools & Manuf.*, 48(1), 107–111.

Nalla, R.K., Altenberger, I. , Noster, U., Liu, G. Y., Scholtes, B.and Ritchie, R.O.(2003). “On the influence of mechanical surface treatments /deep rolling and laser shock peening on the fatigue behavior of Ti-/6Al-/4V at ambient and elevated temperatures.” Mater. Sci. Eng. A.355 , 216-230.

Narutaki, N. and Murakoshi, A. (1985). “Study on Machining of Titanium Alloys.” *CIRP Annals*, 32 (1), 65-69.

Navneet, K. and Davim, J.P.(2015). “Design-of-experiments application in machining titanium alloys for aerospace structural components.” *Measurement*, 61, 280-290.

Nemat, M. and Lyons, A.C.(2000). “An investigation of the surface topography of ball burnished mild steel and aluminium.”*Int. J. Adv. Manuf. Technol*.16, 469-473.

Nikos. C. Tsourveloudis (2010). “Predictive modeling of the Ti6Al4V alloy surface roughness.” J. Int. Robot Syst., 60, 513‑530.

Ohidul Alam, M.d. and Haseeb, A.S.M.A.(2002). “Response of Ti–6Al–4V and Ti–24Al– 11Nb alloys to dry sliding wear against hardened steel.”*Tribol. Int*., 35, 357–362.

Ohkubo,C., Shimura, I., Aoki, T., Hanatani, S., Hosoi, T., Hattori,M., Oda, Y. and Okabe, T.(2003). “Wear resistance of experimental Ti–Cu alloys.” *Biomaterials* , 24, 3377–3381.

Oosthuizen, G.A., Akdogan,G., Dimitrov, D. and Treurnicht, N.F. (2010). “A Review of the Machinability of Titanium Alloys.”*R & D J. of the South African Ins. Mech.l Eng.*, 26, 43-52.

Ozel, T. and Karpat, Y.(2005). “Predictive modeling of surface roughness and tool wear in hard turning using regression and neural networks.”*Int.J.of Mac. Tools and Manufac*., 45, 467–479.

Papsev, D. D. (1978). “Finishing & hardening with cold working.” Moskva

Phadke. M.S.(1989).*Quality Engineering Using Robust Design*, AT & T, Prentice Hall International, Englewood Cliffs, New Jersey.

Prevéy, P.S., Hornbach,D.J., Jacobs, T.L. and Ravindranath, R. (2002). “Improved Damage Tolerance in Titanium Alloy Fan Blades with Low Plasticity Burnishing.” *In: Proc. of Int. Surface Eng. Conf.*, Columbus, OH, 1-4.

Prevéy,P.S., Jayaraman, N., Ravi and Ravindranath.(2004a). “Mitigation of FOD and Corrosion Fatigue Damage in 17-4 PH Stainless Steel Compressor Blades with Surface Treatment.” In: *9th Nat.Turbine Engine High Cycle Fatigue Conf*.

Prevéy,P.S., Jayaraman, N., Ravi and Ravindranath.(2004b). “HCF performance and FOD tolerance improvement in Ti-6Al-4V vanes with LPB treatment.” In: *Proc. 42nd AIAA Aero. Sci. Reno, NV*, 9(1-4).

Pu,Z.,. Song,G.-L., Yang,S., Outeiro, J.C.,Dillon Jr,O.W., Puleo.D.A .and Jawahir,I.S.(2012). “Grain refined and basal textured surface produced by burnishing for improved corrosion performance of AZ31B Mg alloy.” *Corrosion Sci*., 57, 192‑201

Q, Wu.(2007). “Serrated chip formation and tool-edge wear in high-speed machining of advanced aerospace materials.” Utah State University, Logan, Utah.

Qiu, M., Zhang, Y.Z., Zhang, J.H. and Zhu, J.(2006). “Microstructure and tribological characteristics of Ti–6Al–4V alloy against GCr15 under high speed and dry sliding.” *Mater. Sci. Eng*., 434A, 71–75

Radziejewska, J. and Skrzypek, S. J.(2009). “Microstructure and residual stresses in surface layer of simultaneously laser alloyed and burnished steel.” *J. Mater.Process Technol*., 209(4), 2047-2056.

Rahim, E.A.; Sasahara, H (2010). “Surface integrity in MQL drilling nickel-based superalloy. Key Engineering.” *Materials*, 447- 448,811-815.

Rahim, E.A.; Sasahara, H (2011). "An analysis of surface integrity when drilling inconel 718 using palm oil and synthetic ester under MQL condition." *Mach.Sci. and Tech.-An Int. J.*,15(1),76-90.

Rahman,M., Zhi-Gang, W. and Yoke-San, W. (2006). "A review on high-speed machining of titanium alloys."*JSME Int. J. Series C*. 49(1), 11-20.

Rajasekariah R. and. Vaidyanathan, S. (1975). "Increasing the wear-resistance of steel components by ball burnishing." *Wear,* 34, 183 – 188.

Rajesham and Jem Cheong Tak.(1989). "A study on the surface characteristics of burnished components." *J. of Mech. Working Tech*., 20, 129-138

Ramakrishna, P.K and Shunmugam, M.S.(1987)."Investigation into surface topography, microhardness and residual stress in boring trepanning association machining." *Wear,* 119, 89–100.

Ramana, M.V., Srinivasulu, K. and Rao, G.K.M. (2011)."Performance evaluation and selection of optimal cutting conditions in turning of Ti-6Al-4V alloy under different cooling conditions."*Int. J. Innov.Technol. Creative Eng*., 1(5), 10-21.

Ramesh, S., Karunamoorthy, L. and Palanikumar, K.(2012). "Measurement and analysis of surface roughness in turning of aerospace titanium alloy (gr5)." *Measurement*, 45(5), 1266-1276.

Rastee, D., Koyee, Rocco, E. and Siegfried, S.(2014). "Application of Taguchi coupled Fuzzy Multi Attribute Decision Making (FMADM) for optimizing surface quality in turning austenitic and duplex stainless steels." *Measurement*, 58,375-386.

Ribeiro, M.V., Moreira, M.R.V. and Ferreira, J.R. (2003). "Optimization of titanium alloy (Ti-6Al–4V) machining." *J.Mater. Process.Technol*., 143-144,458-463.

Rigney, D.A.(1992). "Some thoughts on sliding wear." *Wear* 152, 187–192.

Rodney, B., Gerhard, W. and Collings, E W.(1994). "Materials Properties Handbook." *ASM International*, Materials Park, OH

Rodríguez, A., L.N. López de Lacalle, A., Celaya, A., Lamikiz, J. and Albizuri.(2012). "Surface improvement of shafts by the deep ball-burnishing technique." *Surf.Coat. Technol*., 206, 2817–2824.

Ross P.J.(1996). "Taguchi techniques for quality engineering: loss function, orthogonal experiments, parameter and tolerance design." *McGraw-Hill*, New York.

Röttger, K. (2002). "Walzen hartgedrehter Oberflaechen." PhD. Dissertation, Technical University of Aachen.

Ruseva and Fuks .(1978). " Surface layer properties after burnishing by different methods." *Russian Eng. J.* 58,28–30.

Sahin, Y.and A.R. Motorcu, (2004). "Surface roughness prediction model in machining of carbon steel by PVD coated cutting tools." *Am. J. Applied Sci*., 1: 12-17

Sahin, Y. and Motorcu,A.R. (2005). "Surface roughness model for machining mild steel with coated carbide tool." *Mater.Des*., 26(4), 321-326.

Sartkulvanich,P., Altan, T., Jasso, F.and Rodriguez, C. (2007). "Finite element modelling of hard roller burnishing: an analysis on the effects of process parameters upon surface finish and residual stress." *J.Manufac. Sci. Eng., Transac. of the ASME* , 129,705–716.

Sasahara, H.T and Obikawa,T. (2004). "Prediction model of surface residual stress within a machined surface by combining two orthogonal plane models." *Int. J. of Mach. Tools and Manuf*., 44(7-8), 815-822

Sayahi M., Sghaier S. & Belhadjsalah H. (2013). "Finite element analysis of ball burnishing process: comparisons between numerical results and experiments." *Int. J. Adv. Manuf. Technol.,* (2013) 67:1665–1673

Schutz, R.W. and Thomas, D. E.(1988). "Corrosion of Titanium and Titanium Alloys."*Metals Handbook*-13(9), ASM, Materials Park, OH.

Sellars, C., and Tegart, W.M. (1966). "On the mechanism of hot deformation." *Acta Metall.* 14, 1136–1138

Selvakumar. S., Ravikumar, R. and Raja, K.(2012). "Implementation of response surface methodology in finish turning on titanium alloy Gr.2."*European J Sci. Res*., 81(3), 436-445.

Shapiro and Frolov (1970). "Influence of surface work hardening on the fatigue properties of wrought iron." *Russian Eng. J.* L, 52–53.

Shiou, F.J. and Chen, C.H.(2003a). "Determination of optimal ball-burnishing parameters for plastic injection moulding steel."*Int. J. Adv. Manuf. Technol*., 3,177-185.

Shiou, F.J. and Chen, C.H.(2003b). "Freedom surface finish of plastic injection mold by using ball-burnishing process."*J. Mater. Process Technol*.140 , 248 - 254.

Shirsat, U.M. and Ahuja, B.B.(2005). "Effect of lubricant on surface finish and surface hardness of burnished component." *IE (I)J. MC*.,86, 91-94.

Shokrani,A., .Dhokia, V. and Newman, S.T.(2012). "Environmentally conscious machining of difficult-to-machine materials with regard to cutting fluids." *Int.J.Mach.Tools Manuf*., 57, 83–101.

Silveira,E., Atxaga,G and Irisarri, A.M.(2008)."Failure analysis of a set of compressor blades." *Eng.Fail. Anal*.,15,666-674.

Skalski, K., Morawski, A. and Przybylski, W. (1995). "Analysis of contact elastic-plastic strains during the process of burnishing." *Int. J.of Mech. Sci*., 37(5), 461–472.

Sokovic, M. and Mijanovic, K. (2001). "Ecological aspects of the cutting fluids and its influence on quantifiable parameters of the cutting processes." *J of Mater. Process Technol*., 109, 181–189.

Sreejith, P.S. and Ngoi, B.K.A.(2000). "Dry machining – machining of the future."*J of Mater. Process Technol*., 101, 289–293.

Srinivasa Rao, D.,Suresh Hebbar, H., Komaraiah, M. and Kempaiah,U. N.(2008). "Investigations on the Effect of Ball Burnishing Parameters on Surface Hardness and

Wear Resistance of HSLA Dual-Phase Steels."*Mater.and Manufac. Process*., 23, 295–302

Straffelini, G. and Molinari, A. (1999). "Dry sliding wear of Ti–6Al–4V alloy as influenced by the counterface and sliding conditions." *Wear*, 236, 328–338.

Streicher, R.M., Weber, H., Schon, R. and Semlitsch, M.(1991). "New surface modifcation for Ti-6Al-7Nb alloy: oxygen diffusion hardening (ODH)."*Biomater*., 12, 125-129.

Suh, N P.(1973). "The delamination theory of wear." *Wear*, 25, 111–124.

Tan,M.J. and Zhu, X.J.(2006). "Dynamic recrystallization in commercially pure titanium." *J. of Achiev.Mater. Manufac. Eng*., 18, 183-186.

Taguchi, G.(1986). "Introduction to quality engineering: designing quality into product and processes." *Asian Productivity Organisation*,Tokyo.

Tao Zhang (2013). "The Effects of Ball Burnishing for Aerospace Blade Material 17-4 PH Steel", *A Thesis report for Master of Science Degree in Mechanical Engineering*, The University of Toledo.

Tao Zhang , Nilo Bugtai and Ioan D. Marinescu.(2015). "Burnishing of aerospace alloy: A theoretical–experimental approach." *J. of Manu. Systems*, 37, 472–478.

Thamizhmanii, S. and Hassan, S.(2009). "An experimental work on multi-roller burnishing process on difficult to cut material–titanium alloy."*Int. J. Integ.Eng*., 1 , 1–6.

Timoshchenko and Dubenko (1976). "Selection of optimum technological parameters for diamond burnishing of chromium coated blanks." *Russian Eng. J.* 56,57–58.

Tolga Bozdana (2005). "On the mechanical surface enhancement techniques in aerospace industry – a review of technology." *Aircraft Eng. and Aero. Technol.: An Int. J.*, 77(4), 279-292.

Tolga Bozdana and Nalla R. K.(2003). “On the influence of mechanical surface treatments (deep rolling and laser shock peening) on the fatigue behaviour of Ti-6Al-4V at ambient and elevated temperatures.” *Mater.Sci. and Eng. A*, 355, 216-230.

Torbilo, V. M (1974). “Diamond Burnishing.” Moskva.

Travieso-Rodriguez J. A., Dessein G. and Gonzalez-Rojas H. A. (2011). “Improving the surface finish of concave and convex surfaces using a ball burnishing process.”*Mat. and Manufac.Process.*, 26(12),1494-1502.

Tsuji, N., Tanaka, S. and Takasugi, T. (2008). “Evaluation of surface modified Ti–6Al–4V alloy by combination of plasmacarburizing and deep-rolling.” *Mater. Sci. Eng. A* 488, 139–145.

Velasco-Ortega, E.(2010). “In vitro evaluation of cytotoxicity and genotoxicity of a commercial titanium alloy for dental implantology.” *Mutat Res*., 702(1), 17-23.

Venkatesh, C. and Venkatesan, R.(2015). “Optimization of process parameters of hot extrusion of SiC/Al 6061 composite using Taguchi's technique and upper bound technique.”*Mater.and Manufac.Process*, 30 (1), 85-92.

Vikramkumar CH R. and Ramamoorthy B.(2007). “Performance of coated tools during hard turning under minimum fluid application”. *J. Mater. Process Technol*., 185(1–3) B, 210–216.

Wakabayashi, T., Sato, H. and Inasaki, I.(1998). “Turning using extremely small amounts of cutting fluids.” *JSME Int. J*., 41, 143-148.

Wang L Yu X, (1999). “Effect of various parameters on the surface roughness of an aluminum alloy burnished with a spherical surfaced polycrystalline diamond tool.”*Int. J. Mach. Tools Manuf.*, 39, 459-469.

Wang, T., Wang, D.P., Gang, G., Gong, B.M. and Song, N.X.(2009). “40Cr nano-crystallization by ultrasonic surface rolling extrusion processing.” *J. of Mech. Eng*., 45 (4), 177–183.

Webzell, S., (2007). “Exotic Substrates, www.machinary.”co.uk, 39-40.

WestmanEL (2003). "Development of an inverse modelling programming system for evaluation of Ti-6Al-4V gleeble experiments." Master's thesis, Lulea University of Technology

Wilks, J. and Wilks,E.(1991)."Properties and Applications of Diamond.", *Butterworth Heinemann*, 17-20.

Wonga, C.C., Hartawan, A and Teo.W.K.(2014). " Deep Cold Rolling of Features on Aero-Engine Components." *Procedia CIRP*, 13, 350-354.

Wu,X.,Tao,N.,Hong,Y.,Liu,G.,Xu,B.,Lu,J.and Lu, K. (2005). "Strain-induced grain refinement of cobalt during surface mechanical attrition treatment."*Acta Materialia*, 53(3), 681-691.

Xiaoping,Y. and Richard, L.C.(1999). "Machining titanium and its alloys." *Mach.Sci. and Technol.*, 3(1), 107-139.

Xuanyong, L., Paul, K., Chub, C. and Dinga.(2004). "Surface modification of titanium, titanium alloys and related materials for biomedical application."*Mater. Sci. and Eng*., R 47, 49–121.

Yasuhiro, M. and Kei, D.(2011). "Surface Age Hardening and Wear Properties of Beta-Type Titanium Alloy by Laser Surface Solution Treatment." *Mater. Transac.*, 52(4) , 714 – 718.

Yerramareddy, S. and Bahadur, S.(1992). "The effect of laser surface treatments on the tribological behavior of Ti–6Al–4V." *Wear*, 157, 245–262.

You-Li Zhu, Kan Wang Li and Yuan-Lin Huang,(2009)."Evaluation of an Ultrasound- Aided Deep Rolling Process for Anti-Fatigue Applications." *J. of Mat. Eng. and Per.*,18(81036-1040.

Yuan, S.M., Yan, L.T., Liu, W.D. and Q. Liu.,Q.(2011). "Effects of cooling air temperature on cryogenic machining of Ti–6Al–4V alloy." *J of Mat. Proces. Tech*., 211(3), 356-362.

Zaborski,A.,Tubielewicz,K.and Major, B.(2000). “Contribution of burnishing to the microstructure and texture in surface layers of carbon steel.” *Arch. of Metall*., 45(4), 333–341.

Zaya,K., Maawada, E. Brokmeiera, H.-G., Wagnera, L. and Genzelc, Ch.(2011) “Influence of mechanical surface treatments on the high cycle fatigue performance of TIMETAL 54M.” *Mat. Sci. and Eng.: A* , 528(6), 2554–2558.

Zhuang, W.and Wicks, B. (2004). “Multipass low-plasticity burnishing induced residual stresses: Three-dimensional elastic-plastic finite element modeling.” *Proc IMechE C J Mech Eng Sci* 218:663–668.

Zhuang,W., Liu, Q., Djuguma, R., Sharpa, P.K. and Paradowska, A.(2014). “Deep surface rolling for fatigue life enhancement of laser clad aircraft aluminium alloy.” *App. Sur. Sci*., 320, 558–562.

Zhang, P., Lindemann, J., Ding, W.J. and Leyens, C.(2010). “Effect of roller burnishing on fatigue properties of the hot-rolled Mg–12Gd–3Y magnesium alloy.”*Mater.Chem. and Phy*.,124 , 835–840

Zou, B.,Chen, M., Huang, C. and An, Q.(2009). “Study on surface damages caused by turning NiCr20TiAl nickel-based alloy.” *J. Mater.Process. Technol*., 209, 5802–5809.

Zoya, Z.A. and Krishnamurthy. R. (2000). “The performance of CBN tools in the machining of titanium alloys.”*J. Mater.Process. Technol*., 100, 80-86

Zwicker, J., Etzold, U. and Moser, T.(1985). “Abrasive properties of oxide layers on TiAl15-Fe2.5 in contact with high density polyethylene Titanium.” *Sci. Technol*., 2, 1343-1350.

LIST OF PUBLICATIONS

I INTERNATIONAL JOURNAL PAPERS

1. Goutam D. Revankar, Raviraj Shetty, Shrikantha S. Rao and Vinayak N. Gaitonde (2014). "Analysis of surface roughness and hardness in Titanium alloy machining with polycrystalline diamond tool under different lubricating modes." *Materials Research, 17(4), 1010-1022*.

2. Goutam D. Revankar, Raviraj Shetty, Shrikantha S. Rao and Vinayak N. Gaitonde (2014). "Selection of optimal process parameters in ball burnishing of Titanium Alloy." *Machining Science and Technology: An International Journal, Taylor and Francis 18(3), 464-483.*

3. Goutam D. Revankar, Raviraj Shetty, Shrikantha S. Rao and Vinayak N. Gaitonde, (2014). "Analysis of surface roughness and hardness in ball burnishing of titanium alloy." *Measurement ,Elesvier 58, 256-268.*

4. Raviraj Shetty, Tony K.Jose, Goutam.D.Revankar, Srikanth.S.Rao and Diwakar Shetty.S.(2014). "Surface roughness analysis during turning of Ti-6Al-4V under near dry machining using statistical tool." *International Journal of Current Engineering and Technology, 4(3), 2061-2067.*

5. Raviraj Shetty, Anajwal Denim, Goutam.D.Revankar, Srikanth.S.Rao and Divakar Shetty.S.(2014). "Characterization of microstructure and tribological study on heat treated Ti-6Al-4V.", *International Journal of Current Engineering and Technology, 4(3), 2183-2188.*

COMMUNICATED

6. Goutam D. Revankar, Raviraj Shetty, Shrikantha S. Rao and Vinayak N. Gaitonde,(2015). "Wear resistance enhancement in titanium alloy due to burnishing." *Journal of materials research and technology* (JMRT-D-15-00153).

II CONFERENCE

1. Goutam D. Revankar, Raviraj Shetty, Diwakar shetty and Shrikantha S. Rao.(19th Aug., 2012). ''Mathematical modelling of burnishing force on ball burnishing of titanium alloy using response surface methodology.'' *Proceedings of International conference in Mechanical and Industrial Engineering (ICMIE 2012),* Goa,India.

2. Goutam D. Revankar, Raviraj Shetty, Shrikantha S. Rao, and Vinayak N. Gaitonde.(7th-8th Dec.,2013). "Response surface model for surface roughness during finish turning of titanium alloy under minimum quantity lubrication." *Proceedings of international conference on emerging Trends in engineering and technology (ICETET'2013),* Phuket, Thailand.

VITAE

The author, Goutam D Revankar was born on 13th August, 1973 in Sirsi, Uttar Kanara (Karnataka).He obtained his primary education from Shri.C.D.O.Jain English Medium School.Gadag. He completed his secondary education from Sri Rajeshwari Vidyaneketan, Hulkoti and higher secondary education from J.T.College, Gadag. He pursued his Bachelor's Degree in Mechanical Engineering in 1995 and Master's Degree in Production Technology in 1997 from B.V.B College of Engineering and Technology,Hubli. He worked as a lecturer for 6 months in Anjuman Polytechnic,Gadag. He joined as Assistant Professor, Department of Mechanical Engineering in Tontadarya College of Engineering, Gadag in 1999. Currently, he is working in the same college as Associate Professor, Department of Mechanical and Dean (Planning).

The author has published a part of his research work in the form of papers in five International Journal and two papers in International Conferences. The papers in International Conferences have been presented in ICMIE 2012 Goa and ICETET 2013 Thailand.